

**АВТОМАТИКА  
и  
ТЕЛЕМЕХАНИКА**

*cm*  
**Vol. 21, No. 7, July, 1960**

**Translation Published February, 1961**

**SOVIET INSTRUMENTATION AND  
CONTROL TRANSLATION SERIES**

# Automation and Remote Control

(The Soviet Journal *Avtomatika i Telemekhanika* in English Translation)

■ This translation of a Soviet journal on automatic control is published as a service to American science and industry. It is sponsored by the Instrument Society of America under a grant in aid from the National Science Foundation, continuing a program initiated by the Massachusetts Institute of Technology.

THE UNIVERSITY  
OF MICHIGAN  
- 1960  
ENGINEERING  
LIBRARY



## SOVIET INSTRUMENTATION AND CONTROL TRANSLATION SERIES

### *Instrument Society of America Executive Board*

**Dr. Ralph H. Tripp**  
*President*

**J. Johnston, Jr.**  
*Past President*

**Philip A. Sprague**  
*President-elect-Secretary*

**Henry J. Noebels**  
*Dept. Vice President*

**E. A. Adler**  
*Dept. Vice President*

**Adelbert Carpenter**  
*Dept. Vice President*

**Nathan Cohn**  
*Dept. Vice President*

**Francis S. Hoag**  
*Dept. Vice President-elect*

**John C. Koch**  
*Treasurer*

**Nelson Gildersleeve**  
*Dist. I Vice President*

**H. Kirk Fallin**  
*Dist. II Vice President*

**John R. Mahoney**  
*Dist. III Vice President*

**F. R. Gilmer**  
*Dist. IV Vice President*

**Milton M. McMillen**  
*Dist. V Vice President*

**Otto J. Lessa**  
*Dist. VI Vice President*

**J. Howard Park, III**  
*Dist. VII Vice President*

**Roy Horton**  
*Dist. VIII Vice President*

**Robert C. Mann**  
*Dist. IX Vice President*

**Kenneth S. Vriesen**  
*Dist. X Vice President*

**John J. McDonald**  
*Dist. XI Vice President*

### *Headquarters Office*

**William H. Kushnick**  
*Executive Director*

**Charles W. Covey**  
*Editor, ISA Journal*

**Herbert S. Kindler**  
*Director, Tech. & Educ. Services*

**Ralph M. Stotsenburg**  
*Director, Promotional Services*

**Ira S. French**  
*Director, Public Relations*

### *ISA Publications Committee*

**Charles O. Badgett, Chairman**

**Jere E. Brophy**

**George A. Larsen**

**Joshua Stern**

**Dr. Enoch J. Durbin**

**Thomas G. MacAnespie**

**Frank S. Swaney**

**Prof. Richard W. Jones**

**John E. Read**

**Richard A. Terry**

### *Translations Advisory Board of the Publications Committee*

**Jere E. Brophy, Chairman**

**T. J. Higgins**

**S. G. Eskin**

**G. Werbizky**

■ This translation of the Soviet Journal *Avtomatika i Telemekhanika* is published and distributed at nominal subscription rates under a grant in aid to the Instrument Society of America from the National Science Foundation. This translated journal, and others in the Series (see back cover), will enable American scientists and engineers to be informed of work in the fields of instrumentation, measurement techniques, and automatic control reported in the Soviet Union.

The original Russian articles are translated by competent technical personnel. The translations are on a cover-to-cover basis and the Instrument Society of America and its translators propose to translate faithfully all of the scientific material in *Avtomatika i Telemekhanika*, permitting readers to appraise for themselves the scope, status, and importance of the Soviet work. All views expressed in the translated material are intended to be those of the original authors and not those of the translators nor the Instrument Society of America.

Publication of *Avtomatika i Telemekhanika* in English translation started under the present auspices in April, 1958, with Russian Vol. 18, No. 1 of January, 1957. The program has been continued with the translation and printing of the 1958, 1959, and 1960 issues.

Transliteration of the names of Russian authors follows the system known as the British Standard. This system has recently achieved wide adoption in the United Kingdom, and is currently being adopted by a large number of scientific journals in the United States.

Readers are invited to submit communications on the quality of the translations and the content of the articles to ISA headquarters. Pertinent correspondence will be published in the "Letters" section of the ISA Journal. Space will also be made available in the ISA Journal for such replies as may be received from Russian authors to comments or questions by American readers.

### *1960 Volume 21 Subscription Prices:*

Per year (12 issues), starting with Vol. 21, No. 1

<i>General: United States and Canada</i> . . . . .	\$35.00
<i>Elsewhere</i> . . . . .	38.00

*Libraries of nonprofit academic institutions:*

<i>United States and Canada</i> . . . . .	\$17.50
<i>Elsewhere</i> . . . . .	20.50

*Single issues to everyone, each* . . . . . \$ 6.00

1957 Volume 18, 1958 Volume 19, and 1959 Volume 20 issues also available. Prices upon request.

See back cover for combined subscription to entire Series.

*Subscriptions and requests for information on back issues should be addressed to the:*

**Instrument Society of America**  
313 Sixth Avenue, Pittsburgh 22, Penna.

Translated and printed by Consultants Bureau Enterprises, Inc.

Copyright © 1961 by the Instrument Society of America



# Automation and Remote Control

*A translation of Avtomatika i Telemekhanika, a publication of the Academy of Sciences of the USSR*

## EDITORIAL BOARD OF AVTOMATIKA I TELEMEXHANIKA

D. I. Ageikin	V. A. Ilin	A. Ya. Lerner	A. A. Tal'
M. A. Aizerman	A. G. Iosuf'yan	A. M. Letov	(Corresp. Secretary)
A. B. Chelyustkin	V. V. Karibskii	(Assoc. Editor)	V. A. Trapeznikov
(Assoc. Editor)	A. V. Khranoi	V. S. Malev	(Editor in Chief)
E. G. Dudnikov	B. Ya. Kogan	B. N. Petrov	Ya. Z. Tsypkin
N. Ya. Festa	V. S. Kulebakin	Yu. P. Portnov-Sokolov	G. M. Ulanov
	S. A. Lebedev	B. S. Sotskov	A. A. Voronov
			S. V. Yablonskii

Vol. 21, No. 7

Russian Original Dated July, 1960

February, 1961

## CONTENTS

	PAGE	RUSS. PAGE
Estimating the Mean Square Deviation from a Given Trajectory. <u>E. A. Barbashin</u> . . . . .	661	941
Investigation of the Periodic Behavior of Relay Systems with Extremum Regulation. <u>I. S. Morosanov</u> . . . . .	668	951
Continuous Extremum Control Systems in the Presence of Random Noise. <u>A. A. Pervozvanskii</u> . . . . .	673	958
Investigation of a Servosystem with an Electromagnetic Induction Clutch Which Operates with Low Null Currents. <u>P. F. Klubnikin</u> . . . . .	678	964
The Maximum Dynamic Characteristic Values of Servomechanism Components of Servosystems. I. <u>G. A. Nadzhafova</u> . . . . .	685	973
Calculation of Static Characteristics of "Nozzle-Baffle" Elements. <u>E. A. Andreeva</u> . . . . .	691	982
Dynamic Characteristics of a "Jet Amplifier - Servomechanism" System. <u>B. D. Kosharskii</u>	701	997
Determination of Maximum Error of a Binary Multiplier. <u>Yang Hsi-zeng</u> . . . . .	709	1007
Exponential Converters with a Logarithmic Transformation Law. <u>A. I. Novikov</u> . . . . .	714	1015
Transformer Distance Transmission by Means of Two Phase Contactless Induction Potentiometers. <u>Yu. M. Pul'er</u> . . . . .	722	1026
Contactless Semiconductor Switching Elements. <u>E. V. Miller</u> . . . . .	728	1035
Calculation and Construction of Induction Clutches. <u>M. S. Mirenskii</u> . . . . .	736	1046
Effect of Magnetization Irregularity on the Static Characteristics of Cores. II. <u>G. D. Kozlov</u> . . . . .	744	1057
A Transistorized Magnetic Amplifier. <u>R. A. Lipman</u> and <u>M. V. Ol'shvang</u> . . . . .	755	1073
A New Method of Spectral Measurements by Means of Photosensitive Layers. <u>W. Lueck</u> . .	762	1084
LETTERS TO THE EDITOR		
An Error in the Article "Effect of Fluctuations on the Simplest Parametric Systems" by <u>V. I. Tikhonov</u> . <u>I. A. Bol'shakov</u> . . . . .	765	1088
DISCUSSION		
On the Book "Elements of Structural Synthesis of Relay Control Circuits" by V. N. Roginskii. <u>V. I. Shestakov</u> . . . . .	767	1090
Reply to V. I. Shestakov's Critical Review of the Book "Elements of Structural Synthesis of Relay Control Circuits" by V. N. Roginskii. <u>V. N. Roginskii</u> . . . . .	771	1094
Erratum. . . . .	775	1098

# General Information

1. Name of the person or organization: \_\_\_\_\_

2. Address: \_\_\_\_\_

3. City: \_\_\_\_\_

4. State: \_\_\_\_\_

5. Zip: \_\_\_\_\_

6. Telephone: \_\_\_\_\_

7. Fax: \_\_\_\_\_

8. E-mail: \_\_\_\_\_

9. Date: \_\_\_\_\_

10. Signature: \_\_\_\_\_

11. Title: \_\_\_\_\_

12. Organization: \_\_\_\_\_

13. Department: \_\_\_\_\_

14. Position: \_\_\_\_\_

15. Date of birth: \_\_\_\_\_

16. Date of death: \_\_\_\_\_

17. Date of marriage: \_\_\_\_\_

18. Date of divorce: \_\_\_\_\_

19. Date of remarriage: \_\_\_\_\_

20. Date of separation: \_\_\_\_\_

21. Date of remarriage: \_\_\_\_\_

22. Date of separation: \_\_\_\_\_

23. Date of remarriage: \_\_\_\_\_

24. Date of separation: \_\_\_\_\_

25. Date of remarriage: \_\_\_\_\_

26. Date of separation: \_\_\_\_\_

27. Date of remarriage: \_\_\_\_\_

28. Date of separation: \_\_\_\_\_

29. Date of remarriage: \_\_\_\_\_

# ESTIMATING THE MEAN SQUARE DEVIATION FROM A GIVEN TRAJECTORY

E. A. Barbashin

Sverdlovsk

Translated from *Avtomatika i Telemekhanika*, Vol. 21, No. 7, pp. 941-950, July, 1960

Original article submitted March 19, 1960

New methods for estimating the mean square deviation from a given trajectory are given. The estimates obtained provide a method of choosing the external influences so that this mean square value will be small. Conditions are given for the existence of motion exactly over a given trajectory.

We consider the system of differential equations

$$\frac{dx_i}{dt} = \sum_{k=1}^n a_{ik}(t) x_k + \sum_{k=1}^m b_{ik} u_k(t) \quad (i = 1, 2, \dots, n; m \leq n). \quad (1)$$

Here  $b_{ik}$  are constants,  $u_k(t)$  scalar functions, which we shall call control functions, and  $a_{ik}(t)$  continuous functions of time. The system may be written in the following matrix form:

$$\frac{dx}{dt} = A(t)x + \sum_{k=1}^m b_k u_k(t), \quad (2)$$

where the vectors  $b_k (b_{1k}, b_{2k}, \dots, b_{nk})$  will be assumed to be linearly independent.

Suppose for  $t_0 \leq t \leq t_0 + T$  we have given a curve  $x_1 = f_1(t)$  ( $i = 1, 2, \dots, n$ ), or, in vector form,  $x = f(t)$ . It is required to find a system of control functions  $u_k(t)$  for which the solution  $x_1(t)$  of system (1), with initial conditions  $x_1(t_0) = f_1(t_0)$ , will coincide with the given functions  $x_1 = f_1(t)$  for  $t_0 \leq t \leq t_0 + T$ . In other words, it is required to choose the control functions so that the given trajectory will be realized.

From the theory of dynamic programming it is clear that for  $m < n$  this problem need not even have a solution. In this case [1, 2] there remains the question of choosing a system of control functions which will yield the best approximation to the given trajectory. However, it should be noted that even in the simplest case, when one attempts to guarantee a minimum of the mean square deviation from a given trajectory, the existent methods [2, 3] lead to solving boundary value problems for systems of ordinary differential equations, in which the form of the system changes when the functions  $f_i(t)$  change.

Ya. N. Roitenberg [4], following an idea of A. Ya. Lerner, indicated another approach to solving the prob-

lem: he described a method of constructing piecewise constant control functions guaranteeing that the trajectory  $x = x(t)$  of Equation (2) intersects the given trajectory  $x = f(t)$  at prescribed moments of time  $t_0, t_1, \dots, t_r$  in the interval  $[t_0, t_0 + T]$ . However, this method of solution may prove to be unsatisfactory in many cases for the simple reason that small perturbations in the control functions found in this manner lead to the loss of the property for which they were constructed; i.e., the perturbed trajectory of Equation (2) may not intersect the given trajectory at a single moment of time in the given interval.

In this paper, following the first of the two directions indicated for solving the problem, we give up the aim of making the deviation a minimum, preferring to indicate an approach whereby the deviation may simply be made small. We assume that the deviation  $\|x\|$  of the quantity of interest to us may be associated with the deviation  $\|y\|$  of another quantity by means of the inequality

$$\|z\| \leq A \|y\|, \quad (3)$$

and assume that the minimum  $\|y\|$  is easily found. In this case, one may replace the problem of finding  $\min \|x\|$  by the problem of finding  $\min \|y\|$ . Since these are different problems, we obtain a somewhat worse approximation, which, however, may prove to be accurate in practice. Such an approach to the problem decreases significantly the calculational difficulties, since the method, while still leading to the solution of a system of ordinary differential equations, may be carried through once and for all for a given matrix  $A(t)$ , and is suitable when the given trajectory  $f(t)$  is varied, as well as when the control vectors  $b_i$  are. This solution admits a simple geometrical interpretation; consequently, it may be modelled, in the sense that a simple calculational analog device, using continuously varying parameters, may be employed in place of complicated digital computers to solve the problem.

In this paper the question of estimating the mean square value of the deviation is considered; the question



of estimating the maximum deviation will be taken up in a succeeding paper.

### 1. Estimate for the Mean Square Deviation

In Equation (2) we introduce the change of variables  $z = x - f(t)$  and obtain the new equation

$$\dot{z} = A(t)z + \sum_{k=1}^m b_k u_k(t) + A(t)f(t) - \dot{f}(t). \quad (4)$$

With the aim in mind of estimating the solution to Equation (4) determined by the initial condition  $z(t_0) = 0$ , and for simplicity, setting  $t_0 = 0$  in all that follows, we write the solution  $z(t)$  according to Cauchy's formula ([5], page 172)

$$z(t) = F(t) F^{-1}(0) \left[ \sum_{k=1}^m b_k u_k(\tau) + A(\tau)f(\tau) - \dot{f}(\tau) \right] d\tau. \quad (5)$$

Here  $F(t)$  is the fundamental matrix satisfying the equation

$$\dot{F}(t) = A(t)F(t),$$

$F^{-1}(t)$  being the inverse matrix.

Introducing the notation

$$y(t) = \sum_{k=1}^m b_k u_k(t) + A(t)f(t) - \dot{f}(t), \quad (6)$$

we obtain

$$z(t) = \int_0^t F(t) F^{-1}(\tau) y(\tau) d\tau. \quad (7)$$

**Theorem 1.** There exists a least positive constant  $L$  such that

$$\|z\| = \left[ \int_0^T \sum_{i=1}^n z_i^2(t) dt \right]^{1/2} \leq L \left[ \int_0^T \sum_{i=1}^n y_i^2(t) dt \right]^{1/2}. \quad (8)$$

The number  $L$  may be found from the formula

$$L^2 = \int_0^T \sum_{i=1}^n x_i^2(t) dt, \quad (9)$$

where the functions  $x_i(t)$  satisfy the system of equations

$$\begin{aligned} \dot{x}_i &= \sum_{k=1}^n a_{ik}(t) x_k - \frac{p_i}{\lambda}, \\ \dot{p}_i &= - \sum_{k=1}^n a_{ki}(t) p_k + x_i \quad (i = 1, 2, \dots, n) \end{aligned} \quad (10)$$

under the boundary conditions

$$x_i(0) = 0; \quad p_i(T) = 0;$$

$$\int_0^T \sum_{i=1}^n p_i^2(t) dt = \lambda^2 \quad (i = 1, 2, \dots, n). \quad (11)$$

The number  $L$  is also equal to the largest value of  $\lambda$  for which the boundary value problem (10)-(11) is solvable.

However, the solution of the boundary value problem (10)-(11) may entail considerable difficulty; therefore, we shall present a convenient method of estimating the number  $L$ .

**Theorem 2.** The inequality  $L \leq L_1$ , holds, where

$$L_1^2 = \int_0^T \int_0^t \sum_{i,k=1}^n w_{ik}^2(t, \tau) d\tau dt. \quad (12)$$

Here  $w_{ik}(t, \tau)$  designate the elements of the matrix  $F(t)F^{-1}(\tau)$ . We note that, if  $A$  is a constant matrix, then  $F(t)F^{-1}(\tau) = F(t - \tau)$ .

### 2. Choice of the Control Functions

After  $L$  or  $L_1$  is found by some means or another, in order to obtain the most accurate estimate of the mean square deviation, it is necessary to choose the control functions so that the quantity

$$\|y\| = \left( \int_0^T \sum_{i=1}^n y_i^2(t) dt \right)^{1/2}$$

is a minimum. For convenience we use the notation

$$r(t) = \dot{f}(t) - A(t)f(t).$$

The problem consists in choosing for each value  $t$  such values  $u_1(t), u_2(t), \dots, u_m(t)$ , which will guarantee the value of the quantity  $\|y\|$  to be a minimum. But the quantity  $\|y\|$  will be minimal if, and only if, for each value  $t$  in the interval  $[0, T]$ , the quantity

$$|y(t)| = \left| \sum_{i=1}^m b_i u_i(t) - r(t) \right|$$

is also minimal. Here  $|y(t)|$  denotes the length of the vector  $y(t)$ .

We consider now the hyperplane  $Q$  spanned by the vectors  $b_1, b_2, \dots, b_m$ . It is clear that the magnitude  $|y(t)|$  determines the distance from the point  $A$ , whose radius-vector is  $r(t)$ , to some point  $B$  with radius-vector  $\sum_{i=1}^m b_i u_i(t)$ , lying on the plane  $Q$ .

Thus,  $|y(t)|$  will be the least for the given  $t$ , if the number  $u_i(t)$  is chosen so that the point  $B$  is the

projection of the point A onto the plane Q, that is so that  $|\mathbf{y}(t)|$  will be the distance from the point A to the plane Q.

According to [6] (page 205), we have

$$AB^2 = \frac{\Gamma(b_1, b_2, \dots, b_m, r(t))}{\Gamma(b_1, b_2, \dots, b_m)}, \quad (13)$$

where

[illegible]

and

$$\Gamma(\mathbf{b}_1, \mathbf{b}_2, \dots, \mathbf{b}_m) = \begin{vmatrix} (\mathbf{b}_1, \mathbf{b}_1) & (\mathbf{b}_1, \mathbf{b}_2) & \dots & (\mathbf{b}_1, \mathbf{b}_m) \\ \vdots & \vdots & \ddots & \vdots \\ (\mathbf{b}_m, \mathbf{b}_1) & (\mathbf{b}_m, \mathbf{b}_2) & \dots & (\mathbf{b}_m, \mathbf{b}_m) \end{vmatrix}$$

is Gramme determinant,  $(b_i, b_k)$  denoting the scalar product. Since the vectors  $b_1, b_2, \dots, b_m$  are linearly independent,  $\Gamma(b_1, b_2, \dots, b_m) \neq 0$ .

Let  $u_1(t), \dots, u_m(t)$  be chosen to minimize  $\|\mathbf{y}(t)\|$ ; then

$$(y(t), b_k) = \left( \sum_{i=1}^m b_i u_i(t) - r(t), b_k \right) = 0$$

( $k = 1, 2, \dots, m$ ), since the vector  $\mathbf{y}(t)$  is orthogonal to all of the vectors  $\mathbf{b}_k$ .

To determine  $u_i(t)$ , we have the system of equations

$$\sum_{i=1}^m (\mathbf{b}_k, \mathbf{b}_i) u_i(t) = (\mathbf{r}(t), \mathbf{b}_k) \quad (k = 1, 2, \dots, m). \quad (14)$$

The determinant of this system is equal to  $\Gamma(\mathbf{b}_1, \mathbf{b}_2, \dots, \mathbf{b}_m)$  and therefore is different from zero.

Denoting  $H^2 = \min \int_0^T |\dot{y}(t)|^2 dt$ , according to

(13) we have

$$H^2 = \frac{1}{\Gamma(\mathbf{b}_1, \mathbf{b}_2, \dots, \mathbf{b}_m)} \int_0^T \Gamma(\mathbf{b}_1, \mathbf{b}_2, \dots, \mathbf{b}_m, \mathbf{r}(t)) dt. \quad (15)$$

These formulas take on a particularly simple form if the system of vectors  $\mathbf{b}_1, \mathbf{b}_2, \dots, \mathbf{b}_m$  is orthogonal, i.e.,

if  $(\mathbf{b}_i, \mathbf{b}_k) = 0$  for  $i \neq k$  and  $(\mathbf{b}_i, \mathbf{b}_i) = 1$ . In this case, we have  $u_i(t) = (\mathbf{x}(t), \mathbf{b}_i)$  ( $i = 1, 2, \dots, m$ ):

$$H^2 = \int_0^T \mathbf{r}^2(t) dt - \sum_{i=1}^m \int_0^T (\mathbf{r}(t), \mathbf{b}_i)^2 dt. \quad (15')$$

If there is only one control function, then

$$u(t) = \frac{(\mathbf{r}(t), \mathbf{b})}{|\mathbf{b}|^2}$$

and

$$H^2 = \int_0^T \mathbf{r}^2(t) dt = \frac{1}{b^2} \int_0^T (\mathbf{r}(t), \mathbf{b})^2 dt. \quad (15'')$$

Formula (15) indicates that the exact realization of the given trajectory is possible only if, at each moment of time,

$$l'(b_1, b_2, \dots, b_m, r(t)) = 0. \quad (16)$$

Equation (16) means that the curve  $z = r(t)$  lies in the plane spanned by the vectors  $b_1, b_2, \dots, b_m$ .

Otherwise, the solvability conditions for the system

$$\sum_{i=1}^m \mathbf{b}_i u_i(t) - \mathbf{r}(t) = 0 \text{ could be formulated in purely}$$

algebraic language ([7], page 40).

### 3. Choice of the Optimal System of Control Vectors

Having found  $H$ , we obtain the formula  $\|z\| \leq LH$  for estimating the mean square deviation. If the quantity  $H$  is large, then, in order to decrease  $\|z\|$ , one must enlarge the collection of control functions. If, however, the set of control functions may not be enlarged, then in certain problems, for a given trajectory  $x = f(t)$ , one may always choose an optimal system of control vectors  $b_1, b_2, \dots, b_m$ , i.e., a system guaranteeing a minimal value for  $H$ .

We consider the matrix  $C = \{c_{jk}\}$ , where

$$c_{ik} = \int_0^T r_i(t) r_k(t) dt, \text{ and } r_1(t) \text{ are the projections of}$$

the vector  $\mathbf{r}(t)$ . The eigenvalues of this matrix are non-negative. We arrange them in increasing order:

$$\lambda_1 \geq \lambda_2 \geq \dots \geq \lambda_n \geq 0.$$

To each eigenvalue  $\lambda_k$  there corresponds at least one eigenvector  $\mathbf{b}_k$ ; it is known ([6], page 20) that it is possible to orthonormalize a system of eigenvectors. Thus, we obtain an orthogonal system of eigenvector for the matrix  $\mathbf{C}$ .

**Theorem 3.** The orthonormal system of eigenvectors  $\mathbf{b}_1, \mathbf{b}_2, \dots, \mathbf{b}_m$  of the matrix  $\mathbf{C}$  is an optimal system of control vectors, in that if the system of control functions is taken according to (14), then

$$H^2 = \int_0^T r^2(t) dt - \sum_{i=1}^m \lambda_i = \sum_{k=m+1}^n \lambda_k. \quad (17)$$

We note now that the exact realization of the trajectory by choosing an optimal system of control functions and control vectors may be attained for  $m < n$  only if

$$\lambda_{m+1} = \lambda_{m+2} = \dots = \lambda_n = 0$$

But this means that the equation

$$D(\lambda) = \begin{vmatrix} c_{11} - \lambda & c_{12} & \dots & c_{1n} \\ \dots & \dots & \dots & \dots \\ c_{n1} & c_{n2} & \dots & c_{nn} - \lambda \end{vmatrix} = 0$$

has a zero root of multiplicity  $n-m$ . The conditions of existence of such a root have the form  $D(0) = D'(0) = \dots = D^{(n-m+1)}(0) = 0$ . Geometrically, these conditions mean that the curve  $z = r(t)$  lies in an  $m$ -dimensional linear subspace of the space  $(z_1, z_2, \dots, z_n)$ .

To calculate  $H^2$  from formula (17), it is necessary to know the roots  $\lambda_{m+1}, \dots, \lambda_n$ . It is known ([10], page 80) that

$$H^2 = \frac{1}{2\pi i} \int_R z \frac{D'(z)}{D(z)} dz, \quad (17')$$

where  $R$  is any contour in the complex plane enclosing only the indicated roots of the equation  $D(\lambda) = 0$ . In particular,  $R$  may be taken as the circle of radius  $\epsilon$  and center at the origin, if it is known that  $\lambda_{m+1} < \epsilon < \lambda_m$ . To determine a minimal set of control functions allowing one to attain a trajectory with prescribed accuracy, it is useful to use the reasoning in [10], page 79, or any other known method (for example, the method of Sturm) for determining the number of roots of the equation  $D(\lambda) = 0$ , in the interval  $(0, \epsilon)$ . If this number is equal to  $l$ , then  $n-l$  control functions and  $n-l$  control vectors may be chosen so that the inequality  $H^2 < \epsilon l$  will hold. The best estimate of the accuracy of the approximation in this case provides formula (17') again. In each case, it is useful to remember that the approximation using  $m$  control functions will be most accurate when the coefficients of the powers of  $\lambda$  not surpassing the degree  $m-n$  in the equation  $D(\lambda) = 0$  are small in absolute value.

#### APPENDIX

Proof of Theorem 1. It is easy to see that

$$L^2 = \max \int_0^T \sum_{k=1}^n x_k^2(t) dt$$

under the condition that  $\int_0^T \sum_{k=1}^n y_k^2(t) dt = 1$ .

We shall solve this variational problem on the basis of Pontryagin's maximum principle and the method of paper [3]. According to [3], one should introduce supplementary variables:

$$x_i = z_i \text{ for } i = 1, 2, \dots, n, \\ x_{n+1} = \int_0^t \sum_{k=1}^n x_k^2(t) dt, \quad x_{n+2} = \int_0^t \sum_{k=1}^n y_k^2(t) dt$$

and write the corresponding Hamiltonian system

$$\begin{aligned} \dot{x}_i &= \sum_{k=1}^n a_{ik}(t) x_k + y_i, \quad \dot{x}_{n+1} = \sum_{k=1}^n x_k^2, \quad \dot{x}_{n+2} = \sum_{k=1}^n y_k^2, \\ \dot{p}_i &= - \sum_{k=1}^n a_{ki}(t) p_k - 2p_{n+1} x_i, \quad \dot{p}_{n+1} = \\ &= 0, \quad \dot{p}_{n+2} = 0 \quad (i = 1, 2, \dots, n). \end{aligned} \quad (18)$$

We shall seek  $\max x_{n+1}(T)$  under the condition that  $x_{n+2}(T) = 1$ . According to [3], it is necessary to construct the Hamiltonian function

$$H = \sum_{i,k=1}^n a_{ik} p_i x_k + \sum_{i=1}^n p_i y_i + p_{n+1} \sum_{k=1}^n x_k^2 + p_{n+2} \sum_{k=1}^n y_k^2.$$

The maximum principle tells us that  $y_i$  should be chosen so that  $H$  is a minimum. The condition of  $H$  being minimal takes the form

$$2p_{n+2} y_i + p_i = 0 \quad (i = 1, 2, \dots, n).$$

Bearing in mind the boundary conditions for the system (18):  $x_i(0) = 0, p_i(T) = 0$  for  $i = 1, 2, \dots, n$ ,  $p_{n+1}(T) = -\frac{1}{2}$ ,  $p_{n+2}(T) = \lambda/2$ ,  $x_{n+2}(T) = 1$ , we have

$$p_{n+1}(t) = -\frac{1}{2}, \quad p_{n+2} = \frac{\lambda}{2} \text{ and } y_i(t) = -\frac{p_i(t)}{\lambda}.$$

The essential portion of system (18) may now be rewritten in the form

$$\begin{aligned} \dot{x}_i &= \sum_{k=1}^n a_{ik} x_k - \frac{p_i}{\lambda}, \quad \dot{p}_i = \\ &= - \sum_{k=1}^n a_{ki} p_k + x_i \quad (i = 1, 2, \dots, n). \end{aligned} \quad (19)$$



This system must be solved under the conditions

$$x_i(0) = 0, p_i(T) = 0 \quad (i = 1, 2, \dots, n);$$

$$x_{n+2}(T) = \frac{1}{\lambda^2} \int_0^T \sum_{k=1}^n p_k^2(t) dt = 1. \quad (20)$$

We show now that  $L^2 = \lambda$ , where  $\lambda$  is the largest eigenvalue for which the boundary problem (19)-(20) has a solution. For this purpose, writing the system (19) in matrix form,

$$\dot{\mathbf{x}} = \mathbf{A}(t) \mathbf{x} - \frac{\mathbf{p}}{\lambda}, \quad \dot{\mathbf{p}} = -\mathbf{A}^*(t) \mathbf{p} + \mathbf{x}$$

[here  $\mathbf{A}^*(t)$  denotes the matrix conjugate to  $\mathbf{A}(t)$ ], we take the scalar product of the first equation with  $\mathbf{p}$ , and of the second with  $\mathbf{x}$ . Adding the resulting equations, we obtain

$$(\dot{\mathbf{x}}, \mathbf{p}) + (\dot{\mathbf{p}}, \mathbf{x}) = (\mathbf{A}(t) \mathbf{x}, \mathbf{p}) - (\mathbf{A}^*(t) \mathbf{p}, \mathbf{x}) - \frac{\mathbf{p}^2}{\lambda} + \mathbf{x}^2.$$

Integrating from 0 to T, and remembering the relation

$$(\mathbf{A}(t) \mathbf{x}, \mathbf{p}) = (\mathbf{x}, \mathbf{A}^*(t) \mathbf{p}),$$

we obtain

$$(\mathbf{x}, \mathbf{p}) \Big|_0^T = \int_0^T \mathbf{x}^2 dt - \frac{1}{\lambda} \int_0^T \mathbf{p}^2 dt$$

or

$$L^2 = \lambda,$$

since, by virtue of condition (20),

$$(\mathbf{x}(t), \mathbf{p}(t)) \Big|_0^T = 0, \quad \int_0^T \mathbf{p}^2(t) dt = \lambda^2.$$

We now turn to some remarks on the connection between our considerations and the simplest concepts of functional analysis ([9], page 114). Formula (7) defines a linear operator W taking the vector function  $\mathbf{y}$  of the Hilbert space  $L_{2n}(0, T)$  into a function of the same space. The operator W is bounded and has norm L which will now be found. The adjoint operator  $W^*$  has the form [2]

$$W^* \mathbf{y} = \int_0^T (\mathbf{F}^*(t))^{-1} \mathbf{F}^*(\tau) \mathbf{y}(\tau) d\tau; \quad (21)$$

the inverse operators  $W^{-1}, (W^*)^{-1}$  are given by the formulas

$$W^{-1} \mathbf{z} = \dot{\mathbf{z}} - \mathbf{A}(t) \mathbf{z}, \quad (W^*)^{-1} \mathbf{z} = -\dot{\mathbf{z}} - \mathbf{A}^*(t) \mathbf{z} \quad (22)$$

If we introduce the notation

$$[\mathbf{y}, \mathbf{z}] = \int_0^T (\mathbf{y}(t) \mathbf{z}(t)) dt,$$

then, of course,

$$[W \mathbf{y}, \mathbf{z}] = [\mathbf{y}, W^* \mathbf{z}].$$

The variational problem which has been solved is the problem of finding the maximum of the functional

$$I = [W \mathbf{y}, W \mathbf{y}] - \lambda [\mathbf{y}, \mathbf{y}] = [W^* W \mathbf{y}, \mathbf{y}] - \lambda [\mathbf{y}, \mathbf{y}].$$

The variation  $\delta I$  is found by the formula

$$\delta I = 2 [W^* W \mathbf{y}, \delta \mathbf{y}] - 2\lambda [\mathbf{y}, \delta \mathbf{y}].$$

Since  $\delta I = 0$ , it follows that  $W^* W \mathbf{y} - \lambda \mathbf{y} = 0$ , or

$$\int_0^T \int_0^T (\mathbf{F}(\alpha) \mathbf{F}^{-1}(t))^* \mathbf{F}(\alpha) \mathbf{F}^{-1}(\tau) \mathbf{y}(\tau) d\tau d\alpha - \lambda \mathbf{y} = 0. \quad (23)$$

Thus, the value  $\lambda = L^2$  of interest to us is the largest eigenvalue of the operator  $W^* W$ . Equation (23) is an integral equation. Using formula (22), it is easy to go from it to the differential equation

$$\mathbf{y} - \lambda W^{-1} W^* \mathbf{y} = 0,$$

which, written in detail, assumes the form

$$\frac{d}{dt} \left( \frac{d\mathbf{y}}{dt} + \mathbf{A}^*(t) \mathbf{y} \right) - \mathbf{A}(t) \left( \frac{d\mathbf{y}}{dt} + \mathbf{A}^*(t) \mathbf{y} \right) + \frac{\mathbf{y}}{\lambda} = 0. \quad (23)$$

This equation should be considered together with the easily deduced conditions  $d\mathbf{y}/dt + \mathbf{A}^*(t) \mathbf{y} = 0$  at  $t = 0$ ,

$$\mathbf{y}(T) = 0, \text{ and also the condition } \int_0^T \mathbf{y}^2(t) dt = 1.$$

The substitution of the variables  $d\mathbf{y}/dt + \mathbf{A}^*(t) \mathbf{y} = -\mathbf{x}/\lambda$ ,  $\mathbf{p} = -\lambda \mathbf{y}$  into Equation (23') again leads to the boundary value problem (19)-(20). However, the purpose of our remarks is not to rederive conditions (19)-(20), but to indicate the applicability of direct methods in the search for  $L^2$ . One of such methods is, for example, the method of steepest descent ([9], page 541).

Proof of Theorem 2. We have  $\|z\|^2 = \int_0^T z_k^2(t) dt$ .  
Since

$$z_i(t) = \sum_{k=1}^n \int_0^t w_{ik}(t, \tau) y_k(\tau) d\tau,$$

then

$$\begin{aligned} \|z\|^2 &= \int_0^T \sum_{i=1}^n \left[ \sum_{k=1}^n \int_0^t w_{ik}(t, \tau) y_k(\tau) d\tau \right]^2 dt \leq \\ &\leq \int_0^T \sum_{i=1}^n \left[ \int_0^t \sqrt{\sum_{k=1}^n w_{ik}^2(t, \tau)} \sqrt{\sum_{k=1}^n y_k^2(\tau)} d\tau \right]^2 dt. \end{aligned}$$

Using the Bunyakovski-Schwartz inequality ([8], page 242), we obtain

$$\|z\|^2 \leq \int_0^T \sum_{i=1}^n \int_0^t \sum_{k=1}^n w_{ik}^2(t, \tau) d\tau \int_0^t \sum_{k=1}^n y_k^2(\tau) d\tau dt.$$

When  $t$  in the second integral is replaced by  $T$ , the inequality is only strengthened. The inequality

$$\|z\|^2 \leq \|y\|^2 \int_0^T \int_0^t \sum_{k=1}^n w_{ik}^2(t, \tau) d\tau dt$$

gives the required result.

Proof of Theorem 3. Since the quadratic form

$$I(\beta_i) = \sum_{i,k=1}^n c_{ik} \beta_i \beta_k = \int_0^T \left( \sum_{k=1}^n \beta_k r_k(t) \right)^2 dt \quad (24)$$

is positive-definite, its eigenvalues, that is, the eigenvalues of the matrix  $C$ , will be nonnegative. If the system of vectors  $b_1, b_2, \dots, b_m$  is orthonormal, then according to formula (15'), we have

$$H^2 = \int_0^T r^2(t) dt - \sum_{k=1}^m (b_k, r(t))^2 dt.$$

It is necessary to choose the system of vectors in such a manner that the sum  $\sum_{k=1}^m \int_0^T (b_k, r(t))^2 dt$  will be the largest possible. Consider the first term of this sum:

$$\begin{aligned} I_1 &= \int_0^T (b_1, r(t))^2 dt = \sum_{i,k=1}^n \int_0^T r_i(t) r_k(t) dt b_{1i} b_{1k} = \\ &= \sum_{i,k=1}^n c_{ik} b_{1i} b_{1k} = I(b_{1i}). \end{aligned}$$

Here  $b_{1k}$  are the projections of the vector  $b_1$ . The problem reduces to finding the maximum of the quadratic form  $I(b_{1i})$  under the condition  $\sum_{i=1}^n b_{1i}^2 = 1$ .

It is known ([8], page 28), that this maximum is equal to the largest eigenvalue  $\lambda_1$ , and is attained for the eigenvector  $b_1$  corresponding to this number. To satisfy the condition that the succeeding term

$$I_2 = \int_0^T (b_2, r(t))^2 dt = I(b_{2i})$$

be a maximum under the subsidiary conditions

$(b_1, b_2) = 0$ ,  $b_2^2 = 1$ , it is necessary to take  $b_2$  as the eigenvector corresponding to the eigenvalue  $\lambda_2$ . According to the extremal theory of quadratic forms ([8], page 28) the maximum  $I_2$  will be equal to  $\lambda_2$ . If  $\lambda_1 = \lambda_2$ , then for  $b_2$  one should choose, among the infinite set of eigenvectors of the multiple root  $\lambda_1$ , a vector which is orthogonal to  $b_1$ . Proceeding analogously, we obtain the complete solution to the problem.

Since  $\int_0^T r^2(t) dt = \sum_{i=1}^n c_{ii} = \sum_{i=1}^n \lambda_i$  is an invariant

quadratic form  $I$ , formula (17) is obvious.

Example. We consider the system

$$\dot{x}_1 = x_2 + b_1 u(t), \quad \dot{x}_2 = -x_1 + b_2 u(t) \quad (25)$$

and attempt to find  $u(t)$  so that the solution of this system is realized by motion along the trajectory  $x_1 = t-1$ ,  $x_2 = t+1$  for  $0 \leq t \leq 1$ .

First, we calculate  $L_1$  (Theorem 2). The fundamental matrix for the system (25) has the form

$$F(t) = \begin{vmatrix} \cos t & \sin t \\ -\sin t & \cos t \end{vmatrix}$$

from which

$$F(t) F^{-1}(\tau) = F(t - \tau) = \begin{vmatrix} \cos(t - \tau) & \sin(t - \tau) \\ -\sin(t - \tau) & \cos(t - \tau) \end{vmatrix}.$$

Thus, formula (12) yields

$$L_1 = T = 1.$$

We introduce the change of variables  $z_1 = x - t + 1$ ,  $z_2 = y - t + 1$  into the system (25). The new system takes the form

$$\dot{z}_1 = z_2 + b_1 u + t, \quad \dot{z}_2 = -z_1 + b_2 u - t. \quad (26)$$

We obtain  $r_1(t) = -t$  and  $r_2(t) = t$ . If  $b_1^2 + b_2^2 = 1$ , then formula (15\*) gives

$$u(t) = (b_2 - b_1)t, \quad H^2 = \frac{2 - (b_2 - b_1)^2}{3}. \quad (27)$$

Thus,

$$\|z\| \leq L_1 H = \left( \frac{2 - (b_2 - b_1)^2}{3} \right)^{1/2}.$$

We now attempt to find a vector  $b(b_1, b_2)$  so that the approximation will be the most accurate. First, we calculate the elements of the matrix  $C$ , entering into Theorem 2. As a result, we obtain

$$c_{11} = \frac{1}{3}, \quad c_{12} = c_{22} = -\frac{1}{3}.$$

The characteristic equation of the matrix is

$$\lambda^2 - \frac{2}{3}\lambda = 0, \text{ from which } \lambda_1 = \frac{2}{3}, \quad \lambda_2 = 0. \text{ According to}$$

Theorem 3, the control vector  $b$  may be chosen so that  $H = 0$ , and then the trajectory will be realized exactly. The vector  $b$  we are seeking should be the eigenvector of the matrix  $C$ , corresponding to the value  $\lambda_1 = 2/3$ .

To determine  $b_1$  and  $b_2$ , we have the system

$$c_{11}b_1 + c_{12}b_2 = \lambda_1 b_1,$$

$$c_{21}b_1 + c_{22}b_2 = \lambda_1 b_2, \quad b_1^2 + b_2^2 = 1,$$

from which we find  $b_1 = -\sqrt{2}/2$ ,  $b_2 = \sqrt{2}/2$ . From formula (27) it follows that  $u(t) = \sqrt{2}t$ . Otherwise, the optimal values of  $b_1$  and  $b_2$  may be found immediately from formula (27).

## LITERATURE CITED

1. R. Bellman, "Notes on control processes. 1. On the minimum of maximum deviation," *Quart. Appl. Math.* **14** (1957).
2. R. Bellman, *Some Aspects of the Mathematical Theory of Control Processes*, Rand Corporation (1958) chap. 4.
3. L. I. Rozonoér, "The L. S. Pontryagin maximum principle in the theory of optimal systems. II", *Avtomatika i Telemekhanika* **20**, 11 (1959).
4. Ya. N. Roitenberg, "Some problems in the Theory of dynamic programming," *Prikl. Matem. i Mekh.* **23**, 4 (1959).
5. V. V. Nemytskii and V. V. Stepanov, *Qualitative Theory of Differential Equations* [in Russian] (Gostekhizdat, 1949).
6. F. R. Gantmakher, *Theory of Matrices* [in Russian] (Gostekhizdat, 1953).
7. V. I. Smirnov, *Course in Higher Mathematics* [in Russian] (Gostekhizdat, 1949) vol. 3, part 1.
8. R. Courant and D. Hilbert, *Methods of Mathematical Physics* [Russian translation] (Gostekhizdat, 1933) vol. 1.
9. L. V. Kantorovich and G. N. Akilov, *Functional Analysis in Normed Spaces* [in Russian] (Fizmatgiz, 1959).
10. M. A. Lavrent'ev and B. V. Shabat, *Methods of the Theory of Functions of a Complex Variable* [in Russian] (Gostekhizdat, 1951).

\* See English translation.



# INVESTIGATION OF THE PERIODIC BEHAVIOR OF RELAY SYSTEMS WITH EXTREMUM REGULATION

I. S. Morosanov

Moscow

Translated from *Avtomatika i Telemekhanika*, Vol. 21, No. 7, pp 951-957, July, 1960

Original article submitted December 12, 1959

On the basis of the approximate calculation of the periodic behavior of relay systems with extremum regulation (RSÉR) [5], we have determined the areas within which self-oscillations exist in such systems for linear object units of any kind. We have also considered some methods for stabilizing these systems (at high frequencies).

At the present time, we are acquainted with two types of relay systems with extremum regulation (RSÉR), those in which the quantitative output magnitude of the object is tied (or fixed), and those in which it is floating with respect to the circuit extremum level (Figs. 1a and 1b).

In systems with a fixed level, the quantization is determined only by means of increments in the forbidden direction,\* the first increment being exactly computed with respect to the extremum [1]. In systems with floating regulation, the quantization is determined by taking into account increments occurring in both directions, the starting point being determined by the initial conditions and independent of the extremum position [2, 3, 4].

We have carried out below a comparative analysis of these systems in terms of the index of periodic behavior, which is a basic characteristic of SÉR.

## 1. Computation of the Parameters of the Periodic Behavior

We will assume that in RSÉR with a floating grid the quantization of the level of the initial conditions is chosen so that the extremum of the statistical characteristic of the object coincides with one of the quantization levels. Then we may use the same model (Fig. 2) in the determination of the index of the periodic behavior of both systems. We will make use of the method of balancing of harmonics in the same form that was outlined in paper [5] for application to extremum systems. From the known frequency characteristics for the linear links  $K_1(j\omega)$  and  $K_2(j\omega)$ , and the system  $K_0(j\omega)$ , we get the equivalent frequency characteristic of the extremum system (Fig. 3):

$$K(j\omega) = K_0^2\left(j\frac{\omega}{2}\right) K_1^2\left(j\frac{\omega}{2}\right) K_2(j\omega) e^{j\frac{\pi}{2}}. \quad (1)$$

The amplitude  $Y_1$  and the oscillation frequency  $\omega$  are outputs for the object and are associated with the parameters of the extremum regulator  $\kappa$  (which is

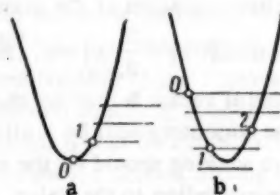


Fig. 1.

quantized in steps corresponding to the level) and the coefficient of amplification  $k_p$  by means of the following relations:

$$Y_1 = \frac{8k_p^2 k}{\pi^2} |K(j\omega)|, \quad (2)$$

$$\kappa = \frac{8k_p^2 k}{\pi^2} |K(j\omega)| f(\alpha), \quad (3)$$

where  $f(\alpha) = 1 + \sin \alpha$  for RSÉR with an extremum index based upon the deviation (increment), and  $f(\alpha) \approx 2 \alpha / \omega$ , for RSÉR with an extremum indicator based upon the integral of the deviation, and the supplementary angle with respect to  $\pi$  of the phase difference of the first harmonic of the expansion of the periodic sequences at the input and output of the regulator. The angle  $\alpha$  is measured as shown in Fig. 3.

If, in a system with a floating grid, the statistical quantization of the extremum does not coincide with either quantization level, the amplitude of the system oscillations will be larger, and the oscillation frequency will be lower, than that obtained from Equations (2) and (3). This is due to the fact that the factual magnitude of the increment, as computed with respect to the extremum, exceeds  $\kappa$  by  $0 \leq \Delta\kappa < \kappa$ ; this is determined from the initial conditions.

\*We will call increments in the forbidden, or the allowed, direction increments in the output magnitude corresponding to their distance from, or their closeness to, the extremum.

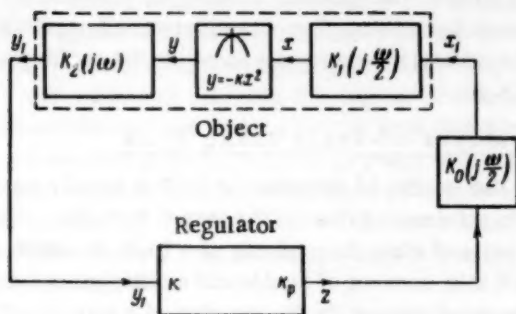


Fig. 2.

Paper [5] has determined the regions in which periodic solutions for the RSER studied in this article exist, and has shown that they satisfy the necessary conditions for stable self-oscillation. The sufficient conditions for stable self-oscillation of RSER are unknown. Papers [3, 6] show the possibility of the existence of complex periodic operation, due to multiple switches, over a period.

## 2. Regions within Which Simple Self-Oscillations Exist for RSER

Let us determine the regions within which simple self-oscillations exist.

Let us make use of the conditions existing during the time of switchover in the system [5] (Fig. 4):

$$Y_1 \cos(\omega t_x - \theta) - Y_1 = -x, \quad (4)$$

where

$$t_x = \frac{1}{\omega} \left( \alpha + \frac{\pi}{2} + \theta \right) \quad (5)$$

is the switchover time,  $Y_1$  and  $\theta$  are the modulus and phase of the equivalent frequency characteristics of system (1).

It is obvious that simple self-oscillations exist if  $2Y_1 > \kappa > Y_1$ , i.e.,  $Y_1 > Y_1 \cos(\omega t_x - \theta) > 0$ ; therefore

$$\frac{\pi}{2} > \alpha > 0. \quad (6)$$

Thus, the boundary of the region in which simple self-oscillations exist is determined by the frequency  $\omega_0$ , which corresponds to the point  $K(j\omega)$  [(1)], lying on the negative real semiaxis ( $\alpha = 0$ , Fig. 3).

In systems whose extremum indicator is the integral of the increment, the conditions at the switchover time are given by

$$\int_{0/t_0}^{t_x} [Y_1 \cos(\omega t - \theta) - Y_1] dt = -x. \quad (7)$$

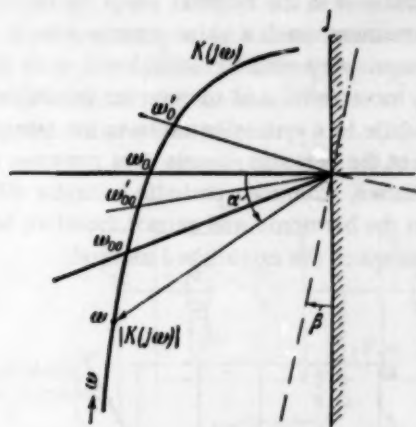


Fig. 3.

For this case, the limiting conditions for the existence of self-oscillations are given by

$$\begin{aligned} & \int_{0/t_0}^{t_x} [Y_1 \cos(\omega t - \theta) - Y_1] dt = \\ & = \int_{t_x}^t [Y_1 \cos(\omega t - \theta) - Y_1 \cos(\omega t_x - \theta)] dt, \end{aligned} \quad (8)$$

where  $t$  is determined by the first maximum of the integral in the right side of Equation (8).

Substituting the value of  $t_x$  from (5), we get

$$\begin{aligned} & Y_1 \frac{1}{\omega} \left( \frac{\pi}{2} + \alpha \right) \\ & \int_0^{\frac{1}{\omega} \left( \frac{\pi}{2} + \alpha \right)} [\cos \omega t - 1] dt = \\ & = Y_1 \frac{1}{\omega} \left( \frac{3\pi}{2} - \alpha \right) \int_0^{\frac{1}{\omega} \left( \frac{\pi}{2} + \alpha \right)} [\cos \omega t - \cos(\frac{\pi}{2} + \alpha)] dt. \end{aligned} \quad (9)$$

From this we get the following equation for  $\alpha$ :

$$\cos \alpha - \left( \frac{\pi - 2\alpha}{3} \right) \sin \alpha = \frac{\pi/2 + \alpha}{3}, \quad (10)$$

which, for  $0 < \alpha < 2\pi$ , has the solution  $\alpha = 0.367$ . This means that the region for which simple self-oscillations exist for this system is determined by the frequency  $\omega_0$ , for which the phase of  $K(j\omega) = -(\pi - 0.367)$  (Fig. 3).

An effort to realize operation at frequencies above the indicated boundary leads to the appearance of re-

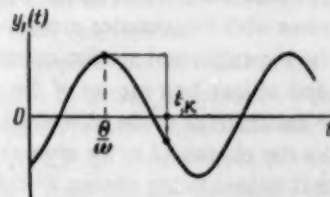


Fig. 4.

peated switchovers in the system when the deviations from the extremum reach a value greater than 2 quantized steps. As a result, in RSER based upon simple increments, increments lead to complex (multiple) oscillations, while, in a system based upon the integral of the increment, the periodic process does not even become established. Complex periodic behavior differs sharply from the harmonic, and cannot, therefore, be analyzed by means of the established method.

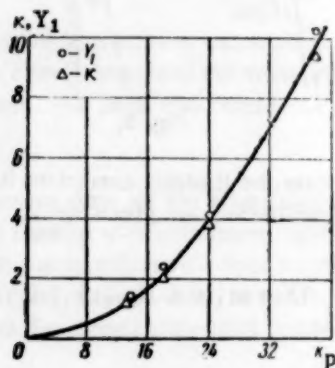


Fig. 5.

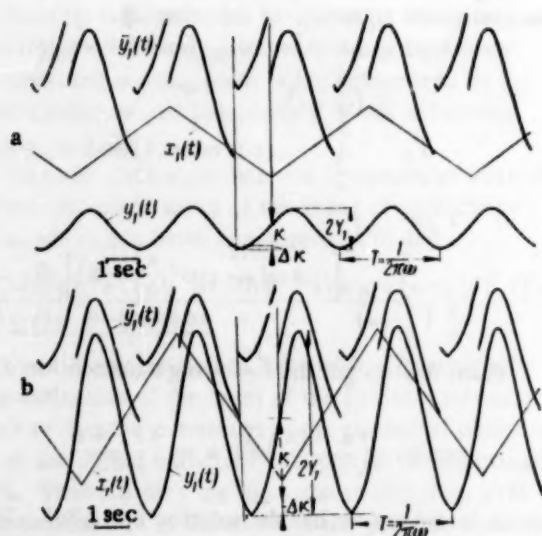


Fig. 6.  $\bar{y}_1(t)$  — quantized with respect to the level of  $y_1(t)$ .

For increases in the case of RSER with floating grid quantization, pictures were taken during experiments of periodic processes with frequencies close to the boundary frequency. The experimental system consisted of an actual operator and object in a set-up of the type MN-8. The output for the critical mode of operation ( $\alpha = 0$ ) was realized by the choice of  $\kappa$  for several fixed values of  $\kappa_p$ , the initial values being chosen so that the statistical extremum was close to one of the quantization levels. Comparison of the computed and experimental data

(Fig. 5) shows a sufficiently satisfactory agreement between the results. Two examples of self-oscillation at the critical frequency are shown in the oscillograms in Fig. 6.

### 3. Means of Stabilizing RSER

The quality of operation of RSER is usually evaluated by the minimum values of the output hunting. From this point of view, the synthesis of a RSER, in which we do not take account of accidental excitations, is subject to the requirements for the creation of a system with a maximum self-oscillation frequency. The critical self-oscillation frequency in RSER may be basically increased if we prevent repeated switchovers in the system. In order to do this, for example, we open (or disconnect) the system for a short time when the output exceeds two quantization levels (with respect to the extremum value) [1]. However, this procedure requires a preliminary knowledge of the self-oscillation frequency, which may not always be available. For example, in some cases, the same regulator must, without resetting, alternately regulate an entire series of objects, all the objects having the same structure, but each linear unit having a different time constant and having extremum statistical characteristics of different curvature.

The prevention of repeated false switchovers in RSER without first narrowing the self-adjustment region

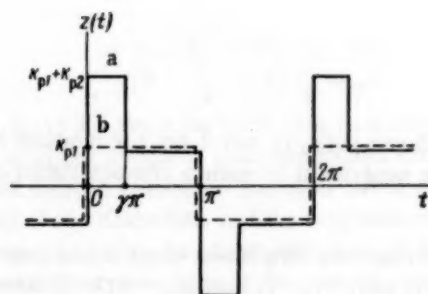


Fig. 7.

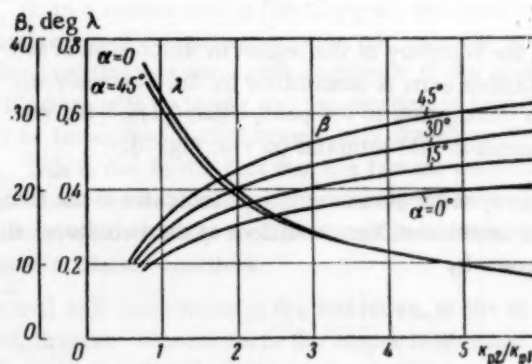


Fig. 8.



of the system is accomplished by the use of a special logical device which either permits or forbids switch-over, depending upon the previous situation. The structure and manner of realizing this logical device will be discussed below. We wish to note at once, however, that such a solution is useful only for a system with a floating grid which is quantized with respect to a level, since it is only in such a system that we can have a definite regulation process both before and after a passage through an extremum.

The region within which simple self-oscillations exist widens in this case to  $\alpha = -0.339$  for RSÉR with an extremum indicator based upon the deviation, and to  $\alpha = 0.168$  for an extremum indicator based upon the integral of the deviations (Fig. 3,  $\omega_0^*$  and  $\omega_{00}^*$ , respectively).

Further widening of the region in which self-oscillations exist for RSÉR may be obtained with the aid of so-called pulse stabilization, as outlined in the appendix of the articles on the usual operation of relay systems in papers [7, 8]. In contrast to [8], where a precise computation of the stabilization effect is made, we will make use of the approximate method of evaluating the effect, using as the basis of our computations the method of balancing the harmonics. In essence, harmonic stabilization consists in forcing the system to move in the direction of the extremum after a change in sign is obtained during scanning. This occurs due to a previous mutilation in the series of regular pulses  $z(t)$  at the regulator output, as shown in Fig. 7a. It is obvious that the first harmonic of the series in Fig. 7a leads the first harmonic of the series in Fig. 7b by a phase angle  $\beta$ . This leads us to the following method for determining the indices of periodic operation of the stabilized system: we use a method of computation which is similar to that outlined in Section 1, but we use a system of coordinates which is rotated by an angle  $\beta$  in the direction of the phase lead (Fig. 3).

The parameter  $\gamma$ —the relative duration of the corrective pulse—must, for the above-outlined reasons, be independent of the self-oscillation frequency; this can only be realized in systems with floating grid quantization. Actually, in order to obtain a corrective pulse in such a system after the passage through the extremum, we can make use of the fixation times of the allowed increments. For example, for RSÉR, due to the fact that  $(1 - \gamma)\pi$  of the half-period  $z(t)$  is equal to  $(\omega_k - \theta)$  of period  $\varphi_1(t)$ , we get

$$\gamma = 0.75 - \frac{\alpha}{2\pi}. \quad (11)$$

Having determined  $\gamma$ , we can compute  $\beta$  as the difference in the phase angles of the first harmonics in the expansion of the series shown in Fig. 7.

In Fig. 8 we show the family of  $\beta$  curves as functions of the relative values of the corrective impulse  $k_{p2}/k_{p1}$  (Fig. 7); the parameter of this family of curves

is  $\alpha$ . In Fig. 7, we also plot the curves for  $\lambda < 1$ , where  $\lambda$  is the transmission coefficient; we must take the value of  $\lambda$  into account in the regulatory circuit in order to maintain the same coefficient of amplification as for the unstabilized system.

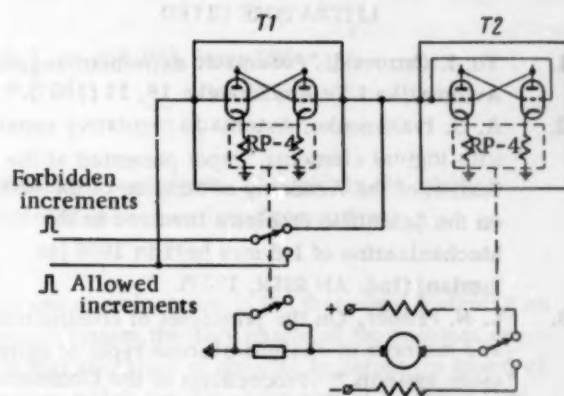


Fig. 9.

Let us examine the circuit of Fig. 9, which permits us to utilize both methods of increasing the self-oscillation frequency in RSÉR. At the input to the circuit, we apply the fixation impulses of the forbidden and allowed increments. The trigger T2 (with one symmetrical output) represents the output relay as in any extremum relay regulator. Trigger T1 (with two outputs) fulfills the following logical functions: 1) it forbids every second fixation pulse of the forbidden increment if it was not preceded by a fixation pulse of the allowed increment; 2) it permits a third fixation pulse of the forbidden increment even if an increment of the allowed fixation has not been received. As we can see from the circuit, the logical operation of the trigger T1 corresponds exactly to the requirement for the formation of a corrective pulse during pulse stabilization. In this manner, the circuit described above prevents repeated switchovers, maintains the system within the extremum region during false switchovers prior to the time that the extremum is reached, and generates a regular series of pulses, shown in Fig. 7a, independently of the absolute values of the self-oscillation frequencies of the system.

## SUMMARY

1. The limits of the region within which simple self-oscillations exist in relay SÉR for object units of any type have been determined.
2. We propose that, in order to increase the self-oscillation, use be made of corrective pulses and of measures which prevent repeated switchovers. The given circuit for the concrete realization of these methods for increasing the frequency is independent of the absolute value of the self-oscillation frequency.

3. We have shown that RSER with floating level grid quantization possess a more elastic structure, in the sense that they are more "self-regulating" under conditions in which the parameters of the regulated object change.

#### LITERATURE CITED

1. Yu. I. Ostrovskii, "Pneumatic extremum-regulator," *Avtomatika i Telemekhanika* **18**, 11 (1957).†
2. A. G. Ivakhnenko, "Automatic regulatory systems with logical elements," Paper presented at the Session of the Academy of Science of the USSR on the Scientific Problems Involved in the Mechanization of Industry held in 1956 [in Russian] (Izd. AN SSSR, 1957).
3. L. N. Filtner, "On the principles of construction and methods of analysis of some types of extremum systems," Proceedings of the Conference on the Theory and Application of Discrete Automatic Systems [in Russian] (Izd. AN SSSR, 1960).
4. V. V. Kazakevich, R. V. Kornilov, and N. G. Khristoforov, "Electronic extremum regulators," Proceedings of the Conference on the Theory and Application of Discrete Automatic Systems [in Russian] (Izd. AN SSSR, 1960).
5. I. S. Morosanov, "Computation of stable behavior in systems with extremum regulation with independent hunting," Proceedings of the Conference on the Theory and Application of Discrete Automatic Systems [in Russian] (Izd. AN SSSR, 1960).
6. V. V. Kazakevich, Theory of an Ideal Model of Extremum Regulation, *Avtomatika i Telemekhanika* **21**, 3 (1960).†
7. Ya. Z. Tsypkin, "Stabilization of automatic regulation relay systems," *Convegno sui problemi dell' automatismo* (Conference on Automation Problems), Milan, 1 (Consiglio Nazionale Delle Ricerche, Rome, 1958).
8. N. A. Korolev, "Pulse stabilization of automatic regulation relay systems," *Avtomatika i Telemekhanika* **18**, 5 (1957).†

† See English translation.

# CONTINUOUS EXTREMUM CONTROL SYSTEMS IN THE PRESENCE OF RANDOM NOISE

A. A. Pervozvanskii

Leningrad

Translated from *Avtomatika i Telemekhanika*, Vol. 21, No. 7, pp 958-963, July, 1960

Original article submitted December 14, 1959

The dynamics of one class of continuous systems of extremum control is investigated. The drift in the position of the extremum, and also the high frequency interference, are regarded as random functions of time.

The extremum control systems are viewed as working on the principle of proportional search. In contrast to discrete systems, the trial pulse is separated from the working action not in time but in the range of frequencies used. Such devices were first described in the book [1], where first attempts were also made to analyze their dynamic behavior, and also to provide qualitative estimates on the impact of random noise.

The block diagram of an extremum system of this type is shown in Fig. 1. The generator of the trial pulses delivers them in the form of a periodic function of time (it is usually either a sine or a square wave). The trial pulse is fed to the controlled object. As shown later, the amplitude of the fundamental harmonic component at the output of the controlled system is approximately proportional to the magnitude of the rate of change of the characteristic (that is, to the derivative of the function representing the dependence of the output on the input).

The magnitude of the indicated amplitude and, thus, of the rate of change obtained with the aid of a demodulator, can be regarded as an error signal of a typical control system; by using a controller the error is made to approach zero, i.e., to bring the system to the extremum point.

Thus, if the value of the rate of change is found:

$$k(x) = \frac{df}{dx},$$

then the motion of the control unit can be performed in accordance with the equation

$$\frac{dx}{dt} = \alpha k(x),$$

where  $\alpha > 0$  when the search is for a maximum, but  $\alpha < 0$  when it is for a minimum.

In view of the formulated conditions, the time constant

$\frac{1}{\alpha \frac{dk}{dx}}$  should be much less than the period

$2\pi/\omega_0$  of the trial pulses.

It was already shown in [1] that, when designing an extremum system, the very nature of the problem demands that two kinds of changes in output (or input) of the system which are not under control be taken into account: a) a slow drift — a gradual change of the characteristic, which includes the slipping away of the extremum point to be followed by the controller, and b) high-frequency disturbances.

If the former type is regarded as a useful signal (as the term is used in the theory of optimum filters), and if the controller is adjusted accordingly to provide optimum performance, the latter appears to be just interference in the controller which should be filtered out.

There is usually a frequency band between the frequencies of the drift and of the noise which, on the whole, is free from the uncontrollable changes. It seems natural that use should be made of this range in generating trial pulses. In actual practice, however, the band may be fairly narrow, and we shall see that the frequency thus selected for the trial signals will not be distinct enough from the frequencies of the useful signal and, in consequence, not distinct enough from the working frequencies of the controller, which is inadmissible.

In view of the above difficulties, objections were raised in [1] against such systems being widely used for practical purposes. Nevertheless, the basis of the working of an extremum controller, as described above, has some very important good points, the fundamental one being the comparative ease with which the search for an extremum dependent on several coordinates, when the working action is continuous (in time), can be realized (see, for example, its mathematical analysis in [2]). It is very important, therefore, from the practical point of view to be able to find an answer to the question as to whether the bandwidth of the testing signals is in fact limited only to the frequency band which is noise-free. When the noise is of a random character (this case is of particular interest as the noise localized at one frequency does not cause the above-mentioned difficulties), it should not, if properly filtered, exert a decisive influence on the working of the system even when the fre-



quency of the trial pulses is definitely within the noise band.

Let us examine an object such that the extremum of its characteristic is searched for changes only in one co-

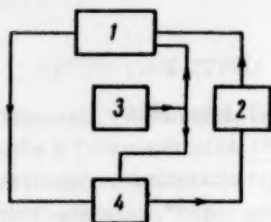


Fig. 1. 1) Object, 2) control unit, 3) generator of the trial pulses, 4) demodulator.

ordinate. Its idealized block-diagram given in Fig. 2a contains a linear dynamic input with transfer function  $\bar{K}_1(p)$  ( $p \equiv \frac{d}{dt}$ ), a nonlinear static element with characteristic  $y = f(x)$  which has a single extremum in the considered range, and the linear dynamic output with transfer function  $K_2(p)$ .

We assume that some external disturbances which it is not possible to control are acting both on the input ( $Z_1$ ) and on the output ( $Z_2$ ) of the object. Each disturbance is thought to consist of two components:

$$Z_1 = Z_{10} + Z_{11}, \quad Z_2 = Z_{20} + Z_{21}, \quad (1)$$

where the 0 subscript denotes the components which correspond to the slow drift (useful signal), the subscript 1 denotes the component corresponding to interference.\*

The components  $Z_{11}$  and  $Z_{21}$  can be represented in the form (see, for example, [3])

$$\begin{aligned} Z_{11} &= A_1 \sin \omega_0 t + B_1 \cos \omega_0 t, \\ Z_{21} &= A_2 \sin \omega_0 t + B_2 \cos \omega_0 t, \end{aligned} \quad (2)$$

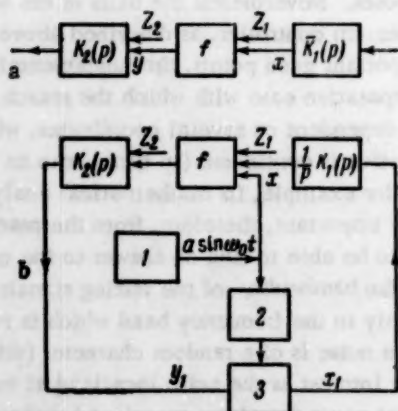


Fig. 2. 1) Generator of trial pulses, 2) phase-shifter, 3) demodulator.

where  $\omega_0$  is the frequency of the trial pulses;  $A_1, B_1, A_2, B_2$  are slowly varying random functions (compared with  $\sin \omega_0 t$ ) uncorrelated to one another (or to  $Z_{10}$  or  $Z_{20}$ ).

A signal proportional to the displacement of the workpiece (the working signal) and the trial disturbance  $a \sin \omega_0 t$  from the generator of the trial signals act on the input of the object. To simplify the matter, it is assumed that the trial pulse excites the input of the nonlinear block  $x$ . The transfer function of the workpiece is represented as  $1/p \bar{K}_1(p)$ , where the operator  $K_1(p)$  characterizes the dynamics of the operating device, as well as the characteristics of the auxiliary compensating networks. The latter, though not indispensable, are introduced in order to improve the dynamic properties of the system as a whole.

The output  $y_1$  of the object is fed to the demodulating device to determine the amplitude of the fundamental harmonic of the output signal.

An ideal demodulator operating on the basis of the relation

$$x_1 = b \frac{\omega_0}{\pi} \int_0^{\frac{2\pi}{\omega_0} + t} y_1 \sin(\omega_0 t + \varphi) dt, \quad (3)$$

is considered where the phase difference  $\varphi$  is introduced by means of a phase-shifter, the lag being due to the passing of the testing signal through the object, that is,

$$\varphi \approx \text{Arg } K_2(j\omega_0). \quad (4)$$

Other types of demodulating devices can be analyzed; for example, a device with synchronous filters [1, 2] where the product of the output and the testing signals  $y_1 b \sin(\omega_0 t + \varphi)$  is fed through a filter. However, with sufficiently efficient filtering of the higher harmonics, there is basically no fundamental difference between the latter device and the ideal demodulator.

With the assumptions as above, we show in Fig. 2b the whole scheme of the extremum control system; for the sake of simplicity, the notation  $K_1(p) = \bar{K}_1(p) \bar{K}_1(p)$  was introduced.

We now proceed to analyze the scheme. We expand the expression for the signal at the output of the nonlinear member:

$$y = f(x + Z_1 + a \sin \omega_0 t) + Z_2$$

into a Taylor's series about the point  $x + Z_{10}$ :

$$\begin{aligned} y &= Z_2 + f(x + Z_{10}) + \\ &+ f'(x + Z_{10}) [(A + a) \sin \omega_0 t + B_1 \cos \omega_0 t] + \dots \end{aligned} \quad (5)$$

\*It is obvious that the component  $Z_{20}$  (the drift either up or down of the characteristic) provides no useful information.



As the ideal demodulation takes place in successive members, it is possible from the start to retain in the formula for  $y$  only the terms with the fundamental frequency (with an accuracy up to the terms containing derivatives of the order higher than two). We thus obtain

$$y^* = A_2 \sin \omega_0 t + B_2 \cos \omega_0 t +$$

$$f'(x + Z_{10}) [(A_1 + a) \sin \omega_0 t + B_1 \cos \omega_0 t].$$

Should  $f(x)$  be a second-degree parabola

$$f(x) = -\frac{x^2}{2},$$

then

$$f'(x) = -x \quad (6)$$

and the quantity  $y^*$  proves linearly dependent on  $x$ .

We shall write down the transformation of the signal  $y^*$  after it has passed through the linear part of the characteristic of the object. We represent  $y^*$  as

$$\begin{aligned} y^* &= [A_2 + f'(x + Z_{10})(A_1 + a)] \sin \omega_0 t + \\ &+ [B_2 + f'(x + Z_{10})B_1] \cos \omega_0 t = \\ &= A_y \sin \omega_0 t + B_y \cos \omega_0 t. \end{aligned} \quad (7)$$

When a linear differential operator operates on the product of a harmonic function of time and an arbitrary function  $u(t)$ ,† we can write the result as

$$\begin{aligned} K_2(p) [u(t) \sin \omega_0 t] &= \sin \omega_0 t K_{21}(p) u(t) + \\ &+ \cos \omega_0 t K_{22}(p) u(t), \\ K_2(p) [u(t) \cos \omega_0 t] &= \cos \omega_0 t K_{21}(p) u(t) - \\ &- \sin \omega_0 t K_{22}(p) u(t), \end{aligned} \quad (8)$$

where

$$K_{21}(p) = \operatorname{Re} K_2(p + j\omega_0),$$

$$K_{22}(p) = \operatorname{Im} K_2(p + j\omega_0).$$

Hence,

$$\begin{aligned} y_1 &= \sin \omega_0 t [K_{21}(p) A_y - K_{22}(p) B_y] + \\ &+ \cos \omega_0 t [K_{22}(p) A_y + K_{21}(p) B_y] \end{aligned} \quad (9)$$

(only the fundamental frequency components are kept).

In view of the fact that the amplitude changes little within a period, we obtain, at the output of the demodulator,

$$\begin{aligned} x_1 &= b \{ [\cos \varphi K_{21}(p) + \sin \varphi K_{22}(p)] [A_2 + \\ &+ f'(x + Z_{10})(A_1 + a)] + \\ &+ [\sin \varphi K_{21}(p) - \cos \varphi K_{22}(p)] [B_2 + \\ &+ f'(x + Z_{10})B_1] \}. \end{aligned} \quad (10)$$

The equation of the closed-loop system, dependent on the "tracking error"  $\epsilon = x + Z_{10}$ , takes the form

$$\begin{aligned} \epsilon &= \frac{b}{p} K_1(p) \{ [\cos \varphi K_{21}(p) + \\ &+ \sin \varphi K_{22}(p)] [A_2 + f'(\epsilon)(A_1 + a)] + \\ &+ [\sin \varphi K_{21}(p) - \cos \varphi K_{22}(p)] [B_2 + \\ &+ f'(\epsilon)B_1] \} = Z_{10}. \end{aligned} \quad (11)$$

The obtained equation is nonlinear. Furthermore, when  $A_1, B_1 \neq 0$ , its coefficients are random functions of time; it proves impossible to analyze the equation in a general case.

We shall not consider (11) further (unless the high-frequency noise at the input of the object is absent). We shall then have to deal with an equation describing a system equivalent to a system which consists of one linear part and one nonlinear element  $f'(\epsilon)$ .

This can be investigated for arbitrary  $f(x)$  by the method of statistical linearization (see, for example, [4]).

Let  $M\{Z_{10}\} = M\{Z_{22}\} = 0$ ; then also  $M\{\epsilon\} = 0$ , and  $f'(\epsilon)$  is approximately equal to  $f'(\epsilon) = k(\sigma_\epsilon)\epsilon$ ,

where  $k(\sigma_\epsilon) = \frac{2}{\pi \sigma_\epsilon} \int_0^\infty f'(\epsilon) \psi(\epsilon) d\epsilon$ , and  $\psi(\epsilon) = \frac{1}{2\pi\sigma_\epsilon} \exp\left(-\frac{\epsilon^2}{2\sigma_\epsilon^2}\right)$  is the probability density of  $\epsilon$  (it

is assumed that  $\epsilon$  has a Gaussian distribution).

Equation (11) takes the form

$$\begin{aligned} &\left\{ 1 - \frac{ab}{p} K(\sigma_\epsilon) K_1(p) [\cos \varphi (K_{21}(p) - \right. \\ &- K_{22}(p)) + \sin \varphi (K_{21}(p) + K_{22}(p))] \} \epsilon = \\ &= Z_{10} + \frac{b}{p} K_1(p) \{ (\cos \varphi K_{21}(p) + \sin \varphi K_{22}(p)) A_2 + \\ &+ (\sin \varphi K_{21}(p) - \cos \varphi K_{22}(p)) B_2 \} \end{aligned} \quad (12)$$

or

$$\begin{aligned} \Phi(p)\epsilon &= Z_{10} + \Phi_1(p) A_2 + \\ &+ \Phi_2(p) B_2. \end{aligned}$$

†The above rules can be easily derived by using the Leibnitz formula.

One can obtain a formula for the variance of  $\epsilon$  by regarding the above as a linear equation

$$\sigma_{\epsilon}^2 = \frac{1}{2\pi} \int_{-\infty}^{\infty} \left\{ \frac{S_0(\omega)}{|\Phi(j\omega)|^2} + \frac{S_2(\omega) [|\Phi_1(j\omega)|^2 + |\Phi_2(j\omega)|^2]}{|\Phi(j\omega)|^2} \right\} d\omega, \quad (13)$$

where  $S_0(\omega)$  is the spectral density of  $Z_{10}$ , and  $S_2(\omega) = S_{A2}(\omega) = S_{B2}(\omega)$  are the spectral densities of the "amplitudes" of high-frequency noise.

When the expression  $S_{Z2}(\omega)$  for the spectrum of the noise itself is at one's disposal,  $S_2(\omega)$  is evaluated with the aid of the formula [3]

$$S_2(\omega) = \frac{2}{\pi} \int_0^{\infty} \cos \omega \tau d\tau \int_0^{\infty} S_{Z2}(\omega) \cos(\omega - \omega_0) \tau d\omega \quad (14)$$

We also notice that (13) can be simplified by making use of the formula

$$|\Phi_1(j\omega)|^2 + |\Phi_2(j\omega)|^2 = \{ |K_{21}(j\omega)|^2 + |K_{22}(j\omega)|^2 \} \frac{b^2}{\omega^2} |K_1(j\omega)|^2, \quad (15)$$

which can easily be obtained.

The integrals on the right-hand side of (13) have been tabulated (see, for example, [4]), and their values expressed directly in terms of the coefficients of the transfer functions  $K_1(p)$  and  $K_2(p)$ , the parameters which determine the spectral densities of the external disturbances, as well as by the linearization coefficient  $k(\sigma_{\epsilon})$ . When the integration has been performed, we see that (13) becomes an equation in  $\sigma_{\epsilon}$  which usually is solved graphically.

When  $f(x)$  represents the equation of the second-degree parabola,  $f(x) = -x^2/2$ , then Equation (11) becomes linear [ $k(\sigma_{\epsilon}) = -1$ ].

If the quantity  $1/T = ab$  is introduced (which actually gives the gain coefficient of the controlling device), it is then obvious that  $\sigma_{\epsilon}^2 = c_0 + c_1 (1/a^2)$ , where  $c_0$  and  $c_1$  are independent of the choice of the amplitude  $a$  of the testing signal.

It is advisable that the selection of the optimum value of  $a$  be in accordance with the condition for the minimum total error  $\Delta$ , which can be given, for example, by the expression

$$\Delta = a + 2\sigma_{\epsilon},$$

that is, in the form of a sum of systematic deviations due to the trial disturbance and of random deviations due to disturbances not under control. ••

As the first approximation, we have

$$a_{\text{opt}} = \sqrt[4]{4c_1}.$$

Some examples of the evaluation of systems are now given:

1. Let

$$K_1(p) = \frac{1}{T_1 p + 1}, \quad K_2(p) = 1, \quad \varphi = 0,$$

$$S_0(\omega) = \frac{\sigma_0^2 T_0}{T_0^2 \omega^2 + 1}, \quad S_2(\omega) = T_0 \sigma_a^2.$$

Then

$$\sigma_{\epsilon}^2 = \sigma_0^2 \frac{T_0(T_1 + T_0)}{T_0^2 + T(T_1 + T_0)} + \sigma_a^2 \frac{T_0}{2a^2 T^2},$$

$$a_{\text{opt}} \approx \sqrt[4]{\frac{2T_0}{a^2 T^2} \sigma_a^2}.$$

$$2. \text{ Let } K_1(p) = 1, \quad K_2(p) = \frac{1}{T_2 p + 1}, \quad \varphi = \text{Arg } K_2(j\omega).$$

The external acting forces are given by the same expression as in the first example.

Then

$$\sigma_{\epsilon}^2 = \sigma_0^2 \frac{T_0}{T_0^2} \frac{2T_2^2 c^4 + 2T_2 T_0 c^2 + 2T_2 T_0 c + T T_0}{T_2^2 c^4 + T_2 T_0 c^4 + T T_0 c^2 + T^2} +$$

$$+ \sigma_a^2 \frac{c T_0}{2a^2 T} \frac{2T_2 c^2 + T}{T_2 c^2 + T},$$

where

$$c = \cos \varphi = \frac{1}{\sqrt{1 + T_2^2 \omega^2}}.$$

The condition  $\omega \ll \omega_0$  was used in the calculations. Then [whatever the order of  $K_2(p)$ ]  $K_{21}(j\omega)$  and  $K_{22}(j\omega)$  can be represented by the formulas of the type  $(a_0 j\omega + a_1)/(b_0 j\omega + b_1)$ , that is, only the terms linear in  $\omega$  are retained in the numerator as well as in the denominator.

It is obvious that the methods described here can also be applied to analyze a more involved case, viz., to find the extremum of a function of several variables, in particular, when the construction of autocontrolled systems by the methods given in [2] is technically

‡It is advisable to assume in the calculations that, within the range of realizable frequencies,  $\omega \ll \omega_0$ .

•• But if one starts with the supposition that the quantity given is the coefficient  $b$ , then the optimum value of the amplitude  $a$  becomes different. In the examples given below, it is obvious that  $a_{\text{opt}} = 0$  ( $T = \infty$ ). This conclusion is in agreement with the one reached in [5, 6] for the case of a simpler discrete system where the magnitudes of the working and of the trial steps were assumed equal or proportional.

### LITERATURE CITED

1. Ch'ien Hsueh-sên, Technical Cybernetics [Russian translation] (IL, 1956).
2. A. A. Krasovskii, "The dynamics of continuous systems of extremum control based on the gradient method," Izd. Akad. Nauk SSSR, Otdel. Tech. Nauk, Avtomatika i Énergetika No. 3 (1959).

3. B. R. Levin, Theory of Random Processes with Applications to Radio (Izd. Sovetskoe Radio, 1957).
4. A. A. Fel'dbaum, "Steady-state processes in a simple discrete extremal system with random noise present," *Avtomat. i Telemekh.* 20, 8 (1959).††
5. A. A. Pervozvanskii, "Application of Markov chains to the evaluation of steady-state errors in extremum regulators," *Izv. Akad. Nauk, Otdel. Tech. Nauk* No. 3 (1960).

†† See English translation.

be written in the following form:

an inertial load at the system output. Equation (1) can

be written in the form (1), then, considering that there is only

one input in system (1), and  $u_1 = u_2 = u$ , we obtain

and  $u_1 = u_2 = u$  (function for the third and the fourth equa-

tions to the control, i.e., if we substitute  $u_1 = u_2 = u$  in

If we neglect the magnetic flux, the time axis

$$\begin{aligned} (3) \quad & M_{\pm}(z) = M_{\pm}(z) \frac{1}{z} = M_{\pm}(z) \frac{1}{z} = M_{\pm}(z) \frac{1}{z} \\ (4) \quad & (0 < z) \quad \frac{1}{z} = \frac{1}{z} + \frac{1}{z} = \frac{1}{z} + \frac{1}{z} \\ (5) \quad & (0 < z) \quad \frac{1}{z} = \frac{1}{z} + \frac{1}{z} = \frac{1}{z} + \frac{1}{z} \end{aligned}$$



# INVESTIGATION OF A SERVO SYSTEM WITH AN ELECTROMAGNETIC INDUCTION CLUTCH WHICH OPERATES WITH LOW-NULL CURRENTS

P. F. Klubnikin

Moscow

Translated from *Avtomatika i Telemekhanika*, Vol. 21, No. 7, pp 964-972, July, 1960

Original article submitted November 18, 1959

In this article, we analyze a servosystem where a reversible electromagnetic induction clutch which operates with low null currents is used. A method of increasing the stability margin of such a system is considered. The experimental results are also given.

At the present time, reversible electromagnetic clutch drives are used to an ever-increasing extent in automatic control systems [1]. The reasons for this are that their design is simple and that they have good dynamic properties. For instance, a clutch drive has a minimum number of parts in the system, a minimum weight per given output power, it can be linked in a simple manner with a semiconductor amplifier, etc.

It is known [1] that, for the normal operation of an automatic control system which has an induction clutch drive, so-called null currents, which must not fall below a certain given magnitude, are transmitted through the clutch control windings. An attempt to reduce the null currents leads to unstable operation of the system, since, apart from other effects, the drive characteristics become nonlinear.

In servosystems, the presence of large null currents in the clutch control windings results in superfluous energy losses, which cause the heating of parts. Therefore, it is desirable to reduce the null currents to a minimum. In this article, we shall investigate a servosystem with an induction clutch operating with low null currents. We shall also explore the possibility of increasing the system stability margin.

## 1. Operational Characteristics of a Servo-system with Small Clutch Null Currents

On the basis of the clutch motion equations [1], for the servosystem illustrated in Fig. 1, we have the following system of equations:

$$\begin{aligned} I \frac{d\theta}{dt} &= M_{to} - M_l \\ M_{to} &= C_0 [(B_1^2 - B_2^2) n_0 - \theta (B_1^2 + B_2^2)], \\ F_1 \left( B_1, \frac{dB_1}{dt}, \dots, i_1, \frac{di_1}{dt}, \dots \right) &= 0, \\ F_2 \left( B_2, \frac{dB_2}{dt}, \dots, i_2, \frac{di_2}{dt}, \dots \right) &= 0, \\ T_1 \frac{di_1}{dt} + i_1 &= k_a \varphi'(\varepsilon) + i_0, \end{aligned}$$

$$\begin{aligned} T_2 \frac{di_2}{dt} + i_2 &= k_a \varphi'(-\varepsilon) + i_0, \\ \varepsilon &= k_T (E - \theta), \end{aligned} \quad (1)$$

where  $\theta$  is the angular velocity of the clutch output shaft,  $I$  is the clutch rotor moment of inertia,  $M_{to}$  is the clutch shaft torque,  $M_l$  is the loading moment,  $C_0$  is the proportionality coefficient [1],  $B_1$  and  $B_2$  are the values of magnetic induction in the air gaps of the first and the second electromagnet, respectively,  $i_1$  and  $i_2$  are the currents in the control windings,  $T_1$  and  $T_2$  are the coefficients which depend on the control windings inductance,  $k_a$  is the amplifier amplification factor,  $i_0$  is the null current intensity in the control windings,  $\varepsilon$  is the amplifier input voltage,  $E$  is the voltage supplied to the system input, and  $n_0$  is the turning speed of the clutch electromagnets.

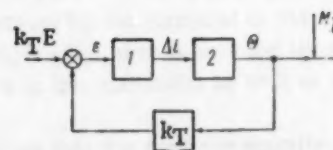


Fig. 1. 1) Amplifier; 2) clutch drive.

If we neglect the magnetic flux rise time with respect to the current, i.e., if we substitute the  $B_1 = f_1(i_1)$  and  $B_2 = f_2(i_2)$  functions for the third and the fourth equations in system (1), then, considering that there is only an inertial load at the system output, Equations (1) can be written in the following form:

$$\begin{aligned} I_1 \frac{d\theta}{dt} &= M_1 - M_2 - \frac{0}{n_0} (M_1 + M_2), \quad M = f(i), \\ T_1 \frac{di_1}{dt} + i_1 &= k_a \varphi'(\varepsilon) + i_0 \quad (i_1 > 0) \\ T_2 \frac{di_2}{dt} + i_2 &= k_a \varphi'(-\varepsilon) + i_0 \quad (i_2 > 0), \quad \varepsilon = k_T (E - \theta). \end{aligned} \quad (2)$$



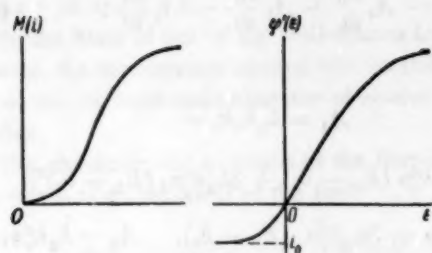


Fig. 2.

Here  $I_1 = I + I_L r^2$ ,  $I_L$  is the load moment of inertia,  $r$  is the reductor gear ratio, and  $M_1$  and  $M_2$  are the moments acting on the rotor due to the first and the second electromagnets.

The approximate shape of the  $M=f(i)$  and  $i=\varphi'(\epsilon)$  functions is shown in Fig. 2.

We shall denote:  $M_1 - M_2 = f_1(\Delta i)$ , and  $M_1 + M_2 = f_2(\Delta i)$ , where  $\Delta i = i_1 - i_2$ . The approximate shapes of the  $f_1(\Delta i)$  and  $f_2(\Delta i)$  functions are shown in Fig. 3.

Then, assuming that  $T_{1,2} = \text{const}$ , after elementary transformations (2), we obtain

$$\begin{aligned} \frac{I_1}{f_2(\Delta i)} \frac{d\theta}{dt} + \theta &= n_0 \frac{f_1(\Delta i)}{f_2(\Delta i)}, \\ T_1 T_2 \frac{d^2 \Delta i}{dt^2} + (T_1 + T_2) \frac{d \Delta i}{dt} + \Delta i &= \\ &= k_a \varphi(\epsilon) + k_a \frac{T_1 + T_2}{2} \frac{d \varphi(\epsilon)}{dt} + k_a \frac{T_2 - T_1}{2} \frac{d \varphi''(\epsilon)}{dt}, \\ \epsilon &= k_T (E - \theta), \end{aligned} \quad (3)$$

where

$$\varphi(\epsilon) = \varphi'(\epsilon) - \varphi'(-\epsilon), \quad \varphi''(\epsilon) = \varphi'(\epsilon) + \varphi'(-\epsilon).$$

Thus, a servosystem of the simplest form with small null currents in the clutch control windings is described by a nonlinear system of equations with variable coefficients (3). It is important to note that the coefficient in front of the derivative  $\theta$  in the first equation of system (3) changes considerably if  $\Delta i$  varies.

Its maximum value is equal to  $T_{\max} = \frac{I_1 n_0}{2M_0(i_0)}$ , i.e., it is completely determined by the null current  $i_0$  magnitude. For instance, for  $i_0 \rightarrow 0$ ,  $T_{\max} \rightarrow \infty$ . In the latter case, the system of equations (1) assumes the form

$$\begin{aligned} I \frac{d\theta}{dt} &= M_{t0} - M_t \\ M_t &= C_0(n_0 - \theta) B^2 \text{sign } \epsilon, \\ F\left(B, \frac{dB}{dt}, \dots, i, \frac{di}{dt}, \dots\right) &= 0, \\ T_1 \frac{di_1}{dt} + i_1 &= k_a \varphi(\epsilon) \quad \left(\text{for } \frac{d\epsilon}{dt} > 0\right), \\ T_2 \frac{di_2}{dt} + i_2 &= k_a \varphi(\epsilon) \quad \left(\text{for } \frac{d\epsilon}{dt} < 0\right), \\ \epsilon &= k_T (E - \theta). \end{aligned} \quad (4)$$

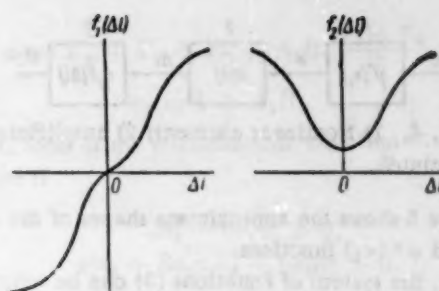


Fig. 3.

The analysis of this system of equations is more complicated than the analysis of system (3).

Practice shows that the basic problem which has to be solved if the clutch is to operate with small null currents is the problem of securing the system stability.

The investigation of the servosystem stability by using Equations (3) or (4) is a rather complicated problem. An attempt to solve this equation by introducing a number of simplifying assumptions leads to contradiction with regard to the results obtained in experimental investigation of such systems.

In connection with the above-mentioned, one important fact should be emphasized. It is not at all necessary to reduce the null currents to zero.

Energy balance calculations show that the losses due to small null currents (for instance, constituting 10 to 15% of the maximum currents) are very small and entirely admissible even in servosystems. On the other hand, a reduction of null currents to zero complicates the system stabilization and its design to a considerable extent, since the more complicated system of Equations (4) has to be investigated in this case.

Finally, by using the general motion stability theory it is also in this case possible, in principle, to select system parameters for which the system is stable; however, large amplification factors cannot be thereby secured and, consequently, the system accuracy will be low.

Let us consider one of the methods for increasing the system stability margin for small null currents — the method of compensating the nonlinear characteristics.

## 2. The Method of Increasing the System Stability Margin for Small Null Currents

Let us introduce an additional inertialess link with the characteristic  $\varphi^*(\epsilon_1)$  in the servosystem chain, as is shown in Fig. 4. Let the  $\varphi^*(\epsilon_1)$  function be such that the following condition is satisfied:

$$0 = n_0 F(k_a \varphi^*[\varphi^*(\epsilon_1)]) = n_0 a \epsilon_1, \quad (5)$$

where

$$F(\Delta i) = \frac{f_1(\Delta i)}{f_2(\Delta i)}.$$

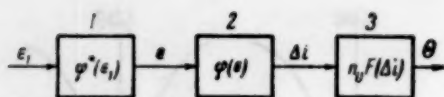


Fig. 4. 1) Nonlinear element; 2) amplifier; 3) clutch.

Figure 5 shows the approximate shapes of the  $\varphi(\epsilon)$ ,  $F(\Delta i)$ , and  $\varphi^*(\epsilon_1)$  functions.

Then, the system of Equations (3) can be written in the following form\*:

$$\begin{aligned} \frac{T_1}{f_2(\Delta i)} \frac{d\theta}{dt} + \theta &= n_0 F(\Delta i), \\ T_1 T_2 \frac{d^2 \Delta i}{dt^2} + (T_1 + T_2) \frac{d\Delta i}{dt} + \Delta i &= \\ &= k_a \varphi_1(\epsilon_1) + k_a \frac{T_1 + T_2}{2} \frac{d\varphi_1(\epsilon_1)}{dt}, \\ \epsilon_1 &= k_r (E - \theta), \end{aligned} \quad (6)$$

where  $\varphi_1(\epsilon_1) = \varphi[\varphi^*(\epsilon_1)]$ .

The system of Equations (6) differs from the system (3) by the form of the current difference  $\Delta i$  vs. error curve.

We shall investigate the stability of a servosystem with an additional link in the case where condition (5) is satisfied.

By expanding the  $F(\Delta i)$  and  $\varphi_1(\epsilon_1)$  functions into the power series

$$\begin{aligned} F(\Delta i) &= \\ &= k_2 \Delta i + k_3 \Delta i^2 + k_4 \Delta i^3 + \dots, \quad \varphi_1(\epsilon_1) = \\ &= k_1 \epsilon_1 + \alpha \epsilon_1^2 + \alpha_2 \epsilon_1^3 + \dots \end{aligned}$$

and by substituting them in (6) while neglecting the fourth and the subsequent terms, we obtain

$$\begin{aligned} T^*(\Delta i) \frac{d\theta}{dt} + \theta &= n_0 k_2 \Delta i + n_0 k_3 \Delta i^2 + n_0 k_4 \Delta i^3, \\ T_1 T_2 \frac{d^2 \Delta i}{dt^2} + (T_1 + T_2) \frac{d\Delta i}{dt} + \Delta i &= \\ &= k_a k_1 \epsilon_1 + k_a \alpha \epsilon_1^2 + k_a \alpha_2 \epsilon_1^3 + \\ &+ k_a \frac{T_1 + T_2}{2} (k_1 + 2\alpha \epsilon_1 + 3\alpha_2 \epsilon_1^2) \frac{d\epsilon_1}{dt}, \\ \epsilon_1 &= k_r (E - \theta), \end{aligned} \quad (7)$$

where  $T^*(\Delta i) = I_1 n_0 / f_2(\Delta i)$ .

Let us apply to the system a constant action  $E_0$ . Then, according to (7), the equations for the servosystem stimulated motion will be of the following form:

$$\begin{aligned} T^*(\Delta i) \frac{d\theta}{dt} + \theta &= B_1 \Delta i + B_2 \Delta i^2 + B_3 \Delta i^3, \\ T_1 T_2 \frac{d^2 \Delta i}{dt^2} + (T_1 + T_2) \frac{d\Delta i}{dt} + \Delta i &= \\ &= -A_1 \theta + A_2 \theta^2 - A_3 \theta^3 - \end{aligned}$$

$$-A_4 \frac{d\theta}{dt} + A_5 \frac{d^2 \theta}{dt^2} - A_6 \frac{d^3 \theta}{dt^3}, \quad (8)$$

where

$$\begin{aligned} A_1 &= k_a k_1 k_r + \\ &+ 2k_a k_r^2 \alpha (E_0 - \theta_0) + 3k_a k_r^3 \alpha_1 (E_0 - \theta_0)^2, \\ A_2 &= k_a k_r^2 \alpha + 3k_a k_r^3 \alpha_1 (E_0 - \theta_0), \quad A_3 = k_a k_r^3 \alpha_1, \\ A_4 &= A_1 \frac{T_1 + T_2}{2}, \\ A_5 &= A_2 \frac{T_1 + T_2}{2}, \quad A_6 = A_3 \frac{T_1 + T_2}{2}, \\ B_1 &= n_0 k_2 + 2n_0 k_3 \Delta i_0 + 3n_0 k_4 \Delta i_0^2, \\ B_2 &= n_0 k_3 + 3n_0 k_4 \Delta i_0, \quad B_3 = n_0 k_4. \end{aligned}$$

Here,  $\theta_0$  and  $\Delta i_0$  are the respective steady-state values of the angular velocity and the current difference at the system output, or the particular solutions of (8).

The  $T^*(\Delta i)$  function can be well approximated by the relation

$$T^*(\Delta i) = \frac{T_0 + \alpha_2 \Delta i^2}{1 + \alpha_3 \Delta i^2},$$

where  $T_0$ ,  $\alpha_2$ , and  $\alpha_3$  are constant coefficients.

In stability investigation, we shall use the methods of the Lyapunov general theory of motion stability [3].

Let us consider the first approximation of the system of Equations (8). After reduction to the normal Cauchy form, we obtain:

$$\begin{aligned} \frac{dx}{dt} &= z, \quad \frac{dy}{dt} = \frac{B_1}{T_0} x - \frac{1}{T_0} y, \\ \frac{dz}{dt} &= -\left(\frac{1}{T_1 T_2} + \frac{A_4 B_1}{T_0 T_1 T_2}\right) x + \\ &+ \left(\frac{A_4}{T_0 T_1 T_2} - \frac{A_1}{T_1 T_2}\right) y - \frac{T_1 + T_2}{T_1 T_2} z, \end{aligned} \quad (9)$$

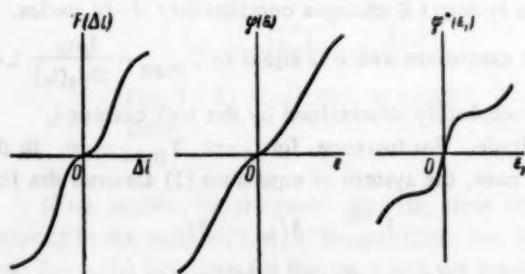


Fig. 5.

\*In order to simplify calculations, the last term of the second equation in (3) is assumed to be equal to zero, since the magnitudes of  $T_1$  and  $T_2$  differ little from each other, and  $d\varphi(\epsilon)/dt \gg d\varphi^*(\epsilon)/dt$ . It can be shown that the retention of this term would not affect the results to be obtained later.

where  $x = \Delta i$  and  $y = \theta$ .

On the basis of one of the well-known Lyapunov theorems, the servosystem motion will be stable if all roots of the characteristic equation of system (9) are negative.

The characteristic equation of the first-approximation system of equations is of the form

$$a_0 p^3 + a_1 p^2 + a_2 p + a_3 = 0,$$

where

$$a_0 = T_0 T_1 T_2, \quad a_1 = T_1 T_2 + T_0 T_1 + T_0 T_2,$$

$$\begin{aligned} (T_1 T_2 + T_0 T_1 + T_0 T_2)^2 - 3 T_0 T_1 T_2 \left[ T_0 + T_1 + T_2 + \frac{1}{2} (T_1 + T_2) A_1 B_1 \right] &> 0, \\ (T_1 T_2 + T_0 T_1 + T_0 T_2)^2 \left[ T_0 + T_1 + T_2 + \frac{1}{2} (T_1 + T_2) A_1 B_1 \right] + 3 T_0 T_1 T_2 (T_1 T_2 + \\ + T_0 T_1 + T_0 T_2) (1 + A_1 B_1) - 6 T_0 T_1 T_2 \left[ T_0 + T_1 + T_2 + \frac{1}{2} (T_1 + T_2) A_1 B_1 \right]^2 &> 0. \end{aligned} \quad (11)$$

An analysis of inequalities (11) shows that the  $A_1 B_1$  product must be a sufficiently small quantity (positive or negative) if these inequalities are to be satisfied. For instance, for  $T_0 = 0.15$ ,  $T_1 = 0.05$ , and  $T_2 = 0.01$ , the system will be stable if the product  $A_1 B_1$  value lies in the  $-3 < A_1 B_1 < 1$  interval.

We shall determine the conditions for the smallness of the  $A_1 B_1$  value by developing the expression for this product:

$$\begin{aligned} A_1 B_1 = & \\ = & k_{\alpha} k_1 k_2 k_3 n_0 + k_{\alpha} k_1 k_2 (2 n_0 k_3 \Delta i_0 + 3 n_0 k_4 \Delta i_0^2) + \\ + & 2 \alpha k_{\alpha} k_2^2 (E_0 - \theta_0) (k_2 n_0 + 2 n_0 k_3 \Delta i_0 + 3 n_0 k_4 \Delta i_0^2) + \\ + & 3 \alpha_1 k_{\alpha} k_2^3 (E_0 - \theta_0)^2 (k_2 n_0 + 2 n_0 k_3 \Delta i_0 + 3 n_0 k_4 \Delta i_0^2). \end{aligned} \quad (12)$$

It is obvious from expression (12) that the value of  $A_1 B_1$  can be small only if the  $\alpha$  and  $\alpha_1$  coefficients are negative. Actually, the values of  $\Delta i_0$  and  $E_0 - \theta_0$  are positive.† The  $k_3$  coefficient is also positive, which can be readily demonstrated if we consider the character of the  $F(\Delta i)$  function (Fig. 5). The  $k_4$  coefficient can be negative; however, it has a small value. Therefore, the terms in brackets in (12) in the operating range of  $\Delta i$  variations are positive. The first term in (12), which represents the amplification factor of an open linearized system for  $E_0 = 0$ , has a comparatively large value (it is usually equal to 500-1000 and over). Consequently, the value of the  $A_1 B_1$  product can be reduced only by considering the last two terms in (12) for negative values of  $\alpha$  and  $\alpha_1$ , ‡ i.e., only if the  $\varphi^*(\epsilon_1)$  function is defined.

It can be readily shown that the necessary form of the  $\varphi^*(\epsilon_1)$  function, for which the  $\alpha$  coefficient is negative, can be obtained by satisfying condition (5).

$$\begin{aligned} a_2 &= T_0 + T_1 + T_2 + A_1 B_1 \frac{T_1 + T_2}{2}, \\ a_3 &= 1 + A_1 B_1. \end{aligned}$$

All roots of the characteristic equation will be negative if

$$\begin{aligned} 2a_1^2 - 6a_0 a_2 &> 0, \\ a_1^2 a_2 + 3a_0 a_1 a_3 - 6a_0 a_2^2 &> 0. \end{aligned} \quad (10)$$

By substituting the values of the characteristic equation coefficients in (10), we obtain

The condition (5) will be called the condition for the linear compensation of the clutch static characteristic.

Actually, it can be seen from Fig. 5 that the series obtained by expanding the  $\varphi^*(\epsilon_1)$  function must have a negative sign in front of the second term, i.e.,

$$\varphi^*(\epsilon_1) = r_1 \epsilon_1 - r_2 \epsilon_1^2 + \dots \quad (13)$$

This follows also from the manner of composing the  $\varphi^*(\epsilon_1)$  function, which can be written in the following form:

$$\varphi_1^*(\epsilon_1) = \epsilon_{12} + \left[ \epsilon(\theta_1) - \frac{\theta_1}{n_0 a} \right],$$

where  $\theta_1$  is the fixed value of the  $\theta(\epsilon)$  function, and  $\epsilon_{12}$  is the corresponding value of  $\epsilon$ .

Then, by writing the function which approximates the amplifier characteristic in the form

$$\varphi(\epsilon) = k_{\alpha} \epsilon + k_y \epsilon^2 + \dots$$

and substituting here the value of  $\epsilon$  from (13), we obtain

$$\begin{aligned} \varphi_1(\epsilon_1) = & \\ = & k_{\alpha} r_1 \epsilon_1 - (k_{\alpha} r_2 - k_{\alpha} r_1^2) \epsilon_1^2 - 2 k_{\alpha} r_1 r_2 \epsilon_1^3 + \dots \end{aligned} \quad (14)$$

† Obviously, due to the symmetry of the clutch characteristics for a negative signal at the system input, this remains valid if Equations (8) are composed with respect to the negative increment.

‡ The  $\alpha_1$  coefficient can also be positive. This depends on the actual system parameter values.



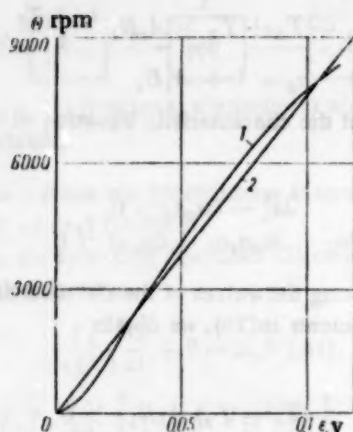


Fig. 6.

Under the condition where  $k_{a1}r_2 > k_{a1}i_0^2$ , which can always be satisfied, the signs in front of the second and the third terms in series (14), which correspond to terms with  $\alpha$  and  $\alpha_1$ , are negative.

Thus, it follows from the above that a linear compensation of the clutch static characteristic provides the possibility of increasing the stability margin of a servo-system with a clutch operating with small null currents. This is confirmed by experiments, the results of which are presented below.

### 3. Experimental Results

The experiments were performed with a drive which had the following parameters: rotor radius: 26 mm; rotor thickness: 0.5 mm; rotor moment of inertia:  $I = 0.07 \text{ g-cm-sec}^2$ ; maximum ampere-turns in the control winding: 550 a. t.; the number of poles in the spider: 6; angular velocity of electromagnet poles:  $n_0 = 11,800 \text{ rpm}$ ; the maximum output shaft torque:  $M_{to} \approx 3 \text{ kg-cm}$ ; the maximum output shaft power: 100 w.

The clutch operation was regulated by means of an electronic amplifier (the maximum control current: 100 ma). In order to simplify the experiments, the  $\varphi^*(\epsilon_1)$  function was reproduced by means of a standard KNB nonlinear electronic unit.

It should be noted that the practical realization of the  $\varphi^*(\epsilon_1)$  function in the system does not require a special unit; it can be secured by using nonlinear resistors, for instance, thyrites, which are connected to the input of the amplifier which controls the clutch. This is especially easy to arrange in the case where amplifiers based on semiconductor elements are used.

Figure 6 shows the dependences of the clutch output shaft speed on the amplifier voltage (1) before and (2) after compensation of the characteristic for  $i_0 = 0.08i_{\max}$ .

Figure 7 shows the frequency characteristics of a closed system (the relative amplitude  $A_0/A_{00}$ , where  $A_{00}$  is the input voltage amplitude and  $A_0$  is the velocity amplitude at the system output, and the phase  $\beta$ ) for

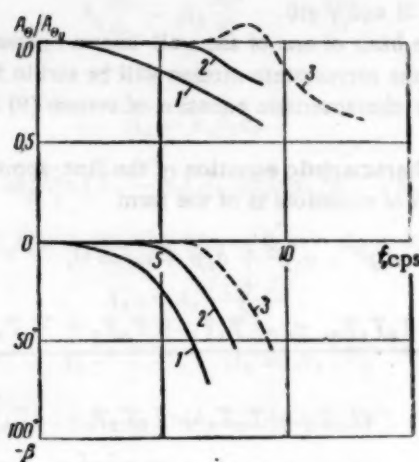


Fig. 7.

$i_0 = 0.08i_{\max}$  when the nonlinear element is absent (curves 1) and when the nonlinear element is present (curves 2). For the sake of comparison, system characteristics for normal (large) null currents  $i_0 = 0.32i_{\max}$  (curves 3) are shown by dotted lines in the same figure. In all cases, the  $k = k_a k_1 k_2 k_T n_0$  coefficient was chosen in such a manner that the system was stable for any input signals; it was equal to 36.4, 118, and 1500, respectively. The frequency characteristics were plotted for the large input signal  $\theta_0 = 0.5\theta_{\max} = 4710 \text{ rpm}$ .

It is obvious from Fig. 7 that the application of linear compensation of the clutch characteristics makes it possible to increase the system stability margin and, consequently, to increase its accuracy for small null currents.

As was to be expected on the basis of the above theoretical investigation, experiments showed that, for small null currents, the system stability is disturbed only when a voltage  $E$  is supplied to the system input, and it depends only on the magnitude of this voltage (i.e., on the value of  $A_1 B_1$ ). This causes the appearance of self-oscillations in the control currents which lead to their simultaneous rise. This is illustrated by the oscillograms shown in Fig. 8.

The oscillations which appear in the system if its stability is disturbed are of a complicated character, and they should be studied separately.

It should be noted that the system efficiency is not affected if it is unstable in the above sense; however, the energy loss arising in this causes rapid heating in clutch drives with a power of over 100 w, and, therefore, unstable system operating conditions are inadmissible.

### SUMMARY

1. A servosystem where a drive with a reversible electromagnetic induction clutch which operates with small null currents [ $i = (0.02-0.08)i_{\max}$ ] is used is described by a system of nonlinear differential equations with variable constants. The over-all amplification factor of a linearized system for which a stable system



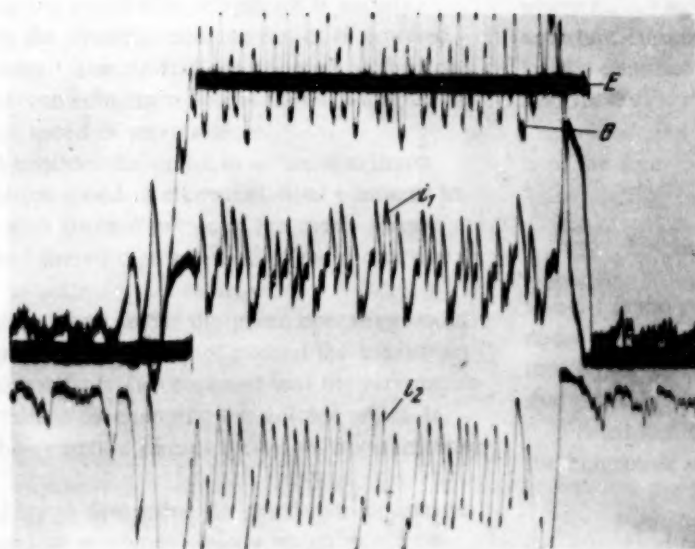
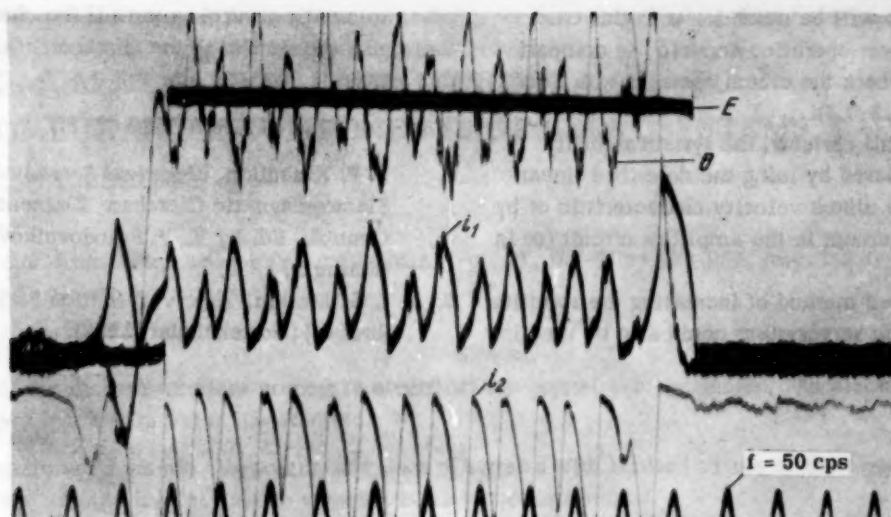
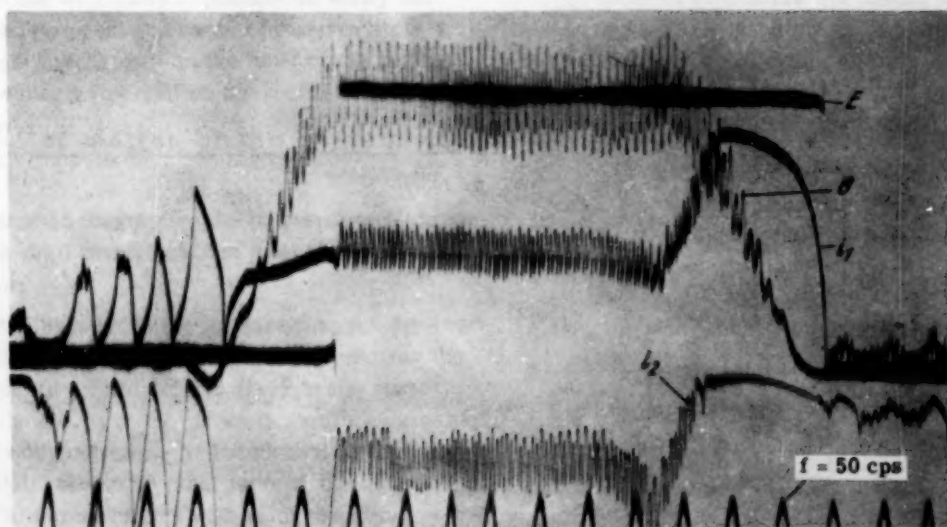


Fig. 8.



operation is possible will be much lower in this case, which leads to a lower operation accuracy in comparison with a system where the clutch operates with large null currents [ $i = (0.2-0.3)I_{max}$ ].

2. For small null currents, the system stability margin can be increased by using the described linear compensation of the clutch velocity characteristic or by using a nonlinear element in the amplifier circuit (or in the amplifier itself).

3. The described method of increasing the stability margin of a nonlinear servosystem could also be used in

other automatic control systems if the characteristics of their units are similar to the characteristics described in this article.

#### LITERATURE CITED

1. P. F. Klubnikin, Electrical Servomechanisms with Electromagnetic Clutches. Elements of Automatic Control. Ed. by V. V. Solodovnikov [in Russian] (Mashgiz, 1958) 2.
2. I. G. Malkin, Theory of Motion Stability [in Russian] (Gostekhizdat, 1952).

# THE MAXIMUM DYNAMIC CHARACTERISTIC VALUES OF SERVOMECHANISM COMPONENTS OF SERVO SYSTEMS. I

G. A. Nadzhafova

Moscow

Translated from *Avtomatika i Telemekhanika*, Vol. 21, No. 7, pp 973-981, July, 1960

Original article submitted April 1, 1960

The problem of the shortest transient process in electrical servosystems is considered. An electric dc servomechanism with independent excitation is investigated.

The maximum dynamic characteristic values of systems with limited values of the torque, the angular velocity, and the voltage supplied to the servomechanism are determined.

The operation speed of servosystems is mainly determined by the dynamic characteristics of powered servomechanisms. The limitations imposed on the coordinates of servomechanisms do not permit an arbitrary increase in the speed of servosystems.

We shall consider the problem of the maximum possible operation speed of electrical final elements in servosystems with limited values of the motor torque, the motor rpm, and the voltage supplied to the motor armature.

It is assumed that, under the given operating conditions, the motor heating does not exceed the maximum allowable values. It is also assumed that the servomechanism is controlled by changing the voltage which is supplied to the armature circuit for a constant excitation flux.

We shall try to determine the maximum operation speed of electrical servomechanisms which would be compatible with the limitations imposed on the system. These evaluations will make it possible to verify the maximum possible operation speed of a servosystem or to select a final mechanism on the basis of the technological requirements imposed on the servosystem.

## 1. Equation of Motion of the Servomechanism

The schematic diagram of the servosystem is shown in Fig. 1. We shall investigate the power-controlled electric motor.

In order to investigate the servomechanism dynamic characteristics, we must know the equation relating the monitoring quantity - the voltage  $U_A$  - to the output shaft rotation angle  $\alpha_2$  or  $\alpha_1$ . If we neglect the armature reaction, the eddy currents, the inductance in the motor armature circuit, and some other factors, the equation of the motor armature circuit will be of the form

$$U_A - E_{\text{mot}} = I_A R_A \quad (1)$$

where  $E_{\text{mot}} = k_e \Phi \omega_1$  is the motor counter-emf,  $I_A$  is the armature current,  $R_A$  is the armature winding resistance,  $k_e$  is a constant coefficient, and  $\Phi$  is the motor excitation flux.

The equation of motion of the electric motor shaft is of the form

$$I \frac{d\omega_1}{dt} = M_{\text{mot}} - M_L \quad \text{or} \quad I \frac{d^2\alpha_1}{dt^2} = M_{\text{mot}} - M_L \quad (2)$$

where  $I$  is the motor and load moment of inertia, reduced to the motor shaft,  $M_{\text{mot}} = k_m \Phi I_A$  is the motor torque,  $M_L$  is the load moment, reduced to the motor shaft, and  $k_m$  is a constant coefficient.

From Eqs. (1) and (2), we obtain the equation for the controlled servomechanism in the following form:

$$I \frac{d^2\alpha_1}{dt^2} + \frac{k_e k_m \Phi^2}{R_A} \frac{d\alpha_1}{dt} = \frac{k_m \Phi}{R_A} U_A - M_L \quad (3)$$

In order to generalize the obtained results, we shall represent Eq. (3) in a system of dimensionless coordinates by introducing the following relative quantities:

$\alpha_1 - \alpha_{\text{ass}} / \alpha_{\text{bas}} = x$  is the deviation of the motor shaft rotation angle from the assigned value,  $\omega_1 - \omega_{\text{ass}} / \omega_{\text{bas}} =$

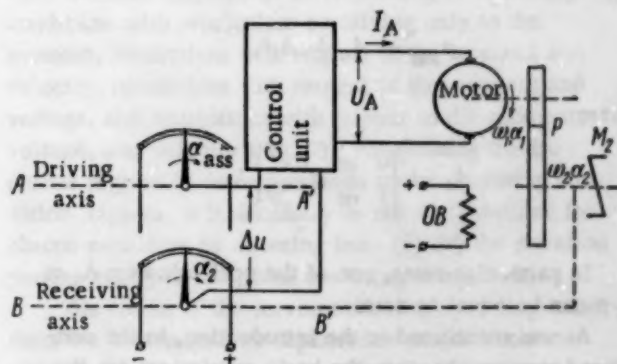


Fig. 1.



$\gamma$  is the deviation of the motor angular velocity from the assigned value,  $U_A/U_{A\text{bas}} = u$  is the control voltage,  $I_A/I_{A\text{bas}} = i_A$  is the armature current,  $I_L/I_{A\text{bas}} = i_L$  is the load current ( $I_L = M_L/k_m \Phi$ ),  $\omega_{\text{ass}}/\omega_{\text{bas}} = \varphi$  is the rate of change in the driving action  $\alpha_{\text{ass}}$ , and  $t/T_{\text{bas}} = \tau$  is the dimensionless time.

For the basic quantities, we shall use: the nominal voltage, the short-circuit motor current, the boundary velocity, and the drive electromechanical and angular constants, which are equal to

$$T_{\text{bas}} = \frac{I_{\text{bas}}}{k_m \Phi I_{A\text{bas}}} = \frac{GD^2 n_0}{375 M_{\text{sc}}}, \quad \alpha_{\text{bas}} = T_{\text{bas}} \omega_{\text{bas}}$$

Let us write the equations of motion (3) and (2) for the accepted type of driving actions in terms of dimensionless quantities:

$$\frac{d^2 x}{d\tau^2} + \frac{dx}{d\tau} = u - i_L - \varphi, \quad (4)$$

$$\frac{d^2 x}{d\tau^2} = i_A - i_L, \quad \frac{dx}{d\tau} = y. \quad (5)$$

The considered types of driving actions are given below.

## 2. Characteristics of Loads, Driving Actions, and Restrictions

In the majority of cases, servosystems are either not loaded with the static resistance moment, when they have to overcome only the load inertia forces, or they are loaded with resistance moments, which are due either to the overbalancing load or to dry friction forces.

In connection with this, in the first part of this paper, we shall consider the inertial forces ( $I \neq 0$  and  $M_L = 0$ ) and the constant resistance moment ( $I \neq 0$  and  $M_L = \text{const}$ ) as loads reduced to the motor shaft.

The behavior of a system loaded with inertial forces and the dry friction moment ( $I \neq 0$  and  $M_L = M_T \sin \omega$ ) will be investigated in the second part of this article.

For the driving actions, we shall use the actions defined by a class of reproducible functions of the following form:

$$\alpha_{\text{ass}} = A_0 + A_1 t,$$

where

$$A_0 = \begin{cases} 0 & \text{or } t < 0, \\ 1 & \text{or } t \geq 0. \end{cases}$$

In particular cases, one of the coefficients  $A_0$  or  $A_1$  can be equal to zero.

As was mentioned in the introduction, in the considered servomechanism, the basic restrictions are the

restrictions with respect to the moment, velocity, and voltage, i.e., the following conditions hold:

$$\left| \frac{d^2 x}{d\tau^2} \right| \leq i_{\text{ma}}, \quad \left| \frac{dx}{d\tau} \right| \leq y_{\text{ma}}, \quad |u| \leq u_{\text{ma}}.$$

The above coordinate restrictions are interlinked by the servomechanism mechanical characteristic (Fig. 2). As can be seen from the mechanical characteristic equation

$$\omega_1 = \frac{U_A}{k_e \Phi} - M \frac{R_A}{k_e k_m \Phi^2},$$

the torque developed by the motor, the motor angular velocity, and the armature voltage are closely related by the static dependence  $\omega_1 = f(M, U_A)$ . Therefore, the mechanical characteristic is limited by a certain polygon, which contains the region of maximum allowable values of these quantities. The corresponding sides of this polygon of maximum allowable values limit either the maximum moment ( $i_{\text{ma}}$ ), or the moment ( $i_{\text{ma}}$ ) and voltage ( $u_{\text{ma}}$ ), or the moment ( $i_{\text{ma}}$ ), the voltage ( $u_{\text{ma}}$ ), and the angular velocity ( $y_{\text{ma}}$ ). In dependence on operating conditions, either  $d^2 x/d\tau^2$ , or  $d^2 x/d\tau^2$  and  $dx/d\tau$  and  $d^2 x/d\tau^2$  and  $u$ , or  $d^2 x/d\tau^2$ ,  $u$ , and  $dx/d\tau$  will be limited. The regions of possible operating conditions for the case where  $i_L = 0$  and  $\varphi = 0$  are shown in Fig. 3.

With regard to the requirements for the optimum conditions in a control process where the maximum operating speed is to be attained, it is necessary to ensure that one of the restricted coordinates is maintained at its maximum value during particular motion stages [1, 2].

## 3. Equations of Isochrone Regions

In order to determine the maximum capabilities of servomechanisms with regard to their operation speed, it is necessary to establish relations between the initial mismatch values and the optimum transient process times, during which the mismatches are reduced to zero.

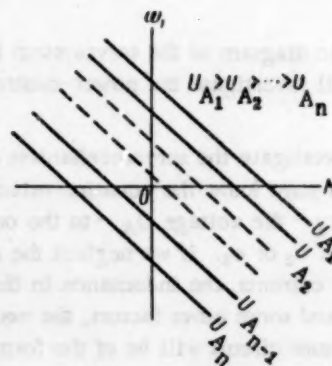


Fig. 2.



For this purpose, it is convenient to use the method of isochrones, which was first used by A. Ya. Lerner in the investigation of optimum systems [3]. The isochrones represent the totality of initial states of a dynamic system from which it passes into an assigned state in the minimum possible time for an optimum control law.

For plotting the region of isochrones, it is necessary to integrate Eq. (4) and to reverse the direction of time  $\tau$  readings, while the time at which the transient process is completed is taken as the initial time. For the accepted reading direction, the time  $\beta = \tau_0 - \tau$ , where  $\tau_0 = \beta_0$  is the transient process time (the isochrone time).

If only the motor torque is limited, the isochrone region equation is of the form

$$x_0 = \mp \frac{i_{ma}\beta_0^2}{4} - \frac{y_0\beta_0}{2} \pm \frac{1}{4i_{ma}} \left( i_L - \frac{y_0}{\beta_0} \right)^2 \beta_0^2. \quad (6)$$

In this equation,  $x_0$  is the initial mismatch between the servosystem receiving and driving axes,  $y_0$  is the initial mismatch between the angular velocities of the receiving and the driving axes,  $\beta_0$  is the isochrone time [i.e., the transient process time during which the servosystem, under optimum control conditions, passes from the initial state, which is determined by the tracing point  $(x_0, y_0)$  on the  $(x, y)$  phase plane, to the assigned state, namely, to the state defined by the point with the coordinates  $(x = 0, y = 0)$ ,  $i_{ma}$  is the maximum allowable motor current, which is proportional to the maximum torque value, and  $i_L$  is the load current due to the constant resistance moment.

If the motor torque and angular velocity are limited, the isochrones are described by the equation

$$x_0 = \pm y_{ma}\beta_0 \pm \frac{y_{ma}^2}{2(i_{ma} \pm i_L)} \pm \frac{(y_{ma} \mp y_0)^2}{2(i_{ma} \mp i_L)}. \quad (7)$$

In this equation,  $y_{ma}$  is the maximum value of the servomechanism velocity.

If the motor torque and the voltage supplied to the armature circuit are limited, the isochrone equation will be of the following form:

$$x_0 = (\varphi \mp u_{ma} + i_L) \beta_0 \mp \frac{y^2}{2(i_{ma} \pm i_L)} \pm \frac{(y_0 \mp y_x)^2}{2(i_{ma} \mp i_L)} - \frac{(\varphi \mp u_{ma} \mp i_{ma})y}{i_{ma} \pm i_L} \mp y_0, \quad (8)$$

where  $u_{ma}$  is the maximum armature voltage,  $y_x$  is the velocity for which the maximum voltage is attained, and  $y$  is the present velocity on the mechanical characteristic portion which corresponds to  $u = u_{ma}$ . In order to determine Eq. (8), the present value of velocity  $y$  must be expressed in terms of  $y_0$ . For this, we use the expressions for the connection times  $\beta_1$  and  $\beta_2$ , where

$\beta_1$  is the braking time, and  $\beta_2$  is the sum of the time  $\beta_1$  and the motion time  $\Delta\beta$  for the constant maximum voltage:

$$\beta_1 = \frac{y}{i_{ma} \pm i_L}, \quad \beta_2 = \beta_0 \pm \frac{y_0 - y_x}{i_{ma} \mp i_L},$$

$$\Delta\beta = \ln \frac{i_{ma} \mp i_L}{u_{ma} \mp \varphi - y \mp i_L}, \quad \beta_2 = \beta_1 + \Delta\beta.$$

In dependence on the initial system state  $(x_0, y_0)$ , a well-defined time  $\beta_1$  must be secured for a given isochrone time. In connection with this, there is, on the one hand, a well-defined relation between  $y_0$  and  $y$  and, consequently, between  $\beta_1$  and  $\beta_2$  on the other hand. By using the values  $y \geq y_x$ , we plot the  $\beta_1 = \varphi_1(y)$  and  $\Delta\beta = \varphi_2(y)$  curves. For every given  $y$ , we find the corresponding  $\beta_2$  and, consequently, the value of  $y_0$ .

If the motor torque, voltage, and angular velocity are limited, the isochrone is described by the equation

$$x_0 = \mp y_{ma}(\beta_0 - 1) \mp \frac{(y_x \mp y_0)(u_{ma} \mp \varphi - y_{ma} \mp i_L)}{i_{ma} \mp i_L} \mp (u_{ma} \mp \varphi - y_{ma} \mp i_L) \ln \frac{i_{ma} \mp i_L}{u_{ma} \mp \varphi - y_{ma} \mp i_L} \pm \frac{y_L^2}{2(i_{ma} \mp i_L)} \pm \frac{(y_x \mp y_0)^2}{2(i_{ma} \mp i_L)} - y_0. \quad (9)$$

The isochrones consist of closed curves composed of two branches, which are described by the above equations, and of lines corresponding to the restriction of the system coordinates.

In order to plot the isochrone regions, we must determine the limits of the servomechanism operating conditions.

#### 4. Determination of the Operating Condition Limits

The servomechanism operating conditions differ from each other with respect to the number of restrictions imposed on the system coordinates. In our case, we shall consider the regions corresponding to operating conditions with restrictions pertaining only to the moment, restrictions with respect to the moment and velocity, restrictions with respect to the moment and voltage, and restrictions with respect to the moment, voltage, and velocity (Fig. 3). For plotting the isochrone regions in correspondence to the operating condition regions, it is necessary to use well-defined isochrone equations by choosing from (6)-(9) the equation corresponding to the given operating conditions.

The limits of the servomechanism operating conditions are determined in dependence on the isochrone time  $\beta_0$ . However, the determinations with respect to time are necessary, but not sufficient, conditions.

Within limits of the found time determinations, it is necessary to provide determinations with respect to the initial conditions.

If, according to the motor operating conditions, no restrictions are imposed on voltage and angular velocity, the regime characterized by restrictions only with respect to the moment will apply for any  $\beta_*$ . The isochrones corresponding to this case, plotted according to Eq. (6), are shown in Fig. 4.

If the working mechanism imposes a certain given restriction on the motor speed, while no restrictions with respect to voltage are present, two regimes are possible. For  $\beta_* < \beta_{*11}$ , there will be only one restriction with respect to the moment; for  $\beta_* > \beta_{*11}$ , two

restrictions are possible. The isochrone limiting time is determined by the expression

$$\beta_{*11} = \frac{y_{ma}}{i_{ma} + i_L}. \quad (10)$$

In order to find the equation for the regime limit, we shall determine  $\beta_*$ , assuming that the system motion corresponds to the limiting case, i.e., although the system attains the maximum speed, the braking begins at the moment when this speed is attained. In this,

$$\beta_* = \mp \frac{y_0}{i_{ma} \mp i_L} + \frac{2y_{ma} i_{ma}}{i_{ma}^2 - i_L^2}. \quad (11)$$

By using Eqs. (7) and (11), we find the regime limits:

$$x_0 = \pm \frac{y_0^2}{2(i_{ma} \mp i_L)} \mp \frac{2y_{ma}^2 i_{ma}}{(i_{ma} \pm i_L)^2 (i_{ma} \mp i_L)} \pm \frac{y_{ma}^2 i_{ma}}{(i_{ma} \pm i_L)^3}. \quad (12)$$

Figure 5 represents the division of the phase plane into regions with respect to the character of the optimum process phase trajectory when restrictions with respect to the moment and speed are present.

In the region represented by the shaded area A, the phase trajectories are limited only with respect to the moment. The isochrones for the initial conditions valid for this region are found from Eq. (6), and, for initial conditions valid outside this region, Eq. (7), which takes into account the restriction with respect to speed, holds. Figure 5 shows examples of isochrones corresponding to different operating conditions.

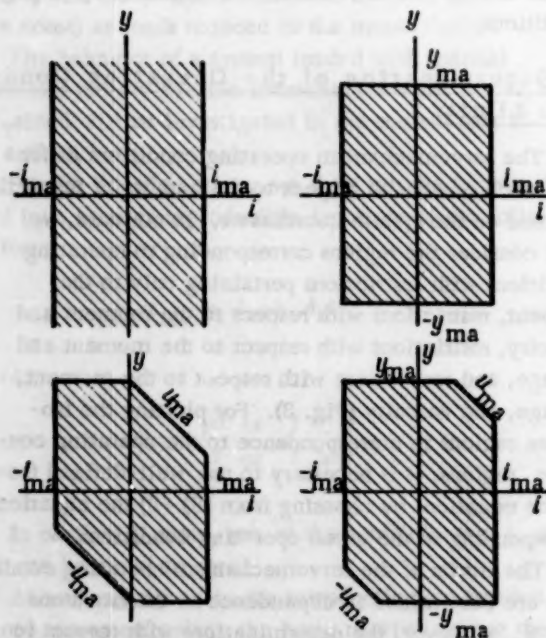


Fig. 3. Regions of motion restrictions.

In the case where a definite restriction is imposed not only on the moment, but also on the motor speed and voltage, three kinds of operating conditions should be distinguished, namely, the regime characterized by a restriction only with respect to the moment, the regime with moment and voltage restrictions, and, finally, the regime where all three coordinates are limited.

In correspondence with the above-mentioned, there are two isochrone limiting time values  $\beta_{*11}$  and  $\beta_{*12}$ . If

$$\beta_* < \beta_{*11} = \frac{y_x}{i_{ma} + i_L}, \quad (13)$$

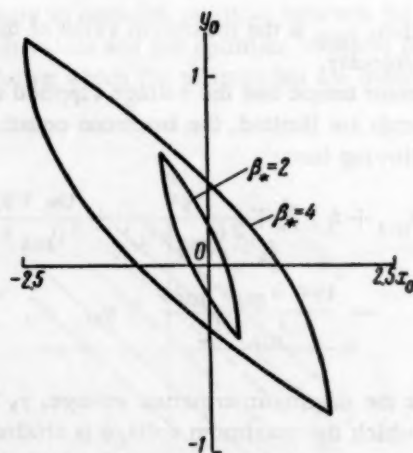


Fig. 4. Isochrones for the case where only the motor torque is limited ( $i_{ma} = 0.25$ ;  $i_L = 0.05$ ).

we have a regime with restrictions only with respect to the moment, and, if

$$\beta_{\text{li1}} < \beta_* < \beta_{\text{li2}} = \beta_{\text{li1}} + \Delta\beta_{\text{max}} \quad (14)$$

where  $\Delta\beta_{\text{max}} = \ln \frac{i_{\text{ma}} + i_L}{u_{\text{ma}} - \varphi - y_{\text{ma}} + i_L}$ , we have

regimes with restriction only with respect to the moment, as well as with restrictions with respect to the moment and voltage. In this case, a regime with all three kinds of restrictions will not be present.

If  $\beta_* > \beta_{\text{li2}}$ , all three kinds of operating conditions will be present.

In the case under consideration, the phase plane is divided by two boundary curves into regions corresponding to the above operating conditions.

The equation of the boundary curve which separates the region where only the moment is restricted from the region where both the moment and the voltage are restricted (speed restrictions are not present) is determined in a similar manner. In this, the isochrone time  $\beta_*$ , which corresponds to the limiting case, is expressed by the relation

$$\beta_* = \frac{y_x}{i_{\text{ma}} \mp i_L} \mp \frac{y_0 \mp y_x}{i_{\text{ma}} \mp i_L} \quad (15)$$

The operating conditions boundary is determined by the equation

$$x_0 = \mp \frac{y_x^2}{2(i_{\text{ma}} \pm i_L)} \pm \frac{y_0^2 - y_x^2}{2(i_{\text{ma}} \mp i_L)} \quad (16)$$

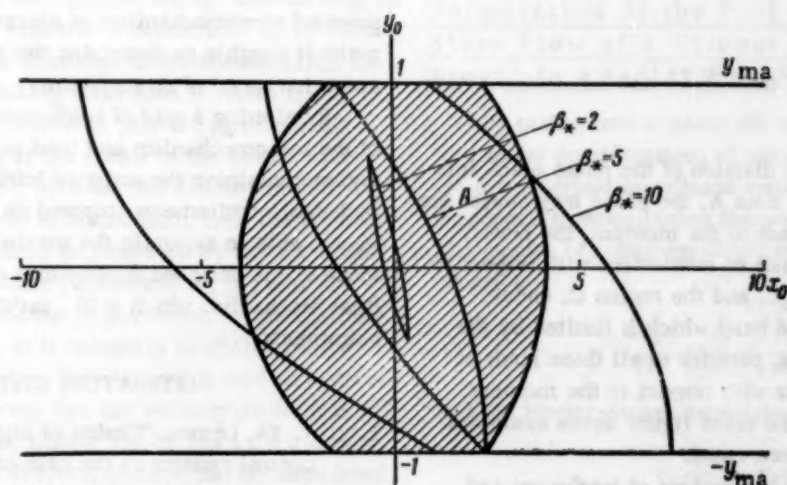


Fig. 5. Isochrones and boundary lines for the case of moment and speed restrictions ( $i_{\text{ma}} = 0.25$ ;  $i_L = 0.05$ ;  $\varphi = 0$ ;  $y_{\text{ma}} = 1.0$ ).

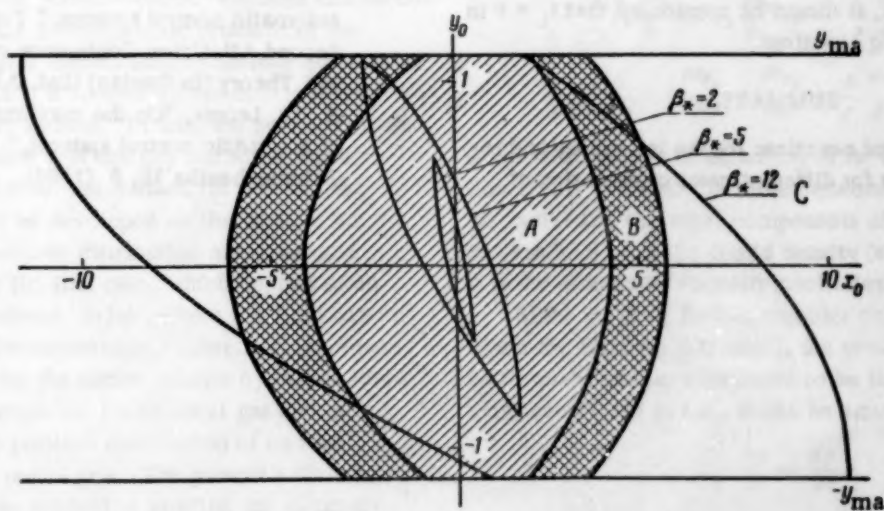


Fig. 6. Isochrones and boundary curves in the case of restrictions with respect to the moment, voltage, and speed ( $i_{\text{ma}} = 0.25$ ;  $i_L = 0.05$ ;  $\varphi = 0$ ;  $u_{\text{ma}} = 1.25$ ;  $y_x = 1.0$ ;  $y_{\text{ma}} = 1.15$ ).



The equation of the boundary curve which separates the region where the moment and the voltage are restricted from the region where the moment, the voltage,

and the speed are restricted is obtained by eliminating the limiting isochrone time which is expressed by the relation

$$\beta_0 = \frac{y_{ma}}{i_{ma} \pm i_L} + \ln \frac{i_{ma} \mp i_L}{u_{ma} - y_{ma} \mp \varphi \mp i_L} + \frac{u_{ma} \mp y_0 \mp \varphi - i_{ma}}{i_{ma} \mp i_L}. \quad (17)$$

The regime boundary to be found is described by the equation

$$x_0 = \pm (y_{ma} \mp y_0) \mp \frac{y_{ma}^2}{2(i_{ma} \mp i_L)} \pm \frac{(y_0 \mp y_x)(u_{ma} \mp \varphi \mp i_L)}{i_{ma} \mp i_L} \pm \frac{(y_0 \mp y_x)^2}{2(i_{ma} \mp i_L)} \pm (\varphi \mp u_{ma} \mp i_L) \ln \frac{i_{ma} \mp i_L}{u_{ma} - y_{ma} \mp \varphi \mp i_L}, \quad (18)$$

where

$$y_x = u_{ma} - \varphi - i_{ma}.$$

Figure 6 shows the division of the phase plane into regions. In the shaded area A, the phase trajectories are limited only with respect to the moment, the doubly shaded area B corresponds to restrictions with respect to the moment and voltage, and the region C, encompassing the unshaded band which is limited by the maximum speed values, pertains to all three kinds of restriction - restrictions with respect to the moment, voltage, and speed. The same figure shows examples of isochrones for all three cases.

The asymmetry in the regions of isochrones and regime boundaries which are shown in Figs. 4, 5, and 6 is a consequence of the effect of the load current  $i_L$ , which is due to the overbalancing load. If the load current is absent, it should be considered that  $i_L = 0$  in the corresponding equations.

#### SUMMARY

The obtained equations for the isochrones and regime boundaries for different cases of operation of

powered servomechanisms of electrical servosystems make it possible to determine the maximum possible operation speed of servosystems.

By plotting a grid of isochrones for different values of the servomechanism and load parameters when the region containing the assigned initial mismatches and technical requirements imposed on the system is known, we are able to ascertain the maximum possible operation speed of the designed servosystem or to select a suitable final mechanism which will satisfy the technical requirements.

#### LITERATURE CITED

1. A. Ya. Lerner, "Design of high-speed automatic control systems in the case of limited values of the controlled device coordinates," Transactions of the Second All-Union Conference on Automatic Control Theory [in Russian] (Izd. AN SSSR, 1955) 2.
2. A. A. Fel'dbaum "On the synthesis of optimum automatic control systems," Transactions of the Second All-Union Conference on Automatic Control Theory [in Russian] (Izd. AN SSSR, 1955) 2.
3. A. Ya. Lerner, "On the maximum operation speed of automatic control systems," *Avtomatika i Telemekhanika* 15, 6 (1954).

# CALCULATION OF STATIC CHARACTERISTICS OF "NOZZLE-BAFFLE" ELEMENTS

E. A. Andreeva

Moscow

Translated from *Avtomatika i Telemekhanika*, Vol. 21, No. 7,

pp 982-996, July, 1960

Original article submitted March 7, 1960

This article presents a calculation method for plotting the static discharge and power characteristics of a "nozzle-baffle" element for compressible and incompressible viscous fluids.

One of the basic elements in pneumatic and hydraulic automation is the "nozzle-baffle" throttle (Fig. 1). The operation of this element is determined by its static characteristics: by the discharge characteristic, i.e., the dependence of the working fluid mass  $G$  which is discharged through the throttle on pressure  $p_0$ , before the baffle, on pressure  $p_e$  at the radius of the nozzle end-face, and on distance  $h$  between the nozzle and the baffle, and by the power characteristic, i.e., the dependence of the force  $F$  which is generated by the jet action on the baffle on the same parameters  $p_0$ ,  $p_e$ , and  $h$ .

In developing a calculation method for plotting the static characteristics, it is necessary to distinguish between two cases: a) when the element is used in hydraulic devices, which means that the working medium is a viscous incompressible liquid, and b) when the element is used in pneumatic devices, when it can be considered that the working medium is an ideal viscous gas.

In the first case, the method of plotting the static discharge  $G = G(p_0, p_e, h)$  and power  $F = F(p_0, p_e, h)$  characteristics of the "nozzle-baffle" element can be obtained by solving the hydrodynamic problem of the steady-state flow of a viscous incompressible liquid in the radial gap which is formed by the nozzle end-face and the baffle plate surface. In this, the pressure distribution along the radius  $r$  of the gap has to be found.

In the second case, the method for plotting the characteristics can be developed on the basis of the equation for the pressure distribution along the gap radius as found for the first case, which applies to an infinitely small volume  $2\pi r h dr$ , where the fluid can be considered to be incompressible. After this, the equation is integrated for the entire volume by taking into account the state equation for an ideal gas and, as a result, we find the pressure distribution of an ideal viscous gas in the radial gap. The present article investigates a calculation method of plotting the static discharge and power characteristics of a "nozzle-baffle" element for a viscous incompressible and a viscous compressible fluid. Brief information on this work has been published in [6] and [9].

## 1. THE CASE OF A VISCOUS INCOMPRESSIBLE LIQUID

### Formulation of the Problem of Steady-State Flow of a Viscous Incompressible Liquid in a Radial Gap

By taking into account the axial symmetry of the flow under consideration, which makes it convenient to use a cylindrical coordinate system  $(r, z)$ , this problem is reduced to determining the pressure field  $p = p(r, z)$ . The system of equations which consists of the continuity equation

$$\frac{\partial v_r}{\partial r} + \frac{v_r}{r} + \frac{\partial v_z}{\partial z} = 0 \quad (1)$$

and the Navier-Stokes equations

$$v_r \frac{\partial v_r}{\partial r} - v_z \frac{\partial v_r}{\partial z} = -\frac{1}{\rho} \frac{\partial p}{\partial r} + \nu \left( \frac{\partial^2 v_r}{\partial r^2} + \frac{\partial^2 v_r}{\partial z^2} + \frac{1}{r} \frac{\partial v_r}{\partial r} - \frac{v_r}{r^3} \right), \quad (2)$$

$$v_r \frac{\partial v_z}{\partial r} + v_z \frac{\partial v_z}{\partial z} = -\frac{1}{\rho} \frac{\partial p}{\partial z} + \nu \left( \frac{\partial^2 v_z}{\partial r^2} + \frac{\partial^2 v_z}{\partial z^2} + \frac{1}{r} \frac{\partial v_z}{\partial z} \right), \quad (3)$$

is the basic system of equations to be used in the solution of this problem. In these equations,  $v_r$  and  $v_z$  are the radial and the axial components of the velocity vector (cm/sec),  $\rho$  is the liquid density (kg-sec<sup>2</sup>/cm<sup>4</sup>), and  $\nu$  is the kinematic viscosity coefficient (cm<sup>2</sup>/sec).

Since we shall further consider only those cases where the distance  $h$  is small, the pressure under the baffle plate can be considered to be independent of the axial coordinate  $z$ , i.e., it can be assumed that

$$\frac{\partial p}{\partial r} = \frac{dp}{dr}.$$

For this, Eqs. (1), (2), and (3) form a closed system:

$$\frac{\partial v_r}{\partial r} + \frac{v_r}{r} + \frac{\partial v_r}{\partial z} = 0, \quad (4)$$

$$v_r \frac{\partial v_r}{\partial r} + v_z \frac{\partial v_r}{\partial z} = -\frac{1}{\rho} \frac{dp}{dr} + \nu \left( \frac{\partial^2 v_r}{\partial r^2} + \frac{\partial^2 v_r}{\partial z^2} + \frac{1}{r} \frac{\partial v_r}{\partial r} - \frac{v_r}{r^2} \right), \quad (5)$$

the solution of which, with the consideration of the boundary conditions

$$v_r(r, 0) = 0, \quad v_z(r, 0) = 0, \\ v_r(r, h) = 0, \quad v_z(r, h) = 0, \quad (6)$$

$$p(r_e) = p_e, \quad (7)$$

$$\int_0^h v_r dz = \frac{Q}{2\pi r}, \quad (8)$$

where  $Q$  is the volumetric liquid discharge ( $\text{cm}^3/\text{sec}$ ), yields the pressure distribution  $p = p(r)$  in which we are interested and, besides, the velocity fields  $v_r = v_r(r, z)$  and  $v_z = v_z(r, z)$ .

By using the concept of the stream function  $\psi = \psi(r, z)$ , which, by definition, must transform the continuity equation (4) into an identity, the system of equations (4) and (5) and the corresponding boundary conditions (6)-(8) can be conveniently represented in the form of the equation which determines the stream function:

$$\frac{\partial \psi}{\partial z} \left( \frac{\partial^3 \psi}{\partial z^3 \partial r} - \frac{2}{r} \frac{\partial^2 \psi}{\partial z^2} \right) - \left( \frac{\partial \psi}{\partial r} \right) \left( \frac{\partial^3 \psi}{\partial z^3} \right) = \\ = r \nu \left( \frac{\partial^4 \psi}{\partial z^4} + \frac{\partial^4 \psi}{\partial z^2 \partial r^2} - \frac{1}{r} \frac{\partial^2 \psi}{\partial z^2 \partial r} \right), \quad (9)$$

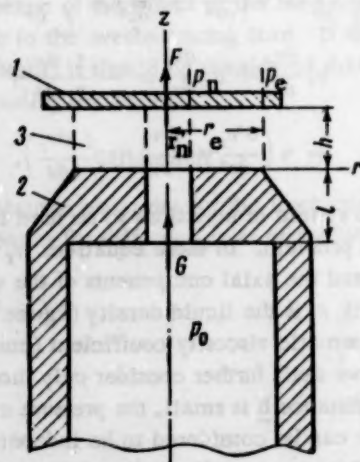


Fig. 1. Diagram of the "nozzle-baffle" element. 1) Baffle; 2) nozzle; 3) radial gap;  $r_n$  is the nozzle radius, and  $r_e$  is the end-face radius;  $p_n$  is the pressure at the nozzle radius, and  $p_e$  is the pressure after throttling.

the relations which determine the velocity fields with respect to the stream function:

$$v_r = \frac{1}{r} \frac{\partial \psi}{\partial z}, \quad v_z = -\frac{1}{r} \frac{\partial \psi}{\partial r}, \quad (10)$$

and the equation which determines the pressure field with respect to the velocity fields:

$$\frac{1}{\rho} \frac{dp}{dr} = -v_r \frac{\partial v_r}{\partial r} - v_z \frac{\partial v_r}{\partial r} + \\ + \nu \left( \frac{\partial^2 v_r}{\partial z^2} + \frac{\partial^2 v_r}{\partial r^2} + \frac{1}{r} \frac{\partial v_r}{\partial r} - \frac{v_r}{r^2} \right). \quad (11)$$

In solving Eq. (9) by taking into account relations (10), it is necessary to consider the boundary conditions (6) and (8), and in integrating Eq. (11), condition (7) must be taken into account.

Thus, after integrating Eq. (9) and taking into account (10) and (11), we shall obtain the velocity field under the baffle plate and the pressure distribution in the radial gap.

#### Analysis of Some Known Solutions

Before obtaining the general solution of the problem, let us determine to what extent the solutions obtained for certain coarse approximations correspond to the actual conditions.

If we assume that the liquid is not viscous ( $\nu = 0$ ), we shall obtain the Bernoulli integral as the solution of Eqs. (2) and (3):

$$\frac{p}{\rho} + \frac{v_r^2}{2} = \frac{p_e}{\rho} + \frac{v_{r_e}^2}{2},$$

where

$$v_r = \frac{G}{2\pi r h \rho}, \quad v_{r_e} = \frac{Q}{2\pi r_e h \rho}.$$

For this, the pressure field in criterion form will be

$$B - B_e = -12.5 A^2 (\alpha^2 - 1), \quad (13)^*$$

where

$$B = \frac{p h^4 \rho}{\mu^2 r_e^2 \cdot 10^3}, \quad B_e = \frac{p_e h^4 \rho}{\mu^2 r_e^2 \cdot 10^3},$$

$$A = \frac{G h}{\pi \mu r_e^2 \cdot 10^3}, \quad \alpha = \frac{r_e}{r};$$

$p$  is the pressure under the baffle plate at the radius  $r$  ( $\text{kg}/\text{cm}^2$ ),  $p_e$  is the pressure at the nozzle end-face radius ( $\text{kg}/\text{cm}^2$ ),  $\mu$  is the dynamic viscosity coefficient ( $\text{kg}\cdot\text{sec}/\text{cm}^2$ ),  $r_e$  is the nozzle end-face radius ( $\text{cm}$ ),  $h$  is the gap between the nozzle and the baffle ( $\text{cm}$ ),  $r$  is the present radius ( $\text{cm}$ ), and  $G$  is the mass discharged ( $\text{kg}\cdot\text{sec}/\text{cm}$ ).

\* As in Russian [Publisher's note].



If we neglect the inertia terms in Eqs. (2) and (3), but consider that the liquid is viscous, the pressure field will be of the form

$$B - B_e = 6A \ln \alpha. \quad (14)$$

This relation is given in [2].

Paper [3] provides the approximate solution of the system of equations (1)-(3):

$$B - B_e = 6A \ln \alpha - 12.5A^2(\alpha^2 - 1). \quad (15)$$

Paper [4] provides the equation for the pressure distribution in the radial gap:

$$B - B_e = 6A \ln \alpha - 19.3A^2(\alpha^2 - 1), \quad (16)$$

which represents a linear combination of approximate solutions (13) and (14), and secures a parabolic radial velocity component distribution in the axial direction. This assumption determines the coefficient in front of the term that characterizes the pressure field in the case where viscosity is neglected.

In Fig. 2, all the above solutions are compared with each other and with the experimental data borrowed from [4].

Curves 1, 2, 4, and 3 correspond to solutions (13), (14), (15), and (16), respectively. The solid lines pertain to divergent flow, and the dotted lines pertain to convergent flow. The points mark the experimental data which were processed in terms of the same criteria; the white and black points correspond to divergent and convergent flows, respectively. The experiments were performed with a nozzle with  $r_n = 0.384$  cm and  $r_e = 5.24$  cm. Water was used as the working liquid. Divergent flow was investigated for the gap  $h = 0.0367$  cm between the nozzle and the baffle plate, the discharge  $Q = 36.4$  cm<sup>3</sup>/sec, and the temperature  $t = 12^\circ\text{C}$ , while the dynamic viscosity coefficient was  $\mu = 0.0124$  g/cm $\cdot$ sec. Convergent flow was investigated for  $h = 0.0356$  cm,  $Q = 9.61$  cm<sup>3</sup>/sec,  $t = 14^\circ\text{C}$ , and  $\mu = 0.0117$  g/cm $\cdot$ sec.

An analysis of the diagrams in Fig. 2 makes it possible to draw the following conclusions:

1. Solutions (13) and (14) do not accurately represent the actual pressure distribution pattern; curves 1 and 2, which correspond to these solutions, do not even qualitatively agree with experimental data.

2. Solution (15) reflects the pressure distribution pattern more accurately, but the corresponding curve 4 still deviates to a great extent from the experimental curve.

3. Equation (16) yields a pressure distribution which is in good agreement with the experimental distribution for divergent flow (solid curve 3), while the correspondence is less accurate for convergent flow (dotted line 3). However, this equation, since it is a semiempirical equation, is not rigorously defined, and, therefore, we cannot be sure that it will agree well with experimental data under different conditions.

Therefore, it became necessary to find a more rigorous solution of this problem.

#### Determination of the Stream Function and of the Velocity Field

By using the same procedure as in [1], we shall assume that the stream function can be represented as the series

$$\psi(r, z) = \sum_{k=1}^{\infty} \frac{a_k(z)}{r^{k-1}}. \quad (17)$$

By substituting (17) in Eq. (9) and in relations (10), after some transformations, we obtain

$$\begin{aligned} & -\frac{2}{r^2} a_1' a_1'' - \sum_{i=1}^{\infty} \frac{2}{r^{i+2}} \sum_{k=1}^{i+1} a_k' a_{i-k+2}'' - \\ & - \sum_{i=1}^{\infty} \frac{1}{r^{i+2}} \left[ \sum_{k=1}^i (i-k+1) (a_k' a_{i-k+2}'' - \right. \\ & \left. - a_k''' a_{i-k+2}) \right] = \\ & = v \left[ \sum_{i=1}^{\infty} \frac{i(i+2)}{r^{i+2}} a_{i+1}'' + \frac{a_1^{IV}}{r^0} + \frac{a_2^{IV}}{r} + \frac{a_3^{IV}}{r^2} + \sum_{i=1}^{\infty} \frac{a_{i+3}^{IV}}{r^{i+2}} \right], \end{aligned} \quad (18)$$

$$v_r = \sum_{k=1}^{\infty} \frac{a_k(z)}{r^k}, \quad v_z = \sum_{k=1}^{\infty} \frac{a_k(z)}{r^{k+1}} (k-1). \quad (19)$$

By now equating in (18) the coefficients in front of terms with equal powers of  $r$ , we shall obtain the following system of ordinary differential equations with respect to the  $a_k = a_k(z)$  function:

$$\begin{aligned} a_1^{IV} &= 0, \\ a_2^{IV} &= 0, \\ a_3^{IV} &= -\frac{2}{v} a_1' a_1'', \\ &\dots \dots \dots \end{aligned} \quad (20)$$

$$\begin{aligned} a_{i+3}^{IV} &= -\frac{2}{v} \sum_{j=1}^{i+1} a_j' a_{i-j+2}'' - \frac{1}{v} \sum_{j=1}^i (i-j+1) \\ & (a_j' a_{i-j+2}'' - a_j''' a_{i-j+2}) - i(i+2) a_{i+1}'' \\ & (i = 1, \dots, \infty). \end{aligned}$$

By integrating these equations, the  $a_k = a_k(z)$  functions are determined with an accuracy equal to that of the arbitrary constants. The substitution of these functions in (19) makes it possible to determine the

velocity distribution after finding the arbitrary constants by using conditions (6) and (8).

By using the notation

$$V_z = \frac{v_z}{6\nu_0\zeta(1-\zeta)} \frac{35}{\text{Re}} \left(\frac{r}{h}\right)^2 \frac{1}{\zeta},$$

$$V_r = \left[ \frac{v_r}{6\nu_0\zeta(1-\zeta)} - 1 \right] \frac{35}{\text{Re}} \frac{r}{h}; \quad (21)$$

$$= \frac{z}{h}, \quad \text{Re} = \frac{v_0 h}{\nu}, \quad v_0 = \frac{Q}{2\pi r h}$$

and noting that the functions  $a_k = 0$  for even values of  $k$ , the found velocity distribution law can be represented in the following form:

in the first approximation ( $k = 1$ )

$$V_z = 0, \quad V_r = 0; \quad (22)$$

in the second approximation ( $k = 3$ )

$$V_z = (1-\zeta)(1-2\zeta)(\zeta^2-\zeta-1),$$

$$V_r = 7\left(\zeta^4 - 12\zeta^3 + \frac{7}{2}\zeta^2 - \frac{7}{2}\zeta - \frac{1}{7}\right); \quad (23)$$

in the third approximation ( $k = 5$ )

$$V_z = (1-\zeta)(1-2\zeta)(\zeta^2-\zeta-1) + \left(\frac{h}{r}\right)^2 \frac{1}{1-\zeta} \times$$

$$\times \left( \frac{4}{9}\zeta^7 - 2\zeta^6 + \frac{8}{3}\zeta^5 - \frac{12}{5}\zeta^4 + \frac{4}{3}\zeta^3 + \frac{256}{15}\zeta - \frac{16}{5} \right) -$$

$$- \text{Re} \frac{h}{r} \frac{1}{1-\zeta} \left( \frac{32}{35}\zeta^9 - \frac{16}{5}\zeta^8 + \frac{19}{3}\zeta^7 - \frac{9}{2}\zeta^6 - \right.$$

$$\left. - \frac{48}{35}\zeta^5 + \frac{17}{5}\zeta^4 - \frac{6}{5}\zeta^3 - \frac{26}{231}\zeta + \frac{53}{770} \right), \quad (24)$$

$$V_r = 7\left(\zeta^4 - 2\zeta^3 + \frac{1}{2}\zeta^2 + \frac{1}{2}\zeta - \frac{1}{7}\right) + \left(\frac{h}{r}\right)^2 \times$$

$$\times \frac{1}{1-\zeta} \left( \zeta^7 - 4\zeta^6 + \frac{14}{3}\zeta^5 - 3\zeta^4 + \frac{4}{3}\zeta^3 + \frac{64}{5}\zeta - \frac{8}{5} \right) -$$

$$- \text{Re} \frac{h}{r} \frac{1}{1-\zeta} \left( \frac{8}{5}\zeta^9 - 8\zeta^8 + \frac{57}{4}\zeta^7 - 9\zeta^6 - \right.$$

$$\left. - \frac{12}{5}\zeta^5 + \frac{51}{10}\zeta^4 - \frac{3}{2}\zeta^3 - \frac{13}{154}\zeta + \frac{53}{1540} \right)$$

#### The Pressure Field

By substituting now the expressions (22), (23), and (24) in Eq. (11)<sup>†</sup> and by integrating it while taking into account (7), we obtain the pressure distribution:

in the first approximation

$$p - p_e = \frac{7G\mu}{\pi\phi h^3} \ln \frac{r}{r_e} + 0.125 \frac{G^2}{\pi^2\phi h^3} \left( \frac{1}{r_e^2} - \frac{1}{r^2} \right) \quad (25)$$

and in the criterion form

$$B - B_e = 6A \ln \alpha - 12.5A^2(\alpha^2 - 1); \quad (26)$$

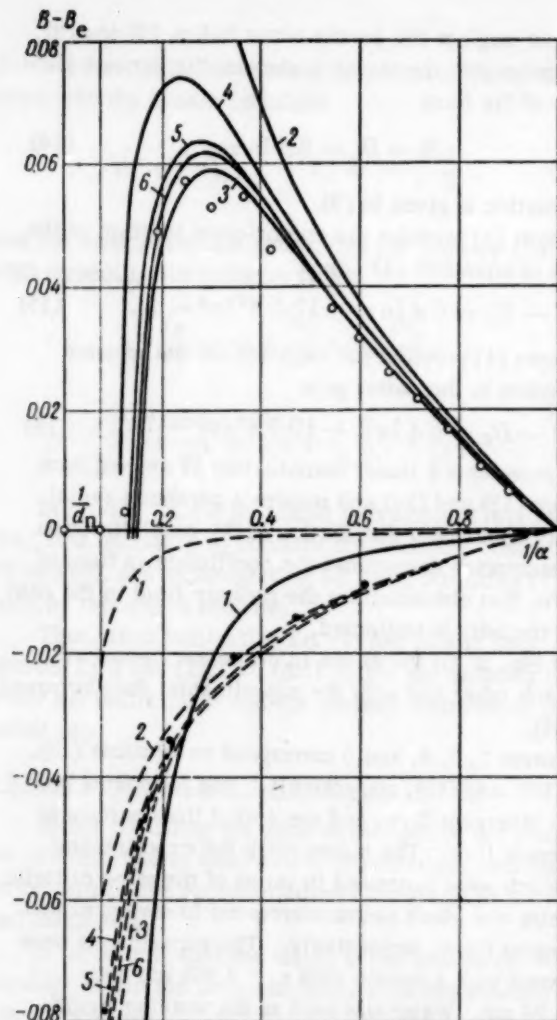


Fig. 2. Pressure distribution along the baffle plate radius.  $B - B_e = (p - p_e) \cdot h^4 \rho / \mu^2 r_e^2 \cdot 10^{-2}$  is the dimensionless pressure drop.

in the second approximation

$$p - p_e = \frac{6G\mu}{\pi\phi h^3} \ln \frac{r}{r_e} + 0.1678 \frac{G^2}{\pi^2\phi h^3} \left( \frac{1}{r_e^2} - \frac{1}{r^2} \right) \quad (27)$$

and in the criterion form

$$B - B_e = 6.4 \ln \alpha - 16.78A^2(\alpha^2 - 1); \quad (28)$$

in the third approximation

$$p - p_e = \frac{6G\mu}{\pi\phi h^3} \ln \frac{r}{r_e} + 0.1678 \frac{G^2}{\pi^2\phi h^3} \left( \frac{1}{r_e^2} - \frac{1}{r^2} \right) +$$

$$+ 0.001425 \frac{G^3}{\pi^3\phi h^4} \left( \frac{1}{r_e^4} - \frac{1}{r^4} \right) +$$

$$+ 0.0003675 \frac{G^3}{\pi^3\phi h^4} \left( \frac{1}{r_e^4} - \frac{1}{r^4} \right) \quad (29)$$

<sup>†</sup> It should be noted that, here, the  $v_z = v_z(r, z)$  and  $v_r = v_r(r, z)$  functions which are represented by a finite number of terms of the series are substituted in (11), which leads to contradiction:  $dp/dr$  depends on  $z$ . In order to eliminate this contradiction, averaging with respect to  $z$  is used.

and in the criterion form

$$B - B_e = 6A \ln \alpha - 16.78A^2(\alpha^2 - 1) - 0.142A^2\beta^2(\alpha^4 - 1) - 3.67A^3(\alpha^4 - 1), \quad (30)$$

where  $\beta = h/r_e$ .

Figure 2 shows a comparison between the obtained pressure distribution relations (26), (28), and (30) and experimental data. It is obvious from the comparison that Eqs. (26), (28), and (30) (curves 4, 5, and 6 correspond to these equations in Fig. 2) define pressure distributions which are the closer to the experimental distribution, the larger the number of terms of the series that are taken into account. For convergent flow, these equations provide a better agreement with experimental data than Eq. (16).

Thus, Eqs. (26), (28), and (30) for the pressure distribution under the baffle plate, which are obtained by solving the hydrodynamic problem and which are in good agreement with experimental data, can be used for calculating the pressure distribution as well as for determining the static discharge and power characteristics. It is obvious from Fig. 2 that the third approximation (curve 6) provides only an insignificant improvement in accuracy in comparison with the second approximation (curve 5), but it yields an equation which is much more complicated for use in calculations. Therefore, for determining the pressure field as well as the discharge and the power characteristics, it is advisable to use the second approximation (28).

#### The Discharge Characteristics

If we consider that the liquid flowing through the nozzle is not viscous, this will permit us to express the pressure  $p_n$  at the nozzle radius in terms of pressure  $p_0$  before the baffle and in terms of discharge  $G$ . In this case,

$$p_n = p_0 - \frac{\rho}{2} \bar{v}_n^2, \quad (31)$$

where

$$\bar{v}_n = \frac{1}{h} \int_0^h v_{rn} dz = \frac{G}{2\pi r_n h \rho}. \quad (32)$$

With this, Eq. (31) in the criterion form will be

$$B_n - B_0 = -12.5A^2\alpha_n^2 \quad (33)$$

where

$$B_c = \frac{p_n h^4 \rho}{\mu^2 r_e^2 10^3}, \quad B_0 = \frac{p_0 h^4 \rho}{\mu^2 r_e^2 10^3}, \quad \alpha_n = \frac{r_n}{r_e}. \quad (34)$$

By applying now Eqs. (26), (28), and (30) to the point  $r = r_n$ , i.e., by substituting in them  $\alpha = \alpha_n$  and  $B = B_n$  and eliminating  $B_n$  from them according to

Eq. (33), we shall obtain the following discharge characteristics of the "nozzle-baffle" element:

In the first approximation

$$B_0 - B_e = 6A \ln \alpha_n + 12.5A^2, \quad (35)$$

in the second approximation

$$B_0 - B_e = 6A \ln \alpha_n + (16.78 - 4.28\alpha_n^2)A^2, \quad (36)$$

in the third approximation

$$B_0 - B_e = 6A \ln \alpha_n + (16.78 - 4.28\alpha_n^2)A^2 - 0.142A^2\beta^2(\alpha_n^4 - 1) - 3.67A^3(\alpha_n^4 - 1). \quad (37)$$

If we take into account the viscosity of the liquid flowing through the nozzle, the discharge characteristic in the second approximation will be of the form

$$B_0 - B_e = 6A \ln \alpha_n + 8 \frac{A}{\alpha_n} + (16.78 - 29.28\alpha_n^2 + 50\alpha_n^4\beta), \quad \alpha_n = \frac{r_n}{h}, \quad (38)$$

where  $l$  is the nozzle length (cm).

Figure 3 shows the family of discharge characteristic curves (36) with respect to  $\alpha_n$ , which are plotted in terms of criteria that do not contain the nozzle parameters:

$$A^* = \frac{G}{\pi \mu h \cdot 10^3}, \quad B^* = \frac{p h^3 \rho}{\mu^3 \cdot 10^{12}}.$$

It is obvious from the figure that the curves intersect and that they have pressure drop values for which discharge does not occur at all. However, neither of these conditions can actually be realized. The contradiction can be explained by the fact that a finite number of terms of the series were used and that the liquid flow losses in the  $0 \leq r \leq r_n$  region were not taken into account. This contradiction limits the regions where the solutions are valid in the following manner:

for  $\alpha_n < 1.98$

$$A_{\text{lim}} = \frac{4.09 - 6 \ln \alpha_n}{(16.78 - 4.28\alpha_n^2)},$$

and for  $1.98 < \alpha_n < 1.98^2$

$$A_{\text{lim}} = \frac{6 \ln 1.98^2 - 6 \ln \alpha_n}{4.28(1.98^4 - \alpha_n^2)}.$$

Figure 4 shows a comparison between the discharge characteristics for different gaps  $h$  between the nozzle and the baffle, calculated according to the second-approximation equation (38), and experimental data which were processed in terms of the same criteria. The theoretical curves are shown by solid lines, and the experimental curves are represented by solid lines with points. The experimental data, which were borrowed



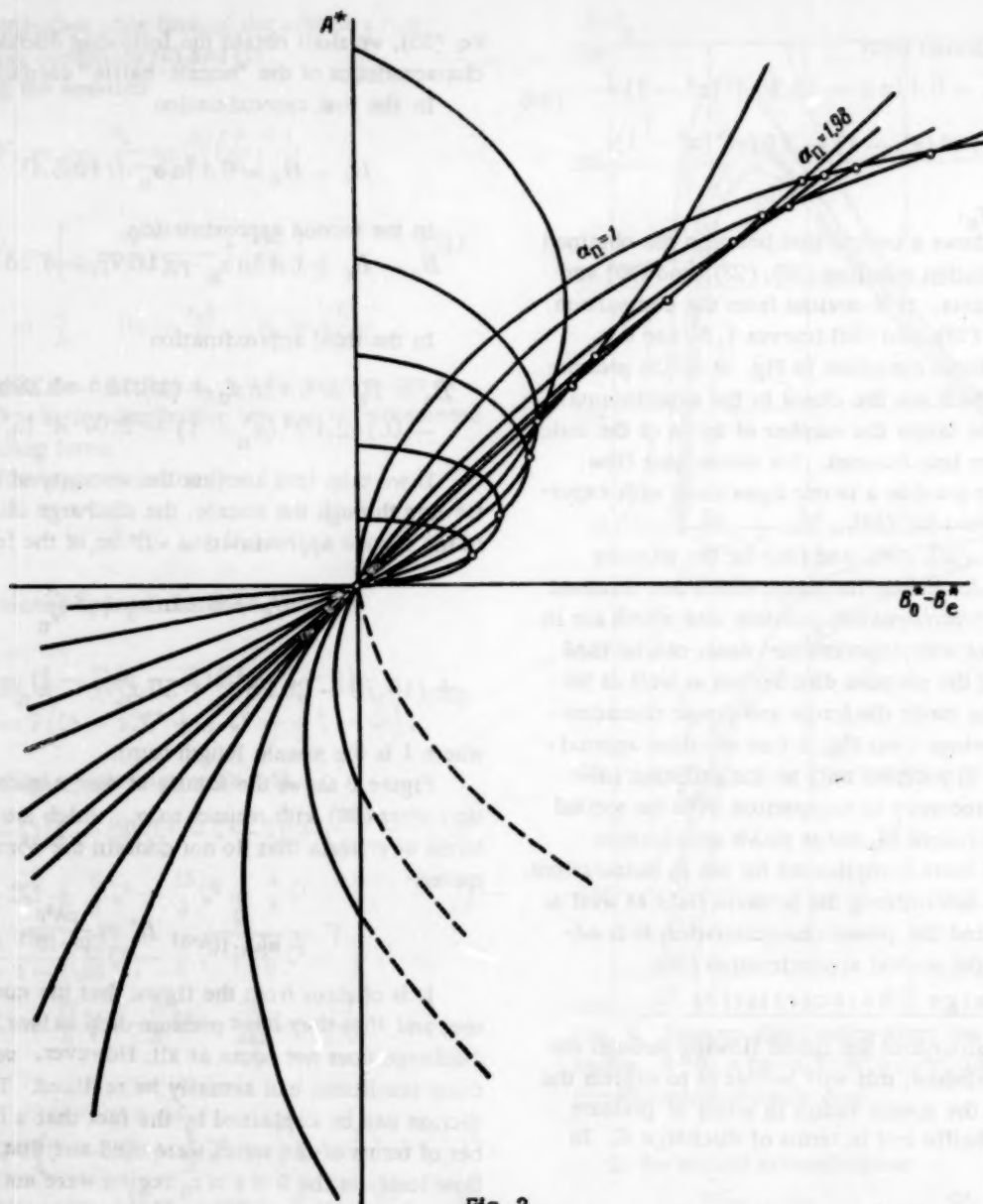


Fig. 3.

from [5], were obtained for a nozzle with  $d_n = 0.6$  mm and  $d_e = 0.95$  mm, where the working liquid was AMG-10 oil at  $t = 50^\circ\text{C}$  with the density  $\rho = 8.66 \times 10^{-7}$  kg·sec<sup>2</sup>/cm<sup>4</sup>, and the dynamic viscosity coefficient  $\mu = 8.66 \times 10^{-8}$  kg·sec/cm<sup>2</sup>.

It is obvious from the comparison that a good quantitative agreement is secured for numbers  $A \leq 2$  and  $B - B_e \leq 30$ , while, for numbers  $A > 2$  and  $B - B_e > 30$ , a good qualitative agreement and an insufficient quantitative agreement is obtained. This unsatisfactory quantitative agreement can be explained by the fact that the solution was obtained for laminar flow and that the discharge  $A$  values exceed the maximum value.

#### The Power Characteristic

Equations (26), (28), and (30) express the law of pressure distribution under the baffle plate in those cases

where  $r_n \leq r \leq r_e$ . Moreover, the pressure at the baffle center, where  $r = 0$ , can be considered to be known, since, here,  $p = p_0$ .

Let us assume that the pressure between the points  $r = 0$  and  $r = r_n$  is linearly distributed, i.e.,

$$p = p_0 - \frac{p_0 - p_n}{r_n} r. \quad (39)$$

Thus, the pressure distribution over the entire baffle surface is known.

After integration, we obtain the following power characteristics of the "nozzle-baffle" element: in the first approximation

$$D = 3A (\alpha_n^2 - 1) + 12.5A^2 \alpha_n^2 \left( \frac{1}{3} - 2 \ln \alpha_n \right); \quad (40)$$

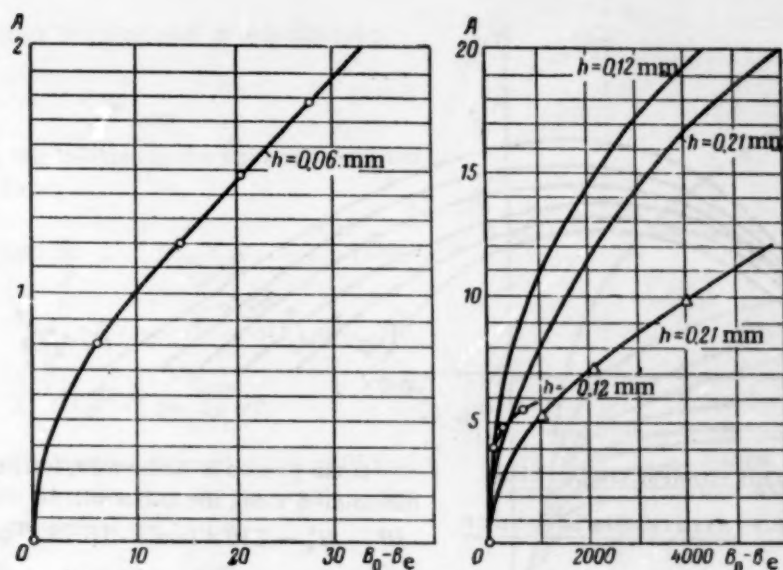


Fig. 4.

in the second approximation

$$D = 3A(\alpha_n^3 - 1) + 16.78A^2\alpha_n^2(0.248 - 2 \ln \alpha_n); \quad (41)$$

in the third approximation

$$D = 3A(\alpha_n^3 - 1) + 16.78A^2\alpha_n^2(0.248 - 2 \ln \alpha_n) - 14.28A^2\beta^2(1 - \alpha_n^2) - 3.675A^3(1 - \alpha_n^2)^2; \quad (42)$$

where

$$D = \frac{Fh^3p}{\pi\mu^2r_e^2r_n^210^3}.$$

Figure 5 shows the family of power characteristic curves (41) with respect to  $\alpha_n$ , which are expressed in terms of the criteria

$$D^* = \frac{Fp}{\pi\mu^2 \cdot 10^3}, \quad B_0^* = \frac{p_0 h^2 p}{\mu^2 \cdot 10^3}, \quad B_e^* = \frac{p_e h^2 p}{\mu^2 \cdot 10^3}.$$

It is obvious from the figure that:

1) If  $r_e/h = \text{const}$ , for an increase in  $\alpha_n$ , the

derivative  $\left. \frac{dD^*}{d(B_0^* - B_e^*)} \right|_{(B_0^* - B_e^*)=0}$  decreases, i.e., if

$r_n$  decreases for the same pressure drop value  $\Delta p$  at the "nozzle-baffle" throttle, the force becomes smaller;

2) If  $\alpha_n = \text{const}$ ,  $h = \text{const}$ , and  $\Delta p = \text{const}$ , while

$r_e$  increases,  $\left. \frac{dD^*}{d(B_0^* - B_e^*)} \right|_{(B_0^* - B_e^*)=0}$  becomes

larger, and the force increases, i.e., if  $r_n$  and  $r_e$  increase by the same amount, the force becomes larger;

3) If  $r_n = \text{const}$ ,  $h = \text{const}$ , and  $\Delta p = \text{const}$ , while  $r_e$  increases, it can be readily shown that

$\left. \frac{dD^*}{d(B_0^* - B_e^*)} \right|_{B_0^* - B_e^*=0}$  increases, i.e., the force becomes larger;

4) If  $r_e = \text{const}$  and  $h = \text{const}$ , the larger  $\alpha_n$ , i.e., the smaller  $r_n$ , the smaller the  $\Delta p$  values for which the force becomes negative;

5) If  $\alpha_n = \text{const}$  and  $h = \text{const}$ , the larger  $r_e$  and  $r_n$ , the larger the  $\Delta p$  values for which the force becomes negative;

6) If  $r_n = \text{const}$  and  $h = \text{const}$ , the larger  $r_e$ , the larger the  $\Delta p$  values for which the force becomes negative.

Thus, by solving the system of hydrodynamic equations for an incompressible viscous liquid, we have obtained the following characteristics:

1) the pressure field under the baffle

$$B - B_e = 6A \ln \alpha - 16.78(\alpha^2 - 1)A^2, \quad (43)$$

2) the discharge characteristic

$$B_0 - B_e = 6A \ln \alpha_n + (16.78 - 4.28\alpha_n^2)A^2, \quad (44)$$

3) the power characteristic

$$D = 3A(\alpha_n^3 - 1) + 16.78A^2\alpha_n^2(0.248 - 2 \ln \alpha_n). \quad (45)$$

Consequently, if we know the pressure drop  $B_0 - B_e$  at the "nozzle-baffle" throttle and the nozzle parameters  $\alpha_n$ , we can find the discharge  $A$  from Eq. (44), and, if we know  $A$ , we can determine the force  $D$  by using (45) and the pressure field  $B - B_e$  under the baffle by using (43). The obtained results are valid only for laminar flow.

If the "nozzle-baffle" element is used in pneumatic devices, where the working fluid is air, the pressure field and the discharge and power characteristics for an ideal viscous gas must be obtained. For calculating the pressure field of a viscous compressible fluid, we shall use the pressure distribution obtained for a viscous incompressible fluid and applied to an infinitely small region.



Fig. 5.

## 2. THE CASE OF A VISCOUS COMPRESSIBLE FLUID

### Determination of the Pressure Field under the Baffle

By using relation (28), we shall write the expression for the pressure drop  $dp$  for an infinitely small element with the radius  $dr$ , where the liquid can be considered to be incompressible, i.e., where  $\rho = \text{const}$ :

$$dp = -\frac{6G\mu}{\pi h^3 p} \ln \frac{r+dr}{r} - 0.1678 \frac{G^2}{\pi^2 h^2 p} \left[ \frac{1}{(r+dr)^2} - \frac{1}{r^2} \right]. \quad (46)$$

By expanding  $\ln(r+dr)/r$  into a power series with respect to  $dr$ , and by neglecting small quantities of the second order, we obtain

$$dp = -\frac{6G\mu}{\pi h^3 p} \frac{dr}{r} + 2 \cdot 0.1678 \frac{G^2 dr}{\pi^2 h^2 r^3 p}. \quad (47)$$

If we consider the fluid to be an ideal gas and assume that the flow is polytropic, we obtain

$$\rho = \rho^* \left( \frac{p}{p_{\text{atm}}} \right)^{1/n}, \quad (48)$$

where  $n$  is the polytropic exponent, and  $\rho^*$  is the density at atmospheric pressure  $p_{\text{atm}}$ .

If we substitute relation (48) in relation (47) and integrate the obtained expression, we shall find the pressure distribution along the radius, which will have the following form when expressed in terms of criterion numbers:

$$B \frac{n+1}{n} - B_e \frac{n+1}{n} = \frac{n+1}{n} [6A \ln \alpha - 16.78A^2(\alpha^2 - 1)] B_{\text{atm}}^{\frac{1}{n}} \quad (49)$$

where

$$B = \frac{ph^4 p^*}{\mu^2 r_e^2 \cdot 10^3}, \quad B_e = \frac{p_e h^4 p^*}{\mu^2 r_e^2 \cdot 10^3}, \\ B_{\text{atm}} = \frac{p_{\text{atm}} h^4 p^*}{\mu^2 r_e^2 \cdot 10^3}, \quad A = \frac{Gh}{\pi \mu r_e^2 \cdot 10^3}, \quad \alpha = \frac{r_e}{r}.$$

If the process is isothermic, i.e.,  $n = 1$ , the pressure distribution along the radius will be

$$B^2 - B_e^2 = 2 [6A \ln \alpha - 16.78A^2(\alpha^2 - 1)] B_{\text{atm}} \quad (50)$$

An approximate solution of the system of hydrodynamic equations for a viscous compressible fluid has been obtained in [7], which is here presented in terms of the same criteria numbers:

$$B \frac{n+1}{n} - B_e \frac{n+1}{n} = \frac{n+1}{n} [6A \ln \alpha - 21A^2(\alpha^2 - 1)] B_{\text{atm}}^{\frac{1}{n}} \quad (51)$$

### The Discharge Characteristic

If the fluid flowing through the nozzle is considered to be compressible, but not viscous, then, by means of the St. Venant-Wenzel equation, we can express the pressure  $p_n$  at the nozzle radius in terms of the pressure  $p_0$  in front of the baffle and the discharge  $G$ :

$$\frac{n-1}{n} \left[ B_0^{\frac{n-1}{n}} - B_n^{\frac{n-1}{n}} \right] = 12.5 \frac{B_{\text{atm}}^{\frac{1}{n}}}{h^{2/n}} \alpha_n^2$$

where

$$B_0 = \frac{p_0 h^4 p^*}{\mu^2 r_e^2 \cdot 10^3}, \quad B_e = \frac{p_e h^4 p^*}{\mu^2 r_e^2 \cdot 10^3}. \quad (52)$$

By applying relation (49) to the point  $r = r_n$ , i.e., assuming that  $\alpha = \alpha_n$  and  $B = B_n$  in this relation, and by using relation (52), we shall obtain the discharge characteristic for a polytropic fluid outflow from the "nozzle-baffle" element:

$$\frac{n-1}{n} \left[ B_0^{\frac{n-1}{n}} - B_n^{\frac{n-1}{n}} \right] = 12.5 A^2 \alpha_n^2 \frac{B_{\text{atm}}^{1/n}}{B_n^{2/n}}, \\ B \frac{n+1}{n} - B_e \frac{n+1}{n} = \frac{n+1}{n} [6A \ln \alpha_n - 16.78A^2(\alpha_n^2 - 1)] B_{\text{atm}}^{1/n} \quad (53)$$



If the fluid outflow is considered to be isothermic,

$$\rho = p \frac{\rho^*}{p_{atm}} \quad (54)$$

By substituting this relation in the Bernoulli equation for a compressible fluid:

$$\int_{p_0}^{p_n} \frac{p_{atm}}{p^*} \frac{dp}{p} + \frac{\bar{v}_r^2}{2} = 0, \quad (55)$$

where

$$\bar{v}_r = \frac{1}{h} \int_0^h v_r dz = \frac{G p_{atm}}{2\pi r_n h p^*},$$

and by integrating the obtained expression, we shall find the relation between the pressure  $p_n$  at the nozzle radius and the pressure  $p_0$  in front of the baffle:

$$\ln \frac{B_0}{B_n} = 12.5 A^2 \alpha_n \frac{B_{atm}}{B_n^2} \quad (56)$$

If we apply relation (49) to the point  $r = r_n$  and use relation (56), we obtain the discharge characteristic for an isothermic outflow from the "nozzle-baffle" element:

$$B_0 = \sqrt{B_e^2 + 2[6A \ln \alpha_n - 16.78 A^2 (\alpha_n^2 - 1)] B_{atm}} \times \exp \frac{12.5 A^2 \alpha_n^2 B_{atm}}{B_e^2 + 2[6A \ln \alpha_n - 16.78 A^2 (\alpha_n^2 - 1)] B_{atm}} \quad (57)$$

Figure 6 shows a comparison between the discharge characteristics calculated according to Eq. (57), which are represented by a solid line, and experimental data for different distances between the nozzle and the baffle plate, which are plotted as solid lines with points. The experimental data, which were taken from [8], were obtained for a nozzle with  $r_n = 0.613$  mm and  $r_e = 1.61$  mm. The working fluid was air, for which  $\rho^* = 11.8 \times 10^{-10}$  kg·sec<sup>2</sup>/cm<sup>4</sup>,  $\mu = 1.845 \times 10^{-10}$  kg·sec/cm<sup>2</sup>,  $t = 20^\circ\text{C}$ , and  $p_{atm} = 746$  mm Hg.

It is obvious from relation (57) that, for a certain value of  $A$ , the expression

$$B_e^2 + 2[6A \ln \alpha_n - 16.78 A^2 (\alpha_n^2 - 1)] B_{atm}$$

becomes equal to zero, and  $B_0$  becomes indeterminate. If we develop this indeterminacy, we find that  $B_0 \rightarrow \infty$  for

$$B_e^2 + 2[6A \ln \alpha_n - 16.78 A^2 (\alpha_n^2 - 1)] B_{atm} \rightarrow 0.$$

Consequently, the calculated discharge characteristics will have asymptotes, whose equation will be

$$B_e^2 + 2[6A \ln \alpha_n - 16.78 A^2 (\alpha_n^2 - 1)] B_{atm} = 0. \quad (58)$$

It can be seen from Fig. 6 that the theoretical characteristics are qualitatively in good agreement with experimental data, while their quantitative agree-

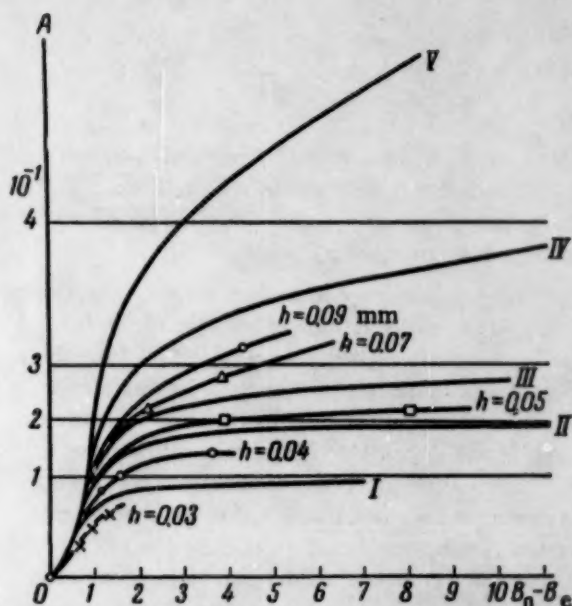


Fig. 6. Dependence of the discharge of a viscous compressible fluid through the "nozzle-baffle" throttle on the pressure drop at the throttle for different gaps between the nozzle and the baffle plate.

ment is not satisfactory. The quantitative disagreement becomes greater with an increase in the gap  $h$  between the nozzle and the baffle. The correction for the theoretical characteristic, which is obtained by taking into account the viscosity of the fluid flowing through the nozzle, is negligibly small and does not reduce the disagreement between the theoretical and experimental curves. Consequently, the quantitative disagreement can be explained by the fact that the outflow becomes turbulent, while the turbulence increases with an increase in the gap  $h$  between the nozzle and the baffle, and also by the fact that the discharge values exceed the maximum value.

#### The Power Characteristic

Relation (49) describes the pressure distribution along the end-face radius for  $r_n \leq r \leq r_e$ . Moreover, it is assumed that, for  $0 \leq r \leq r_n$ , the pressure changes according to the equation

$$p = p_0 - \frac{p_0 - p_n}{r_n} r. \quad (59)$$

Thus, the pressure distribution law for the entire baffle plate surface is known. By integration over the surface, we obtain the power characteristics of the "nozzle-baffle" element for a viscous compressible fluid:

$$D = \frac{1}{3} B_0 + \frac{2}{3} B_n - B_e + \left( \frac{B_{atm}}{B_e} \right)^{\frac{1}{n}} (12A - 4 \cdot 16.78 A^2) \left( \frac{1}{6} \alpha_n^2 + \frac{1}{3\alpha_n} - \frac{1}{2} \right). \quad (60)$$

where

$$D = \frac{Fh^4\rho^*}{\pi\mu^2 r_n^2 r_e^2 10^2}.$$

If  $n \neq 1$ ,  $B_n$  is determined by relation (52), and the discharge criterion A is determined by relation (53). If  $n = 1$ ,  $B_n$  is determined by relation (56), and the discharge criterion A is determined by relation (57).

Figure 7 provides a comparison between experimental data and the calculated characteristic of the force action on the baffle, which was obtained for isothermic flow according to Eq. (60). The characteristics were determined in dependence on the distance  $h$  between the nozzle and the baffle for a certain given pressure drop. The experimental data, which were borrowed from [8], are represented by the line I, and the theoretical curve is shown by the line II. The criterion  $D^* = F/\pi p_e r_n^2$  is plotted on the axis of ordinates, and  $B_e = p_e h^4 \rho^* / \mu^2 r_e^2 \cdot 10^2$  is plotted on the axis of abscissas. The experiments and calculations were performed for air for  $r_n = 0.5$  mm,  $\alpha_n = 4.45$ ,  $p_0 - p_e = 0.5$  kg/cm<sup>2</sup>,  $\mu = 1.845 \times 10^{-10}$  kg·sec/cm<sup>2</sup>, and  $\rho^* = 11.8 \times 10^{-10}$  kg·sec<sup>2</sup>/cm<sup>4</sup>.

It is obvious from the figure that, also in this case, a good qualitative agreement is observed, while the results do not agree quantitatively, which also indicates that the flow is turbulent and that the discharge A values exceed the maximum values.

#### SUMMARY

1. The pressure field under the baffle plate and the discharge and the power characteristics of a "nozzle-baffle" element for a compressible and an incompressible viscous liquid flow were obtained.

2. The applicability limits for the theoretical discharge characteristic were established.

3. The theoretical characteristics for an incompressible fluid were compared with experimental data. A good agreement was observed for Reynolds numbers smaller than 800. For Reynolds numbers larger than 800, a good qualitative agreement was observed, while the quantitative correspondence was not satisfactory.

4. We compared the theoretical characteristics for a compressible fluid with experimental data, and it was found that a good qualitative agreement exists even in the region of discharge A values which exceed the maximum value.

5. We investigated the influence of the nozzle parameters  $r_n$  and  $r_e$  on the discharge and the power characteristics.

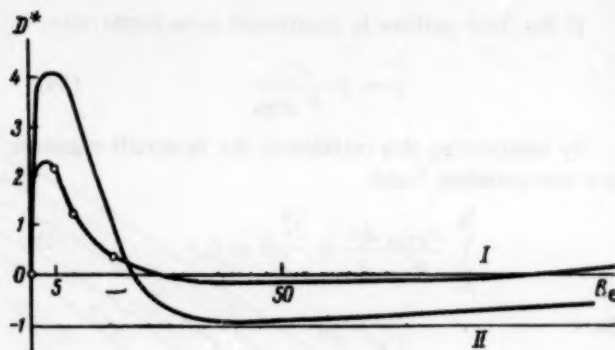


Fig. 7. Dependence of the force acting on the baffle plate from the side of the viscous compressible fluid stream on the gap between the nozzle and the baffle.

#### LITERATURE CITED

1. N. A. Slezkin, "Viscous liquid flow in a cone and between two cones," *Matematicheskii Sbornik* **42**, 1 (1935).
2. T. M. Bashta, *Aircraft Hydraulic Drives and Units* [in Russian] (Oborongiz, 1951).
3. N. P. Shumskii, "Results of experimental and theoretical investigations of control devices of the 'nozzle-baffle' type," *Systems, Devices, and Elements in Pneumatic and Hydraulic Automation* [in Russian] (Izd. AN SSSR, 1959).
4. J. H. McGinn, "Observations on the radial flow of water between fixed parallel plates," *Appl. Scient. Res. A*, **5**, 4 (1955).
5. I. M. Krassov and B. G. Turbin, "Dynamic effect of flow in a 'nozzle-baffle' hydraulic amplifier," *Avtomatika i Telemekhanika* **20**, 12 (1959).†
6. E. A. Andreeva, "Calculation of static characteristics of the 'nozzle-baffle' element," *Systems, Devices, and Elements in Pneumatic and Hydraulic Automation* [in Russian] (Izd. AN SSSR, 1959).
7. M. Raymond Comolet, "Nombre de Reynolds critique d'un écoulement visqueux, radial divergent entre deux plans parallèles," *L'Académie des sciences, Paris, Comptes rendus* **244**, 11 (Fevrier, 1957).
8. V. N. Dmitriev, *Experimental and Theoretical Investigation of a Pneumatic Relay of the "Nozzle-Baffle" Type: Dissertation for the Degree of Candidate of Technical Sciences* (Institute Avtomatika i Telemekhaniki AN SSSR, 1955).
9. E. A. Andreeva, "Calculation of static characteristics of a pneumatic 'nozzle-baffle' element," *Problems in Pneumatic and Hydraulic Automation* [in Russian] (Izd. AN SSSR, 1960).

† See English translation.

# DYNAMIC CHARACTERISTICS OF A "JET AMPLIFIER - SERVOMECHANISM" SYSTEM

B. D. Kosharskii

Khar'kov

Translated from *Avtomatika i Telemekhanika*, Vol. 21, No. 7,

pp. 997-1006, July, 1960

Original article submitted December 30, 1959

The structural layouts and the basic dynamic characteristics of a linearized "jet amplifier - servomechanism" system are investigated for the cases where single- and two-stage amplifiers are used.

Theoretical and experimental frequency characteristics are given.

The aim of the present article is to determine the basic dynamic characteristics of a linearized "jet amplifier - servomechanism" system for the parameter interval which is encountered in industrial devices.

Figure 1 shows the schematic and the structural layouts of elements in a "single-stage amplifier - servomechanism" system. The presence of a velocity feedback section in this layout is determined by the fact that, when the servomechanism is immobile, the pressure drop in the receiving nozzles of the nozzle plate differs from the pressure drop behind the receiving nozzles when the servomechanism piston moves. The hydraulic phenomena which occur in this case have been considered in detail in [1].

The jet tube motion is generally described by the differential equation\*

$$\frac{1}{L_{jt}} \left( I_{jt} \frac{d^2 \sigma_j}{dt^2} + H_{jt} \frac{d \sigma_j}{dt} + M_{jt} \sigma_j \right) = M_c, \quad (1)$$

where  $I_{jt}$  is the moment of inertia of the jet amplifier kinematic system, equal to  $2 \times 10^{-3}$  kg·cm·sec<sup>2</sup>,  $H_{jt}$  is the coefficient of viscous friction, which arises due to the fact that the jet tube end is immersed in the amplifier oil tank (on the basis of our experimental data, which are given in [2], the value of  $H_{jt}$  depends on the input signal frequency  $\omega$  and is equal to  $1.1 \times 10^{-3} \sqrt{\omega}$  kg·cm·sec),  $M_c$  is the control moment which is applied to the jet tube,  $M_{c \max} = 35 \times 10^{-3}$  kg·cm,  $\sigma_j$  is the linear deviation of the jet tube end with respect to its equilibrium position,  $\sigma_{j \max} = 0.15$  cm,  $L_{jt}$  is the jet tube length from the rotation axis to the outlet section of the conical endpiece, equal to 16.6 cm, and  $M_{jt}$  is the moment due to the mass of statically unbalanced elements of the amplifier kinematic system which is reduced to the jet tube and is equal to  $2 \times 10^{-3}$  kg·cm.

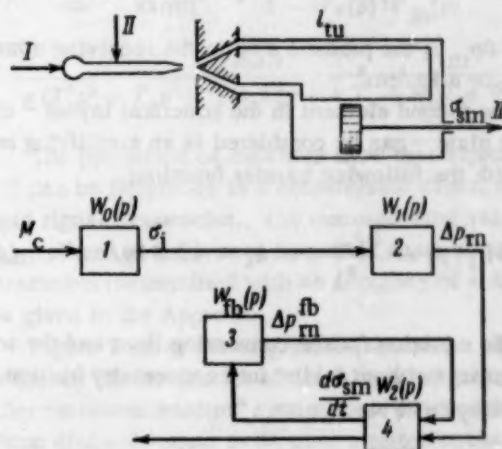


Fig. 1. I) Working agent feed; II) control moment; III) to regulating unit; 1) jet tube; 2) nozzle plate; 3) velocity feedback; 4) connecting lines and servomotor.

The transfer function of the first element in the structural layout - the jet tube - will be written in the following form:

$$W_0(p) = \frac{\sigma_j}{M_c} = \frac{k_0}{T_1^2 p^2 + T_2 p + 1}, \quad (2)$$

where

$$k_0 = L_{jt} / M_{jt}, \quad T_1^2 = I_{jt} / M_{jt}, \quad T_2 = H_{jt} / M_{jt}.$$

\* This equation is somewhat different from the similar equation given in [2], since a combination of a jet tube with two springs can be considered as a particular case, which is encountered only in certain types of regulators.



With the numerical values, this equation will be

$$W_0(p) = \frac{8200}{p^3 + 0.54 \sqrt{\omega} p + 1}.$$

In order to obtain the over-all jet amplifier characteristic, it is necessary to consider the equation which characterizes the pressure variation in the receiving nozzles when the jet tube is deflected. This dependence, which has been considered in [1], has a rather complicated form; however, it can be considered as linear if we assume with a certain degree of accuracy that the oil does not move in the receiving nozzles. According to the obtained experimental data, this characteristic remains unchanged in a wide range of the working medium pressure values at the jet tube inlet ( $p_{jc} = 3-20 \text{ kg/cm}^2$ ) and is described by the equation

$$\Delta p_{rn} = 0.8 p_{jc} \frac{\sigma_j}{\sigma_{j \max}}, \quad (3)$$

where  $\Delta p_{rn}$  is the pressure drop in the receiving nozzles, and  $p_{jc} = 8 \text{ kg/cm}^2$ .

The second element in the structural layout - the nozzle plate - can be considered as an amplifying section with the following transfer function:

$$W_1(p) = \frac{\Delta p_{rn}}{\sigma_j} = k_1 = 42.8 \text{ kg/cm}^2. \quad (4)$$

The equation for the connecting lines and the servomechanism (without taking into account dry friction and pure delay) will be:

$$m_t \frac{d^2 \sigma_{sm}}{dt^2} + h_t \frac{d \sigma_{sm}}{dt} = \Delta p_{rn} F_{sm} \quad (5)$$

where  $m_t = m_{pl} + m_0$ ;  $m_{pl}$  is the servomechanism piston mass and the reduced mass of all kinematic system links connected to the piston, approximately equal to  $0.11-0.13 \text{ kg} \cdot \text{sec}^2/\text{cm}$ , and  $m_0$  is the mass of the working liquid in the servomechanism cylinder and connecting lines, which is reduced to the piston;  $h_t = h_{pl} + h_{cy} + h_{tu}$  is the coefficient which characterizes the magnitude of viscous friction of the servomechanism mobile parts and of the working liquid in the cylinder and the connecting lines.

The magnitude of  $h_{pl} + h_{cy} < 0.0005 \text{ kg} \cdot \text{sec}/\text{cm}$ , and can be neglected in practice. Moreover, the following notation was used in Eq. (5):  $\sigma_{sm}$  is the servomechanism piston stroke ( $\sigma_{sm \max} = 20 \text{ cm}$ ), and  $F_{sm}$  is the servomechanism piston surface area, equal to  $50.2 \text{ cm}^2$ .

According to [3], the value of  $m_0$  is determined from the equation

$$m_0 = F_{sm} \frac{\gamma_o}{g} \left[ \sigma_{sm \max} + l_{tu} \left( \frac{d_{sm}}{d_{tu}} \right)^2 \right], \quad (6)$$

where  $l_{tu}$  is the over-all length of the connecting lines from the amplifier to the servomechanism (cm), equal to double the route length  $L$ ,  $d_{tu}$  is the connecting lines diameter, equal to 1 cm, and  $\gamma_o$  is the oil specific weight, equal to  $0.0009 \text{ kg/cm}^3$ .

With the numerical values,  $m_0 = 0.0009 + 0.003 l_{tu} \text{ kg} \cdot \text{sec}^2/\text{cm}$ .

Consequently,

$$m_t = 0.13 + 0.003 l_{tu}. \quad (7)$$

On the basis of Poiseuille's law, since the working liquid flow in the connecting lines is laminar, we can write

$$h_t \approx h_{tu} = 8\pi\mu l_{tu} e \left( \frac{d_{sm}}{d_{tu}} \right)^4, \quad (8)$$

where  $l_{tu} e$  is the equivalent length of the connecting lines, where all local resistances are taken into account, and  $\mu$  is the dynamic viscosity coefficient of the working liquid - transformer oil - for  $\gamma_o = 0.0009 \text{ kg/cm}^3$  and a viscosity of 2E, equal to  $\mu = 12 \times 10^{-8} \text{ kg} \cdot \text{sec}/\text{cm}^2$ .

In numerical form,  $h_t = 0.0124 l_{tu} e \text{ kg} \cdot \text{sec}/\text{cm}^2$ .

Equation (5) does not reflect the characteristics of the section under consideration with sufficient accuracy, since it does not take into account the effect of "pure delay", which is determined by the acceleration time  $\tau_a$  in the channel and the pressure propagation time  $\tau_p$  in the line.

The total "pure delay" time (without taking into account the elasticity of the connecting lines) is determined from the expression

$$\tau = \tau_a + \tau_p = \frac{\gamma_o d_{tu}^2}{32g\mu} + \frac{l_{tu}}{\lambda_o}, \quad (9)$$

where  $\lambda_o$  is the pressure propagation rate in the connecting oil line, equal to  $12 \times 10^4 \text{ cm/sec}$ .

In numerical form,  $\tau = 0.239 + l_{tu}/(12 \times 10^4)$ .

If we consider the delay, instead of Eq. (5), we shall write

$$\left( \frac{m_t}{F_{sm}} p + \frac{h_t}{F_{sm}} \right) \sigma_{sm} = \Delta p_{rn} e^{-p\tau}. \quad (10)$$

The section transfer function will be

$$W_2(p) = \frac{\sigma_{sm}}{\Delta p_{rn}} = \frac{e^{-p\tau}}{(T_3^2 p^2 + T_4 p) k_2} \quad (11)$$

where  $k_2 T_3^2 = m_t/F_{sm}$  and  $k_2 T_4 = h_t/F_{sm}$ .

If, for the case under consideration, we conventionally assume that  $l_{tue} \approx 1.2 l_{tu}$ † and consider that the

†The actual value of the  $l_{tue}$  depends on the device operating conditions and has to be accurately determined in each individual case.

$k_2$  coefficient is a proportionality factor, numerically equal to unity, we obtain

$$T_3^2 = (25 + 0.6l_{tu}) \cdot 10^{-4} \frac{\text{kg} \cdot \text{sec}^2}{\text{cm}^2},$$

$$T_4 = 3 \cdot 10^{-4} l_{tu} \frac{\text{kg} \cdot \text{sec}}{\text{cm}^2}.$$

According to [1], the velocity feedback equation will be

$$\Delta p_{rn}^{fb} = -0.92 \frac{\gamma_0 k_a}{g F_{rn}} \frac{d\sigma_{sm}}{dt} \times \left[ 2 \left( \sum_{i=0}^{i=m} \Delta F_{ri} v_{aFi} + \sum_{j=n}^{j=s} \Delta F_{rj} v_{aFj} \right) - k_a \frac{d\sigma_{sm}}{dt} \left( \sum_{i=0}^{i=m} \Delta F_{ri} - \sum_{j=n}^{j=s} \Delta F_{rj} \right) \right], \quad (12)$$

where  $F_{rn}$  is the receiving nozzle surface area, equal to  $0.27 \text{ cm}^2$ ,  $k_a = F_{sm}/F_{rn} \cos \beta$  ( $\beta$  is the receiving nozzle tilt angle with respect to the jet tube axis; for  $\beta = 0^\circ 30'$ ,  $k_a = 180$ ),  $\Delta F_{ri}$  and  $\Delta F_{rj}$  are the elementary receiving nozzle surface areas covered by the jet (the index  $i$  pertains to a nozzle completely covered with the jet, and the index  $j$  pertains to a nozzle partially covered by the jet)†, and  $v_{aFi}$  and  $v_{aFj}$  are the average jet velocities at the elementary area  $\Delta F_r$ .

The absolute value of the second term of the expression in square brackets in (12) is smaller than the first term value 25- to 60-fold, and it can be neglected. Therefore, instead of Eq. (12), we can write

$$\Delta p_{rn}^{fb} \approx -1.84 \frac{k_a \gamma_0}{g F_{rn}} \left( \sum_{i=0}^{i=m} \Delta F_{ri} v_{aFi} + \sum_{j=n}^{j=s} \Delta F_{rj} v_{aFj} \right) \frac{d\sigma_{sm}}{dt}.$$

If the jet tube is in the middle position, the quantity in parentheses is equal to  $F_{rn} v_{aFav}$ , where  $v_{aFav}$  is the average jet velocity at the transition section (for  $p_{jc} = 8 \text{ kg/cm}^2$ ,  $v_{aFav} = 780 \text{ cm/sec}$ ).

The expression in parentheses can be replaced by a simpler relation:

$$\sum_{i=0}^{i=m} \Delta F_{ri} v_{aFi} + \sum_{j=n}^{j=s} \Delta F_{rj} v_{aFj} \approx k_j F_{rn} v_{rav}$$

where  $k_j$  varies from 1.5 to 2.0 in dependence on the jet tube deflection; we assume that  $k_j \approx 1.75$ .

The velocity feedback equation, in its final form, will be

$$\Delta p_{rn}^{fb} = -1.84 \frac{k_a k_j \gamma_0 v_{aFav}}{g} \frac{d\sigma_{sm}}{dt}. \quad (13)$$

The velocity feedback transfer function will be determined by the expression

$$W_{fb}(p) = \frac{\Delta p_{rn}^{fb}}{\sigma_{sm}} = -k_{fb} T_s p, \quad (14)$$

where

$$k_{fb} T_s = 1.84 \frac{k_a k_j \gamma_0 v_{aFav}}{g} = 0.42 \frac{\text{kg} \cdot \text{sec}}{\text{cm}^2}$$

The transfer function of the entire "single-stage amplifier - servomechanism" system will be

$$W_{am}(p) = \frac{\sigma_{sm}}{M_c} = \frac{W_0(p) W_1(p) W_2(p)}{1 - W_3(p) W_{fb}(p)} = \frac{k_0 k_1 e^{-p\tau}}{p (T_1^2 p^2 + T_2 p + 1) (k_2 T_3^2 p + k_3 T_4 + k_{fb} T_s e^{-p\tau})}. \quad (15)$$

The performed calculations show that expression (15) can be simplified to a considerable extent for low input signal frequencies. The corresponding values of  $W_{am}(p)$  and of the system frequency characteristic parameters (determined with an accuracy of  $\sim 5\%$ ) are given in the Appendix.

Figure 2 shows the amplitude (a) and the phase (b) frequency characteristics of the "single-stage amplifier - servomechanism" system for a servomechanism piston diameter equal to 80 mm, a piston stroke of 200 mm, and for connecting line lengths equal to  $l_{tu} = 10-100 \text{ m}$  (which corresponds to a distance of 5-50 m from the regulator to the servomechanism).

In order to verify the calculation formulas, we processed the oscillograms obtained in testing a "single-stage amplifier - servomechanism" system. In the tests, the jet tube was rigidly connected to a mechanical generator of sinusoidal oscillations, i.e., the  $\sigma_j$  coordinate was subjected to forced sinusoidal oscillations.

In this case, instead of Eq. (15), the following equation is used for describing the system transfer function:

$$W_{am}^*(p) = \frac{\sigma_{sm}}{\sigma_{sm}} = \frac{k_0^* k_1 e^{-p\tau}}{p (k_2^* T_3^2 p + k_3^* T_4 + k_{fb}^* T_s e^{-p\tau})},$$

where  $k_j^* = 1$ .

As can be seen from Fig. 3, the agreement between the theoretical values and the experimental data (white points) is entirely satisfactory.

†This has been treated in detail in [1].

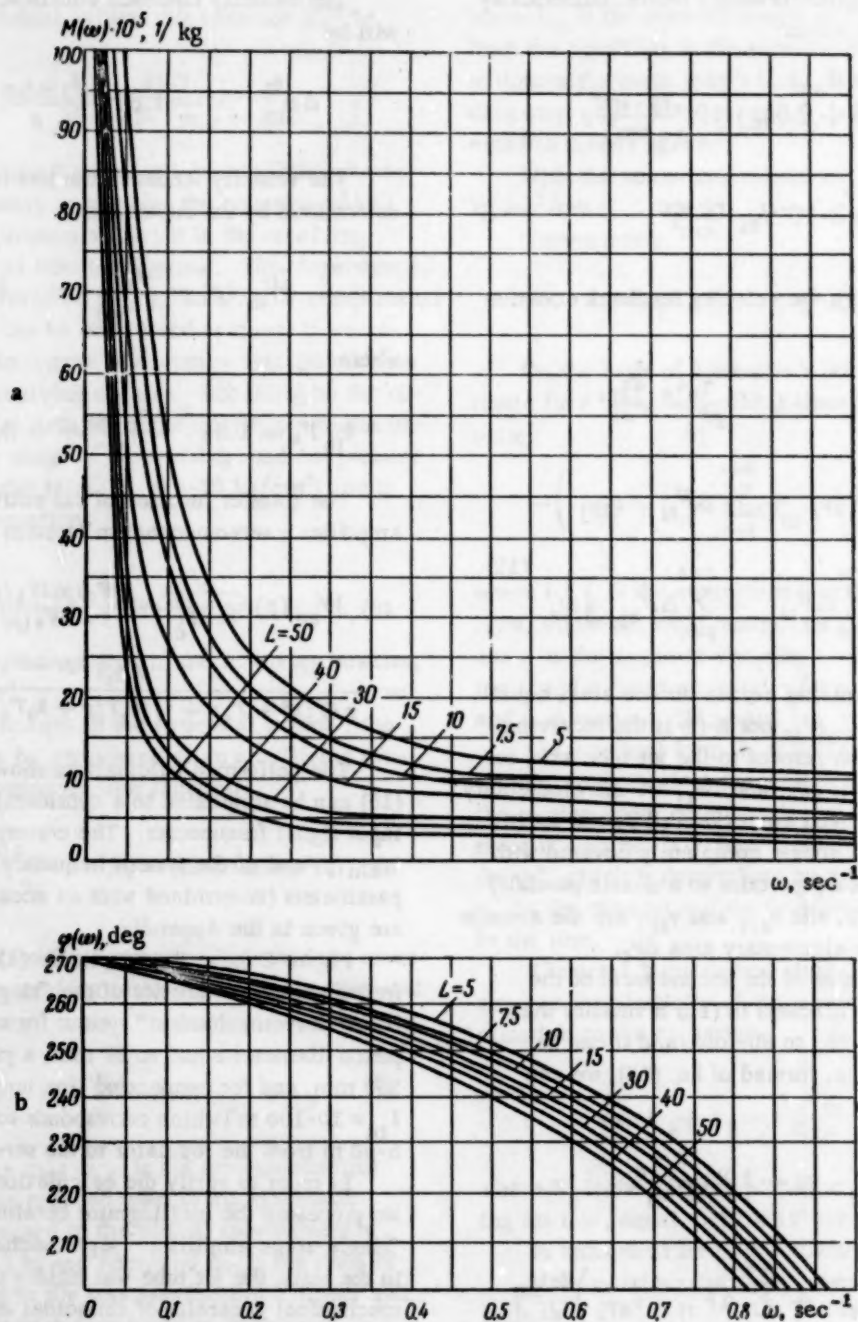


Fig. 2.

The "two-stage amplifier-servomechanism" system (Fig. 4) operates with different working medium pressures in the jet and the gate valve stages ( $p_{jc} = 8 \text{ kg/cm}^2$  and  $p_{vs} = 12-15 \text{ kg/cm}^2$ ).

Since, in the first amplification stage, the receiving nozzles are directly built into the gate valve piston, which follows the jet tube displacement, this element can be considered as a closed circuit with a feedback coefficient equal to unity [2].

Considering that the oil flow velocity in the gate valve receiving nozzles is slight and can be neglected,

the open-circuit equation of motion will be written thus:

$$m_v \frac{d^2 \sigma_v}{dt^2} + h_v \frac{d \sigma_v}{dt} = k_1 p_{jc} \frac{\sigma_c}{\sigma_{j \max}} F_{dv}, \quad (16)$$

where  $m_v$  is the mass of the gate valve parts and of the working liquid in the valve which is reduced to the piston and is approximately equal to  $0.0002 \text{ kg} \cdot \text{sec}^2/\text{cm}$ ,  $h_v$  is the coefficient characterizing the mag-



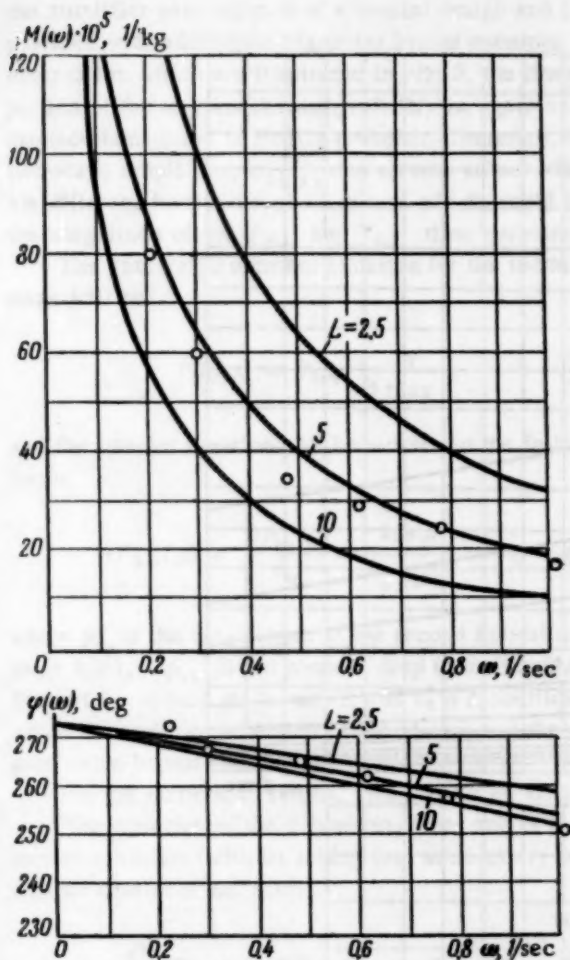


Fig. 3. The amplitude and the phase frequency characteristics of a "single-stage amplifier - servo-mechanism" system.

nitude of viscous friction in the gate valve element (it is assumed that  $h_v = 0.03 \text{ kg} \cdot \text{sec}/\text{cm}$ ,  $F_{dv}$  is the surface area of the small driving piston, equal to  $12.6 \text{ cm}^2$ , and  $\sigma_v$  is the gate valve linear displacement).

Equation (16) can be written in the following form:

$$(T_{3.1}^2 p^2 + T_{4.1} p) \sigma_v = \sigma_j, \quad (17)$$

where

$$T_{3.1}^2 = \frac{m \sqrt{j_{\max}}}{k_1 p_{jc} F_{dv}} = 3.7 \cdot 10^{-7} \text{ sec}^2,$$

$$T_{4.1} = \frac{h_v \sigma_j}{k_1 p_{jc} F_{dv}} = 0.5 \cdot 10^{-4} \text{ sec}.$$

The open-circuit transfer function will be

$$W_{1.1}^*(p) = \frac{\sigma_v}{\sigma_j} = \frac{1}{T_{3.1}^2 p^2 + T_{4.1} p} \quad (18)$$

The transfer function of the gate valve element is determined by the expression

$$W_{1.1}(p) = \frac{W_{1.1}^*(p)}{1 + W_{1.1}^*(p)} = \frac{1}{T_{3.1}^2 p^2 + T_{4.1} p + 1}. \quad (19)$$

The values of the  $T_{3.1}$  and  $T_{4.1}$  time constants mainly depend on the gate valve device design.

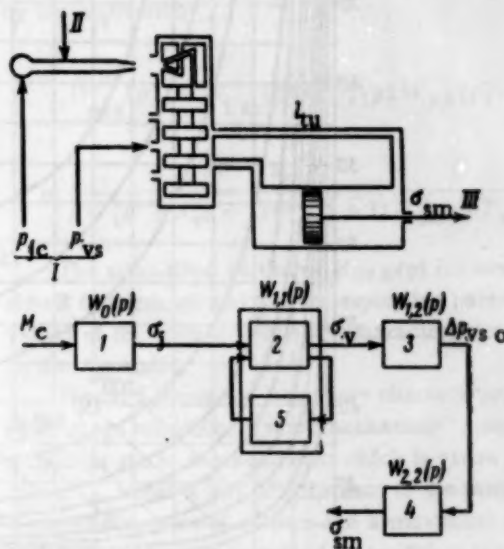


Fig. 4. Schematic diagram and the structural layout of a "two-stage amplifier - servo-mechanism" system. I), II), and III) same designation as in Fig. 1; 1) jet tube; 2) driving gate valve; 3) driven gate valve; 4) connecting lines and servomotors; 5) rigid feed-back.

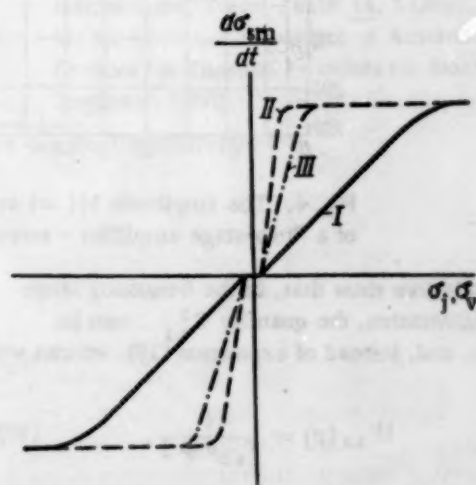


Fig. 5. Characteristics of single- and two-stage amplifiers. I) For a single- or two-stage amplifier if additional triangular bypass openings are provided in the gate valve; II) for a two-stage amplifier with rectangular bypass openings in the gate valve; III) for a two-stage amplifier with round bypass openings.

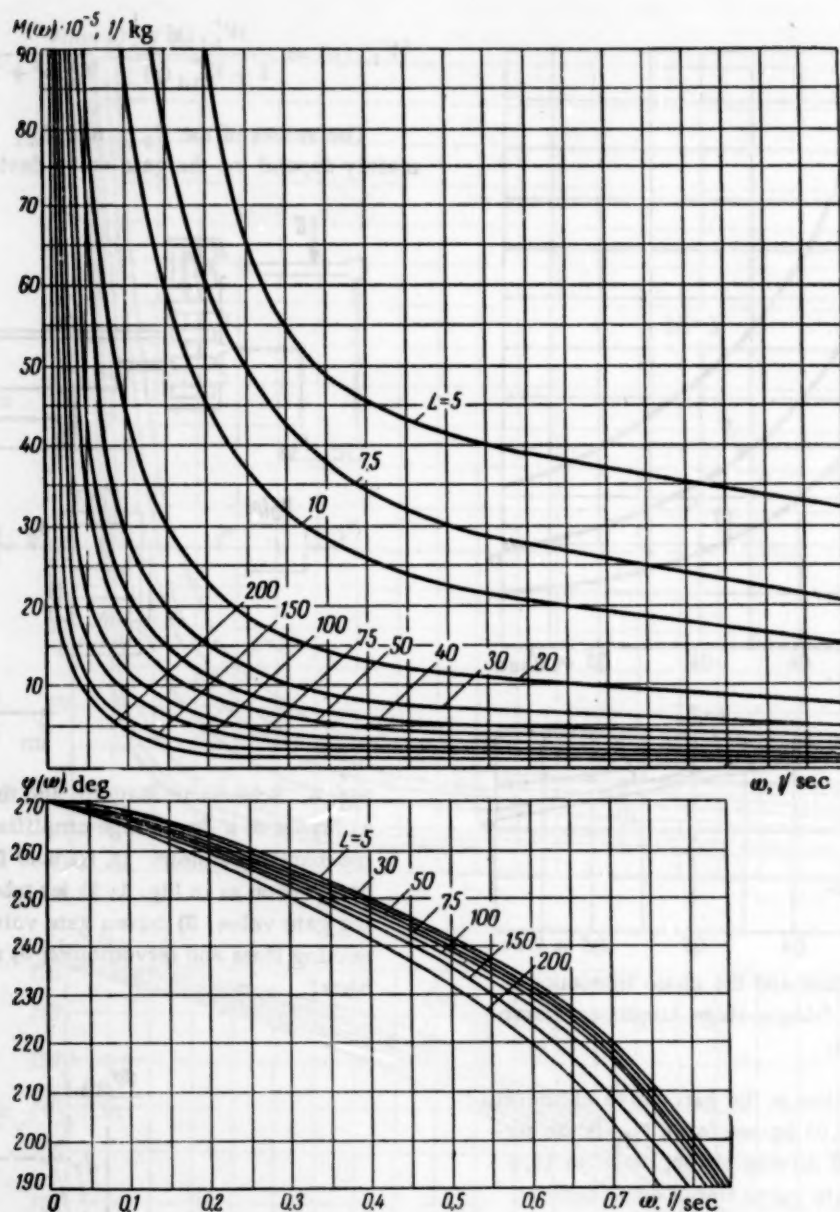


Fig. 6. The amplitude  $M(\omega)$  and the phase  $\varphi(\omega)$  frequency characteristics of a "two-stage amplifier - servomechanism" system.

Calculations show that, in the frequency range under consideration, the quantity  $T_{2.1}^2$  can be neglected, and, instead of expression (19), we can write

$$W_{1.1}(p) = \frac{1}{T_{4.1}p + 1}. \quad (20)$$

Thus, the transfer function of the first amplification stage in a two-stage amplifier will be

$$\begin{aligned} W_{1 \text{ am}}(p) &= W_0(p) W_{1.1}(p) = \\ &= \frac{k_0}{(T_1^2 p^2 + T_2 p + 1)(T_{4.1} p + 1)}. \end{aligned} \quad (21)$$

One of the basic advantages of "single-stage amplifier - servomechanism" systems which are used in hydraulic regulators, is a small insensitivity zone and a considerable length of the linear portion of the curve which characterizes the dependence of the servomechanism piston velocity on the input signal magnitude (Fig. 5). In many cases, the fulfillment of this condition is indispensable if a satisfactory regulation quality is to be secured.\*\*

Experiments show that, in two-stage amplifiers, the above-mentioned dependence is similar to the dependence for single-stage amplifiers only in the case where

\*\*For instance, in the case where two-pulse feed regulators for boiler units with hydraulic feedback are used.

the amplifier gate valve is of a special design and is provided with additional triangular bypass openings. In other cases, which are illustrated in Fig. 5, the linear portion of the servomechanism velocity vs. gate valve displacement curve is greatly reduced. Therefore, in two-stage amplifiers,  $\sigma_{j \max}$  can assume values which are different from those given above, which would affect the magnitude of the  $T_{3.1}$  and  $T_{4.1}$  time constants.

The gate valve element equation for the second stage will be

$$\Delta p_{vs0} = k_2 p_{vs} \frac{\sigma_v}{\sigma_{j \max}}, \quad (22)$$

and the transfer function will be written in the following form:

$$W_{1.2}(p) = \frac{\Delta p_{vs0}}{\sigma_v} = \frac{k_2 p_{vs}}{\sigma_{j \max}} = k_2', \quad (23)$$

where  $p_{vs}$  is the oil pressure at the second amplification stage inlet,  $\Delta p_{vs0}$  is the pressure drop in the connecting lines at the second stage outlet, and  $k_2$  is a coefficient which depends on the design of the pistons and the driven gate valve bypass openings.

For the numerical values,  $W_{1.2}(p) = 64 \text{ kg/cm}^3$ .

The equation of the connecting lines and of the servomechanism (without taking into account dry friction) will be similar to Eq. (10):

$$m_t \frac{d^2 \sigma_{sm}}{dt^2} + h_t \frac{d \sigma_{sm}}{dt} = \Delta p_{vs0} F_{sm} e^{-p\tau}, \quad (24)$$

However,  $m_t$ ,  $h_t$ ,  $F_{sm}$ ,  $\sigma_{sm}$ , and  $\tau$  can assume values which are different from those given above, since, in the case of two-stage amplifiers, different servomechanism types can be used and, correspondingly, the dimensions of the connecting lines can be different.

The section transfer function will be

$$W_{2.2}(p) = \frac{\sigma_{sm}}{\Delta p_{vs0}} = \frac{e^{-p\tau}}{p(T_{3.2}^2 p + T_{4.2})}, \quad (25)$$

where  $T_{3.2}^2 = m_t/F_{sm}$  and  $T_{4.2} = h_t/F_{sm}$ .

The over-all transfer function of the "two-stage amplifier - servomechanism" system will be determined by the expression

$$W_{0aa}(p) = W_{1am}(p) W_{1.2}(p) W_{2.2}(p) = \frac{k_0 k_2' e^{-p\tau}}{p(T_1^2 p^2 + T_2 p + 1)(T_{4.1} p + 1)(T_{3.2}^2 p + T_{4.2})} \quad (26)$$

The simplified values of  $W_{0aa}(p)$  for low input signal frequencies and the corresponding parameter values of the system frequency characteristics are given in the Appendix.

Figure 6 shows the frequency characteristics of a "two-stage amplifier - servomechanism" system (for the amplifier static characteristic which is given in Fig. 5, curve 1), where a servomechanism of the same type with a piston diameter of 80 mm and a maximum stroke of 200 mm for a route length of up to 200 m (i.e., for  $l_{tu} \leq 400 \text{ m}$ ) is used.

#### LITERATURE CITED

1. B. D. Kosharski, "Some problems in the design of hydraulic jet amplifiers", *Avtomatika i Telemekhanika* 17, 7 (1956).††
2. S. Z. Dushkas, and S. L. Cahn, "Analysis of some hydraulic components used in regulators and servomechanisms," *Trans. ASME* 74, 4 (May, 1952).
3. M. M. Gordon, *Calculation of Automatic Control Devices for Thermal Processes* [in Russian] (Metalurgizdat, 1956).

†† See English translation.



System	Input signal frequency, cps	Simplifications used	System transfer function $W_{\text{am}}(p) = \frac{a_{\text{ym}}}{A_C}$	Frequency characteristics	Values of the frequency characteristic parameters
Single-stage amplifier - servomechanism	$\omega > 0.3$	The transfer function and the frequency characteristic parameters are reduced with respect to theoretical dependences	$\frac{k_0 k_1 e^{-p\tau}}{p(T_1^2 p^2 + T_2 p + 1)(k_2 T_2^2 p + k_2 T_4 + k_{\text{fb}} T_6 e^{-p\tau})}$	Amplitude $M_{\text{am}}(\omega) = \frac{k_0 k_1}{\sqrt{R^2 + S^2}}$ Phase $\varphi_{\text{am}}(\omega) = \arctg \frac{S \cos \omega\tau - R \sin \omega\tau}{R \cos \omega\tau + S \sin \omega\tau}$	$R = k_2 T_1^2 T_2^2 \omega^4 - k_{\text{fb}} T_1^2 T_6 \omega^3 \sin \omega\tau - (k_2 T_2^2 + k_2 T_4 + k_{\text{fb}} T_2 T_6 \cos \omega\tau) \omega^2 + k_{\text{fb}} T_6 \omega \sin \omega\tau$ $S = (k_2 T_2 T_2^2 + k_2 T_1^2 T_4 + k_{\text{fb}} T_1^2 T_6 \cos \omega\tau) \omega^3 - k_{\text{fb}} T_2 T_6 \omega^2 \sin \omega\tau - (k_2 T_4 + k_{\text{fb}} T_6 \cos \omega\tau) \omega$
	$\omega = 0.05 - 0.3$	The transfer function is defined with respect to theoretical dependences, and the frequency characteristic parameters are reduced with respect to the simplified expressions	$\frac{k_0 k_1 e^{-p\tau}}{p(T_1^2 p^2 + T_2 p + 1)(k_2 T_2^2 p + k_2 T_4 + k_{\text{fb}} T_6 e^{-p\tau})}$	$\varphi_{\text{am}}(\omega) = \arctg \frac{S \cos \omega\tau - R \sin \omega\tau}{R \cos \omega\tau + S \sin \omega\tau}$	$R = -(k_2 T_2^2 + k_2 T_4 + k_{\text{fb}} T_2 T_6 \cos \omega\tau) \omega^2 + k_{\text{fb}} T_6 \omega \sin \omega\tau$ $S = (k_2 T_1^2 T_4 + k_{\text{fb}} T_1^2 T_6 \cos \omega\tau) \omega^3 - (k_2 T_4 + k_{\text{fb}} T_6 \cos \omega\tau) \omega$
	$\omega < 0.15$	The transfer function and the frequency characteristic parameters are reduced with respect to the simplified expressions	$\frac{k_0 k_1 e^{-p\tau}}{p(k_2 T_2^2 p + k_2 T_4 + k_{\text{fb}} T_6 e^{-p\tau})}$	$R = k_{\text{fb}} T_6 \omega \sin \omega\tau$ $S = -\omega(k_2 T_4 + k_{\text{fb}} T_6 \cos \omega\tau)$	
Two-stage amplifier - servomechanism	$\omega > 0.5$	The transfer function and the frequency characteristic parameters are defined with respect to theoretical dependences	$\frac{k_0 k_2 e^{-p\tau}}{p(T_1^2 p^2 + T_2 p + 1)(T_{4.1} p + 1)(T_{3.2} p + T_{4.2})}$	Amplitude $M_{\text{am}}(\omega) = \frac{k_0 k_2}{\sqrt{R_1^2 + S_1^2}}$ Phase $\varphi_{\text{Oad}}(\omega) = \arctg \frac{-(S_1 \cos \omega\tau + R_1 \sin \omega\tau)}{R_1 \cos \omega\tau - S_1 \sin \omega\tau}$	$R_1 = (T_2 T_{3.2}^2 T_{4.1} + T_1^2 T_{3.2}^2 + T_1^2 T_{4.1} T_{4.2}) \omega^4 - (T_{3.2}^2 + T_{4.1} T_{4.2} + T_2 T_{4.2}) \omega^3$ $S_1 = T_1^2 T_{3.2}^2 T_{4.1} \omega^5 - (T_{3.2}^2 T_{4.1} + T_2 T_{3.2}^2 + T_2 T_{4.1} T_{4.2}) \omega^3 + T_{4.2} \omega$
	$\omega = 0.15 - 0.5$		$\frac{k_0 k_2 e^{-p\tau}}{p(T_1^2 p^2 + T_2 p + 1)(T_{3.2} p + T_{4.2})}$	$\varphi_{\text{Oad}}(\omega) = \arctg \frac{-(S_1 \cos \omega\tau + R_1 \sin \omega\tau)}{R_1 \cos \omega\tau - S_1 \sin \omega\tau}$	$R_1 = T_1^2 T_{3.2}^2 \omega^4 - (T_{3.2}^2 + T_2 T_{4.2}) \omega^3$ $S_1 = -(T_2 T_{3.2}^2 + T_2 T_{4.2}) \omega^3 + T_{4.2} \omega$
	$\omega < 0.15$	The transfer function and the frequency characteristic parameters are defined with respect to the simplified expressions			$R_1 = -(T_{3.2}^2 + T_2 T_{4.2}) \omega^3$ $S_1 = -(T_2 T_{3.2}^2 + T_2 T_{4.2}) \omega^3 + T_{4.2} \omega$

# DETERMINATION OF MAXIMUM ERROR OF A BINARY MULTIPLIER

Yang Hsi-zeng

Peiping

Translated from *Avtomatika i Telemekhanika*, Vol. 21, No. 7,

pp. 1007-1014, July, 1960

Original article submitted September 30, 1959

A digital integrator scheme based on a binary multiplier is considered with analysis of its error due to fluctuations in the frequency of output pulses. A formula is derived for the maximum value of this error.

There is, at present, a wide field of application for digital integrators in digital differential analyzers, as well as in specialized computing devices. The accuracy of their work, however, has not until now been investigated [1, 2]. One type of error is considered in the present paper, namely, of a digital integrator based on binary multipliers [3], the error being due to fluctuations in the frequency of its output pulses. The outline of a digital integrator based on binary multipliers is shown in Fig. 1. The input and output pulses of the integrator are shown in Fig. 2.

The pulses  $f$  enter the binary counters  $C_0, C_1, \dots, C_n$ . At the output of each digital place of the counter, pulse series with frequencies  $f \cdot 2^{-1}, \dots, f \cdot 2^{-n}$  were obtained. These pulses proceed to the gates  $B_0, B_1, \dots, B_n$ , controlled by the corresponding digital places of the register. All the outputs of the gates are combined and fed to the output of the integrator. When "1" is retained in a given digital place, then the corresponding gate is open.

The number of pulses at the output of the integrator during time  $T$  is equal to

$$y = T f \sum_{k=1}^n k_k \cdot 2^{-k},$$

where  $k_1$  is the coefficient of the corresponding power of 2 in the binary representation of the number which is in the register;  $k_1$  are either 0 or 1.

We put into this formula  $x = \sum_{k=1}^n k_k \cdot 2^{-k}$ ; this is

the binary representation of the number in the register, and  $T = \sum_0^N \Delta t$  (where  $\Delta t = 1/f$ ) is the time period of travelling of the input pulses. We obtain as a result

$$y = f \sum_0^N x \Delta t \approx f \int_0^T x dt. \quad (1)$$

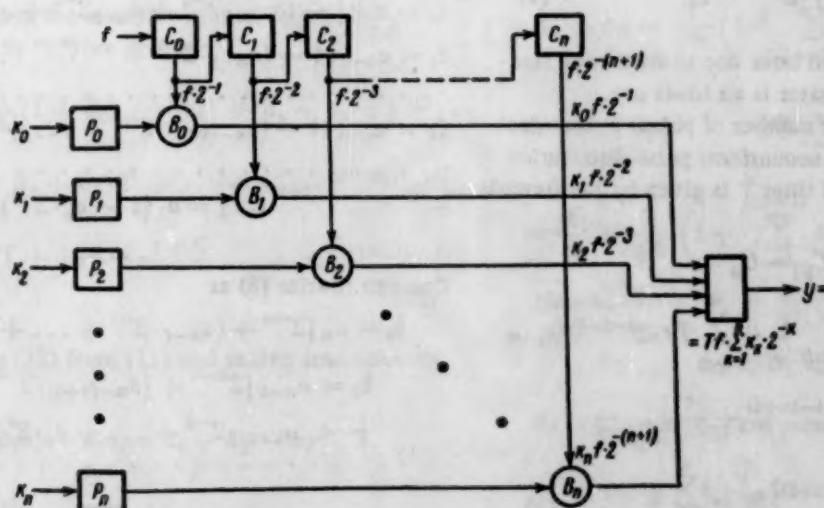


Fig. 1.

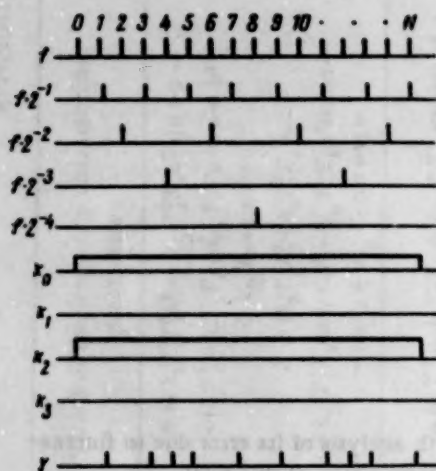


Fig. 2.

### 1. Maximum Frequency Fluctuation of an Integrator

The number of pulses at the output of a sum circuit within the time interval  $T$  is equal to [4]

$$C_{FI} = \sum_{i=0}^n \left[ T f \cdot 2^{i-(n+1)} + \frac{1}{2} \right]_{i.p.} k_i. \quad (2)$$

The subscript "i.p." denotes here that the integral part of the expression in square brackets should be taken. The time  $T$  can be expressed by the number  $N$  of pulses entering the counter  $C$ :

$$T = (a_0 \cdot 2^0 + a_1 \cdot 2^1 + \dots + a_n \cdot 2^n) \frac{1}{f} = \frac{N}{f}. \quad (3)$$

Should the number of pulses, which is determined by the code in the register, be distributed uniformly within the time interval  $2^{n+1}/f$ , then the number of pulses through the sum circuit would be equal to

$$C_u = \sum_{i=0}^n T f \cdot 2^{i-(n+1)} k_i. \quad (4)$$

In this case there is no error due to frequency fluctuation, that is, the integrator is an ideal one.

The difference in the number of pulses in the ideal integrator and one with a nonuniform pulse distribution at an arbitrary moment of time  $T$  is given by the formula

$$\begin{aligned} D &= C_{FI} - C_u = \\ &= \sum_{i=0}^n \left[ T f \cdot 2^{i-(n+1)} + \frac{1}{2} \right]_{i.p.} k_i - \sum_{i=0}^n T f \cdot 2^{i-(n+1)} k_i = \\ &= \sum_{i=0}^n \left\{ \left[ T f \cdot 2^{i-(n+1)} + \frac{1}{2} \right]_{i.p.} - \right. \\ &\quad \left. - T f \cdot 2^{i-(n+1)} \right\} k_i = \sum_{i=0}^n \delta_i. \end{aligned} \quad (5)$$

The above difference gives the error of an actual integrator as compared with the ideal one.

By substituting (3) into (5) and bearing in mind that

$$\sum_{n=2}^n \left[ \frac{1}{2} + a_i 2^{-p} \right]_{i.p.} = 0, \text{ one can express (5) as follows:}$$

$$\delta_0 = \frac{1}{2} k_0$$

$$[a_n - (a_{n-1} \cdot 2^{-1} + a_{n-2} \cdot 2^{-2} + \dots + a_0 \cdot 2^{-n})],$$

$$\delta_1 = \frac{1}{2} k_1 [a_{n-1} - (a_{n-2} \cdot 2^{-1} + \dots + a_0 \cdot 2^{1-n})],$$

$$\delta_k = \frac{1}{2} k_k [a_{n-k} - (a_{n-(k+1)} \cdot 2^{-1} + \dots + a_0 \cdot 2^{k-n})],$$

$$\delta_{n-1} = \frac{1}{2} k_{n-1} [a_1 - a_0 \cdot 2^{-1}], \quad (6)$$

$$\delta_n = \frac{1}{2} k_n a_0.$$

### 2. Positive Error Due to Frequency Fluctuations

As seen from (6), in order to obtain the maximum positive magnitude of  $D$ , it is necessary that the following be satisfied:

$$k_i = 0 \text{ for } a_{n-i} = 0, \quad k_i = 1 \text{ for } a_{n-i} = 1.$$

Were it not so, either some positive terms would be lost ( $k_i = 0$  when  $a_{n-i} = 1$ ), or negative ones added ( $k_i = 1$  when  $a_{n-i} = 0$ ), from the terms in the expression (6) for the error.

In view of the fact that in (6)  $k$  and  $a$  are two-valued variables, one can express the necessary condition for obtaining the maximum positive value of  $D$  in the form

$$k_i = a_{n-i}. \quad (7)$$

We substitute (7) into (5) and, denoting  $2\delta_i$  by  $\xi_i$ , we obtain

$$\xi_0 = a_n [1 - (a_{n-1} \cdot 2^{-1} + a_{n-2} \cdot 2^{-2} + \dots + a_0 \cdot 2^{-n})],$$

$$\xi_1 = a_{n-1} [1 - (a_{n-2} \cdot 2^{-1} + \dots + a_0 \cdot 2^{1-n})],$$

$$\xi_k = a_{n-k} [1 - (a_{n-(k+1)} \cdot 2^{-1} + \dots + a_0 \cdot 2^{k-n})],$$

$$\xi_{n-1} = a_1 (1 - a_0 \cdot 2^{-1}), \quad (8)$$

$$\xi_n = a_0.$$

One can rewrite (8) as

$$\xi_0 = a_n [2^{-n} + (\bar{a}_{n-1} \cdot 2^{-1} + \dots + \bar{a}_0 \cdot 2^{-n})],$$

$$\xi_k = a_{n-k} [2^{k-n} + (\bar{a}_{n-(k+1)} \cdot 2^{-1} + \dots + \bar{a}_0 \cdot 2^{k-n})], \quad (9)$$

$$+ a_{n-(k+2)} \cdot 2^{-2} + \dots + \bar{a}_0 \cdot 2^{k-n}],$$

$$\xi_{n-1} = a_1 (2^{-1} - \bar{a}_0 \cdot 2^{-1}), \quad \xi_n = a_0$$



or

$$\begin{aligned}\xi_0 &= \frac{a_n}{2^n} (1 + \bar{a}_0 \cdot 2^0 + \bar{a}_1 \cdot 2^1 + \dots + \bar{a}_{n-1} \cdot 2^{n-1}), \\ \xi_1 &= \frac{a_{n-1}}{2^{n-1}} (1 + \bar{a}_0 \cdot 2^0 + \bar{a}_1 \cdot 2^1 + \dots + \bar{a}_{n-2} \cdot 2^{n-2}), \\ &\dots \\ \xi_k &= \frac{a_{n-k}}{2^{n-k}} (1 + \bar{a}_0 \cdot 2^0 + \\ &+ \bar{a}_1 \cdot 2^1 + \dots + \bar{a}_{n-(k+1)} \cdot 2^{n-(k+1)}), \\ &\dots \\ \xi_{n-1} &= \frac{a_1}{2^1} (1 + \bar{a}_0), \\ \xi_n &= \frac{a_0}{2^0}\end{aligned}\quad (10)$$

and

$$\Delta_n = 2D = \sum_{p=0}^n \frac{a_p}{2^p} \left[ 1 + \sum_{s=1}^p \bar{a}_{s-1} \cdot 2^{s-1} \right] = \sum_{p=0}^n \xi_p, \quad (11)$$

where the bar over a letter denotes the complement of the given two-valued variable, that is,  $\bar{a}_{n-1} = 1 - a_{n-1}$ .

As seen from (11), the error  $\Delta_n$  consists of  $n+1$  component terms  $\xi_p$  ( $p$  assumes the values from 0 to  $n$ ). It is convenient to write (10) and (11) in terms of the digits "1" and "0". We denote the terms of error which are present when  $a_1 = 1$  by the symbol "1". Inversely, the terms of the error which are absent when  $a_1 = 0$  are denoted by the symbol "0". Now the  $a_1$ , which equal 1 or 0, appear as coefficients of the corresponding power of 2 of the number  $T$ .

It can be shown that taking the complement of all the terms  $\xi_p$  of the error in (11), except  $\xi_0$  and  $\xi_n$  which are in the state "1" (present), will not change the magnitude of the error  $\Delta$ .

Proof. Taking the complements of  $a_1, \dots, a_{n-1}$  ( $a_0$  and  $a_n$  remain "1") we obtain

$$\begin{aligned}\Delta_n &= \frac{a_0}{2^0} + \frac{\bar{a}_1}{2^1} (1 + \bar{a}_0) + \frac{\bar{a}_2}{2^2} (1 + \bar{a}_0 + a_1 \cdot 2^1) + \dots \\ &\dots + \frac{\bar{a}_p}{2^p} (1 + \bar{a}_0 + a_1 \cdot 2^1 + \dots + a_{p-1} \cdot 2^{p-1}) + \dots \\ &\dots + \frac{a_n}{2^n} (1 + \bar{a}_0 + a_1 \cdot 2^1 + \dots + a_{n-2} \cdot 2^{n-2}).\end{aligned}\quad (12)$$

Subtracting (12) from (11) and taking into account that

$$a_i \bar{a}_j - \bar{a}_i a_j = a_i + \bar{a}_j - 1, \quad (13)$$

one can show that

$$\Delta_n - \Delta'_n = 0 \quad \text{or} \quad \Delta_n = \Delta'_n. \quad (14)$$

### 3. Maximum Positive Error

The maximum positive error is attained when all the even terms  $\xi_0, \xi_2, \dots, \xi_{2p}$  of the error are present, and all the odd terms  $\xi_1, \xi_3, \dots, \xi_{2p-1}$  are absent.

Proof. We rewrite (11), putting now  $a_1 = 1$  for even  $i$  and equal 0 for odd  $i$ :

$$\Delta_{pM} = 1, 0, 1, \dots, 0, 1, 0, 1, 0, \dots, 0, 1. \quad (15)$$

It is being taken as valid that with the terms  $\xi_0$  and  $\xi_n$  always present, and all even terms present, and all odd ones absent in the terms  $\xi_{2p-1}, \dots, \xi_{n-1}$ , whatever the combination of presences and absences of the remaining terms  $\xi_1, \xi_2, \dots, \xi_{2p-2}$ , the error

$$\Delta_1 = 1, \xi_1, \xi_2, \dots, \xi_{2p-3}, \xi_{2p-2}, 0, 1, 0, 1, \dots, 0, 1 \quad (16)$$

never exceeds  $\Delta_{pM}$ , that is,  $\Delta_1 \leq \Delta_{pM}$ .

The inequality can be verified by putting  $p = 1, 2, 3, \dots$

We shall show now that the above assumption remains valid when instead of  $\xi_1, \xi_2, \dots, \xi_{2p-1}$  we take  $\xi_1, \xi_2, \dots, \xi_{2p}$ , in other words, that for the error

$$\Delta_2 = 1, \xi_1, \xi_2, \dots, \xi_{2p-3}, \xi_{2p-2}, \xi_{2p-1}, \xi_{2p}, 0, 1, \dots, 0, 1 \quad (17)$$

the inequality  $\Delta_2 \leq \Delta_{pM}$  is valid.

The change from (16) to (17) involves the appearance of two new terms  $\xi_{2p-1}$  and  $\xi_{2p}$ , and they can take any form, depending on their presence or absence. Four combinations are altogether possible: 0, 0; 1, 1; 1, 0; 0, 1.

Each case corresponding to a respective combination is considered separately:

a)  $\xi_{2p-1}$  and  $\xi_{2p}$  are absent (0, 0). Then

$$\Delta_3 = 1, \xi_1, \xi_2, \dots, \xi_{2p-3}, \xi_{2p-2}, 0, 0, 0, 1, 0, \dots, 0, 1. \quad (18)$$

We find the difference

$$\begin{aligned}\Delta_1 - \Delta_3 &= \frac{1}{2^{2p}} \left( 1 + \sum_{s=1}^{2(p-1)} \bar{a}_s 2^s + 2^{2p-1} \right) - \\ &- 2^{2p} \sum_{s=p+1}^{n/2} \frac{1}{2^{2s}} = \\ &= \frac{1}{6} + \frac{1}{2^{2p}} \left( 1 + \sum_{s=1}^{2(p-1)} \bar{a}_s 2^s \right) + \frac{1}{3} \frac{1}{2^{n-2p}} > 0.\end{aligned}$$

Hence,

$$\Delta_3 < \Delta_1 \leq \Delta_{pM}$$

b)  $\xi_{2p-1}$  and  $\xi_{2p}$  are present (1, 1). Then

$$\begin{aligned}\Delta_4 &= 1, \xi_1, \xi_2, \dots, \xi_{2p-3}, \xi_{2p-2}, \\ &1, 1, 0, 1, \dots, 0, 1, 0, 1.\end{aligned}\quad (19)$$

Taking the complements of all the terms in (19), except of  $\xi_0$  and  $\xi_n$ , we obtain the expression

$$\Delta'_4 = 1, \bar{\xi}_1, \bar{\xi}_2, \dots, \bar{\xi}_{2p-3}, \bar{\xi}_{2p-2}, \\ 0, 0, 1, 0, \dots, 1, 0, 1, 1. \quad (20)$$

Taking the complements of  $\xi_1, \dots, \xi_{2p-2}$  in (16), but leaving the remaining terms as they are, we obtain the expression

$$\Delta'_1 = 1, \bar{\xi}_1, \bar{\xi}_2, \dots, \bar{\xi}_{2p-3}, \bar{\xi}_{2p-2}, \\ 0, 1, 0, 1, \dots, 0, 1, 0, 1. \quad (21)$$

We form the difference

$$\Delta'_1 - \Delta'_4 = \sum_{k=p}^{n/2} \frac{1}{2^{2k}} \left[ 1 + \sum_{s=0}^{2(k-1)} a_s 2^s + \sum_{s=k}^{n/2} 2^{2s-1} \right] - \\ - \left\{ \sum_{k=p}^{n/2-1} \frac{1}{2^{2k+1}} \left[ 1 + \sum_{s=0}^{2k-2} a_s 2^s + \sum_{s=k}^{n/2-1} 2^s + 2^{2k-1} \right] + \right. \\ \left. + \frac{1}{2^n} \left[ 1 + \sum_{s=0}^{2p-2} a_s 2^s + \sum_{s=p}^{n/2-1} 2^{2s} + 2^{2p-1} \right] \right\} = \\ = \frac{1}{6} - \frac{1}{3} \frac{1}{2^{n-2p+1}} + \frac{1}{3} \left[ 1 + \sum_{s=0}^{2p-2} a_s 2^s \right] \left[ \frac{2}{2^{2p}} - \frac{1}{2^n} \right] > 0$$

or  $\Delta'_4 < \Delta'_1$ .

It follows from the proof given in Section 2 that  $\Delta'_4 = \Delta_4$ . In addition, we know that  $\Delta'_1 \leq \Delta_{pM}$ . Thus,  $\Delta_{pM} \geq \Delta'_1 > \Delta'_4 = \Delta_4$  and, therefore,  $\Delta_4 < \Delta_{pM}$ .

c)  $\xi_{2p-1}$  is present,  $\xi_{2p}$  absent (1,0). Then

$$\Delta_5 = 1, \xi_1, \xi_2, \dots, \xi_{2p-3}, \xi_{2p-2}, \\ 1, 0, 0, 1, \dots, 0, 1. \quad (22)$$

Taking the complements of all the terms in (22) except of  $\xi_0$  and  $\xi_n$ , we obtain the expression

$$\Delta'_5 = 1, \bar{\xi}_1, \bar{\xi}_2, \dots, \bar{\xi}_{2p-3}, \bar{\xi}_{2p-2}, \\ 0, 1, 1, 0, 1, 0, \dots, 1, 0, 1, 1. \quad (23)$$

Subtracting (23) from (21), we obtain

$$\Delta'_1 - \Delta'_5 = \sum_{k=p}^{n/2} \frac{1}{2^{2k}} \left[ 1 + \sum_{s=0}^{2k-2} a_s 2^s + \sum_{s=k}^{n/2} 2^{2s-1} \right] - \\ - \left\{ \sum_{k=p}^{n/2-1} \frac{1}{2^{2k+1}} \left[ 1 + \sum_{s=0}^{2k-2} a_s 2^s + \sum_{k+1}^{n/2-1} 2^{2s} + 2^{2k-1} \right] + \right. \\ \left. + \frac{1}{2^{2p}} \left[ 1 + \sum_{s=0}^{2p-2} a_s 2^s + 2^{2p-1} \right] + \frac{1}{2^n} \left[ 1 + \sum_{s=0}^{2p-2} 2^{2s} + \right. \right. \\ \left. \left. + 2^{2p-1} \right] \right\} = \frac{1}{3} \left[ \frac{1}{2} + \frac{5}{6} \frac{1}{2^{n-2p}} - \right. \\ \left. - \left( 1 + \sum_{s=0}^{2p-2} a_s 2^s \right) \left( \frac{1}{2^{2p}} + \frac{1}{2^{n-1}} \right) \right] > 0,$$

as

$$1 + \sum_{s=0}^{2p-2} a_s 2^s < 2^{2p-1}.$$

It follows from the relations  $\Delta'_5 = \Delta_5$  and  $\Delta'_1 = \Delta_{pM}$  that  $\Delta_{pM} \geq \Delta'_1 > \Delta'_5 = \Delta_5$  and, consequently,  $\Delta_5 < \Delta_{pM}$ .

d)  $\xi_{2p-1}$  absent,  $\xi_{2p}$  present (0,1). In this case, we obtain

$$\Delta_6 = 1, \xi_1, \xi_2, \dots, \xi_{2p-3}, \xi_{2p-2}, \\ 0, 1, 0, 1, \dots, 0, 1, \quad (24)$$

that is,  $\Delta_6 = \Delta_1$  (see (16)).

We have proved in this way that for any combination of presences and absences of the terms  $\xi_1, \xi_2, \dots, \xi_{2p}$

$$\Delta_2 \leq \Delta_{pM}.$$

This method can be generalized for an arbitrary number of terms, from  $\xi_1$  to  $\xi_{n-1}$ . Therefore, for any combination of presences and absences of  $\xi_1, \dots, \xi_{n-1}$ , we always have  $\Delta_7 \leq \Delta_{pM}$ , where

$$\Delta_7 = 1, \xi_1, \xi_2, \dots, \xi_{2p-3}, \xi_{2p-2}, \\ \xi_{2p-1}, \xi_{2p}, \xi_{2p+1}, \dots, \xi_{n-1}, \xi_n. \quad (25)$$

The magnitude of the maximum positive error can be evaluated from the formula

$$\Delta_{pM} = \frac{1}{2} \left[ \sum_{p=0}^{n/2} \frac{1}{2^{2p}} \left( 1 + \sum_{s=1}^p 2^{2s-1} \right) + \right. \\ \left. + r \frac{1}{2^{n+1}} \left( 1 + \sum_{s=1}^{n/2} 2^{2s-1} \right) \right] = \\ = \frac{1}{6} \left\{ n + \frac{1}{3} \left[ 10 + (-1)^{r+1} \frac{1}{2^n} \right] \right\},$$

where  $r = 1$  if  $n$  is odd and  $r = 0$  if  $n$  is even.

It follows from the proof in Section 2 that the maximum error appears twice for even  $n$  in the operation of an integrator:

1) when the number of input pulses and the value of

the number appearing in the register are  $\sum_{p=0}^{n/2} 2^{n-2p}$ , as

shown above;

2) when the number of input pulses and the value of

the number in the register are  $2^n + \sum_{p=0}^{n/2-1} 2^{n-2p-1} + 1$ .

With  $n$  odd, the maximum positive error also appears twice in the process of the integrator operation:

1) when the number of input pulses and the value of

the number of the register are  $\sum_{p=0}^{(n-1)/2} 2^{(n-1)-2p} + 2^n$ ;

2) when the number of input pulses and the value of

the number of the register are  $\sum_{p=0}^{n/2-1} 2^{n-2p} + 1$ .

#### 4. Maximum Negative Error

In order that the maximum negative error be attained, it is necessary, as seen from (6) that the conditions be established:  $k_1 = 0$  where  $a_{n-1} = 1$ , but  $k_1 = 1$  when  $a_{n-1} = 0$ , that is  $k_k = \bar{a}_{n-k}$ .

The expression for the negative error assumes the form

$$\Delta_n = \sum_{p=0}^n \mu_p = \sum_{p=0}^n \frac{\bar{a}_p}{2^p} \left( 1 + \sum_{s=1}^p a_{s-1} 2^{s-1} \right).$$

It can be shown, as in the case of the positive error, that taking the complements of all the terms  $\mu_p$  of the error, except the fixed  $\mu_0$  and  $\mu_n$  which have the state "1" (they are present), does not change the value of the error  $\Delta_n$ .

To determine the maximum negative error, the same method as for the positive error is used, and we obtain an expression for the maximum negative error:

$$\Delta_n.M = \frac{1}{2} \left\{ \sum_{k=0}^{n/2} \frac{1}{2^{2k}} \left( 1 + \sum_{i=1}^k 2^{2i-1} \right) + r \frac{1}{2^{n+1}} \times \right. \\ \left. \times \left( 1 + \sum_{i=1}^{n/2} 2^{2i-1} \right) \right\} = \frac{1}{6} \left\{ n + \frac{1}{3} \left[ 10 + (-1)^{r+1} \frac{1}{2^n} \right] \right\},$$

where  $r = 1$  for odd  $n$  and  $r = 0$  for even  $n$ .

The error  $\Delta_n.M$  appears twice when  $n$  is even:

1) when the number of input pulses is  $\frac{1}{3}(2^{n+1} + 1)$ ,

and the value of the number in the register is  $\sum_{p=0}^{n/2} 2^{n-2p}$ ;

2) when the number of input pulses is  $\frac{1}{3}(2^n - 1)$ ,

and the value of the number in the register is  $2^n + \sum_{p=0}^{n/2-1} 2^{n-2p-1} + 1$ .

It also appears twice when  $n$  is odd:

1) when the number of input pulses is  $\frac{1}{3}(2^{n+1} - 1)$ ,

and the value of the number in the register is  $2^n +$

$$+ \sum_{p=0}^{(n-1)/2} 2^{(n-1)-2p};$$

2) when the number of input pulses is  $\frac{1}{3}(2^n + 1)$ , and the value of the number in the register is

$$\sum_{p=0}^{n/2-1} 2^{n-2p} + 1.$$

#### SUMMARY

1. If  $n$  is even, the integration error is maximum when the values of the function under the integration sign are

$$\text{either } \sum_{p=0}^{n/2} 2^{n-2p} \text{ or } 2^n + \sum_{p=0}^{n/2-1} 2^{n-2p-1} + 1,$$

2. If  $n$  is odd, the integration error is maximum when the values of the function under the integration

$$\text{sign are either } 2^n + \sum_{p=0}^{(n-1)/2} 2^{(n-1)-2p} \text{ or } \sum_{p=0}^{n/2-1} 2^{n-2p} + 1,$$

3. The maximum integration error increases with the increasing number of members of the integrator.

4. The obtained formula may be applied to evaluate the maximum error of a system with several integrators used for solving equations.

In conclusion, the author wishes to express his sincere thanks to V. V. Karibskii for his assistance in the preparation of this paper.

#### LITERATURE CITED

1. R. E. Sprague, "Fundamental concepts of the differential analyzer method of computation," Math. Tables and Other Aids to Compute, 37 (1952).
2. Lundh Yngvar, "Digital technique for small computation," J. Brit. Inst. Radio Engrs, 19, 1 (January, 1959).
3. A. A. Voronov and G. N. Sokolov, "A device for programming curves of second order, based on a digital integrator," Avtomat. i Telemekh. 20, 2 (1959).\*
4. V. V. Karibskii, "On the error of a linear interpolator for digital programming control," Avtomat. i Telemekh. 20, 6 (1959).\*

\* See English translation.



# EXPONENTIAL CONVERTERS WITH A LOGARITHMIC TRANSFORMATION LAW

A. I. Novikov

Moscow

Translated from *Avtomatika i Telemekhanika*, Vol. 21, No. 7, pp. 1015-1025, July, 1960

Original article submitted January 19, 1960

Exponential converters with a logarithmic transformation law are considered. The basic equations which characterize the operation of converters are given. The errors are analyzed. Various converter variants are studied.

## INTRODUCTION

As a rule, a linear relation between the measured and the received parameter values is required in remote-measurement systems. This is explained by the fact that the taking and interpolation of readings can be conveniently performed on a linear scale, that the quantities to be measured can be added at the receiving end, and that the absolute error within the range can remain constant. A linear relation is usually secured by the application of linear converters.

A linear relation between the measured and the received parameters can be secured not only by means of linear converters. Let there be a converter, which we shall call a functional converter, where the parameter  $x$  to be measured is transformed into the analog  $y$  according to the equation

$$y = f(x). \quad (1)$$

Let us assume that  $x$ , in turn, is a function of  $\lambda$  and that it changes according to the law

$$x = \varphi(\lambda). \quad (2)$$

Then the transformed function, which is to be transmitted through the communication channel, will be

$$y = f[\varphi(\lambda)]. \quad (3)$$

Assume that the receiver contains a device whose characteristic is an inverse function with respect to the converter characteristic:

$$z = f^{-1}(y). \quad (4)$$

We shall call this device an inverse functional converter. Then, at the output of this converter, the received

signal will be equal to the transmitted quantity  $\varphi(\lambda)$ :

$$z = f^{-1}\{f[\varphi(\lambda)]\} = \varphi(\lambda). \quad (5)$$

Thus, the relation between the transmitted  $\varphi(\lambda)$  and the received  $z$  parameters will be linear, although the transformed parameter  $y$  changes nonlinearly in dependence on  $\varphi(\lambda)$ . The linear converter would constitute a particular case of the functional converter.

Certain types of functional converters secure a sufficiently high transformation stability, and they have simple circuits. The exponential converters which are considered below belong to this type.

## Basic Relations

In an exponential converter with a logarithmic transformation law, the voltage, which changes according to the  $Ee^{-t/\tau}$  or the  $E[1-e^{-t/\tau}]$  law, is compared with the data transmitter voltage.

The converter consists of a bridge circuit (Fig. 1).

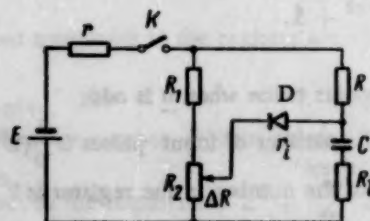


Fig. 1.

A resistor  $R_1$  and a potentiometric data transmitter  $R_2$  are connected to one branch of the bridge, and the resistor  $R$  and capacitor  $C$  are connected to the other branch. A diode  $D$  is provided in the bridge diagonal between the data transmitter  $R_2$  slider and capacitor  $C$ . A rectangular voltage is periodically supplied to the bridge by means of key  $K$  (Fig. 2a).

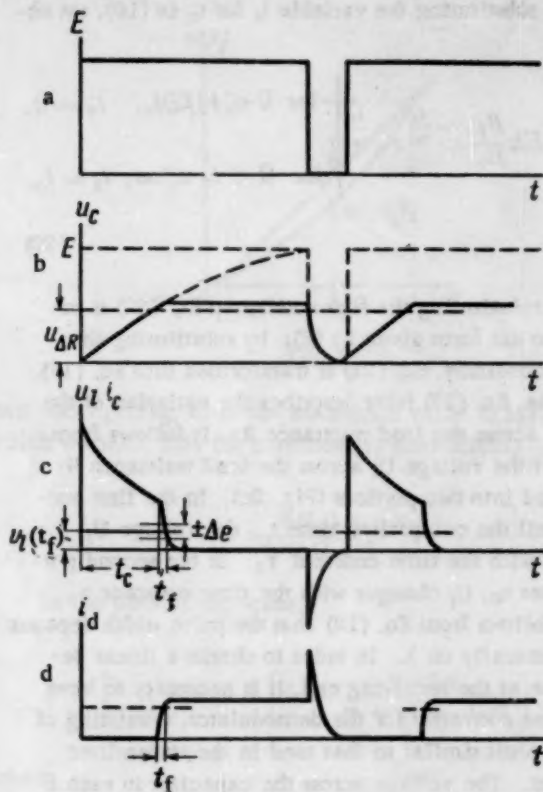


Fig. 2.

In this, the voltage across capacitor C will rise in the manner shown in Fig. 2b, and the current through the capacitor will change according to the diagram in Fig. 2c.

At the comparison time  $t_c$ , when the voltage across the capacitor attains the value  $U_{\Delta R}$ , the diode will be unlocked. The character of the diode current variation is shown in Fig. 2d.

After the time  $t_c$ , the voltage across the capacitor will remain constant up to the video pulse end, since the unlocked diode resistance  $r_1 \ll R$ . The moment of comparison and its corresponding time  $t_c$  can be fixed with respect to the change in the diode circuit current  $i_d$  (Fig. 2d) and with respect to the change in the capacitor circuit current  $i_c$  or the voltage  $U_l$  across the load resistance  $R_l$  (Fig. 2c).

Let us determine the effect of the circuit parameters on the pulse width  $t_c$  and the trailing edge duration  $t_f$  (Fig. 2c). The values of  $t_c$  and  $t_f$  will be determined with respect to variations of the voltage across the resistance  $R_l$ , because this method is the simplest.

The equivalent circuit of a converter in the state preceding the comparison moment is shown in Fig. 3. The equations are of the following form:

$$\frac{E}{P} = i_1(r + R_1 + R_2) - i_2(R_1 + R_2), \quad (6)$$

$$0 = -i_1(R_1 + R_2) + i_2(R_1 + R_2 + R + R_l + \frac{1}{Cp}).$$



Fig. 3.

By solving these equations, we shall find the voltage across the capacitor:

$$U_C = Ek(1 - e^{-\frac{t_1}{CR_0}}), \quad (7)$$

the voltage across the load resistance  $R_l$ :

$$U_l = Ek \frac{R_l}{R_0} e^{-\frac{t_1}{CR_0}}, \quad (8)$$

the voltage at the data transmitter  $R_2$  slider:

$$U_{\Delta R} = Ek \frac{\Delta R}{R_1 + R_2} \left(1 - \frac{rk}{R_0} e^{-\frac{t_1}{CR_0}}\right), \quad (9)$$

where

$$k = \frac{R_1 + R_2}{R_1 + R_2 + r}, \quad (10)$$

$$R_0 = R + R_l + rk, \quad (11)$$

and  $\Delta R$  is the resistance between the data transmitter  $R_2$  slider and the ground.

The present time  $t_1$  changes within the  $0 \leq t_1 \leq t_c$  interval. The pulse width  $t_c$  is determined by the equation

$$U_c + U_l = U_{\Delta R} + \Delta E, \quad (12)$$

where  $\Delta E$  is the diode unlocking voltage.

The reduced expressions yield the equation

$$t_c = CR_0 \ln \frac{m + q(1 - \lambda n)}{1 - \lambda n - \frac{\Delta E}{Ek}}, \quad (13)$$

where

$$m = \frac{R}{R_0}, \quad q = \frac{rk}{R_0}, \quad n = \frac{R_2}{R_1 + R_2}, \quad \lambda = \frac{\Delta R}{R_2}.$$

The parameter  $\lambda$  to be transmitted will change within the interval

$$\lambda_{\min} \leq \lambda \leq 1,$$

where

$$\lambda_{\min} = \frac{R_l}{(R + R_l)n}. \quad (14)$$

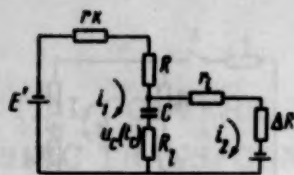


Fig. 4.

For determining the trailing edge duration  $t_f$ , we shall use an equivalent circuit (Fig. 4) which corresponds to the converter state after the comparison time  $t_c$ . The following assumptions were made with regard to this circuit: the current in the  $R_1 R_2$  circuit is assumed to be constant after the comparison time  $t_c$ , since  $R \gg R_1 + R_2$ ; the diode internal resistance is constant and equal to  $r_i$  after unlocking.

The circuit shown in Fig. 4 is described by the equations

$$\begin{aligned} \frac{Ek - U_C(t_c)}{p} &= \\ = i_1 \left( R + R_l + r_k + \frac{1}{Cp} \right) + i_2 \left( R_l + \frac{1}{Cp} \right), \\ \frac{U_C(t_c) - U_{\Delta R}(t_c)}{p} &= \\ = -i_1 \left( R_l + \frac{1}{Cp} \right) + i_2 \left( r_i + \Delta R + R_l + \frac{1}{Cp} \right), \end{aligned} \quad (15)$$

where  $U_C(t_c)$  and  $U_{\Delta R}(t_c)$  are the voltage across the capacitor, and at the data transmitter slider, at the comparison time  $t_c$ , respectively.

By using Eq. (15), we shall determine the voltage  $U_l(t_2)$  across the load resistance  $R_l$  and the current  $i_2(t_2)$  which is transmitted through the diode after the comparison time  $t_c$  (Fig. 2, c and d):

$$U_l(t_2) = Ek \frac{R_l}{R_0} e^{-\frac{t_c}{\tau_1}} e^{-\frac{t_2}{\tau_2}}, \quad (16)$$

$$i_2(t_2) = \frac{Ek_1}{R_0} e^{-\frac{t_c}{\tau_1}} (1 - e^{-\frac{t_2}{\tau_2}}), \quad (17)$$

where

$$\tau_1 = CR_0, \quad (18)$$

$$\tau_2 = C \left[ R_l + \frac{(R + rk)(r_i + \Delta R)}{R + rk + r_i + \Delta R} \right], \quad (19)$$

$$k_1 = \frac{k(R + rk)}{R + rk + r_i + \Delta R}. \quad (20)$$

From (16) we find the trailing edge duration:

$$t_f = \tau_2 \ln \frac{Ek}{U_l(t_f)} \frac{R_l}{R_0} e^{-\frac{t_c}{\tau_1}}. \quad (21)$$

In Eq. (21),  $U_l(t_f)$  is the voltage at the level of which the trailing edge duration  $t_f$  is read.

By substituting the variable  $t_1$  for  $t_c$  in (16), we obtain

$$U_l = Ek \frac{R_l}{R_0} e^{-\frac{t_1}{\tau_1}} e^{-\frac{t_2}{\tau_2}} \begin{cases} \text{for } 0 \leq t_1 \leq t_c, & t_2 = 0, \\ \text{for } 0 < t_2 \leq \infty, & t_1 = t_c. \end{cases} \quad (22)$$

By substituting the first condition, Eq. (22) is reduced to the form given by (8); by substituting the second condition, Eq. (22) is transformed into Eq. (16).

Thus, Eq. (22) fully describes the variation of the voltage across the load resistance  $R_l$ . It follows from (22) that the voltage  $U_l$  across the load resistance  $R_l$  is divided into two portions (Fig. 2c). In the first portion, until the comparison time  $t_c$ , the voltage  $U_l$  changes with the time constant  $\tau_1$ . In the second portion, after  $t_c$ ,  $U_l$  changes with the time constant  $\tau_2$ .

It follows from Eq. (13) that the pulse width depends logarithmically on  $\lambda$ . In order to obtain a linear dependence at the receiving end, it is necessary to have an inverse converter for the demodulator, consisting of an RC circuit similar to that used in the transmitter converter. The voltage across the capacitor in such a converter must change in step and according to the same law as in the converter capacitor, i.e.,

$$U(t) = E(1 - e^{-\frac{t}{\tau}}). \quad (23)$$

By substituting (13) in (23), we obtain

$$U(\lambda) = E \left[ 1 - \frac{1 - \lambda n - \frac{\Delta E}{Ek}}{m + q(1 - \lambda n)} \right]. \quad (24)$$

It follows from (24) that  $U(\lambda)$  changes nonlinearly in dependence on  $\lambda$  (Fig. 5). The nonlinearity is due to the presence of the resistance  $r$  in the converter (Fig. 1), as a result of which the voltage across the data transmitter  $R_2$  changes nonlinearly throughout the range, as follows from Eq. (9).

In the case where  $r = 0$  or  $r \ll R$ , the dependence of  $U(\lambda)$  on  $\lambda$  will be linear:

$$U(\lambda) = E \left( b + \frac{n}{m} \lambda \right), \quad (25)$$

where

$$b = 1 - \frac{1 - \frac{\Delta E}{Ek}}{m} \approx 0. \quad (26)$$

We shall define the degree of nonlinearity of  $U(\lambda)$  in expression (24) by the ratio of the maximum deflec-



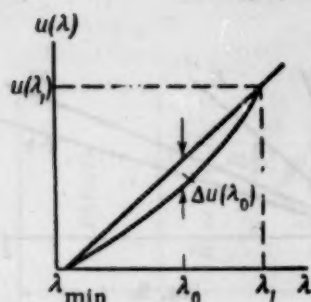


Fig. 5.

tion  $\Delta U(\lambda_0)$  (Fig. 5) to the maximum value  $U(\lambda_1)$ , which we shall call the nonlinearity coefficient:

$$\beta = \frac{\Delta U(\lambda_0)}{U(\lambda_1)}. \quad (27)$$

In the considered case,

$$\beta = \frac{\lambda_0 - \lambda_{\min}}{1 - \lambda_{\min}} - h \left[ 1 - \frac{1 - \lambda_n}{m + q(1 - \lambda_{\min})} \right], \quad (28)$$

where

$$\lambda_0 = \frac{m + q}{nq} - \frac{1}{nq} \sqrt{hnm(1 - \lambda_{\min})}, \quad (29)$$

$$h = \frac{1}{1 - \frac{1 - n}{m + q(1 - n)}}. \quad (30)$$

### Converter Errors

From Eq. (13), it follows that the pulse width  $t_c$  depends on the feed voltage  $E$ . The reduced error due to variations of the feed voltage  $E$  is equal to

$$\delta_{\Delta E} = \frac{\Delta t}{t_{c \max}} = \frac{\ln \frac{1 - \lambda_n - \frac{\Delta E}{E'k}}{1 - \lambda_n - \frac{\Delta E}{Ek}}}{\ln \frac{m + q(1 - n)}{1 - n - \frac{\Delta E}{Ek}}}, \quad (31)$$

where  $E' = E \pm \delta E$ .

TABLE 1

E=50			E=25		
$t_i$ , sec	$t_n$ , sec	$U_I$ , v	$t_i$ , sec	$t_n$ , sec	$U_I$ , v
0	0	0.543	0	0	0.271
0.3	0	0.447	0.3	0	0.223
0.6	0	0.367	0.6	0	0.183
1.068	0	0.271	1.094	0	0.133
1.068	0.02	0.179	1.094	0.02	0.088
1.068	0.04	0.118	1.094	0.04	0.058
1.068	0.08	0.051	1.094	0.08	0.025
1.068	0.12	0.022	1.094	0.12	0.011

Figure 6, a and b, shows the calculated  $U_I$  curves which illustrate the variation of  $t_c$  when the feed voltage  $E$  changes twofold.

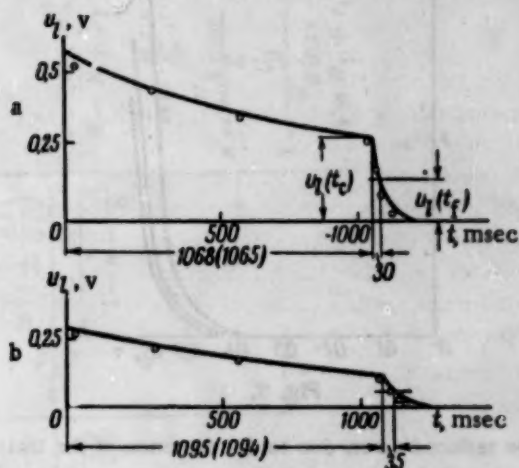


Fig. 6.

The calculation results are given in Table 1.

The calculations were performed according to Eq. (22) for the circuit shown in Fig. 1, where the measured parameters had the following values:  $R_1 = 692 \text{ ohm}$ ,  $\Delta R_2 = R_2 = 700 \text{ ohm}$ ,  $R = 74,460 \text{ ohm}$ ,  $R_n = 818 \text{ ohm}$ ,  $r_1 = 870 \text{ ohm}$ ,  $r = 0$ ,  $C = 20.4 \mu\text{f}$ ,  $\Delta E = 0.35 \text{ v}$ .

For a feed voltage of  $E = 50 \text{ v}$ , the comparison time  $t_c = 1068 \text{ msec}$ , and for  $E = 25 \text{ v}$ ,  $t_c = 1095 \text{ msec}$ .

The experimental curves are marked by points in Fig. 6. The experimentally obtained values of  $t_c$  are in brackets. As follows from Fig. 6, a and b, the theoretical and experimental curves practically coincide.

In calculating the diode bias,  $\Delta E$  is obtained from the condition

$$r_1 = \frac{\Delta E}{I_d} = (3 - 4) R_0. \quad (32)$$

For silicon D-202 diodes,  $\Delta E = 0.35 \text{ v}$ . The characteristics of three specimens of D-202 diodes are given in Fig. 7.

The accuracy in reading the pulse width  $t_c$  is determined by the magnitude of the pulse trailing edge  $t_f$  and by the operation threshold magnitude  $\pm \Delta e$  (Fig.

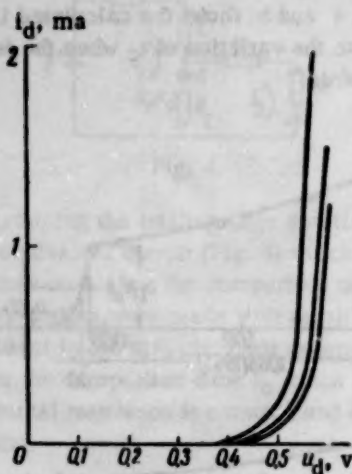


Fig. 7.

2c). The reduced errors due to the presence of the trailing edge  $t_f$  and  $\Delta e$  are equal to

$$\delta_{\Delta t} = \frac{\tau_2}{\tau_1} \frac{\ln \frac{Ek}{U_L(t_f)} \frac{R_L}{R_0} e^{-\frac{t_c}{\tau_1}}}{\ln \frac{m+q(1-n)}{1-n-\frac{\Delta E}{Ek}}} \quad (33)$$

$$\delta_{\Delta e} = \frac{\tau_2}{\tau_1} \frac{\ln \left( 1 \pm \frac{\Delta e}{U_L(t_f)} \right)}{\ln \frac{m+q(1-n)}{1-n-\frac{\Delta E}{Ek}}} \quad (34)$$

respectively.

It follows from (33) and (34) that the errors  $\delta_{\Delta t}$  and  $\delta_{\Delta e}$  depend on the relation

$$\frac{\tau_2}{\tau_1} = \left[ R_L + \frac{(R+rk)(r_1+\Delta R)}{R+rk+r_1+\Delta R} \right] \frac{1}{R_0} \approx \alpha + \frac{R_L + \Delta R_2}{R_0} \quad (35)$$

since

$$r_1 + \Delta R \ll R + rk.$$

For a fixed feed voltage  $E$ , it can be considered that

$$\alpha = \frac{r_1}{R_0} = \text{const}, \quad (36)$$

since the diode internal resistance  $r_1$  changes almost linearly with a change in  $R_0$  (Fig. 8).

The dependence of  $\alpha$  on  $E$  for silicon D-202 diodes is shown in Fig. 9. The variation of  $\tau_2/\tau_1$  in dependence on  $R_0$  is given in Fig. 10. From expression (35) and the diagrams in Fig. 10, it follows that  $\tau_2/\tau_1$  is independent of the capacitance value and is directly propor-

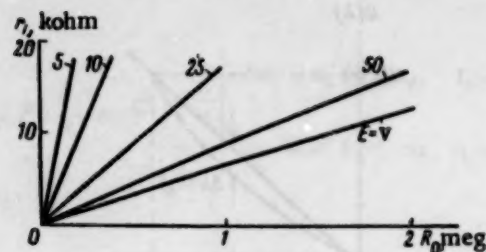


Fig. 8.

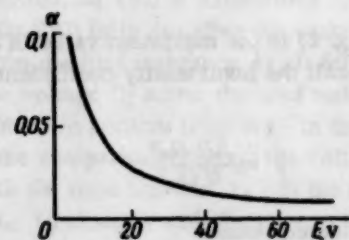


Fig. 9.

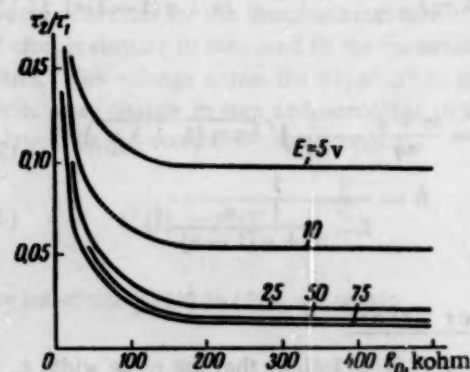


Fig. 10.

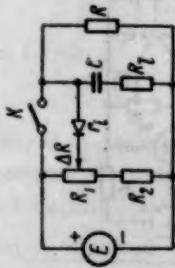
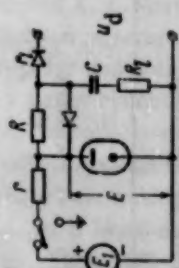
tional to  $\Delta R$  and  $R_L$  and inversely proportional to  $E$  and  $R_0$ . Thus, in order to reduce the trailing edge duration  $t_f$  and the  $\delta_{\Delta t}$  and  $\delta_{\Delta e}$  errors, it is necessary to reduce  $R_L$  and  $\Delta R$  and to increase the feed voltage  $E$  and the resistance  $R$ . The change in the trailing edge duration  $t_f$  when the feed voltage  $E$  changes twofold can be seen in Fig. 6, a and b. The increase in  $t_f$  with an increase in the  $\frac{R_L + \Delta R}{R_0}$  ratio if  $\tau_1$  remains constant and  $\alpha = 0.012$  can be seen in the voltage  $U_L$  oscillograms, which are shown in Fig. 11. The duration  $t_f$  in Figs. 6 and 11 is read at the  $U_L(t_f) = 0.5 U_L(t_c)$  level.

### Converter Circuits

Table 2 provides circuits and equations for some other converters.

In circuit No. 1, when the key  $K$  is closed, capacitor  $C$  is quickly charged to voltage  $E$ . During discharge, the voltage across capacitor  $C$ , which varies exponentially, is compared with the voltage  $U_{\Delta R}$  across the data transmitter.

TABLE 2

Circuit No.	Circuit	Character of operation	Pulse width	Reduced error due to changes in E	Reduced error due to the presence of trailing edge $t_f$	Reduced error due to the presence of operation threshold $\pm \Delta e$	Remark
1		Discharge	$t_c = R_0 C \ln \frac{m}{1-n\lambda - \frac{\Delta E}{E}}$	$v_{\Delta E} = \frac{\ln \frac{1-n\lambda - \frac{\Delta E}{E}}{1-n\lambda - \frac{\Delta E}{E}}}{\ln \frac{m}{1-n\lambda - \frac{\Delta E}{E}}} = \frac{m}{1-n\lambda - \frac{\Delta E}{E}}$	$v_{\Delta t} = \frac{\frac{R_1}{R_0} \frac{t_0}{U_0} e^{\frac{t_0}{\tau_1}}}{\ln \frac{m}{1-n\lambda - \frac{\Delta E}{E}}} = \frac{\tau_2}{\tau_1} \ln \frac{1 \pm \frac{\Delta e}{U_0}}{\frac{m}{1-n\lambda - \frac{\Delta E}{E}}}$	$v_{\Delta e} = \frac{\tau_2}{\tau_1} \ln \frac{1 \pm \frac{\Delta e}{U_0}}{\frac{m}{1-n\lambda - \frac{\Delta E}{E}}}$	$R_0 = R + R_l$ $m = \frac{R}{R_0}$ $n = \frac{R_1}{R_1 + R_2}$ $\lambda = \frac{\Delta R}{R_1}$ $\tau_2 = R_l + \tau_1 + \Delta R_0$ $\Delta R_0 = \frac{\Delta R_1(R_1 + R_2 - \Delta R_1)}{R_1 + R_2}$
2		Charge	$t_c = R_0 C \ln \frac{m}{1-n\lambda - \frac{\Delta E}{E}}$				$R_0 = R + R_l$ $m = \frac{R}{R_0}$ $n = \frac{U_{d \max}}{E}$ $\lambda = \frac{U_d}{U_{d \max}}$ $\tau_1 = R_l + \tau_l$





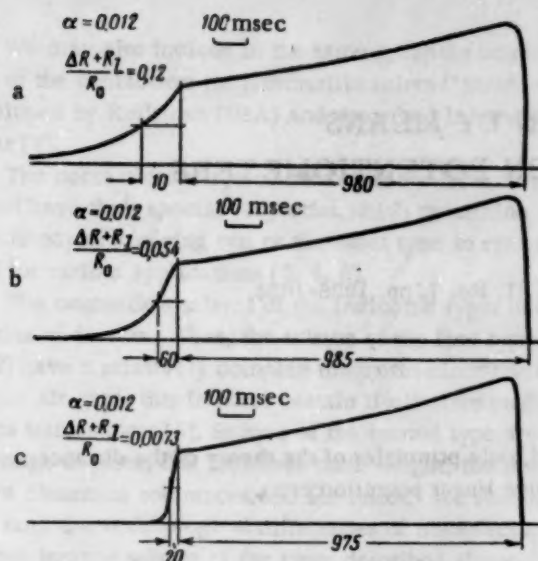


Fig. 11.

If such a converter is used in a remote-measurement system, the voltage in the inverse converter will change linearly with  $\lambda$ :

$$U(\lambda) = E \left( b_1 + \frac{n}{m} \lambda \right), \quad (37)$$

where

$$b_1 = \left( 1 - \frac{\Delta E}{E} \right) \frac{1}{m} \approx 0.$$

This constitutes the difference in principle between this converter and the one considered above.

In a number of cases, the converter can be conveniently controlled by supplying a voltage to the diode input. Such converters are described in Table 2; they are based on circuits Nos. 2 and 3.

The pulse width  $t_c$  in circuit No. 2 directly depends on the feed voltage, and therefore, a stabilivolt is provided at the converter input. In contrast to circuit No. 2, circuit No. 3 does not require stabilized voltage. Its principle of operation is clear from Fig. 12. The voltage  $U(t)$  changes exponentially, and is compared with two steady voltages  $U_0$  and  $U_d$ . The pulse width between  $t_0$  and  $t_d$  does not depend on the exponential voltage amplitude:

$$t_c = t_d - t_0 = CR \ln \frac{U_0}{U_d}.$$

If  $U_0$  is fixed and  $U_d$  changes in correspondence with the parameter to be measured, the pulse width  $t_c$  will change according to the logarithmic law.

In circuit No. 3, when key K is closed, the capacitors in the RC cells, which have equal time constants, are charged to voltage E. After the key is opened, the capacitors discharge through the resistor R. The comparison time of the  $U_c$  and  $U_0$  voltages in one RC cell

is the beginning of reading the pulse width  $t_c$ , and the  $U_c$  and  $U_d$  comparison time in the other RC cell is the end of this pulse reading.

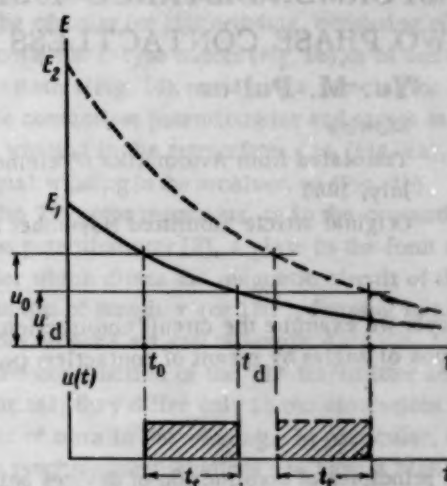


Fig. 12.

As was mentioned above, the comparison time in the converter can be fixed not only with respect to the change in the voltage across the resistance  $R_L$ , but also with respect to changes in the diode circuit current  $i_d$ .

Such a circuit is shown in Table 2 (No. 4). The fixing of  $t_c$  with respect to the  $i_d$  current has a number of advantages. A transistor, which acts as an amplifier at the same time, is used as the comparing element.

The front duration  $t_f$  in such a circuit is reduced by eliminating the resistance  $R_L$  [see Eqs. (19) and (35)]. However, in the construction of such circuits, it is necessary to use stable silicon transistors, which have large emitter-base and emitter-collector reverse resistances, affected only slightly by temperature and voltage variations.

The described converters can be used in the construction of remote-measurement, remote-signalization, and remote-control systems.

#### LITERATURE CITED

1. A. I. Novikov, "Exponential time-pulse converters," *Avtomatika i Telemekhanika* 18, 8 (1957).\*
2. V. A. Il'in and A. I. Novikov, "New principles in the construction of remote-measurement systems with time-pulse and pulse-width modulation," *Avtomatika i Telemekhanika* 19, 8 (1958).\*
3. V. A. Il'in, "Principles of the design of contactless remote-control systems with exponential converters," *Avtomatika i Telemekhanika* 20, 4 (1959).\*
4. V. A. Il'in, A. I. Novikov, S. V. Polyanskii, and E. Ya. Karasik, "The VST-1 time-pulse remote-measurement system," *Byull. Tekhn.-Ekonom. Inform.* 8 (1959).

\*See English translation.

# TRANSFORMER DISTANCE TRANSMISSION BY MEANS OF TWO PHASE CONTACTLESS INDUCTION POTENTIOMETERS

Yu. M. Pul'er

Moscow

Translated from *Avtomatika i Telemekhanika*, Vol. 21, No. 7, pp. 1026-1034,

July, 1960

Original article submitted November 5, 1959

In this paper we examine the circuit construction, operation and basic principles of the theory of the distance transmission of angles by means of contactless two-phase inductive linear potentiometers.

The principles of construction of devices being used at the present time for transformer distance transmission are based upon the application of inductive selsyn elements, which in their method of construction represent, as we know, two- and three-phase machines of the asynchronous type, behaving as transformers and in no way differing in principles from sine-cosine rotary transformers.

Contactless selsyn-transformers, whose construction is likewise based upon the principles of electrical machinery, have found wide application. Of the known types of contactless selsyns, we wish first of all to point out the construction of the type of [1, 2].\* In this, a series of extremely successful constructional solutions has been found for the magnetic circuit of a machine which ensures the necessary changes in the flux linkages between the stationary exciting ring winding

and the stator winding which is of the customary type used in electrical machines. We also wish to point out the second type of known construction, the properties of which consist of a varying constructive displacement between two stages, the input (or output) transformer and the portion similar to an electrical machine. The first stage consists of either a ring transformer, which ensures a flux linkage between its movable and stationary windings which does not change with changes in the rotor position [3, 5], or of an electrical machinery stage of the sine-cosine rotary transformer type, proposed in [6].

\*These constructions have been widely applied, mainly in inductive operation; however, in many cases, they may be used successfully in transformer operation, with the limitations pointed out in [5].

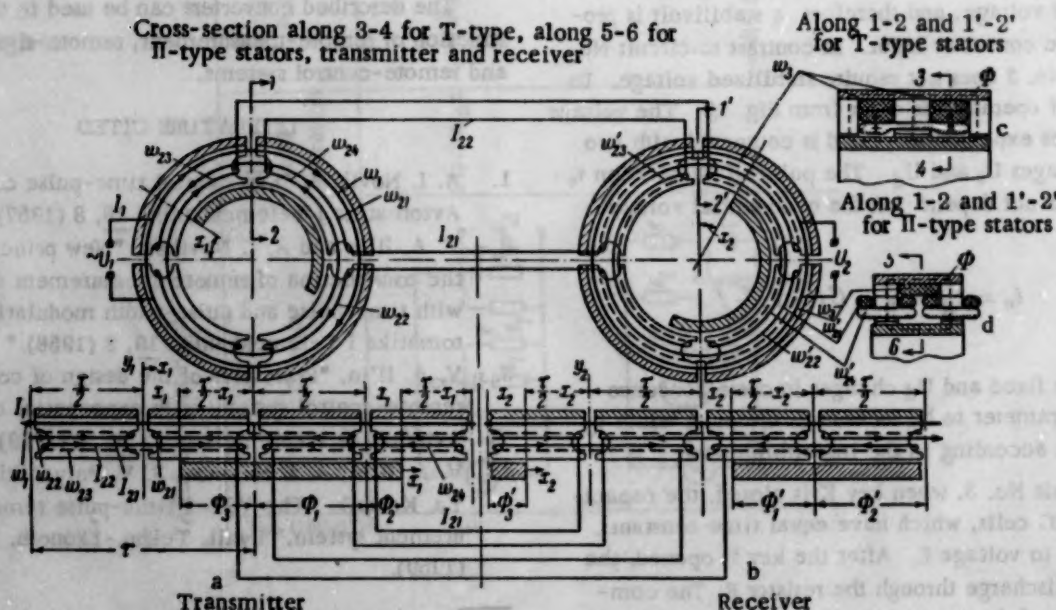


Fig. 1.



We may also include in the same group the construction of the contactless transformerlike selsyn ("Sinchrotel") developed by Kollman (USA) and described in survey paper [7].

The contactless selsyn constructions we have mentioned have their special properties, which determine the expediency of applying one or the other type in systems used for various applications [2, 4, 5].

The contactless selsyns of the indicated types have a series of defects. Thus, the selsyns of the first type [1, 2] have a relatively complex magnetic circuit with double air gaps; this imposes certain limitations on their use as transformers [5]. Selsyns of the second type are two-stage devices; this increases their weight, the number of clearance tolerances, and the losses. We should also note the technological difficulties of manufacturing close-tolerance selsyns of the types described above, and especially the difficulties in manufacturing the close-tolerance rotors. This circumstance limits the possibility of constructing miniature selsyns.

We will show below that if we place, on the stator, a linear inductive potentiometer having a range of  $\pm 90^\circ$  [8], in which the second pair of coils is displaced by  $90^\circ$  with respect to the first pair, the apparatus acquires properties which are analogous to the properties of a selsyn transformer. This analogy consists of the fact that, with the aid of such two-phase inductive potentiometers, there appears another possible construction for a transformer for distance transmission of angular position. Since contactless instruments are of the greatest practical interest, in the present paper we will examine transmission systems using contactless, two-phase, inductive potentiometers. These potentiometers, which do not involve two-stage transformations, are distinguished by their ease of manufacture and can be made to extremely small tolerances.

## 1. Description of the Construction of Two-Phase Induction Contactless Potentiometer-Selsyns (TIP)

The construction of a TIP-transmitter and receiver, connected in a distance transmission circuit, is shown in Fig. 1.

As we see from Fig. 1, a and b, the stators of the TIP transmitter and receiver differ from the contactless induction potentiometer [8], having the well-known construction described above, because it is single-phase and the former have a two-phase winding consisting of two pairs of coils  $w_{21}$ ,  $w_{22}$ , and  $w_{23}$ ,  $w_{24}$  mutually displaced by  $90^\circ$ . Each of these coils covers the central part of the stator for a T-type stator (Fig. 1a) or the lateral part (one or both) for a  $\Pi$ -type stator (Fig. 1d).

Each pair of coils (for example,  $w_{21}$  and  $w_{22}$ ) forming one phase, is interconnected so that the directions of the emf's or currents are opposing.

If we make use of the generally accepted selsyn terminology, then the two-phase transmitter winding con-

sisting of two pairs of coils  $w_{21}$ ,  $w_{22}$  and  $w_{23}$ ,  $w_{24}$  (Fig. 1a) and the receiver coils  $w_{11}$ ,  $w_{12}$  and  $w_{13}$ ,  $w_{14}$  (Fig. 1b) form synchronized windings.

The circular (or ring) winding, consisting of two circular coils for T-type stators (Fig. 1b), or of one coil for  $\Pi$ -type stators (Fig. 1d), remains the same as for an inductive contactless potentiometer and serves as the exciting winding in the transmitter,  $w_1$  (Fig. 1a), and as the signal winding in the receiver,  $w_3$  (Fig. 1b).

The TIP rotor represents, as in the contactless induction potentiometer [8], a plate in the form of a semi-cylinder which closes the magnetic circuit of the stator over an arc of length  $\tau$  (or  $180^\circ$ ), forming in all its positions an even air gap of length  $\delta$ .

The construction of the TIP transmitter and receiver is identical; they differ only in the dimensions and the number of turns in the winding. In particular, the receiver synchronizing windings can have a higher resistance than those of the transmitter, so as to lower the necessary transmitter power, while the higher-resistance signal winding will increase the magnitude of the difference signal.

The stator magnetic circuit may be either a T- or a  $\Pi$ -type (Fig. 1, c and d).

## 2. Principles Behind Remote Transmission by Means of Two-Phase Induction Potentiometers

The circuit of Fig. 1† shows the transmitter and receiver connections for a remote transmission system. We can see from the circuit that, for a current in the transmitter ring winding  $w_1$  due to the ac voltage  $U_1$  when the transmitter rotor is in its mean position (Fig. 1a), i.e., for  $x_1 = 0$ , the total transformation emf and the current  $I_{22}$  in the coils  $w_{23}$  and  $w_{24}$  is zero; but for this rotor position, the total transformation emf is a maximum for coils  $w_{21}$  and  $w_{22}$ , since coil  $w_{21}$  is placed into a position where the flux linkages with the exciting ring winding  $w_1$  are a maximum.

If, in this position of the transmitter rotor ( $x_1 = 0$ ), the receiver rotor were also rotated by  $\tau/2$ , for example, to the right with respect to the first position (considering that the transmitter and receiver axes  $y_1$  and  $y_2$  are parallel), then in this rotor position the voltage  $U$  across signal winding  $w_3 = 0$ . This is due to the fact that for  $x_1 = 0$  the coils  $w_{23}$  and  $w_{24}$  of one phase of the transmitter are deenergized. In this case, as we can see from Fig. 1b, when the receiver rotor is displaced by  $\tau/2$  from the transmitter rotor, i.e., for

$$x_2 \Big|_{x_1=0} = \tau/2 \text{ (or } 90^\circ\text{)}, \text{ the } w_3 \text{ winding has no flux}$$

† The four-conductor connection (Fig. 1) can be replaced by a three-conductor connection by combining two conductors in one of the two pairs of conductors (with current  $I_{21}$  or  $I_{22}$ ).

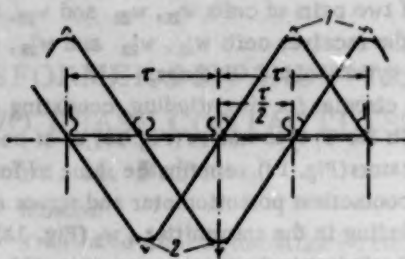


Fig. 2.

linkages with the coils  $w_{21}$  and  $w_{22}$  which are included in the opposite phase. For the indicated rotor position,  $U_2 = 0$ .

We can, on the basis of the same reasoning, see from the circuits of Fig. 1, a and b, that  $U_2$  will also be zero for every  $\tau/2$  (or  $90^\circ$ ) shift of the transmitter rotor if we preserve the mutual  $90^\circ$  rotor displacement. We prove below that the synchronized state of the system  $U_2 = 0$  will occur for a mutual perpendicular displacement of the transmitter and receiver over a whole revolution. We should point out that for the given distance transmission system, as in the known transformer transmission systems, the position of agreement between the transmitter and receiver corresponds to null values of voltage across the receiver signal winding which is connected to the input of the servo-drive amplifier.

We wish, first of all, to indicate that, if it follows from strictly linear dependence curves that dependence of the output voltage upon the rotor position for each winding is synchronized for  $-\tau/2 \leq x_1 \leq \tau/2$  and  $\tau/2 \leq x_1 \leq 3\tau/2$ , then, at the points which determine the boundaries of these intervals, there will theoretically be a break in the continuity of the indicated curves (Fig. 2, curve 1). However, in the actually constructed device, due to the continuity of the field the linear portions are connected by a continuous curve in the region of the maximum or the minimum (Fig. 2, curve 2).

The continuity of the characteristics ensures a stable state in the position of agreement between the transmitter and receiver in those rotor positions which correspond to the regions in the vicinity of the maximum and minimum points.

Let us first examine analytically the operation of the distance transmission system over the interval  $0 < x_1 < \tau/2$  corresponding to the linear part of the ideal theoretical synchronizing winding output voltage characteristic at no-load.

On the basis of the distance transmission circuit construction (Fig. 1) and the scanner construction in the TIP transmitter and receiver (Fig. 1, a and b), and making use of the designations for the currents, fluxes, and displacements indicated in the diagram, we can write the system of equations for the magnetic fluxes in the transmitter and receiver. While writing these equations,

we may neglect the leakage fluxes and also the boundary effects, i.e., we will consider that the specific magnetic conductivity along the gap  $G_0 = \text{const}$  over the range  $0$  to  $\tau/2$ . The behavior of the system for rotor positions corresponding to the neglected zones of the synchronous winding output voltage, and also for arbitrarily large differences, will be examined later.

Taking into account the symmetry of the transmitter and receiver windings (for the transmitter:  $w_{21} = w_{22} = w_{23} = w_{24} = w_2$ ; for the receiver:  $w'_{21} = w'_{22} = w'_{23} = w'_{24} = w'_2$ ), we can write the following equations: for the transmitter

$$\Phi_1 = [I_1 w_1 - (I_{21} w_2 + I_{23} w_2)] G_0 \frac{\tau}{2}, \quad (1)$$

$$\Phi_2 = [I_1 w_1 - (I_{21} w_2 - I_{23} w_2)] G_0 \left( \frac{\tau}{2} - x_1 \right), \quad (2)$$

$$\Phi_3 = [I_1 w_1 + (I_{21} w_2 - I_{23} w_2)] G_0 x_1; \quad (3)$$

for the receiver

$$\Phi'_1 = -(I_{21} w'_2 + I_{23} w'_2) G_0 \left( \frac{\tau}{2} - x_2 \right), \quad (4)$$

$$\Phi'_2 = (I_{21} w'_2 - I_{23} w'_2) G_0 \frac{\tau}{2}, \quad (5)$$

$$\Phi'_3 = (I_{21} w'_2 + I_{23} w'_2) G_0 x_2. \quad (6)$$

In addition, we have for the transmitter primary winding  $w_1$  the relationship

$$\dot{U}_1 = j\omega 10^{-8} w_1 [\dot{\Phi}_1 + \dot{\Phi}_2 + \dot{\Phi}_3] + I_1 Z_{1s}, \quad (7)$$

and for the receiver signal winding  $w_2$ ,

$$\dot{U}_2 = j\omega 10^{-8} w_2 [\dot{\Phi}'_1 + \dot{\Phi}'_2 + \dot{\Phi}'_3]. \quad (8)$$

The emf of the transmitter synchronizing windings, using the current direction shown in Fig. 1a, is determined by the equations

$$E_{21} = j\omega 10^{-8} w_2 [\dot{\Phi}_1 + \dot{\Phi}_2 - \dot{\Phi}_3],$$

$$E_{22} = j\omega 10^{-8} w_2 [\dot{\Phi}_1 + \dot{\Phi}_2 - \dot{\Phi}_3].$$

For the counter-emf in the receiver synchronizing windings, using the current directions shown in Fig. 1b, the actual equations are

$$E'_{21} = -j\omega 10^{-8} [-\dot{\Phi}'_1 + \dot{\Phi}'_2 + \dot{\Phi}'_3],$$

$$E'_{22} = -j\omega 10^{-8} [\dot{\Phi}'_1 + \dot{\Phi}'_2 - \dot{\Phi}'_3].$$

The equations for the currents in the synchronizing windings are

$$\begin{aligned} \dot{E}_{21} + \dot{E}'_{21} &= j\omega 10^{-8} w_1 \times \\ &\times [(\dot{\Phi}_1 + \dot{\Phi}_3 - \dot{\Phi}_2) - (-\dot{\Phi}'_1 + \dot{\Phi}'_3 + \dot{\Phi}'_2)] = \\ &= \dot{I}_{21} Z_{21}, \end{aligned} \quad (9)$$

$$\begin{aligned} E_{22} + \dot{E}'_{22} &= j\omega 10^{-8} w_2 \times \\ &\times [(\dot{\Phi}_1 + \dot{\Phi}_2 - \dot{\Phi}_3) - (\dot{\Phi}'_1 + \dot{\Phi}'_2 - \dot{\Phi}'_3)] = \dot{I}_{22} Z_{22}. \end{aligned} \quad (10)$$

The system of 10 equations in 10 unknowns which we have written down is easily solved if we make the substitutions given below.

Removing the parentheses in Equations (1)-(3) and performing the indicated additions, we get for the transmitter currents

$$\begin{aligned} \dot{\Phi}_1 + \dot{\Phi}_2 + \dot{\Phi}_3 &= \\ &= 2\dot{I}_1 w_1 G_0 \frac{\tau}{2} - 2\dot{I}_{21} w_2 G_0 \left( \frac{\tau}{2} - x_1 \right) - 2\dot{I}_{22} w_2 G_0 x_1, \end{aligned} \quad (11)$$

$$\dot{\Phi}_1 + \dot{\Phi}_3 - \dot{\Phi}_2 = 2\dot{I}_1 w_1 G_0 \left( \frac{\tau}{2} - x_1 \right) - 2\dot{I}_{21} w_2 G_0 \frac{\tau}{2}, \quad (12)$$

$$\dot{\Phi}_1 + \dot{\Phi}_2 - \dot{\Phi}_3 = 2\dot{I}_1 w_1 G_0 x_1 - 2\dot{I}_{22} w_2 G_0 \frac{\tau}{2}. \quad (13)$$

Removing the parentheses in Equations (4)-(6) and performing the indicated additions, we get for the receiver currents

$$\begin{aligned} \dot{\Phi}'_1 + \dot{\Phi}'_2 + \dot{\Phi}'_3 &= -2\dot{I}_{22} w_2 G_0 \left( \frac{\tau}{2} - x_2 \right) + \\ &+ 2\dot{I}_{21} w_2 G_0 x_2, \end{aligned} \quad (14)$$

$$-\dot{\Phi}'_1 + \dot{\Phi}'_2 + \dot{\Phi}'_3 = 2\dot{I}_{21} w_2 G_0 \frac{\tau}{2}, \quad (15)$$

$$-\dot{\Phi}'_1 - \dot{\Phi}'_2 + \dot{\Phi}'_3 = 2\dot{I}_{22} w_2 G_0 \frac{\tau}{2}. \quad (16)$$

Taking into account the symmetry of the transmitter and receiver synchronizing windings, the total leakage resistance of the two winding contours of the synchronizing system equals  $Z_{21} = Z_{22} = Z_2$ , where  $Z_2$  is

total leakage resistance of each of the two contours of the synchronizing windings, through which the currents  $\dot{I}_{21}$  and  $\dot{I}_{22}$  flow.

Substituting (11) in (7), (12) and (15) in (9), and (13) and (16) in (10), we get

$$\begin{aligned} 2j\omega 10^{-8} w_2 \left[ \dot{I}_1 w_1 G_0 \left( \frac{\tau}{2} - x_1 \right) - \dot{I}_{21} (w_2 + w'_2) G_0 \frac{\tau}{2} \right] &= \\ &= \dot{I}_{21} Z_2, \end{aligned} \quad (17)$$

$$\begin{aligned} 2j\omega 10^{-8} w_2 \left[ \dot{I}_1 w_1 G_0 x_1 - \dot{I}_{22} (w_2 + w'_2) G_0 \frac{\tau}{2} \right] &= \\ &= \dot{I}_{22} Z_2, \end{aligned} \quad (18)$$

$$\begin{aligned} 2j\omega 10^{-8} w_2 \left[ \dot{I}_1 w_1 G_0 \frac{\tau}{2} - \dot{I}_{21} w_2 G_0 \left( \frac{\tau}{2} - x_1 \right) - \dot{I}_{22} w_2 G_0 x_1 \right] &= \\ &= \dot{I}_1 - \dot{I}_1 Z_{15}, \end{aligned} \quad (19)$$

where  $Z_{15}$  is the total leakage resistance of the exciting windings.†

From Equations (17) and (18) we get the relations between the primary and secondary currents:

$$\dot{I}_{21} = \frac{2j\omega 10^{-8} w_2 \dot{I}_1 w_1 G_0 \left( \frac{\tau}{2} - x_1 \right)}{Z_2 + j\omega 10^{-8} w_2 G_0 \tau (w_2 + w'_2)}, \quad (20)$$

$$\dot{I}_{22} = \frac{2j\omega 10^{-8} w_2 \dot{I}_1 w_1 G_0 x_1}{Z_2 + j\omega 10^{-8} w_2 G_0 \tau (w_2 + w'_2)}. \quad (21)$$

Let  $j\omega 10^{-8} w_2 G_0 \tau (w_2 + w'_2) = a$ ; after substituting (20) and (21) in (19) we get

$$\begin{aligned} \dot{U}_1 &= j\omega 10^{-8} w_1^2 G_0 \tau \dot{I}_1 \times \\ &\times \left\{ 1 - \frac{4j\omega 10^{-8} w_2 G_0 \tau}{Z_2 + a} \frac{1}{\tau^2} \left[ \left( \frac{\tau}{2} - x_1 \right)^2 + x_1^2 \right] \right\} + \dot{I}_1 Z_{15}. \end{aligned} \quad (22)$$

If we let  $j\omega 10^{-8} w_1^2 G_0 \tau = jx_0$ , then  $j\omega 10^{-8} w_2^2 G_0 \tau = jx_0 \frac{w_2^2}{w_1^2}$ . Let  $\frac{w_2}{w_1} = k_{21}$ ,  $\frac{w_2^2}{w_1^2} = k_{22}$ . Then

$$\begin{aligned} \dot{I}_1 &= jx_0 \dot{I}_1 \times \\ &\times \left\{ 1 - \frac{4jx_0 k_{21}^2}{Z_2 + jx_0 (k_{21}^2 + k_{22})} \left[ \frac{1}{4} - \frac{2x_1}{\tau} \left( 1 - \frac{x_1}{\tau} \right) \right] \right\} + \\ &+ \dot{I}_1 Z_{15}. \end{aligned}$$

Then primary current  $\dot{I}_1$  is determined by the equation

$$\dot{I}_1 = \frac{\dot{U}_1}{jx_0 \left\{ 1 - \frac{4jx_0 k_{21}^2}{Z_2 + jx_0 (k_{21}^2 + k_{22})} \left[ \frac{1}{4} - \frac{2x_1}{\tau} \left( 1 - \frac{x_1}{\tau} \right) \right] \right\} + Z_{15}}.$$

† In the given investigation we neglect, in order to simplify the discussion, the differential leakage of the contactless induction potentiometer [8] and consider that  $Z_{15}$  and  $Z_{25}$  are independent of the rotor position.



Note that formula (23) shows that the primary current is independent of  $x_2$ , i.e., of the position of the receiver rotor. Substituting (14) in (8), we get, for the signal voltage  $\dot{U}_2$  across the  $w_3$  receiver winding (Fig. 1),

$$\dot{U}_2 = j\omega 10^{-8} w_3 \left[ -2\dot{I}_{22} w_2 \left( \frac{\tau}{2} - x_2 \right) + 2\dot{I}_{21} w_2 x_2 \right] G_0 \quad (24)$$

or, substituting (20) and (21),

$$\dot{U}_2 = \frac{2(j\omega)^2 10^{-8} w_3 10^{-8} w_2^2 G_0^2}{(Z_{22} + a)} \frac{\tau^2 w_3}{\tau^2 w_3} \left[ -\left( \frac{\tau}{2} - x_2 \right) x_1 + \left( \frac{\tau}{2} - x_1 \right) x_2 \right].$$

Making use of (22) and (23), we get

$$\dot{U}_2 = \dot{U}_1 \frac{2jx_0 \frac{w_2^2 w_3}{w_1^2 w_1}}{Z_{22} + jx_0(k_{21}^2 + k_{23}^2)} \frac{\frac{w_2}{w_3} \frac{1}{\tau^2} \left[ -\left( \frac{\tau}{2} - x_2 \right) x_1 + \left( \frac{\tau}{2} - x_1 \right) x_2 \right]}{\left\{ 1 - \frac{4jx_0 k_{21}^2}{Z_{22} + jx_0(k_{21}^2 + k_{23}^2)} \left[ \frac{1}{4} - \frac{2x_1}{4} \left( 1 - \frac{x_1}{\tau} \right) \right] \right\} + \frac{Z_{12}}{jx_0}} \quad (25)$$

or

$$\dot{U}_2 = \dot{U}_1 \frac{jx_0 \frac{w_2^2 w_3}{w_1^2 w_1 w_3}}{Z_{22} + jx_0(k_{21}^2 + k_{23}^2)} \frac{\frac{1}{\tau} (x_2 - x_1)}{\left[ 1 - \frac{4jx_0 k_{21}^2}{Z_{22} + jx_0(k_{21}^2 + k_{23}^2)} \left[ \frac{1}{4} - \frac{2x_1}{\tau} \left( 1 - \frac{x_1}{\tau} \right) \right] \right] + \frac{Z_{12}}{jx_0}} \quad (26)$$

Thus, it follows from the expression for the signal voltage  $\dot{U}_2$  (Equation 26) that the latter (if we neglect the stipulated changes in the denominator term) is proportional to the angular difference between the transmitter rotor for  $0 < x_1 < \tau/2$  and the receiver rotor for  $0 < x_2 < \tau/2$ .

In the position in which the transmitter and the receiver agree, their rotors are in a mutually perpendicular position.

We wish also to underline the fact that, for the case where several TIP receivers operate in parallel from one transmitter, there is no mutual interaction between them during mutual disagreement due to the fact that the synchronizing currents  $\dot{I}_{21}$  and  $\dot{I}_{22}$  according to (20) and (21), are independent of the receiver rotors.

Now let us examine the operation of the system for all other possible positions of the transmitter rotor, and, therefore, also for difference angles of large  $\pm \tau/4$  including the regions where the secondary current (or voltage) characteristics bend over.

In order to do this, we will make use of formulas (20) and (21). In the actual construction, the functions  $\dot{I}_{21}$  and  $\dot{I}_{22}$  [formulas (20) and (21)] do not have a discontinuity at  $x_1 = \tau/2$  but change continuously (the discontinuity occurs only for the case of ideal linearity). In order to analyze the system for rotor positions in the vicinity of the points of theoretical discontinuity, and also for differences in position involving these points, the rational periodic functions  $\dot{I}_{21}$  and  $\dot{I}_{22}$  are approxi-

mated by sinusoids. As a result, the currents  $\dot{I}_{21}$  and  $\dot{I}_{22}$  take the form

$$\dot{I}_{21} = k_1 \sin \frac{\pi}{\tau} \left( \frac{\tau}{2} - x_1 \right), \quad \dot{I}_{22} = k_1 \cos \frac{\pi}{\tau} x_1, \quad (27)$$

where

$$k_1 = \frac{jx_0 \frac{w_3}{w_1} I_1 G_0 \tau}{Z_{22} + jx_0 \frac{w_3}{w_1}}.$$

Here  $\dot{I}_1$  is determined from (23); if we take into consideration the small change in the denominator, we can assume, in the given case, that  $\dot{I}_1$  is independent of  $x_1$ .

The indicated substitution corresponds to the fact that in (26) the function  $G_0(\tau/2 - x_1)$  is replaced by  $G_0 \tau \sin \pi/\tau (\tau/2 - x_1) = G_0 \tau \cos(\pi/\tau) x_1$ , and the function  $G_0 x_1/\tau$ , by  $G_0 \tau \sin(\pi/\tau) x_1$ . Analogously,  $G_0(\tau/2 - x_2)$  is replaced by  $G_0 \tau \sin \pi/\tau (\tau/2 - x_2) = G_0 \tau \cos(\pi/\tau) x_2$  and the function  $G_0 x_2/\tau$ , by  $G_0 \tau \sin(\pi/\tau) x_2$ .

Substituting in the expression for the signal voltage (24) the currents  $\dot{I}_{21}$  and  $\dot{I}_{22}$ , taking into account the approximation introduced in formula (26) and bearing in mind the substitution (27) resulting from the latter, we get the following expression for the signal voltage:

$$\dot{U}_2 = k_2 \left[ -\sin \frac{\pi}{\tau} \left( \frac{\tau}{2} - x_2 \right) \sin \frac{\pi}{\tau} x_1 + \sin \frac{\pi}{\tau} \left( \frac{\tau}{2} - x_1 \right) \sin \frac{\pi}{\tau} x_2 \right] = k_2 \sin \frac{\pi}{\tau} (x_1 - x_2). \quad (28)$$

Here  $k_2$ , taking account of the substitution (22), will be determined by the formula

$$k_2 = \frac{jx_0 \frac{w_3}{w_1} \frac{w_2 w_2}{w_1^2} j_1}{Z_{22} + (k_{21}^2 + k_{23}^2)} \quad (29)$$

In (29), as well as in (27), we can practically neglect the insignificant variation in the current  $\bar{I}_1$  due to the location of the transmitter rotor  $x_1$  [see (23)] and consider that  $k_2 \approx \text{const}$ .

Equation (28) determines the character of the changes in the receiver signal voltage for transmitter and receiver corresponding to arbitrarily large differences, and also to zones of theoretical discontinuity of the curves of the synchronizing currents  $\bar{I}_{21}$  and  $\bar{I}_{22}$ .

As we see from (28), the voltage undergoes practically the same type of changes with changes in rotor position and with differences in position between the two rotors as in transformer distance transmission for the known types of selsyns of the electrical machine type.

However, as indicated above, formulas (26) and (28) have been obtained for idealized cases, the first for the triangular, and the second for the sinusoidal, form of these characteristics.

In the actual construction, characteristics (20) and (21) are close to triangles with rounded tops and are periodic, continuous functions. Therefore, a more rigorous analysis of an analogous system for any range of differences in the positions of transmitter and receiver and for all matching positions over an entire revolution will be obtained if we represent the characteristics in (20) and (21) in the form of trigonometric series.

Therefore, we must consider that formula (29) is true only for the basic harmonics of functions (20) and (21). Therefore,

$$U_2 = kU_1 \left[ \sum_{n=1,3,5,\dots} A_2(n) \sin n \left( \frac{\tau}{2} - x_2 \right) \times \right. \\ \left. \times \sum_{1,3,5,\dots} A_1(n) \sin n \frac{\pi}{\tau} x_1 + \right. \\ \left. + \sum_{1,3,5,\dots} A_1(n) \sin n \left( \frac{\tau}{2} - x_1 \right) \sum_{1,3,5,\dots} A_2(n) \sin n \frac{\pi}{\tau} x_2 \right]. \quad (30)$$

is a more rigorous expression for the signal voltage of the system.

## SUMMARY

1. The method of distance transmission by means of two-phase induction potentiometers, which we have examined in this paper, ensures circular tracking having only one stable position for the case in which the transmitter and rotor positions agree.

2. The transmitter and receiver of the distance transmission system considered in this article are elements with single-stage transformation. They are easy to construct and may be built to very small tolerances.

3. The absence of receiver reaction due to changes in its rotor position permits us to operate several receivers in parallel from one transmitter; in the process, the indication of each receiver is automatically brought into agreement with the transmitted signal. This is of basic importance in complex systems in which centralized transmitters operate a great many receivers.

The basic distance transmission properties of contactless two-phase potentiometers which have been examined in this paper permit us to recommend this device for use in automatic installations.

## LITERATURE CITED

1. A. G. Iosif'yan, and D. V. Svecharnik, Selsyns [in Russian] (Gosenergoizdat, 1942).
2. D. V. Svecharnik, Distance Transmission [in Russian] (Gosenergoizdat, 1959).
3. Terman Patent DRP No. 162740, Beckman Patent DRP No. 405156.
4. D. P. Mkrtchyan and V. V. Khrushchev, Single-Phase Selsyns [in Russian] (Sudpromglz, 1957).
5. Yu. M. Pul'er, "Contactless sine-cosine rotational transformer-selsyns," *Elektrichestvo* 1 (1958).
6. I. M. Sadovskii, Author's Certificate No. 56183 and 65902.
7. E. Widermuth, "Inductive distance transmission systems and their building blocks," *Feinwerktechnik* 62, 10 (1958).
8. Yu. M. Pul'er, "Inductive linear potentiometers," *Avtomatika i Telemekhanika* 17, 7 (1956). \*\*

\*\* See English translation.

# CONTACTLESS SEMICONDUCTOR SWITCHING ELEMENTS

E. V. Miller

Leningrad

Translated from *Avtomatika i Telemekhanika*, Vol. 21, No. 7, pp. 1035-1045,

July, 1960

Original article submitted December 28, 1959

Contactless switching element circuits developed to replace relays in automatic control systems are discussed, and also the calculation of these elements. An example is given of their use in a typical automated system.

Many different types of contactless devices which replace this or that relay have been built in recent years both in the USSR and abroad. Such devices have a practically unlimited service life, and do not require any servicing while in use.

The replacement of contact devices with contactless ones is especially important in those automatic control systems which operate in the presence of dust and dirt - for example, in metallurgical plants, ore-concentration factories, flour mills, etc. In the foreign press, there are communications about the development of entire automated systems using contactless switching elements (so-called logic elements), built from semiconductors and rectangular loop magnetic elements.

Only the systems which use semiconductors are discussed in this article.

Elements of switching circuits with contacts are shown in Fig. 1; they may be called "and," "or," "not," and "command," according to the functions they perform.

The existing semiconductor "and," "or," and "not" circuits may be divided into three basic groups:

- 1) using diodes only
- 2) using transistors only
- 3) using both diodes and transducers

Diode circuits are presented, for example, in [5] and [6]. They are very simple and cheap, but when several elements are connected to operate one after the other, a large number of separate power supplies of different amplitude are required; therefore, they are not suitable for the system being developed.

Transistor circuits [3, 5, 6] can be subdivided into two subgroups: a) with series, and b) with parallel connection of the transistors. Like the diode circuits, the series-connected transistor circuits require a separate power supply for each input. Moreover, when elements with series-connected transistors are used, the assembly of a number of elements into a common automatic control circuit becomes very complex.

Elements with parallel-connected transistors permit the use of one power supply for any number of elements

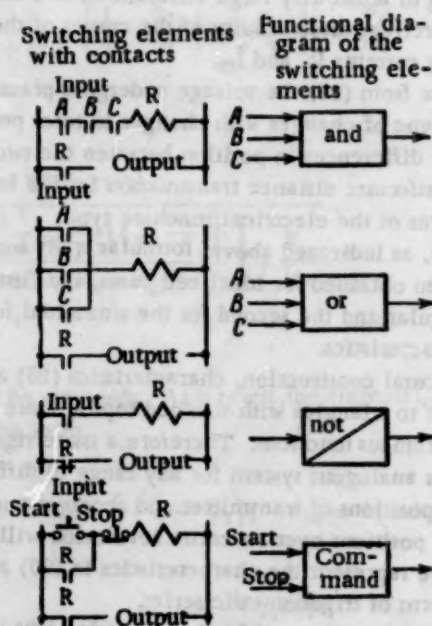


Fig. 1. Basic elements of switching circuits.

in the automated circuit, and are easily assembled into any kind of circuit.

Combined diode-transistor circuits, depending on their use, can be cheaper than transistor circuits (when their use reduces the number of transistors required). By using parallel-connected transistors, it is possible to obtain a system of elements for which only one power supply is required, and these elements will easily combine into various circuits. The "command" ("memory") element is built only from transistors.

The industrial electrification faculty of the remote Northwest Polytechnic Institute (SZPI), as a result of research, developed a system of contactless switching elements using typical semiconductor diodes and transistors. The features of the system developed which differ from existing circuits are:

- a) the possibility of simple combination of the



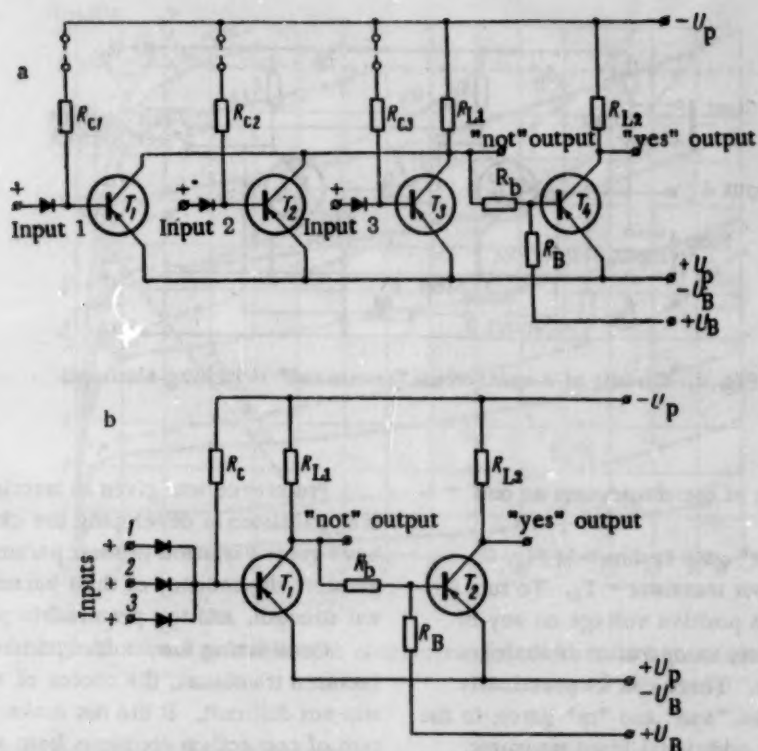


Fig. 2. Circuits of contactless switching elements: a) "and" gate, b) "or" gate.

contactless elements developed for the assembly of different automated switching circuits;

b) the operation of the elements is almost independent of the ambient temperature up to  $50^\circ\text{C}$ ; this is ensured by the use of bias on all elements, and by a suitable choice of the transistor operating modes;

c) the absence of a separate "not" element, and the construction of "and," "or," and "command" elements with two outputs, "yes" and "not"; this reduces the total number of elements required by automatic control circuits.

The input signal to an element can come from any sort of transducer which gives a small voltage (thermocouple, photocell, induction switch), or from switching apparatus with contacts. Moreover, the outputs from the elements can excite the inputs of other contactless elements, or of amplifiers. The separate elements of the circuits developed are described below.

A contactless "and" gate which gives two outputs, "yes" and "not," is depicted in Fig. 2a. The input transistors  $T_1$ ,  $T_2$ , and  $T_3$  have a common load resistance  $R_{L1}$ , and their bases are connected through resistances  $R_{c1}$ ,  $R_{c2}$ , and  $R_{c3}$  to the negative terminal of the power supply. In this case, all three transistors are on in the absence of input signals, a current flows through resistance  $R_{L1}$  and the collector-to-emitter voltage of  $T_1$ ,  $T_2$ , and  $T_3$  is a fraction of a volt. A load resistance  $R_{L2}$  is wired into the collector circuit of output transistor  $T_4$ ,

and its base is connected to the common collector terminal of the input transistors through a voltage divider consisting of resistances  $R_b$  and  $R_B$ . Hence, if one of the transistors  $T_1$ ,  $T_2$ , or  $T_3$  is on, the base current of  $T_4$  will be positive (for a suitable relation between  $R_b$  and  $R_B$ ), and the collector current of  $T_4$  will be very small. Therefore, the potential at the "yes" output point will differ little from the potential at point  $-U_p$ , and will be almost equal to the  $+U_p$  potential at the "not" output point. If a positive signal is impressed on the base of one of the input transistors, it will be cut off, but the "yes" and "not" output potentials will not change, due to the other two transistors, which are still on. If a positive voltage is simultaneously impressed on all the input transistors, they will all be cut off, no current will flow through  $R_{L1}$ , a negative base current will arise in  $T_4$ , and this will cause it to turn on. In this manner, the "yes" and "not" output voltages will change places: the potential on the first will be nearly  $+U_p$  and the second will be nearly  $-U_p$ .

There is a resistance  $R_B$  fed from a low voltage supply  $U_B$  to eliminate the effect of the ambient temperature, and the heating of the transistors themselves, on the output voltages. The temperature has practically no effect on the operation of the gate, if  $U_B$  and  $R_B$  are correctly chosen.

Semiconductor diodes are provided to eliminate the effect of the element currents on the primary transducers,

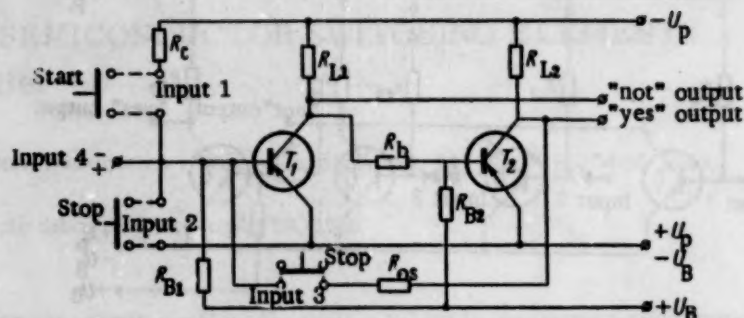


Fig. 3. Circuit of a contactless "command" switching element.

and to prevent interaction of the transducers on one another.

The circuit of the "or" gate is shown in Fig. 2b. Here there is only one input transistor —  $T_1$ . To turn it on, it is sufficient to put a positive voltage on any of the three inputs. Otherwise, its operation is analogous to that of the "and" gate. There can be practically any number of inputs to the "and" and "or" gates; in the first gate, this requires an additional input transistor, diode, and resistance  $R_c$ ; in the second, it is sufficient to add only an input diode.

The described operation of the "and" and "or" gates can occur with input signals from contact or contactless transducers. If one or more inputs of the "and" gate must be connected to the outputs of other contactless elements, then one or more straps (shown by dots in Fig. 2a) must be removed from the  $R_c$  resistances, and the free ends of these resistors are considered as inputs.

The "or" gate, intended for operation with other elements, must be built analogously to an "and" gate, but the  $R_c$  resistances in this case must be connected not to  $-U_p$ , but to  $+U_p$  (the input transistors will be on in the absence of input signals). In this case, the input of each of the transistors must be not positive, but negative, and correspondingly, the "yes" and "not" outputs change places.

The circuit of a "command" element, wired like a fixed bias trigger, is shown in Fig. 3.\* Transistor  $T_1$  is cut off when there are no input signals, and  $T_2$  is on; this is ensured by appropriate relations between the individual resistances in the circuit. When a negative pulse is impressed on input 4, or when the "start" button connected to input 1 is pressed, transistor  $T_1$  turns on, and  $T_2$  is cut off. The cut-off condition of  $T_2$  ensures that a base current will flow into  $T_1$  through resistance  $R_{cs}$ . Thus, when the negative pulse is removed from input 4 (or the "start" button is released),  $T_1$  remains on, and  $T_2$  remains cut off. In order to restore  $T_1$  to cut-off and to turn  $T_2$  on, one need only feed a positive pulse to input 4 (or press the normally open "stop" switch in input 2, or the normally closed switch in input 3).

Preference was given to junction, over point-contact, transistors in developing the circuits, since the latter have great variation in their parameters, a large temperature dependency of their parameters, less mechanical strength, and less permissible power dissipation.

Considering the limited number of types of manufactured transistors, the choice of a junction transistor was not difficult. It did not make sense to build a system of contactless elements from power transistors, since they are large and would require much power, as well as heat sinks. It was better to select small transistors, but with very small transistors, the base current is comparable with leakage and possible noise currents. Hence, it was desirable to choose transistors with base currents not less than one-tenth of a milliamper. Moreover, it was desirable to use hermetically sealed transistors for protection against dust and humidity. Therefore, the most suitable domestically manufactured transistors are the P-13, P-14, and P-15 series. The P-13A has the largest current amplification factor of all these, and thus permits the connecting of the largest number of other elements to its output. Thus, it was used in the elements developed.

It should be noted that silicon transistors are suitable for operation at higher temperatures than germanium, and, when they are manufactured on a large scale, it will become very desirable to use them for automated systems which operate at temperatures higher than  $50^\circ\text{C}$ .

The determination of the parameters of the "and" and "or" gates essentially leads to the choice of the voltages  $U_p$  and  $U_B$ , and the resistances  $R_c$ ,  $R_B$ ,  $R_b$ , and  $R_L$ . The output characteristics of the P-13A transistor are needed for the computation of these parameters. These characteristics, taken for one typical sample of this transistor, are shown in Fig. 4 at temperatures of  $20^\circ\text{C}$  (solid lines), and  $50^\circ\text{C}$  (dotted lines). A load line for the resistance  $R_L$  is drawn on the characteristic for a certain voltage  $U_p$ . The mode must be chosen so that the load line will intersect the characteristic at the

\* In the U.S., this circuit is also known as a binary memory, or "flip-flop" [Publisher's note].

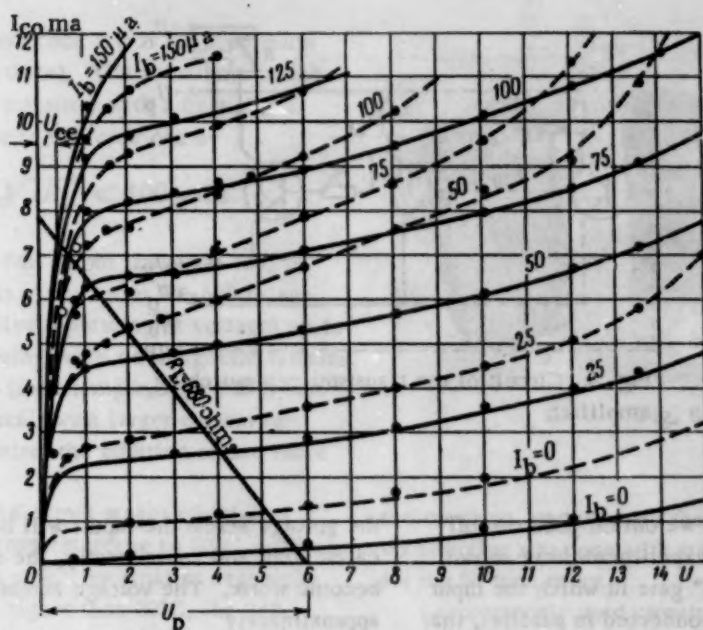


Fig. 4. Experimental output characteristics of the P-13A transistor.

knee of the curve, so as to make the collector current depend almost entirely on the load resistance  $R_L$ . It can be seen from this condition that increasing voltage  $U_p$  causes a large current stability against fluctuations of this voltage, the temperature, and the base current. On the other hand, a long service life of the element is desirable, and this is ensured by lowering the voltage. According to the manufacturer's data on the P-13A transistor, the limiting voltage for a common emitter circuit is 10 volts, so  $U_p$  was set at 6 volts to increase the reliability.

The load resistance, ignoring the voltage drop across the conducting transistor, is determined from the relation

$$R_L \geq \frac{U_p}{I_{me}}$$

The maximum emitter current  $I_{me} = 10$  ma. The resistance  $R_L = 680$  ohms in the circuits. Hence, the collector current will be approximately

$$I_{co} = \frac{U_p}{R_L} = 8.9 \text{ ma.}$$

Drawing the load line corresponding to resistance  $R_L$  (Fig. 4), it can be seen that the base current  $I_b$  must be not less than  $125\text{--}150 \mu\text{a}$ , so that the load will fall on the knee of the output characteristic. Setting  $I_b = 200 \mu\text{a}$  for reserve, and neglecting the voltage drop between emitter and base, we find the resistance

$$R_c = \frac{U_p}{I_b} = \frac{6}{200 \cdot 10^{-6}} = 30\,000 \text{ ohms.}$$

The resistance  $R_b$  is chosen with input transistors  $T_1$ ,  $T_2$ , and  $T_3$  cutoff for the "and" gate (or input transistor  $T_1$  of the "or" gate). In this case, the base current which will ensure that the output transistor  $T_4$  is on in the "and" gate (or  $T_2$  in the "or" gate) must also be  $I_b = 200 \mu\text{a}$ . This will give the sum

$$R_L + R_b \approx \frac{U_p}{I_b} = \frac{6 \cdot 10^6}{200} = 30\,000 \text{ ohms.}$$

Since the resistance  $R_L$  found earlier is small in comparison to  $R_b$ , it can be neglected, and the resistance  $R_b$  can be made 30000 ohms for standardization. The bias voltage amplitude  $U_B$  must be greater than the voltage  $U_{ce}$  (see Fig. 4) to ensure a positive potential on the base of the cut-off transistor  $T_2$  of the "or" gate. The latter is not more than 0.3 volt for different samples of the P-13A transistor, with a resistance  $R_c = 30\,000$  ohms, using characteristics taken at  $+50^\circ\text{C}$ . Therefore,  $U_B$  must be on the order of 0.6 volt.

The inequality

$$\frac{U_{ce} + U_B}{R_b + R_B} R_B < U_B,$$

must be satisfied so that a positive potential will be ensured on the base of the cut-off transistor  $T_2$ ; from this,

$$R_B < \frac{U_B}{U_{ce}} R_b.$$

For the assumed values of  $U_B$ ,  $U_{ce}$ , and  $R_b$ ,

$$R_B < \frac{0.6 \cdot 30\,000}{0.3}, \quad R_B < 60\,000 \text{ ohms.}$$



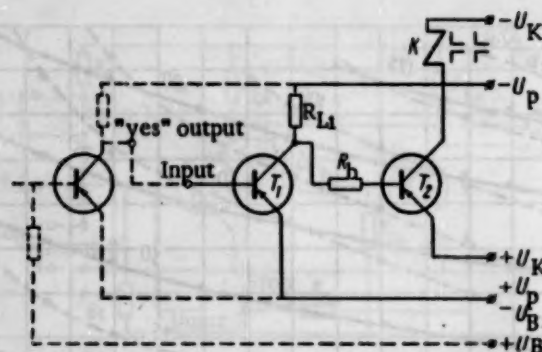


Fig. 5. Circuit of the transistorized switching amplifier.

Making  $R_B = 56000$  ohms, we obtain good cut-off of the output transistor  $T_2$ , as experiments have shown.

It is evident, for the "and" gate in which the input transistors  $T_1$ ,  $T_2$ , and  $T_3$  are connected in parallel, that the voltage drop  $U_{CE}$  will be less than the voltage drop across one transistor. Therefore, the same values of  $U_B$  and  $R_B$  will ensure even better temperature compensation.

Any diodes which have a reverse voltage greater than  $U_p$ , and current rating greater than  $I_b$ , can be used as input diodes. In particular, any of the DGTs-type diodes are suitable. The only other calculation needed for the "command" element is the determination of the resistances for the potentiometer, which comes from the formula [1]

$$R_B \leq \frac{U_B}{I_{cb \max}},$$

$$R_{os} \leq \left( \frac{\beta_{\min}}{1 + \beta} \frac{U_B R_L}{U_p R_B} - 1 \right) R_L; R_b = R_{os}.$$

The amplitude of  $I_{cb}$  at  $20^\circ\text{C}$  is  $30 \mu\text{a}$ , according to the manufacturer's data for the P-13A transistor. We find that

$$I_{cb \max} = I_{cb 20^\circ} \cdot 2^{\frac{I_{\max} - 20}{10}} = 30 \cdot 2^{\frac{80 - 20}{10}} = 240 \mu\text{a}.$$

The minimum amplification factor of the P-13A transistor may be on the order of  $\beta_{\min} = 25$ . Then

$$R_B \leq \frac{0.6}{240 \cdot 10^{-6}}; R_B \leq 2500 \text{ ohms},$$

$$R_{os} \leq \left( \frac{25}{1 + 25} \frac{0.6 \cdot 680}{6 \cdot 2500} - 1 \right) 680;$$

$$R_{os} \leq 10000 \text{ ohms}.$$

When several inputs are connected to the output of one "and" or "or" gate (with the output transistor on),

the voltage across the inputs will be even lower than calculated, and consequently, the operation will not become worse. The voltage across the inputs will be approximately

$$U_{in} = \frac{U_p}{R_L + R_{in}} R_{in},$$

with the output transistor cut off, where  $R_{in}$  is the resistance of all  $n$  input circuits.

Since  $R_{in} = R_c/n$ , then, by setting  $n = 10$  (which is sufficient for the majority of the circuits encountered in practice), we get  $R_{in} = 30000/10 = 3000$  ohms. Then

$$U_{in} = \frac{U_p}{680 + 3000} \cdot 3000 = 0.81 U_p.$$

Consequently, each input current will be  $0.81 I_b = 162 \mu\text{a}$ . Since the calculated base current,  $I_b = 200 \mu\text{a}$ , was chosen with a reserve (instead of  $125$  to  $150 \mu\text{a}$ ), the drop to  $162 \mu\text{a}$  will not make the system operation worse.

It should be noted that the transistors manufactured at present have a large variation in their parameters and characteristics. Therefore, the characteristics of each transistor must be taken into account when such circuits are built.

The elements which are constructed from the P-13A low power junction transistor have a very small output current which is not sufficient to control the coils of the power relays. Hence, amplifiers must be used to increase the power, and they may be transistor or magnetic. The first type is cheaper, lighter, and smaller in size. Therefore, it follows logically to give it preference. The circuit of such an amplifier of the utmost simplicity is shown in Fig. 5. The amplifier uses two transistors  $T_1$  and  $T_2$  (type P4B). The transistor shown in the circuit with dotted lines is the output transistor of the contactless element. The amplifier works as a phase inverter, as does the contactless element itself. The coil of relay K is the load resistance of  $T_2$ ; this relay must operate

at a voltage  $U_K \leq 70$  volts (since this is the maximum voltage rating of the transistor). The maximum power rating ( $P_{\max}$ ) of the P4B transistor with a heat sink is 25 watts. The load power in this case can be

$$P_L \leq 4P_{\max} \sqrt{iP_L} \leq 100 \text{ watts.}$$

An amplifier with a P4B output transistor can, in this way, control the coils of dc series KP-500 relays up to the fifth size, inclusive (operating at voltages up to 70 volts), or series KTP relays with dc magnetic systems. More powerful transistors (for example, type P207) can be used to control relay coils with larger current requirements; this may require the addition of one more amplification stage.

The load power of the output stages mentioned corresponds to ambient temperatures up to 30°C, with the use of a suitable heat sink. For smaller heat sinks or ambient temperatures higher than 30°C, the P4B transistors can control only smaller relays.

For standardization, the first transistor  $T_1$  is also a P4B. The resistance  $R_{L1}$  is chosen on the basis of the base current of  $T_1$ , with a signal impressed on the amplifier input from the output of any of the elements. This current will be

$$I_{b1} = \frac{U_p}{R_L} = \frac{6}{680} \cdot 10^3 = 8.9 \text{ ma.}$$

We find from the output characteristic of the P4B transistor (which is not shown in the article, but appears in handbooks) that the collector current  $I_{co1}$  must be  $\approx 75$  ma so that the voltage  $U_{ce}$  will not be more than 1 volt, if the current  $I_{b1} = 8.9$  ma.

The resistance

$$R_{L1} = \frac{U_p - U_{ce}}{I_{co1}} = \frac{6 - 1}{75 \cdot 10^{-3}} = 68 \text{ ohms.}$$

In finding the necessary base current of  $T_2$ , the load resistance of the coil of the fifth size series KP-500 relay must be taken into account;  $R_K$  is 70.5 ohms at a voltage of 55 volts. A current

$$I_{K2} = \frac{U_K - U_{ce}}{R_K} = \frac{55 - 1}{70.5} = 0.77 \text{ amp.}$$

corresponds to such a resistance (assuming  $U_{ce} = 1$  volt).

The base current  $I_{b2}$  must be  $\geq 50$  ma so that  $U_{ce}$  will not be more than 1 volt.

If the collector of  $T_1$  is directly connected to the base of  $T_2$ , the base current of  $T_2$  will be  $I_{b2} = I_{K1} = 75$  ma with  $T_1$  cut off.

Since this current is larger than necessary, more reliable operation of the amplifier is assured.

An external view of a contactless "command" element (2 units in one case) is shown in Fig. 6; (a) with

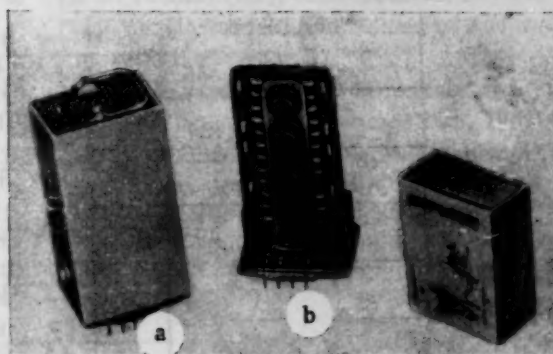


Fig. 6.

the cover on, and (b) with the cover off. The initial construction was done with standard cases and sockets for the IR-type relay.

A commonly used circuit for controlling the machinery for moving and locking the cross-slide of a powerful metal turning lathe (a) and an analogous circuit using contactless elements (b) is shown in Fig. 7.

The control circuits for the motor which moves the cross-slide up and down and the motor which clamps and unclamps the cross-slide by means of a special lever-screw device are shown in Fig. 7a. Relays UR and DR control the slide motion motor, and CC and UC control the clamp-unclamp motor. In order to move the cross-slide upwards, one presses the appropriate button, and the intermediate relay 1 IR is energized. This relay first turns on the unclamp relay UC. When the unclamping process is completed, limit switch LS opens, the unclamping is stopped, and the cross-slide begins to move. After the "up" button is released, or URS opens when maximum travel is reached, relay 1 IR and the coil of the UR are deenergized, and the upward movement ceases. Simultaneously, the clamp relay CC is energized. Clamping of the cross-slide ceases when the overload relay OR operates; its coil is connected in the main circuit of the clamp motor. The operation is analogous for downward motion.

A block diagram of the same device with contactless elements is shown in Fig. 7b. Only the input and output elements are shown in it. All outputs without designations are "yes" outputs, "Not" and other outputs are indicated by appropriate labels.

When the "up" switch is pressed, input signals are fed to the "and/not" element, the "or" gate, and the "and" gate. The connection of an input signal to the "and/not" element removes the signal from the input of the "and<sub>1</sub>" gate in the circuit of the CC coil, and so the latter cannot be energized. A signal is fed from the "or" gate to the "and<sub>2</sub>" gate. A second input to it comes from the "and<sub>3</sub>" gate with a "yes" output. Hence, the UC coil is powered through amplifier A<sub>2</sub>, and begins to unclamp the cross-slide. When the slide is unclamped,

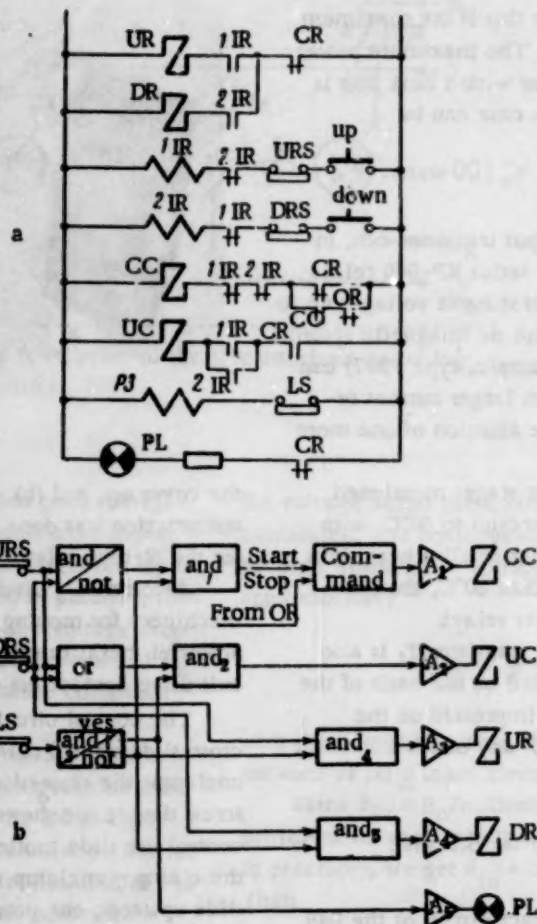


Fig. 7.

the limit switch LS opens, the "and<sub>5</sub>" gate does not give a "yes" output, and consequently, there will be no output signal from the "and<sub>2</sub>" gate. The UC coil is deenergized. The removal of the input signal from the "and<sub>3</sub>" gate will cause its "not" output to cease, and as a result, the UR coil is energized through "and<sub>4</sub>"; and amplifier A<sub>3</sub> (one of the inputs to "and<sub>4</sub>" comes from the "up" switch, which is still pressed). When the "up" switch is released, a second input signal will be impressed on "and<sub>1</sub>" (the first being present from the opening of LS), and consequently, a "start" pulse will be sent to "command." As a result of this, the CC coil of the clamp motor will be energized through amplifier A<sub>1</sub>. Clamping of the cross-slide is begun. It will continue until the OR relay operates; this feeds a "stop" pulse to the "command" element, thus deenergizing the CC coil, and causing the clamping of the slide to stop. Pilot lamp PL (as in the circuit of Fig. 7a) lights when the slide is unclamped. In the circuit being discussed (Fig. 7b), push button switches, limit switches with contacts, and the contacts of the overload relay are shown as input transducers. Replacing these with contactless

elements, if necessary, does not cause any special difficulties. Induction switches can be used as connecting and tracking devices; they can have very small dimensions, since the input signals are of such low power. Contactless relays, which operate from a comparison of voltage drops in the main current circuit with a reference, can be used instead of current-operated contact relays.

The circuit being considered has a relatively small number of relays, and only illustrates the principle of using the elements developed. They can be used with considerably more effectiveness in circuits with a larger number of relays.

The dimensions and weight of equipment which uses the contactless elements described is significantly less than of that using contact relays. The service life is determined by the service life of the transistors and diodes which, according to existing preliminary data, may be years if the operating modes are correctly chosen.

#### LITERATURE CITED

1. Semiconductor Electronics [in Russian] (Gosenergizdat, 1959).



2. N. I. Chistyakov (ed.), Transistor Electronics and Apparatus Construction [in Russian] (Oborongiz, 1959)
3. V. V. Pavlov (ed.), Transistors in Protective Relays, Measuring Instruments, and Telemechanics for Energy-Generating Systems [Russian translation] (Gosenergoizdat, 1958).
4. Ya. A. Fedotov (ed.), Semiconductor Devices and Their Use [in Russian] (Izd. Sovetskoe Radio, 1957 (2nd ed.), 1958 (3rd ed.)).
5. F. V. Malorov, Electronic Numerical Calculating Machines [in Russian] (Gosenergoizdat, 1957).
6. A. I. Kitov, Electronic Numerical Machines [in Russian] (Izd. Sovetskoe Radio, 1956).

## CALCULATION AND CONSTRUCTION OF INDUCTION CLUTCHES

## M. S. Mirenskii

## Moscow

Translated from *Avtomatika i Telemekhanika*, Vol. 21, No. 7, pp. 1046-1056,  
July, 1960

Original article submitted February 24, 1960

The construction of an induction clutch is described; it is simpler to make and more reliable in use than induction clutches described earlier in the literature. A calculation of a hollow rotor is made; it is based on experimental data which confirm the possibility of considering the hollow rotor as a squirrel cage consisting of a finite number of bars. The effective flux, torque, and geometric dimensions of the basic clutch parts are also calculated.

Recently, induction clutches have found use in automatic apparatus where they are intended to operate in servosystems as low-inertia controllable drives. These clutches work on a principle analogous to that of the asynchronous slipping clutches [1]. The operating principle and constructional diagram of the clutch are given in [2]. Induction clutches do not differ in their dynamic properties from two-phase motors with hollow rotors, and are better than dc motors. Their advantage is that powerful magnets, electromagnets, or electronic amplifiers are not required for controlling them.

## 1. Description of the New Clutch Construction

The clutch being examined in this article is separated into two halves in order to simplify the construction and also to increase the reliability in use. Each half

(Fig. 1) consists of a motor 1, star-wheel 2, hollow rotor 3, control winding 4, and stationary flux path 5. Two clutches working on a common gear box must be used so that reverse is possible. The theoretical kinematic diagram of the clutch combination is shown in Fig. 2. To accomplish reverse, the clutches could be combined as shown in Fig. 3. One motor serves as the drive for both clutches in this scheme; it is linked to them through a gear box. However, it can be affirmed that the use of a separate squirrel cage induction motor to drive the second clutch simplifies the construction and makes it more applicable for operation in servo-systems, since the insufficiently reliable and noisy element — the second gear box — is eliminated by doing this. The clutch whose constructional diagram is shown in Fig. 1 is simpler to make and more reliable in use

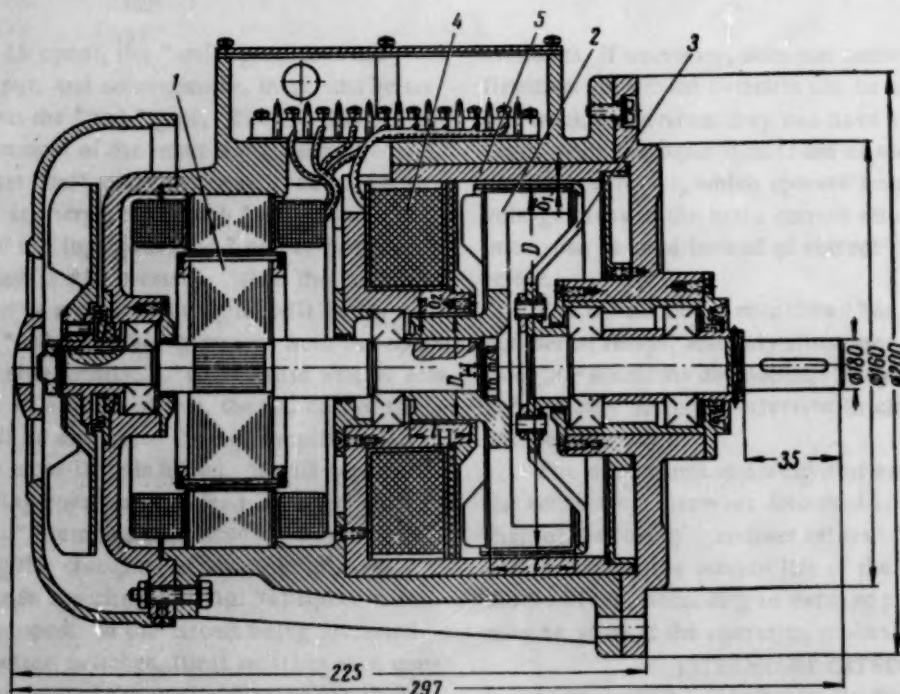


Fig. 1.

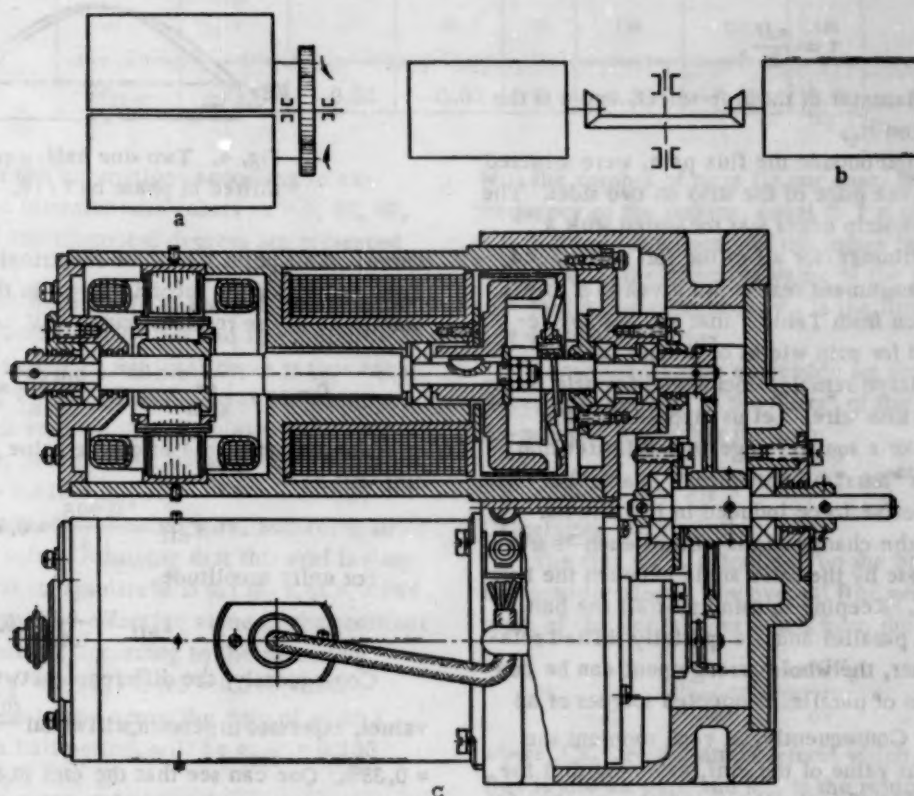


Fig. 2. Combination of the two halves of the clutch with a gear box. a) Using spur gears, b) using bevel gears, c) actual construction of the type of combination shown in a).

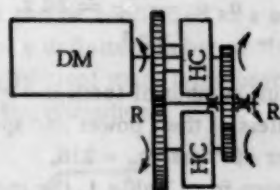


Fig. 3. Diagram showing two half-clutches connected to operate from one drive motor. DM - drive motor, HC - half-clutch, R - gear box.

than the clutch described in [2]. If the double clutch breaks down, it is replaced by another double clutch; in case of failure in a system consisting of two half-clutches, only one of its halves is replaced.

## 2. Calculation of Induction Clutches

Calculations of induction clutches done in the literature, particularly in [2], are based on speculative conclusions, and therefore, the correctness of the calculated formulas is not always confirmed by a check on the finished clutches. This author has succeeded in devising a method for calculating induction clutches, based on data obtained as results of specially designed experiments; the calculation is analogous to that for

electrical machines. One must be able to determine the amplitude of the emf induced in the hollow rotor, the flux magnitude generated by the control winding, and finally, the ohmic resistance of the rotor, in order to calculate the geometric dimensions of the individual elements of the clutch. Therefore, a description of the experiments which permit one to find the comparatively simple solution of the problems enumerated above is presented below.

### Data of the Experimental Investigation of the Hollow Rotor

The hollow rotor, as will be shown below, can be considered as a squirrel cage, in which the distance between bars is very small. The following experiments performed by the author serve as the basis for this statement. A strip of copper foil with a width equal to the axial length of a tooth of the star-wheel is fastened along the inner surface of the stationary flux path within which the star-wheel rotates. The length  $L$  of this strip is changed from experiment to experiment, beginning from the full length  $12\tau$  of the circumference of the internal bore of the flux path, and passing through a series of values equal to  $8\tau$ ,  $2\tau$ ,  $\tau$ ,  $\tau/2$ ,  $\tau/4$ ,  $\tau/18$ , and  $\tau/36$ . In the last experiment, a thin wire was used as the strip.

Assuming the tooth width is  $\tau$ , and the teeth are equally spaced with gap  $\tau$ , we can write



$$\tau = \frac{\pi D}{2z},$$

where  $D$  is the diameter of the star-wheel, and  $z$  is the number of teeth on it.

Two wires, led outside the flux path, were soldered to the middle of the edge of the strip on two sides. The voltage across the strip edges was measured with a vacuum tube voltmeter for all of the foil sizes listed above. The measurement results are given in Table 1.

It can be seen from Table 1 that the voltage remains unchanged for strip widths of  $2\tau$  and above. Likewise, the voltage remains unchanged for strip sizes, from  $\tau/18$  to the thin wire. Let us suppose that the hollow rotor is like a squirrel cage with infinitesimal distance between "bars". Consequently, each "bar" has its own electromotive force induced in it. The harmonic curves of the change in the emf of each "bar" are shifted in phase by the solid angle between the bars being considered. Keeping in mind that all the bars are connected in parallel and are spatially shifted relative to one another, the whole arrangement can be considered as a series of parallel-connected sources of an alternating emf. Consequently, at each moment the total instantaneous value of the emf, assuming that the resistance of the "bars" is the same, will be equal to [4]

$$\sum_{\text{inst}} = \frac{e_1 + e_2 + \dots + e_n}{n}, \quad (1)$$

where  $e$  is the instantaneous value of the emf in a given bar at a given time, and  $n$  is the number of parallel-connected emf's or "bars". If any emf in one or more bars has a negative value at a given time, its amplitude in expression (1) is written with a minus sign. Hence, the measured emf's shown in Table 1 are the total emf of sources connected in parallel and shifted in phase. However, starting with the thin wire and up to the strip which is  $\tau/18$  wide, the amplitude of the emf remains the same. In this parallel connection, the phase shift caused by the spatial shift of the infinitely thin conductors does not cause a noticeable change in the total emf, if the angle is less than a certain value. This may be seen by constructing two arbitrary harmonic curves shifted in phase, let us say, by  $\tau/18$ , or 10 electrical degrees. Let us assume that the emf in each conductor is sinusoidal. Then, for the two curves shown in Fig. 4, and shifted by  $\tau/18$  or 10 electrical degrees relative to one another, it can be said that one of these curves varies as  $\sin \omega t$ , and the other as  $\sin(\omega t - 10)$ . The amplitude is set as unity in both cases. The amplitude of the resultant curve will be defined at the intersection of these

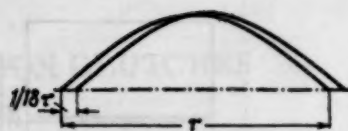


Fig. 4. Two sine half-waves, shifted in phase by  $\tau/18$ .

curves. This point lies at 95 electrical degrees for the first, and 85 for the second curve. In this case, the amplitude of the resultant curve will equal

$$E_{\text{max res}} = \frac{\sin 95^\circ + \sin 85^\circ}{2} = 0.996.$$

Consequently, the effective value of the resultant emf will be

$$E_{\text{eff}} = \frac{0.996}{1.41} = 0.706.$$

For unity amplitude,

$$E_{\text{eff}} = \frac{1}{1.41} = 0.709.$$

Consequently, the difference between the effective values, expressed in percent, will equal  $\frac{(0.709 - 0.706) \cdot 100}{0.709} = 0.38\%$ .

One can see that the emf in the thin conductor and that in the conductor  $\tau/18$  wide can be considered equal. This is confirmed by experiment (see Table 1). It can be considered, on the basis of what has been said, that the number of "bars" in a hollow rotor is

$$n_z = \frac{2\tau z}{18\tau} = 36z.$$

The optimum number of teeth is  $z = 6$  for all clutches, regardless of their power and speed. In this case, the number of "bars"  $n_z = 216$ .

As can be seen from Table 1, the measured voltage decreases according to the degree to which the circumferential strip length is increased. An emf is induced in the "bars" of the strip which is equal in length to the circumference of the hollow rotor; this emf is equal to the emf measured in the strip or thin conductor. We will assume that the emf in the "bar" is sinusoidal, as before. During one-half of the period corresponding to  $\tau$ , 18 harmonic curves which vary sinusoidally as  $\sin(\omega t - \varphi)$  are induced, and are shifted by  $\varphi = 10$  electrical degrees relative to one another. In this case, the total emf at each instant can be determined from expression (1). All these harmonic curves are expressed by the functions:  $\sin(\omega t - 0)$ ,  $\sin(\omega t - 10)$ ,  $\sin(\omega t - 20)$ , ...,  $\sin(\omega t - 180)$ , respectively.

TABLE 1

$L$	$12\tau$	$6\tau$	$2\tau$	$\tau$	$\frac{1}{2}\tau$	$\frac{1}{4}\tau$	$\frac{1}{18}\tau$	$\frac{1}{36}\tau$	Thin wire
$U, \text{V}$	0.068	0.068	0.068	0.133	0.158	0.172	0.175	0.175	0.175

TABLE 2

$\omega t$	0	30	60	90	120	150	180
$\Sigma e_{\text{inst}}$	-0.6	-0.52	-0.30	0	0.30	0.52	0.6

The results of the summations according to expression (1) for the instantaneous values  $\omega t = 0, 30, 60, 90, 120, 150$ , and  $180$  electrical degrees are presented in Table 2.

As can be seen from Table 2, the amplitude of the resultant curve is defined at  $\omega t = 0$  and  $180$  electrical degrees. The amplitude of the total curve is thus equal to  $e_{\text{max res}} = 0.6 e_{\text{max}}$ , where  $e_{\text{max}}$  is the amplitude of one curve which varies sinusoidally as  $\sin(\omega t - \varphi)$ .

Consequently, the effective value of the resultant emf is  $e_{\text{eff res}} = 0.415 e_{\text{max}}$ .

The emf measured in the thin wire, according to Table 1, is  $0.175$  volts. Assuming that this emf is sinusoidal, we find that its amplitude is  $0.175 \cdot 1.41 = 0.247$  volts. Consequently, the effective value of the resultant emf for 18 components, according to the preceding, will equal  $e_{\text{eff res}} = 0.247 \cdot 0.425 = 0.105$  volts.

The voltage measured across the strip of width  $\tau$ , corresponding to a half-period, will be  $e_{\text{eff}} = 0.133$  volts, according to Table 1.

Keeping in mind that the emf in the thin wire does not in fact change sinusoidally, but according to the curve shown in Fig. 5, it can be acknowledged that the measurements approach calculated data rather closely. All this confirms the correctness of the assumption that the hollow rotor can be considered as a squirrel cage which consists of a definite number of "bars" shorted at their ends by cylindrical strips lying beyond the limits of the teeth on the star-wheel.

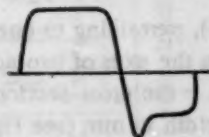


Fig. 5. Oscillogram of the change in the emf in a thin wire, and in a conductor  $\tau/18$  wide.

### 3. Calculation of the emf in One "Bar" of the Rotor

An emf is induced in a rotor "bar" in the same manner as in high-frequency induction machines. A description of the mechanism of inducing the emf and the method of calculating it is given in [3], where the amplitude of the induced emf is determined from the formula

$$E_{\text{eff}} = 2k_b W / \Phi_a \cdot 10^{-8} \text{ volts.}$$

Here,  $k_b$  is a coefficient of the instantaneous emf curve equal to approximately 1.15, according to [3];

$W$  is the number of turns (in our case,  $W = 0.5$ );  $f$  is the frequency of the current, equal to  $f = n/60$  in our case;  $n$  is the angular velocity of the motor in rpm;  $\Phi_a = \Phi_z - \Phi_g$  is the effective value of the flux.

In the last expression,  $\Phi_z$  is the flux of one tooth, and  $\Phi_g$  is the gap flux.

Consequently, the expression for the electromotive force, as it pertains to the "bars" of the rotor and the six-pronged star, takes the form

$$E_{\text{eff}} = 11.5n\Phi_a \cdot 10^{-10} \text{ volts.} \quad (2)$$

### Calculating the Flux $\Phi_a$

The flux  $\Phi_a$  is calculated on the basis of the following considerations. The over-all flux generated by the teeth of the star is determined from the formula

$$\Phi_{\text{ov}} = \frac{0.4\pi AW_g}{R_{\text{ov}}},$$

where  $AW_g$  are the ampere-turns which generate the flux in the air gap, and  $R_{\text{ov}}$  is the reluctance of the air gaps. The flux path has two gaps:  $\delta_1$  - between the star-wheel and the flux path, and  $\delta_2$  - between the hub of the star-wheel and the flux path (see Fig. 1).

Therefore,

$$R_{\text{ov}} = R_1 + R_2, \\ R_1 = \frac{\delta_1 k_b}{S} = \frac{2\delta_1 k_b}{\pi D l}, \quad R_2 = \frac{\delta_2}{\pi D_H l_H}.$$

Here  $R_1$  is the reluctance of the main air gap;  $R_2$  is the reluctance of the air gap between the hub of the star-wheel and the flux path;  $S$  - the cross section of the teeth on the star-wheel, reckoned from the inner diameter of the wheel;  $D$  - the inner diameter of the wheel, in cm;  $l$  - the axial length of a star-wheel tooth, in cm;  $D_H$  - the diameter of the wheel hub;  $l_H$  - the hub length over the part adjacent to the stationary portion of the flux path, in cm (see Fig. 1);  $k_b$  - the Carter coefficient, which accounts for the fact that the wheel is toothed, and is determined from the formula

$$k_b = \frac{t + 10b_1}{b + 10b_1}.$$

In the last expression,  $t = \pi D/6$ ;  $b = \pi D/12$ .

Consequently,

$$R_{\text{ov}} = \frac{2\delta_1 D_H l_H k_b + \delta_2 D l}{\pi D l_H l_H}$$

whence

$$\Phi_{\text{ov}} = \frac{1.26 \cdot 0.85 AW \pi D l_H l_H}{2\delta_1 D_H l_H + \delta_2 D l},$$

where AW are the ampere-turns which generate the flux  $\Phi_{ov}$  in the air gap and in the steel flux path.

The coefficient 0.85 in the last formula takes into account that approximately 85% of the ampere-turns are effective in generating the flux in the air gap.

The flux in one tooth is

$$\Phi_z = \frac{\Phi_{ov}}{6} = \frac{0.56AWDlD_H l_H}{2\delta_1 D_H l_H k_\delta + \delta_2 D l}.$$

The flux  $\Phi_g$  generated in one gap is determined from the following expressions [5]:

$$\Phi_g = 1.55AWl \lg \frac{\delta_1 k_\delta + \frac{\pi m}{4}}{\delta_1 k_\delta},$$

where  $m = \pi D/12$  is the gap width.

One can therefore write

$$\Phi_a = \Phi_z - \Phi_g = \frac{0.56AWDlD_H l_H}{2\delta_1 D_H l_H k_\delta + \delta_2 D l} - 1.55AWl \lg \frac{\delta_1 k_\delta + \frac{\pi m}{4}}{\delta_1 k_\delta}. \quad (3)$$

The amplitudes of the emf's induced in the thin wires of two finished clutches, and the calculated values of the emf's from formulas (2) and (3), were compared in order to check how closely the calculated values approach reality. The results of the comparisons are given in Table 3.

As can be seen, the values computed from formulas (2) and (3) are sufficiently accurate for practical use.

#### 5. Calculating the Ohmic Resistance of the Rotor "Bars"

The computation of the rotor resistance is analogous to that for a squirrel cage. As is known [6], the phase resistance of a squirrel cage is

$$r_{rot} = r_b + \frac{2r_K}{c^2}, \quad (4a)$$

where  $r_b$  is the resistance of a squirrel cage bar;  $2r_K/c^2$  is the resistance of the part of the short-circuiting ring which contacts the "bar". The "bar" resistance of a hollow rotor is

$$r_b = \frac{\rho l}{S},$$

where  $\rho$  is the resistivity of the rotor metal;  $l$  - the "bar" length in meters, taken as the axial length of the

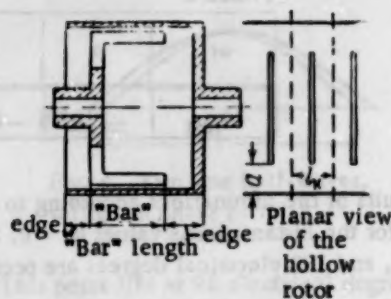


Fig. 6.

star-wheel;  $S = \frac{\pi D \Delta}{n_z}$  - the cross-sectional area of the bar in  $\text{mm}^2$ ;  $D$  - the rotor diameter in mm, and  $\Delta$  - the wall thickness of the hollow cylindrical rotor in mm.

The resistivity  $\rho$  must be chosen on the basis of the expected overheating temperature of the rotor being planned. For aluminum at an overheating temperature of  $100^\circ\text{C}$ ,  $\rho = 0.035$ , and for duralumin at  $150^\circ\text{C}$ ,  $\rho = 0.07$ .

Consequently,

$$r_b = \frac{6.9 \cdot 10^{-3} \rho l}{D \cdot \Delta}. \quad (4b)$$

There are no so-called short-circuiting rings in the hollow rotor, but the edges of the rotor which protrude beyond the limits of the star-wheel (as shown in Fig. 6), can be considered as short-circuiting rings. Therefore, the resistance  $r_K$  in the expression  $2r_K/c^2$  for the edge of the hollow rotor included between the axes of two adjacent "bars" is determined analogously to  $r_b$ :

$$r_K = \frac{\rho l_K}{S_K},$$

where  $l_K = \frac{\pi D}{n_z} = 14.5 \cdot 10^{-6} D$  is the length of the protruding edge (in mm), pertaining to one bar, equal to the distance between the axes of two adjacent "bars" (see Fig. 6);  $S_K = a\Delta$  - the cross section of the edge in  $\text{mm}^2$ ;  $a$  - the edge width in mm (see Fig. 6);  $\Delta$  - the wall thickness of the edge in mm.

Consequently,

$$r_K = \frac{14.5 \cdot 10^{-6} D \rho}{a \cdot \Delta}.$$

The quantity  $c^2$  in the expression  $2r_K/c^2$  is determined from the formula [6]

TABLE 3

Clutch power, watts	Emf measured in a wire equal to the tooth length, volts	Emf computed from formulas (2) and (3)	Error, %
50	0.04	0.047	17.5
500	0.175	0.190	8.5



TABLE 4

Clutch power, watts	Rotor material	Dimensions					Emf in a bar $\tau/18$ wide, volts	Drive motor shaft power during clutch engagement, watts	Rotor bar resistance		Error, %
		$\rho$	a, mm	l, mm	D mm	$\Delta$ , mm			calculated, ohms	from experimental data, ohms	
5	Aluminum	$35 \cdot 10^{-8}$	2	12	42.6	0.4	$14 \cdot 10^{-3}$	14.2	$3.5 \cdot 10^{-3}$	$3.29 \cdot 10^{-3}$	-6.5
20	"	"	4	14	68.6	0.4	$35 \cdot 10^{-3}$	81	$2.71 \cdot 10^{-3}$	$3.28 \cdot 10^{-3}$	+176
50	"	"	4	9	78.6	0.4	$47 \cdot 10^{-3}$	190	$2.42 \cdot 10^{-3}$	$2.51 \cdot 10^{-3}$	+3.
300	Duralumin	$7 \cdot 10^{-8}$	8.5	30	105.5	0.75	$195 \cdot 10^{-3}$	630	$0.30 \cdot 10^{-3}$	$0.3 \cdot 10^{-3}$	0
500	"	"	6.5	45	96.5	0.75	$190 \cdot 10^{-3}$	1520	$0.43 \cdot 10^{-3}$	$0.51 \cdot 10^{-3}$	+19

Note: The values of  $\rho$  are given for a 50 watt clutch with an overheating temperature of  $100^\circ\text{C}$ ; the overheating temperature is  $150^\circ\text{C}$  for clutch powers greater than 50 watts.

$$c = 2 \sin \frac{\pi p}{n_z} = 2 \sin \frac{180.6}{216} = 0.174,$$

where  $p$  is the number of pairs of poles. In our case,  $p$  is equal to the number of teeth, that is,  $p = z = 6$ . Thus,  $c = 0.174$  and

$$\frac{2r_R}{c^2} = \frac{9.66 \cdot 10^{-4} p D}{a \Delta}. \quad (4c)$$

The total phase resistance of the rotor, that is, the "bar" resistance of the hollow rotor and the parts of the rotor edge in contact with them, is found by substituting the values from (4b) and (4c) in (4a):

$$r_{\text{rot}} = \frac{6.9 \cdot 10^{-2} p (a l + 1.4 \cdot 10^{-3} D^2)}{D a \Delta}. \quad (4d)$$

The method shown for determining the ohmic resistance of the rotor "bars" can be checked experimentally. Keeping in mind that the motor shaft power is entirely dissipated in heat as the clutch is engaged, we can write

$$P_{\text{mo}} = M_{\text{st}} n_{\text{mo}} 1.025 \cdot 10^{-3} = \frac{n_z E_{\text{eff}}^2}{r_{\text{rot}}}, \quad (5)$$

where  $P_{\text{mo}}$  is the shaft power of the motor during clutch engagement,  $M_{\text{st}}$  is the starting torque of the clutch, and  $n_{\text{mo}}$  is the motor speed during clutch engagement. Thus,

$$r_{\text{rot}} = \frac{n_z E_{\text{eff}}^2}{P_{\text{mo}}}.$$

Data obtained from finished clutches are compared in Table 4; this permits one to compute the ohmic resistance of a rotor "bar" from formula (4) and from the experimental data as used in formula (5).

#### 6. Calculating the Clutch Torque

During engagement to the motor shaft, a torque is applied equal to the starting torque of the clutch. Consequently, one can write, on the basis of expression (5),

$$M_{\text{st}} = \frac{n_z E_{\text{eff}}^2 \cdot 10^3}{r_{\text{rot}} n_{\text{mo}} 1.025} = \frac{211 \cdot E_{\text{eff}}^2 \cdot 10^3}{r_{\text{rot}} n_{\text{mo}}}. \quad (6)$$

Substituting the value for  $r_{\text{rot}}$  from (4) and for  $E_{\text{eff}}$  from (2) in expression (6), we get

$$M_{\text{st}} = \frac{4 n_{\text{mo}} \Phi_a D a \Delta \cdot 10^{-10}}{p (a l + 1.4 \cdot 10^{-3} D^2)}. \quad (7)$$

The expression for the flux can be put in the form

$$\Phi = \tau l B$$

where  $\tau = \frac{\pi D}{2z}$ ,  $l$  is the tooth length of the star-wheel in cm, and  $B$  is the flux density in gauss.

For the six-pronged star,  $\tau = 0.261 D$  ( $D$  in mm), and one can write

$$\Phi = 0.261 D l B. \quad (8)$$

Substituting  $\Phi$  from (8) in expression (7), we get

$$M_{st} = \frac{27.2 \cdot 10^{-12} n_{mo} D^3 l^2 B^2 a \Delta}{p (al + 1.4 \cdot 10^{-3} D^2)} \quad (9)$$

Since the torque developed by the hollow rotor is caused by the rotor slipping with respect to the rotating star-wheel, the general expression for the clutch torque can be put in the following form:

$$M_c = \frac{27.2 \cdot 10^{-12} n_{mo} s D^3 l^2 B^2 a \Delta}{p (al + 1.4 \cdot 10^{-3} D^2)} \quad (10)$$

where  $s = \frac{n_w - n_{rot}}{n_w}$  is the slip of the hollow rotor with

respect to the star-wheel,  $n_w$  is the speed of the wheel, and  $n_{rot}$  is the rotor speed.

It can be seen by comparing expressions (9) and (10) that the torque is proportional to the slip, if the flux and speed of the motor change very slightly. Consequently, the characteristics  $s = f(M)$ , or  $n = f(M)$  will vary linearly. In reality, the clutches actually made have an  $n = f(M)$  characteristic which is not strictly linear. But to simplify the solution of the problems concerning induction clutches, one can assume that this characteristic is linear. Consequently, the characteristic  $n = f(P_{ms})$ , where  $P_{ms}$  is the power at the clutch shaft in watts, will be parabolic. The maximum power developed by the clutch (the apex of the parabola) will be developed when slip  $s = 0.5$ .

#### 7. Calculating the Geometric Dimensions of the Clutch

The determination of the basic dimensions of the main clutch parts is based on expressions (9) and (10). One must also consider what dimensions are desirable from a standpoint of construction. The values  $n_{mo}$ ,  $B$ ,  $a$ , and  $\Delta$  in expressions (9) and (10) must be determined from a number of variables, keeping the following considerations in mind:

a. Increasing the motor speed reduces the clutch and motor size, and also reduces the exciting ampere-turns. However, the noise of the clutch at higher speeds becomes significant, and the requirements on dynamic balancing of its rotating parts become more stringent.

b. In choosing the flux density  $B$  in the air gap, one must simultaneously check the degree of saturation in the individual parts of the flux path (in the root of a star-wheel tooth, in the hub, and in the cavity of the stationary flux path).

c. The values of  $a$  and  $\Delta$  can be selected on the basis of the data shown in Table 5, for clutches planned to operate at high frequency (400 cps).

TABLE 5

Power range watts	5-50	60-100	125-300	500-1000
$a$ , mm	3	4-5	5-7	8-10
$\Delta$ , mm	0.4	0.55	0.75	1.00

d. The most favorable ratio of  $D$  to 1 is determined from computations using a number of variables.

#### 8. Calculating the Clutch Excitation

In calculating the clutch excitation, one must take into account the ampere-turns necessary for the two air gaps and for the steel flux path. The general expression is written in the form

$$\Sigma AW = AW_{sf} + AW_{\delta_1} + AW_{\delta_2}$$

where  $\Sigma AW$  are the total ampere-turns,  $AW_{sf}$  - the ampere-turns of the steel flux path,  $AW_{\delta_1}$  - the ampere-turns of the main air gap, and  $AW_{\delta_2}$  - the ampere-turns of the air gap between the star-wheel hub and the stationary flux path.

The method of calculating the ampere-turns is shown in various references (see, for example, [6]). In connection with this, one should keep in mind that the flux of the star-wheel goes only in one direction, and therefore, formula (6-5) in [6] takes the form

$$F_{\delta} = 0.8 B_{\delta} \delta.$$

#### 9. Calculating the Drive Motor Power

It was shown above that the clutch develops maximum power when the slip  $s = 0.5$ . Consequently, the drive motor must develop a power of  $P_{mo} = 2P_{mp}$ , where  $P_{mp}$  is the maximum power of the clutch. This means that the nominal power of the motor must be twice the nominal (maximum) clutch power. The overload rating of the drive motor is determined from the following calculation. The starting torque of the clutch, as was shown above, is found from the relation  $M_{st} = 2M_{nom}$ , where  $M_{nom}$  is the nominal clutch torque.

It follows from the preceding that the drive motor speed during clutch engagement is thus equal to  $n_{mo} \approx 2n_{NS}$ , where  $n_{NS}$  is the nominal speed of the clutch.

Consequently, the motor must develop the power

$$P_{mo} = 2n_{NS} 2M_{NS} \cdot 1.025 \cdot 10^{-5} \approx 4P_{NS}$$

as the clutch is engaged.

This means that the motor must develop a maximum power which is twice its nominal power.

Note: The motor slip was not taken into account in the calculations which have been made. Moreover, it has been assumed that the mechanical characteristic of the clutch,  $n_c = f(M_c)$ , is linear.

#### LITERATURE CITED

1. V. S. Sharov, Slipping Clutches [in Russian] (Gosenergoizdat, 1958).
2. V. V. Solodovnikov (ed.), Fundamentals of Automatic Control [in Russian] (Mashgiz, 1959) vol. 2, chap. 1.

3. A. E. Alekseev, "High frequency machines" Electrical Machine Construction [in Russian] (NTOE Press, 1930).
4. A. S. Kasatkin and M. A. Perekalin, Electrotechnology [in Russian] (Gosenergoizdat, 1955).

5. K. Schmidt, Fortschritte im Bau von Mittel und Hochfrequenzmaschinen (ETZ, 1928).
6. P. S. Sergeev (ed.), Design of Electrical Machines [in Russian] (Gosenergoizdat, 1950).

positive saturation  
negative saturation

is the slope of the  
characteristic

is the slope of the  
characteristic

is the slope of the  
characteristic

is the slope of the  
characteristic

is the slope of the  
characteristic

is the slope of the  
characteristic

The effect of magnetic saturation on the static characteristics of the machine is considered. It is shown that the effect of saturation is to reduce the slope of the characteristic and to shift the characteristic towards the origin.

The effect of magnetic saturation on the static characteristics of the machine is considered. It is shown that the effect of saturation is to reduce the slope of the characteristic and to shift the characteristic towards the origin.

The effect of magnetic saturation on the static characteristics of the machine is considered. It is shown that the effect of saturation is to reduce the slope of the characteristic and to shift the characteristic towards the origin.

The effect of magnetic saturation on the static characteristics of the machine is considered. It is shown that the effect of saturation is to reduce the slope of the characteristic and to shift the characteristic towards the origin.

The effect of magnetic saturation on the static characteristics of the machine is considered. It is shown that the effect of saturation is to reduce the slope of the characteristic and to shift the characteristic towards the origin.

The effect of magnetic saturation on the static characteristics of the machine is considered. It is shown that the effect of saturation is to reduce the slope of the characteristic and to shift the characteristic towards the origin.

The effect of magnetic saturation on the static characteristics of the machine is considered. It is shown that the effect of saturation is to reduce the slope of the characteristic and to shift the characteristic towards the origin.



# EFFECT OF MAGNETIZATION IRREGULARITY ON THE STATIC CHARACTERISTICS OF CORES. II

G. D. Kozlov

Moscow

Translated from *Avtomatika i Telemekhanika*, Vol. 21, No. 7, pp. 1057-1072,

July, 1960

Original article submitted November 25, 1959

The effect of magnetization irregularity on the static characteristics of cores is considered. Characteristics obtained by experiment and by calculation are compared. Some recommendations concerning the selection of geometric relations of a divided magnetic circuit are given.

The present paper is devoted to further studies of the magnetization irregularity effect on the core static characteristics. In [1-3], the irregularity in core magnetization was considered for a toroidal magnetic circuit and for a hysteresis loop in the shape of a parallelogram. In this, the slope of the "horizontal" portions of the hysteresis loop was not taken into account (the angle  $\delta = 0$ ). The characteristics of materials used in practice actually have a certain slope in the saturation region (the angle  $\delta \neq 0$ ), which has to be taken into account. This is especially important in analyzing the operation of a divided magnetic circuit.

In the present paper, we shall consider the magnetization irregularity effect on the core characteristics in the case where the material hysteresis loops are of the shape shown in Fig. 1. The dependence of the magnetic characteristics of a core with a divided magnetic circuit on its dimensions and the location of the magnetizing winding will also be considered.

For the sake of simplicity, the effect of the core magnetization irregularity will be analyzed for a toroidal shape of the magnetic circuit.

## 1. Toroidal Magnetic Circuit

In order to determine the  $B = f(F)$  magnetic characteristics of the core when the material hysteresis loops have the shape shown in Fig. 1, it is first necessary to find a mathematical expression for individual branches of hysteresis loops in the  $b = f(h)$  form [3].

Mathematically, individual hysteresis loop branches can be represented in the following manner:

### The Ultimate Hysteresis Loop

#### Rising branch

$$b = \frac{2b_p}{h_s - h_p} \left( h - \frac{h_s + h_p}{2} \right) + \operatorname{tg} \delta \frac{h_s + h_p}{h_s - h_p} (h - h_p), \quad (1)$$

#### descending branch

$$b = \frac{2b_p}{h_s - h_p} \left( h + \frac{h_s + h_p}{2} \right) + \operatorname{tg} \delta \frac{h_s + h_p}{h_s - h_p} (h + h_p), \quad (2)$$

#### positive saturation

$$b = b_p + \operatorname{tg} \delta (h + h_p), \quad (3)$$

#### negative saturation

$$b = -b_p + \operatorname{tg} \delta (h - h_p), \quad (4)$$

Here,  $\operatorname{tg} \delta = \frac{b_s - b_p}{h_s - h_p} = \frac{b_r - b_p}{h_p}$  is the slope of the saturation and maximum magnetization branches of the hysteresis loops.

### Symmetric Hysteresis Loop Cycles

#### Rising branch

$$b = \frac{b_p}{h_s - h_p} [(2h - h_s) - h_p] + \operatorname{tg} \delta \frac{h_s + h_p}{h_s - h_p} h - \operatorname{tg} \delta \frac{h_s + h_p}{h_s - h_p} h_p, \quad (5)$$

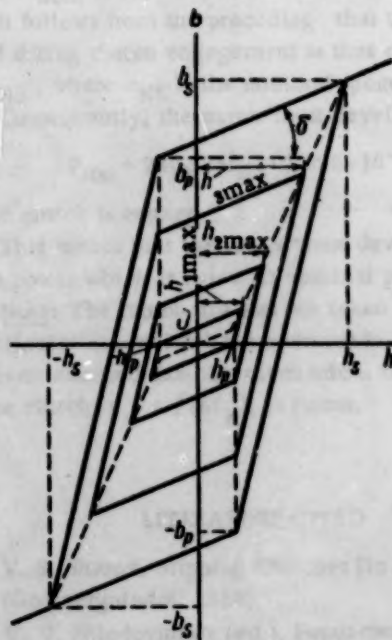


Fig. 1.

descending branch

$$b = \frac{b_p}{h_s - h_p} [(2h + h_m) + h_p] + \operatorname{tg} \delta \frac{h_s + h_p}{h_s - h_p} h + \operatorname{tg} \delta \frac{h_m + h_p}{h_s - h_p} h_p; \quad (6)$$

positive magnetization

$$b = \frac{b_p}{h_s - h_p} (h_m - h_p) + \operatorname{tg} \delta \frac{h_m - h_p}{h_s - h_p} h_p + \operatorname{tg} \delta h, \quad (7)$$

negative magnetization

$$b = -\frac{b_p}{h_s - h_p} (h_m - h_p) - \operatorname{tg} \delta \frac{h_m - h_p}{h_s - h_p} h_p + \operatorname{tg} \delta h. \quad (8)$$

By substituting  $h = h_M$  in Eqs. (5) and (6) or (7) and (8), we can determine the loci of the peaks of symmetric hysteresis loop cycles:

$$b = \frac{b_p}{h_s - h_p} (h_m - h_p) + \frac{\operatorname{tg} \delta}{h_s - h_p} (h_s h_m - h_p^2). \quad (9)$$

For  $h_M \geq h_s$  values, the material magnetization is reversed with respect to the ultimate hysteresis loop. For this, the maximum induction values are determined by the  $h_M$  value, and they lie on the straight line

$$b = b_p + \operatorname{tg} \delta (h_m + h_p). \quad (10)$$

For field strength values  $h_M \leq h_p$ , the material magnetization will not be reversed with respect to the symmetric hysteresis loops; in this case, the maximum induction values will lie on the straight line

$$b = h_M \operatorname{tg} \delta. \quad (11)$$

However, individual layers of the core material will have different field strengths for the same magnetization ampere-turns. Therefore, for determining the total change in the  $B = f(F)$  core induction, Eqs. (1)-(11) should be reduced to the  $b = f(F)$  form and then substituted in Eq. (8) [3]:

$$B = \frac{1}{R_n - R_p} \int_{R_p}^{R_n} b dR. \quad (11a)$$

The transformed Eqs. (1)-(11) will assume the following forms, respectively:

Ultimate Hysteresis Loop

Rising branch

$$b = \frac{2b_p}{F_s - F_p} \left( F \frac{R_n}{R} - \frac{F_s + F_p}{2} \right) + \operatorname{tg} \delta \frac{F_s + F_p}{F_s - F_p} \left( F \frac{R_n}{R} - F_p \right), \quad (12)$$

descending branch

$$b = \frac{2b_p}{F_s - F_p} \left( F \frac{R_n}{R} + \frac{F_s + F_p}{2} \right) + \operatorname{tg} \delta \frac{F_s + F_p}{F_s - F_p} \left( F \frac{R_n}{R} + F_p \right); \quad (13)$$

positive saturation

$$b = b_p + \operatorname{tg} \delta \left( F \frac{R_n}{R} + F_p \right), \quad (14)$$

negative saturation

$$b = -b_p + \operatorname{tg} \delta \left( F \frac{R_n}{R} - F_p \right). \quad (15)$$

Symmetric Hysteresis Loop Cycles

Rising branch

$$b = \frac{b_p}{F_s - F_p} \left[ (2F - F_m) \frac{R_n}{R} - F_p \right] + \operatorname{tg} \delta \left[ -\frac{F_s + F_p}{F_s - F_p} F \frac{R_n}{R} - \frac{F_p}{F_s - F_p} \left( F_m \frac{R_n}{R} - F_p \right) \right] \quad (16)$$

descending branch

$$b = \frac{b_p}{F_s - F_p} \left[ (2F + F_m) \frac{R_n}{R} + F_p \right] + \operatorname{tg} \delta \left[ \frac{F_s + F_p}{F_s - F_p} F \frac{R_n}{R} + \frac{F_p}{F_s - F_p} \left( F_m \frac{R_n}{R} - F_p \right) \right]; \quad (17)$$

positive magnetization

$$b = \frac{b_p}{F_s + F_p} \left( F_m \frac{R_n}{R} - F_p \right) + \operatorname{tg} \delta \left[ F \frac{R_n}{R} + \frac{F_p}{F_s - F_p} \left( F_m \frac{R_n}{R} - F_p \right) \right], \quad (18)$$

negative magnetization

$$b = -\frac{b_p}{F_s - F_p} \left( F_m \frac{R_n}{R} - F_p \right) + \operatorname{tg} \delta \left[ F \frac{R_n}{R} - \frac{F_p}{F_s - F_p} \left( F_m \frac{R_n}{R} - F_p \right) \right]. \quad (19)$$

In order to find the "normal magnetization curve," Eqs. (9)-(11) must be reduced to the following form:

$$b = \frac{b_p}{F_s - F_p} \left[ F_M \frac{R_p}{R} - F_p \right] + \frac{\lg \delta}{F_s - F_p} \left[ F_s F_M \frac{R_p}{R} - F_p^2 \right], \quad (20)$$

$$b = b_p + \lg \delta \left[ F_M \frac{R_p}{R} + F_p \right], \quad (21)$$

$$b = \lg \delta F_M \frac{R_p}{R}. \quad (22)$$

In this case, we shall assume that  $\lg \delta = \frac{b_s - b_p}{F_s - F_p} = \frac{b_r - b_p}{F_p}$  determines the saturation line slope for the

internal layer of the core material ( $R = R_B$ ). For this, the core dimensions are so chosen that the inequality

$$\alpha < \beta \quad (23)$$

is satisfied (case 1 [3]).

Here,  $\beta = h_s/h_p = F_s/F_p$  is the coefficient which characterizes the magnetic material.

In dependence on the maximum value  $F_M$  of magnetization ampere-turns, the alternating magnetization of the core will take place under different conditions.

Three shapes of symmetric alternating magnetization loops can be distinguished: 1) for the  $F_p < F_M \leq \alpha F_p$  values, 2) for the  $\alpha F_p < F_M \leq F_s$  values, and 3) for the  $F_s < F_M \leq \alpha F_s$  values.

The derivations of analytical expressions describing the total change in the core induction  $B = f(F)$  for different alternating magnetization conditions are given in the Appendix. By using these equations, we determined the family of symmetric alternating magnetization loops and the normal magnetization curve for the  $b_p = 1$ ,  $b_s = 1.4$ ,  $\alpha = 2$ , and  $\beta = 4$  values; the results are given in Fig. 2. In plotting the calculated characteristics, the relative quantity  $F/F_p$  was laid off on the axis of abscissas. In this, the maximum value of magnetization ampere-turns was chosen in such a manner that  $F_M/F_p = \alpha$  for the first type of symmetric alternating magnetization loops,  $F_M/F_p = \beta$  for loops of the second type, and  $F_M/F_p = \alpha\beta$  for loops of the third type.

For the sake of comparison, Fig. 3 shows the family of symmetric alternating magnetization loops, obtained experimentally for a core made of the 50 NP material, the dimensions of which are given in Table 1.

Figure 4 shows the  $B = f(F)$  dependence of the ultimate alternating magnetization loop and the "normal magnetization curve" (dotted line), which were plotted separately with respect to the known material parameters  $h_p$ ,  $h_s$ ,  $b_p$ , and  $b_s$ .

From the plotting in Fig. 4, it is obvious that the intersections of the continuations of linear portions of the "normal magnetization curve" with the coordinate

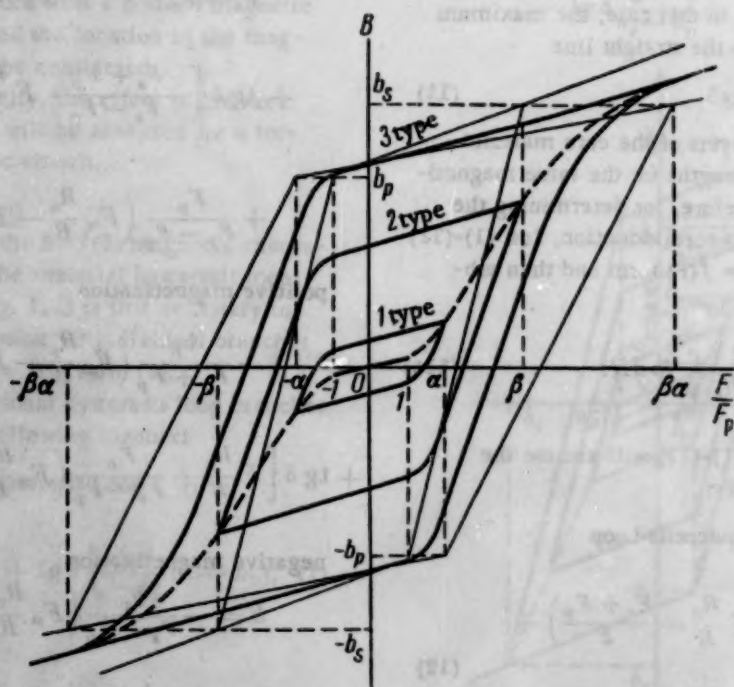


Fig. 2.





Fig. 3.

axes and with each other make it possible to determine the values of  $b_s$ ,  $b_r$ ,  $F_s(\alpha - 1)/\ln\alpha$ , and  $F_p(\alpha - 1)/\ln\alpha$ —by means of which all parameters of the magnetic material can be determined if the value of  $\alpha$  is known.

Thus, if the material hysteresis loop is known, then, for certain given dimensions of the toroidal core, it is possible to plot the family of the core alternating magnetization loops and the "normal magnetization curve." Conversely, by means of simple geometric constructions and calculations, the magnetic material parameters  $h_p$ ,  $h_s$ ,  $b_p$ , and  $b_s$  can be determined with respect to the available experimental "normal magnetization curve."

Let us consider the order of determining these parameters with respect to the experimental "normal magnetization curve."

1) We plot the experimental dependence  $U_{av} = f(F)$  for a core whose dimensions are known. Here,  $U_{av}$  is

the average voltage over a half-period, and  $F$  are the magnetization ampere-turns for a sinusoidal current.

Since the value of  $U_{av}$  is proportional to  $B_{max}$ , it can be considered that the  $U_{av} = f(F)$  dependence is proportional to  $B_{max} = f(F)$ .

2) The "normal magnetization curve"  $B_{max} = f(F)$ , which is obtained experimentally, is plotted in a coordinate system. Then, by continuing the linear portions of the "normal magnetization curve" until they intersect the coordinates and each other, we obtain the X, Y, and Z intersection points (Fig. 4). It is obvious from the plot that the magnitude of OY corresponds to the  $b_r$  value; the projection of OZ on the axis of ordinates corresponds to the  $b_s$  value; the projection of OZ on the axis of abscissas corresponds to the  $F_s(\alpha - 1)/\ln\alpha$  value; and the projection of OX on the axis of abscissas corresponds to the  $F_p(\alpha - 1)/\ln\alpha$  value. Hence, since the value of  $\alpha$  is known, we determine the  $F_p$ ,  $F_s$ ,  $\tan\delta = (b_s - b_r)/F_s$ , and  $b_p = b_r - \tan\delta F_p$  values, and we find the material parameters  $h_p$ ,  $h_s$ ,  $b_p$ , and  $b_s$ .

3) By substituting the found values in Eqs. (38)–(42) (see Appendix), we can calculate the "normal magnetization curve." Moreover, by plotting the theoretical curve in the same coordinate system as the experimental curve, we can estimate the accuracy in determining the magnetic material parameters.

Figure 5 shows the experimental (solid lines) and the theoretical (dotted lines) normal magnetization curves for different cores, the data of which are given in Table 1.

A comparison of characteristics obtained by experiment and by calculation (Fig. 5) shows that, if the material hysteresis loops are represented in the shape

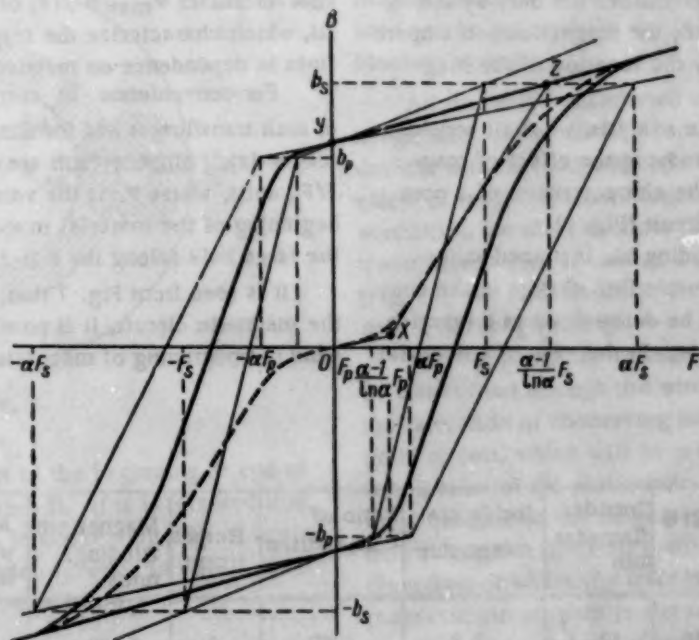


Fig. 4.

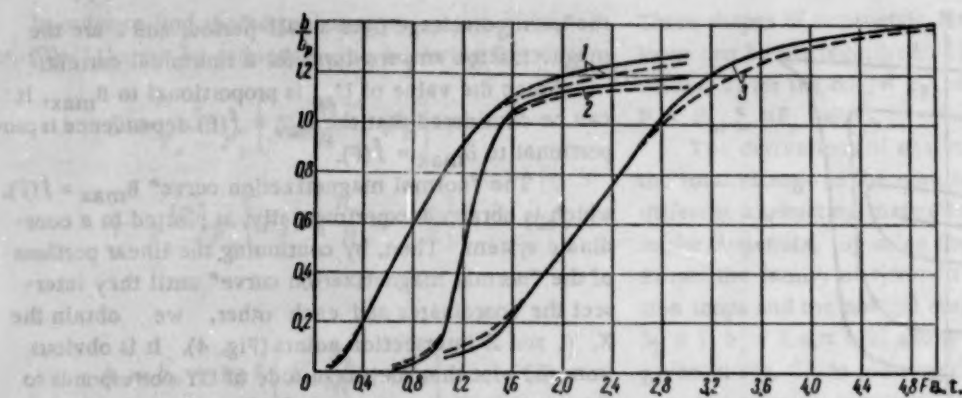


Fig. 5.

of parallelograms, where the slope of "horizontal" portions and the effect of the core magnetization irregularity are taken into account, it is possible to obtain theoretical relations which analytically describe the static core characteristics. For practical purposes, the agreement between the theoretical and experimental characteristics is satisfactory.

## 2. The Divided Magnetic Circuit

The operation principle of devices with divided magnetic circuits is actually based on the irregularity in magnetizing the magnetic circuit along different closed magnetic loops. Therefore, in analyzing the magnetization process in such a magnetic circuit, it is necessary to analyze the irregular magnetization in separate connecting links, as well as in the entire magnetic circuit. In this case, the  $\Phi_{\max} = f(F)$  dependence can be conveniently used for the magnetic regime characteristics of the magnetic circuit.

In divided magnetic circuits, the connecting link magnetic conditions are determined not only by the magnetic circuit dimensions, the magnetization ampere-turns, and by  $F$ , but also by the location of the magnetizing winding.

In order to simplify the analysis, we shall consider a two-hole transfluxor in studying the effect of magnetization irregularity on the characteristics of a core with a divided magnetic circuit (Fig. 6).

If the magnetizing winding  $W_m$  is placed at the connecting link I, the magnetic flux change in the connecting links II and III can be determined as a function of magnetizing ampere-turns. In the case of a material

with the hysteresis loop shown in Fig. 1, the magnetization reversal in the magnetic circuit will first take place around the large hole in the volume which is in contact through link II and then around both holes in the volume which is in contact through link III. The magnetization reversal through link II takes place in the toroidal volume, and the magnetization reversal through link III occurs in a somewhat extended volume, whose shape is similar to a transmission belt. In order to simplify the analysis, the extended volume can be reduced to a toroidal volume without changing either the outside or the inside perimeter lengths  $l_{O2}$  and  $l_{I2}$ , or the volume cross section. The analysis of magnetization reversal processes in toroidal volumes can be entirely replaced by an analysis of these processes in equivalent toroidal cores. Therefore, all the conclusions concerning the magnetization irregularity in toroidal cores (see [3] and Section 1 of the present paper) are applicable to toroidal volumes. Fig. 7 shows the experimental magnetic characteristics  $\Phi_{\max} = f(F)$  of connecting links II and III, which characterize the magnetic flux changes in the links in dependence on magnetizing ampere-turns.

For convenience in comparing the characteristics of such transfluxors and for simplifying the analysis, magnetizing ampere-turns are represented in relative  $F/F_p$  units, where  $F_p$  is the value of ampere-turns at the beginning of the material magnetization reversal around the large hole (along the I-II-I path).

It is seen from Fig. 7 that, for suitable dimensions of the magnetic circuit, it is possible to determine beforehand the beginning of magnetization reversal in con-

TABLE 1

Curve No.	Material type	Outside diameter, mm	Inside diameter, mm	Ratio of core radii, $\alpha$	Height, mm	Magnetizing winding, turns	Measuring winding, turns
1	Ferrite	13	7.8	1.67	3	20	250
2	50NP	27.8	20	1.39	5	20	130
3	KhVP	39.2	28.2	1.39	10	40	120

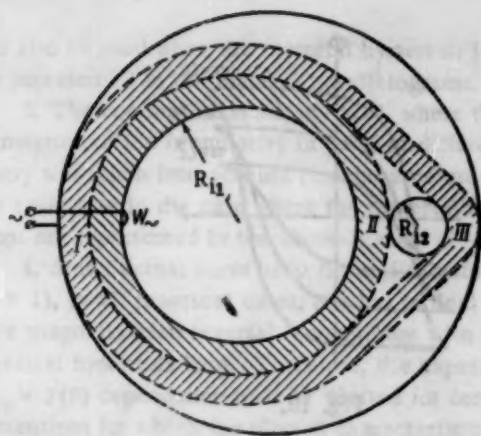


Fig. 6.

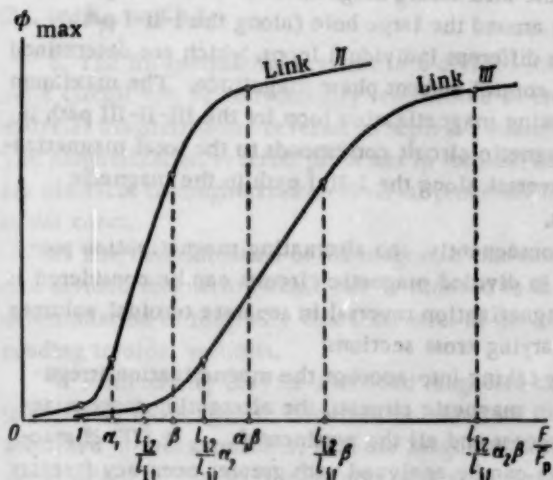


Fig. 7.

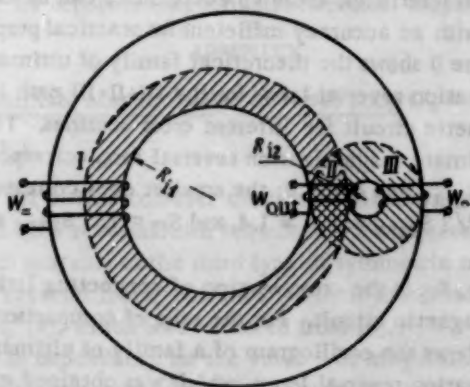


Fig. 8.

necting link III with respect to the beginning or end of magnetization reversal in link II. If it is required that the magnetization reversal in connecting link III begins after the end of magnetization reversal in link II, the following inequality must be satisfied:

$$\beta \leq \frac{l_{i2}}{l_{o1}}, \quad (24)$$

where  $l_{i2}$  is the inside perimeter of the "extended" volume (magnetization reversal along the I-III-I path), and  $l_{o1}$  is the outside perimeter of the toroidal volume (magnetization reversal along the I-II-I path).

Consequently, in this case, the magnetization reversal in the connecting link will occur successively, moving from one connecting link to another as the magnitude  $F$  of the magnetizing ampere-turns increases.

It should be noted here that inequality (24) must be satisfied if a reliable "magnetic decoupling" between individual magnetic circuit components is to be secured (which is necessary in almost all devices where divided magnetic circuits are used). By selecting suitable magnetic circuit dimensions, it is also possible to vary the slope of  $\Phi_{\max} = f(F)$  characteristics, and, for certain materials (for a sufficiently small value of the  $\beta$  coefficient), an equal slope of the  $\Phi_{\max} = f(F)$  characteristics can be obtained for different links in the magnetic circuit. This, in turn, will make it possible to obtain voltage pulses of identical shapes.

If the slopes of the  $\Phi_{\max} = f(F)$  characteristics are to be identical, the following relation must be satisfied:

$$\alpha_2\beta + \frac{1}{\alpha_1\beta} = 2. \quad (25)$$

Here,  $\alpha_2 = l_{o2}/l_{i2}$  is the ratio of the outside perimeter to the inside perimeter (alternating magnetization along the I-III-I path), and  $\alpha_1 = l_{o1}/l_{i1}$  is the ratio of the outside toroidal volume perimeter to the inside perimeter (alternating magnetization along the I-II-I path), where  $l_{i1}$  is the toroidal volume perimeter (alternating magnetization along the I-II-I path).

The devices where the principle of successive magnetization of links in a divided magnetic circuit is used can be successfully applied in distributing and blocking systems.

All the above-mentioned concerning magnetization irregularity can be used in considering the operation of devices with divided magnetic circuits. In studying the effect of magnetization irregularity on the device characteristics, we shall consider the example of a two-hole transfluxor, which is used as a controllable transformer (Fig. 8). We shall describe the operation principle of such a device [4 and 5].

Let a preliminary current pulse of large amplitude be transmitted through the winding  $W$ . This will cause the saturation of connecting links II and III in the magnetic circuit, which will be preserved also after the termination of the preliminary current pulse. Under these conditions, the magnetic flux around the smaller hole (along the III-II-III path) will not change, since, regardless of where the field is directed, a part of the magnetic circuit path is already saturated. Due to the insufficient magnitude of magnetizing ampere-turns, the magnetic flux around the large hole (along the



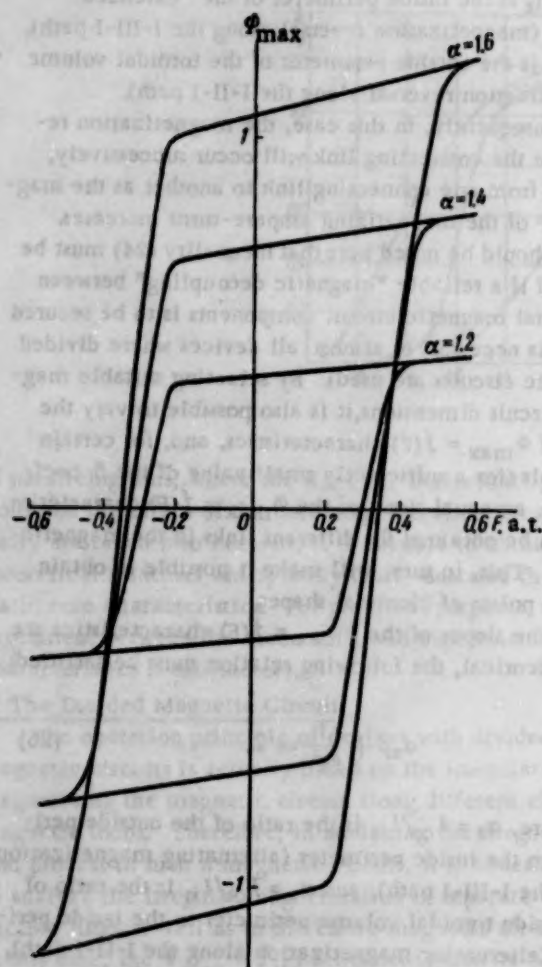


Fig. 9.

III-I-III path) will not change, either. Consequently, no voltage will appear at the  $W_{out}$  winding.

If a control current pulse is now transmitted through the  $W_{=}$  winding, in the direction opposite to the blocking direction, the magnetization reversal in the magnetic circuit will take place around the large hole (along the I-II-I path) in the opposite direction. Under these magnetizing conditions, the magnetization reversal can now take place around the smaller hole (along the III-II-III path). As a result, a voltage, the magnitude of which is proportional to the amplitude of the control current pulse, arises at the  $W_{out}$  winding. This mutual dependence can be explained in the following manner: when the magnetization reversal in the magnetic circuit takes place around the large hole (along the I-II-I path), the magnetic polarity of connecting link II is reversed completely or partially by the control current pulse in dependence on its magnitude. This determines the larger or smaller reversal volume magnetization round the smaller hole (along the III-II-III path).

The alternating magnetization of the magnetic circuit in volumes around the smaller hole (along the III-II-III path) follows the ultimate hysteresis loop,

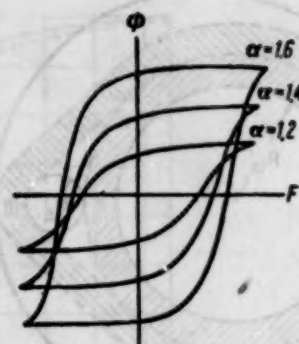


Fig. 10.

while the alternating magnetization of the magnetic circuit around the large hole (along the I-II-I path) follows different individual loops, which are determined by the control current phase magnitude. The maximum alternating magnetization loop for the III-II-III path in the magnetic circuit corresponds to the total magnetization reversal along the I-II-I path in the magnetic circuit.

Consequently, the alternating magnetization processes in divided magnetic circuits can be considered as the magnetization reversal in separate toroidal volumes with varying cross sections.

By taking into account the magnetization irregularity in magnetic circuits, the alternating magnetization process and all the pertinent  $\Phi_{max} = f(F)$  characteristics can be analyzed with greater accuracy (greater than that secured in [5]). Moreover, by taking into account the effect of magnetization irregularity on the static characteristics, these characteristics can be calculated with an accuracy sufficient for practical purposes.

Figure 9 shows the theoretical family of ultimate magnetization reversal loops for the III-II-III path in the magnetic circuit for different cross sections. The large ultimate magnetization reversal loop corresponds to  $S_{II} = S_{max}$  and  $\alpha = 1.6$ ; the smaller ones correspond to  $S_{II} = 2/3 S_{max}$  and  $\alpha = 1.4$ , and  $S_{II} = 1/3 S_{max}$  and  $\alpha = 1.2$ .

Here,  $S_{II}$  is the cross section of connecting link II in the magnetic circuit. For the sake of comparison, Fig. 10 shows the oscillogram of a family of ultimate magnetization reversal loops, which was obtained experimentally by using a transfluxor made of the 65NP material.

#### SUMMARY

1. The representation of the material hysteresis loops in the shape of parallelograms (Fig. 1) is justified since the mutual agreement of the "normal magnetization curves" obtained by calculation and by experiment can be used for practical purposes.

2. The method of determining the core induction as the  $B = f(F)$  function of magnetizing ampere-turns

can also be used when the material hysteresis loops are not represented in the shape of parallelograms.

3. The conclusions reached in [3], where the effect of magnetization irregularity in cores of different geometry was taken into account (for three values of  $\alpha$ ), are valid also in the case where the material hysteresis loops are represented in the above manner (Fig. 1).

4. Since actual cores have finite dimensions ( $\alpha > 1$ ), in all practical cases, one has to deal with the core magnetization reversal loop, and not with the material hysteresis loop. Therefore, the experimental  $U_{av} = f(F)$  dependence must be plotted for cores with dimensions for which the plotted characteristics have considerable linear portions ( $\alpha < 8$ ). This makes it easier to determine the material magnetic parameters ( $h_p$ ,  $h_s$ ,  $b_p$ , and  $b_s$ ).

5. The magnetization reversal in a divided magnetic circuit can be conveniently represented as the material magnetization reversal in separate volumes. The magnetization reversal processes in toroidal volumes are identical to magnetization reversal processes in toroidal cores.

6. The determination of all magnetic characteristics of a divided magnetic circuit can be reduced to the determination of magnetic characteristics of the corresponding toroidal volumes.

7. If inequality (24) for a divided magnetic circuit is satisfied, the magnetic circuit dimensions are characterized in such a manner, that the magnetization reversal in one of the sections begins only after the magnetization reversal ends in the other. Thus, if this inequality is satisfied, a considerable "magnetic decoupling" for separate magnetization reversal loops is secured.

#### APPENDIX

##### a) Ultimate Magnetization Reversal Loop ( $F_s < F_M \leq \alpha F_s$ )

Let us first consider the conditions for the core magnetization reversal with respect to the ultimate loop, which pertains to the third type of symmetric magnetization reversal loops. For this, we shall substitute (12)-(15) in Eq. (8), which was borrowed from [3].

In dependence on the value  $F$  of magnetization ampere-turns, the ultimate magnetization reversal loop will have different functional sections.

##### 1st Section. For $-F_M \leq F \leq F_p$ ,

$$B_1 = \frac{1}{R_n - R_p} \int_{R_n}^{R_p} \left[ -b_p + \lg \left( F \frac{R_n}{R} - F_p \right) \right] dR.$$

By solving this equation, we obtain

$$B_1 = -b_p + \lg \left[ \frac{\ln \alpha}{\alpha - 1} F - F_p \right]. \quad (26)$$

##### 2nd Section. For $F_p \leq F \leq \alpha F_p$ ,

$$B_2 = \frac{1}{R_n - R_p} \left\{ \int_{R_n}^R \left[ \frac{2b_p}{F_s - F_p} \left( F \frac{R_n}{R} - \frac{F_s + F_p}{2} \right) + \right. \right. \\ \left. \left. + \lg \left( \frac{F_s + F_p}{F_s - F_p} \left( F \frac{R_n}{R} - F_p \right) \right) \right] dR + \right. \\ \left. + \int_R^{R_n} \left[ -b_p + \lg \left( F \frac{R_n}{R} - F_p \right) \right] dR \right\}.$$

where  $R = R_n F/F_p$ .

By solving this equation, we obtain

$$B_2 = \frac{1}{\alpha - 1} \frac{b_p}{F_s - F_p} \left[ 2F \left( \ln \frac{F}{F_p} - 1 \right) - \right. \\ \left. - F_s (\alpha - 1) + F_p (\alpha + 1) \right] + \\ + \frac{1}{\alpha - 1} \frac{\lg \alpha}{F_s - F_p} \left[ 2FF_p \left( \ln \frac{F}{F_p} - 1 \right) + \right. \\ \left. + F(F_s - F_p) \ln \alpha + F_p^2 (\alpha + 1) - F_s F_p (\alpha - 1) \right]. \quad (27)$$

##### 3rd Section. For $\alpha F_p \leq F \leq F_s$ ,

$$B_3 = \frac{1}{R_n - R_p} \int_{R_n}^{R_p} \left[ \frac{2b_p}{F_s - F_p} \left( F \frac{R_n}{R} - \frac{F_s + F_p}{2} \right) + \right. \\ \left. + \lg \left( \frac{F_s + F_p}{F_s - F_p} \left( F \frac{R_n}{R} - F_p \right) \right) \right] dR.$$

By solving this equation, we obtain

$$B_3 = \frac{b_p}{F_s - F_p} \left[ \frac{\ln \alpha}{\alpha - 1} 2F - (F_s + F_p) \right] + \\ + \lg \left( \frac{F_s + F_p}{F_s - F_p} \left[ \frac{\ln \alpha}{\alpha - 1} F - F_p \right] \right). \quad (28)$$

##### 4th Section. For $F_s \leq F \leq \alpha F_s$ ,

$$B_4 = \frac{1}{R_n - R_p} \left\{ \int_{R_n}^R \left[ b_p + \lg \left( F \frac{R_n}{R} + F_p \right) \right] dR + \right. \\ \left. + \int_R^{R_n} \left[ \frac{2b_p}{F_s - F_p} \left( F \frac{R_n}{R} - \frac{F_s + F_p}{2} \right) + \right. \right. \\ \left. \left. + \lg \left( \frac{F_s + F_p}{F_s - F_p} \left( F \frac{R_n}{R} - F_p \right) \right) \right] dR \right\}.$$

where  $R = R_n F/F_s$ .

By solving this equation, we obtain

$$B_4 = \frac{1}{\alpha-1} \frac{b_p}{F_s - F_p} \left[ 2F \left( 1 + \ln \frac{\alpha F_s}{F} \right) - \right. \\ \left. - F_s (\alpha + 1) - F_p (\alpha - 1) \right] + \\ + \frac{1}{\alpha-1} \frac{\lg \delta}{F_s - F_p} \left[ 2FF_p \left( 1 - \ln \frac{F}{F_s} \right) + \right. \\ \left. + F(F_s + F_p) \ln \alpha - F_p^2 (\alpha - 1) - F_s F_p (\alpha + 1) \right]. \quad (29)$$

5th Section. For  $\alpha F_s \leq F \leq F_M$ .

$$B_5 = \frac{1}{R_n - R_b} \int_{R_b}^{R_n} \left[ b_p + \lg \delta \left( F \frac{R_n}{R} + F_p \right) \right] dR.$$

By solving this equation, we obtain

$$B_5 = b_p + \lg \delta \left[ \frac{\ln \alpha}{\alpha-1} F + F_p \right]. \quad (30)$$

The mathematical expression for the descending branch of the ultimate magnetization reversal loop is determined in a similar manner.

b) Second Type of Symmetric Magnetization Reversal Loops ( $\alpha F_p < F_M \leq F_s$ ).

For studying this type of magnetization reversal loops, we shall substitute Eqs. (16)-(19) in Eq. (8), which was borrowed from [3]. In dependence on the value  $F$  of magnetization ampere-turns, this type of magnetization reversal will have different functional sections.

1st Section. For  $-F_M \leq F \leq F_p$ .

$$B_1 = \frac{1}{R_n - R_b} \int_{R_b}^{R_n} \left\{ - \frac{b_p}{F_s - F_p} \left( F_M \frac{R_n}{R} - F_p \right) + \right. \\ \left. + \lg \delta \left[ F \frac{R_n}{R} - \frac{F_p}{F_s - F_p} \left( F_M \frac{R_n}{R} - F_p \right) \right] \right\} dR.$$

After solving this equation, we shall have

$$B_1 = - \frac{b_p}{F_s - F_p} \left[ \frac{\ln \alpha}{\alpha-1} F_M - F_p \right] + \\ + \lg \delta \left[ \frac{\ln \alpha}{\alpha-1} F - \frac{F_p}{F_s - F_p} \left( \frac{\ln \alpha}{\alpha-1} F_M - F_p \right) \right]. \quad (31)$$

2nd Section. For  $F_p \leq F \leq \alpha F_p$ .

$$B_2 = \frac{1}{R_n - R_b} \int_{R_b}^R \left\{ \frac{b_p}{F_s - F_p} \left[ (2F - F_M) \frac{R_n}{R} - F_p \right] + \right. \\ \left. + \lg \delta \left[ \frac{F_s + F_p}{F_s - F_p} F \frac{R_n}{R} - \frac{F_p}{F_s - F_p} \left( F_M \frac{R_n}{R} + F_p \right) \right] \right\} dR.$$

$$+ \frac{1}{R_n - R_b} \int_R^{R_n} \left\{ - \frac{b_p}{F_s - F_p} \left( F_M \frac{R_n}{R} - F_p \right) + \right. \\ \left. + \lg \delta \left[ F \frac{R_n}{R} - \frac{F_p}{F_s - F_p} \left( F_M \frac{R_n}{R} - F_p \right) \right] \right\} dR,$$

where  $R = R_B F / F_p$ .

By solving this equation, we obtain

$$B_2 = \frac{1}{\alpha-1} \frac{b_p}{F_s - F_p} \left[ 2F \left( \ln \frac{F}{F_p} - 1 \right) - \right. \\ \left. - F_M \ln \alpha + F_p (\alpha + 1) \right] + \\ + \frac{\lg \delta}{\alpha-1} \frac{1}{F_s - F_p} \left[ F(F_s - F_p) \ln \alpha + \right. \\ \left. + 2F \left( \ln \frac{F}{F_p} - 1 \right) - F_M F_p \ln \alpha + F_p^2 (\alpha + 1) \right]. \quad (32)$$

3rd Section. For  $\alpha F_p \leq F \leq F_M$ .

$$B_3 = \frac{1}{R_n - R_b} \int_{R_b}^{R_n} \left\{ \frac{b_p}{F_s - F_p} \left[ (2F - F_M) \frac{R_n}{R} - F_p \right] + \right. \\ \left. + \lg \delta \left[ \frac{F_s + F_p}{F_s - F_p} F \frac{R_n}{R} - \frac{F_p}{F_s - F_p} \left( F_M \frac{R_n}{R} + F_p \right) \right] \right\} dR.$$

By solving this equation, we obtain

$$B_3 = \frac{b_p}{F_s - F_p} \left[ \frac{\ln \alpha}{\alpha-1} (2F - F_M) - F_p \right] + \\ + \lg \delta \left[ \frac{F_s + F_p}{F_s - F_p} \frac{\ln \alpha}{\alpha-1} F - \frac{F_p}{F_s - F_p} \left( \frac{\ln \alpha}{\alpha-1} F_M + F_p \right) \right].$$

4th Section. For  $-F_p \leq F \leq F_M$ .

$$B_4 = \frac{1}{R_n - R_b} \int_{R_b}^{R_n} \left\{ \frac{b_p}{F_s - F_p} \left( F_M \frac{R_n}{R} - F_p \right) + \right. \\ \left. + \lg \delta \left[ F \frac{R_n}{R} + \frac{F_p}{F_s - F_p} \left( F_M \frac{R_n}{R} - F_p \right) \right] \right\} dR.$$

After solving this equation, we obtain

$$B_4 = \frac{b_p}{F_s - F_p} \left[ \frac{\ln \alpha}{\alpha-1} F_M - F_p \right] + \\ + \lg \delta \left[ \frac{\ln \alpha}{\alpha-1} F + \frac{F_p}{F_s - F_p} \left( \frac{\ln \alpha}{\alpha-1} F_M - F_p \right) \right]. \quad (34)$$

The mathematical expression for the descending branch of this type of symmetric magnetization reversal loops is determined in a similar manner.

c) First Type of Symmetric Magnetization Reversal Loops ( $F_p < F_M \leq \alpha F_p$ ).

In order to determine the  $B = f(F)$  dependence for this type of magnetization reversal loops, we shall sub-



stitute Eqs. (16)-(19) in Eq. (8), which was borrowed from [3]. In dependence on the values  $F$  of magnetizing ampere-turns, the symmetric magnetization reversal loops will have different functional sections.

1st Section. For  $-F_M \leq F \leq F_p$ ,

$$B_1 = \frac{1}{R_H - R_B} \int_{R_1}^{R_1} \left\{ -\frac{b_p}{F_s - F_p} \left[ F_M \frac{R_B}{R} - F_p \right] + \right. \\ \left. + \operatorname{tg} \delta \left[ F \frac{R_B}{R} - \frac{F_p}{F_s - F_p} \left( F_M \frac{R_B}{R} - F_p \right) \right] \right\} dR + \\ + \frac{1}{R_H - R_B} \int_{R_1}^{R_H} \operatorname{tg} \delta F \frac{R_B}{R} dR,$$

where  $R_1 = R_B F_M / F_p$ .

By solving this equation, we obtain

$$B_1 = -\frac{1}{\alpha - 1} \frac{b_p}{F_s - F_p} \left[ F_M \left( \ln \frac{F_M}{F_p} - 1 \right) + F_p \right] + \\ + \frac{\operatorname{tg} \delta}{\alpha - 1} \left\{ F \ln \alpha - \frac{F_p}{F_s - F_p} \left[ F_M \left( \ln \frac{F_M}{F_p} - 1 \right) + F_p \right] \right\}. \quad (35)$$

2nd Section. For  $F_p \leq F \leq F_M$ ,

$$B_2 = \frac{1}{R_H - R_B} \int_{R_1}^R \left\{ \frac{b_p}{F_s - F_p} \left[ (2F - F_M) \frac{R_B}{R} - F_p \right] + \right. \\ \left. + \operatorname{tg} \delta \left[ \frac{F_s + F_p}{F_s - F_p} F \frac{R_B}{R} - \frac{F_p}{F_s - F_p} \left( F_M \frac{R_B}{R} + F_p \right) \right] \right\} dR + \\ + \frac{1}{R_H - R_B} \int_{R_1}^R \left\{ -\frac{b_p}{F_s - F_p} \left[ F_M \frac{R_B}{R} - F_p \right] + \operatorname{tg} \delta \left[ F \frac{R_B}{R} - \right. \right. \\ \left. \left. - \frac{F_p}{F_s - F_p} \left( F_M \frac{R_B}{R} - F_p \right) \right] \right\} dR + \frac{1}{R_H - R_B} \int_{R_1}^{R_H} \operatorname{tg} \delta F \frac{R_B}{R} dR,$$

where  $R = R_B F / F_p$ ,  $R_1 = R_B F_M / F_p$ .

After solving this equation, we obtain

$$B_2 = \frac{1}{\alpha - 1} \frac{b_p}{F_s - F_p} \left[ 2F \left( \ln \frac{F}{F_p} - 1 \right) + \right. \\ \left. + F_M \left( 1 - \ln \frac{F_M}{F_p} \right) + F_p \right] + \\ + \frac{\operatorname{tg} \delta}{\alpha - 1} \frac{1}{F_s - F_p} \left[ F (F_s - F_p) \ln \alpha + \right. \\ \left. + 2FF_p \left( \ln \frac{F}{F_p} - 1 \right) + F_M \left( 1 + \ln \frac{F_M}{F_p} \right) F_p + F_p^2 \right] \quad (36)$$

3rd Section. For  $-F_p \leq F \leq F_M$ ,

$$B_3 = \frac{1}{R_H - R_B} \int_{R_1}^{R_1} \left\{ \frac{b_p}{F_s - F_p} \left[ F_M \frac{R_B}{R} - F_p \right] + \right.$$

$$+ \operatorname{tg} \delta \left[ F \frac{R_B}{R} + \frac{F_p}{F_s - F_p} \left( F_M \frac{R_B}{R} - F_p \right) \right] \right\} dR + \\ + \frac{1}{R_H - R_B} \int_{R_1}^{R_H} \operatorname{tg} \delta F \frac{R_B}{R} dR,$$

where  $R_1 = R_B F_M / F_p$ .

By solving this equation, we obtain

$$B_3 = \frac{1}{\alpha - 1} \frac{b_p}{F_s - F_p} \left[ F_M \left( \ln \frac{F_M}{F_p} - 1 \right) + F_p \right] + \frac{\operatorname{tg} \delta}{\alpha - 1} \left\{ F \ln \alpha + \right. \\ \left. + \frac{F_p}{F_s - F_p} \left[ F_M \left( \ln \frac{F_M}{F_p} - 1 \right) + F_p \right] \right\}. \quad (37)$$

The mathematical expression for the descending branch of this type of symmetric magnetization reversal loops is determined in a similar manner.

d) Normal Magnetization Curve

For determining the mathematical expressions for the "normal magnetization curve", Eqs. (20)-(22) must be substituted in Eq. (8) from [3]. In dependence on the value of  $F_M$ , the "normal magnetization curve" will have functional sections.

Zero Section. For  $0 \leq F_M \leq F_p$ ,

$$B_{0 \max} = \frac{1}{R_H - R_B} \int_{R_1}^{R_H} \operatorname{tg} \delta F_M \frac{R_B}{R} dR.$$

By solving this equation, we obtain

$$B_{0 \max} = \operatorname{tg} \delta \frac{\ln \alpha}{\alpha - 1} F_M. \quad (38)$$

1st Section. For  $F_p \leq F_M \leq \alpha F_p$ ,

$$B_{1 \max} = \frac{1}{R_H - R_B} \left\{ \int_{R_1}^R \left[ \frac{b_p}{F_s - F_p} \left( F_M \frac{R_B}{R} - F_p \right) + \right. \right. \\ \left. \left. + \frac{\operatorname{tg} \delta}{F_s - F_p} \left( F_s F_M \frac{R_B}{R} - F_p^2 \right) \right] dR + \int_R^{R_H} \operatorname{tg} \delta F_M \frac{R_B}{R} dR \right\},$$

where  $R = R_B F_M / F_p$ .

By solving this equation, we obtain

$$B_{1 \max} = \frac{1}{\alpha - 1} \frac{b_p}{F_s - F_p} \left[ F_M \left( \ln \frac{F_M}{F_p} - 1 \right) + F_p \right] + \\ + \frac{1}{\alpha - 1} \frac{\operatorname{tg} \delta}{F_s - F_p} \left[ F_M F_p \left( \ln \frac{F_M}{F_p} - 1 \right) + F_M (F_s - F_p) \ln \alpha + F_p^2 \right]. \quad (39)$$

2nd Section. For  $\alpha F_p \leq F_M \leq F_s$ ,

$$B_{2 \max} = \frac{1}{R_H - R_B} \int_{R_1}^{R_H} \left[ \frac{b_p}{F_s - F_p} \left( F_M \frac{R_B}{R} - F_p \right) + \right.$$

$$+ \frac{\lg \delta}{F_s - F_p} \left( F_s F_M \frac{R_n}{R} - F_p^2 \right) dR.$$

By solving this equation, we obtain

$$B_{2 \max} = \frac{b_p}{F_s - F_p} \left[ \frac{\ln \alpha}{\alpha - 1} F_M - F_p \right] + \frac{\lg \delta}{F_s - F_p} \left[ \frac{\ln \alpha}{\alpha - 1} F_s F_M - F_p^2 \right]. \quad (40)$$

3rd Section. For  $F_s \leq F_M \leq \alpha F_s$ ,

$$B_{3 \max} = \frac{1}{R_n - R_p} \left\{ \int_{R_p}^{R_n} \left[ b_p + \lg \delta \left( F_M \frac{R_n}{R} + F_p \right) \right] dR + \int_{R_n}^{R_M} \left[ \frac{b_p}{F_s - F_p} \left( F_M \frac{R_n}{R} - F_p \right) + \frac{\lg \delta}{F_s - F_p} \left( F_s F_M \frac{R_n}{R} - F_p^2 \right) \right] dR \right\},$$

where  $R = R_B F_M / F_s$ .

By solving this equation, we obtain

$$B_{3 \max} = \frac{1}{\alpha - 1} \frac{b_p}{F_s - F_p} \times \quad (41)$$

$$\times \left[ F_M \left( 1 + \ln \frac{\alpha F_s}{F_M} \right) - F_s - F_p (\alpha - 1) \right] + \frac{1}{\alpha - 1} \frac{\lg \delta}{F_s - F_p} \times \\ \times \left[ F_M (F_s - F_p) \ln \alpha + F_M F_p \left( 1 + \ln \frac{\alpha F_s}{F_M} \right) - F_s F_M - F_p^2 (\alpha - 1) \right].$$

4th Section. For  $\alpha F_s \leq F_M$ ,

$$B_{4 \max} = \frac{1}{R_n - R_p} \int_{R_p}^{R_n} \left[ b_p + \lg \delta \left( F_M \frac{R_n}{R} + F_p \right) \right] dR.$$

By solving this equation, we obtain

$$B_{4 \max} = b_p + \lg \delta \left[ \frac{\ln \alpha}{\alpha - 1} F_M + F_p \right]. \quad (42)$$

#### LITERATURE CITED

1. R. W. Roberts and R. J. Van Nice, "Influence of ID/OD ratio on static and dynamic properties of toroidal cores," *Trans. AIME* 74, pt. 1 (1955).
2. M. A. Rozenblat, "Dependence of static characteristics of toroidal cores on their dimensions," *Avtomatika i Telemekhanika* 19, 8 (1958).
3. G. D. Kozlov, "Effect of magnetization irregularity on the static characteristics of cores," *Avtomatika i Telemekhanika* 21, 1 (1960).
4. J. A. Rajchman, and A. W. Lo, "The transfluxor," *Proc. IRE* 44 (March, 1956).
5. H. W. Abbott and J. J. Suran, "Multihole ferrite core configurations and applications," *Proc. IRE* 45 (August, 1957).

\*See English translation.

# A TRANSISTORIZED MAGNETIC AMPLIFIER\*

R. A. Lipman and M. V. Ol'shvang

Moscow

Translated from *Avtomatika i Telemekhanika*, Vol. 21, No. 7, pp. 1073-1083,

July, 1960

Original article submitted December 18, 1959

This article deals with a transistorized magnetic amplifier, which works as a continuously controlled switch and is based on a pulse-width modulated relaxation-oscillator. The theoretical analysis of the circuit is provided, and experimental results are quoted.

When a transistor (T) is operated as a switch, it becomes possible to make it much more efficient, i.e., to raise the ratio between the power dissipated in the load and that in the transistor. Thus, the output power of the transistor amplifier can be greatly increased.

The switching operation of the transistor is widely used in amplifiers with a continuous input - output characteristic, as well as in purely relay circuits. In the former case, the transistor is periodically switched, and the continuous variation of the mean value of the output power is attained by changing the relative duration of the open-circuited condition of the transistor (in a manner similar to a thyatron or relay-contact amplifier with a continuous control).

There are many circuits which provide a continuously controlled switching operation of the transistor [1-7 and others]. In the majority of them, the control of power transistors is accomplished by means of some type of pulse-width modulation, which transforms the variations in the signal strength into a proportional change in the relative duration of the pulse.

The special characteristic of the circuit proposed by Morgan [7] is the combination of the functions of a power amplifier with those of a pulse-width modulator. Moreover, the power transistor which controls the power in the load also serves as an amplifier for the oscillator with the pulse-width modulation.

The Morgan circuit (Fig. 1a) is based on a blocking-oscillator with a series overloading transformer. The feedback transformer (FBT) has a working winding  $w_0$  which is connected in series with the load impedance  $R_L$  and  $L_L$ , a return winding  $w_r$  which is connected in parallel with the emitter-collector circuit through a large building-out resistor  $R_b$  (a small resistor  $r_b$  serves to supply the bias for the emitter) and a feedback winding  $w_f$  connected in the base circuit. When the feedback current  $i_f$  is positive (Fig. 1a), the transistor is conducting, and the feedback circuit is completed through the emitter circuit of T (rectifier  $B_C$  is then blocked). When  $i_f < 0$ , the transistor becomes blocked, and the feedback circuit is completed through rectifier  $B_C$  and the adjustable resistor  $R_C$ .

Windings  $w_0$  and  $w_r$  have only a few turns; moreover, the resistance of the feedback circuit (both for the conducting and blocked conditions of the transistor), which is connected to windings  $w_0$  and  $w_r$ , is considerably smaller than resistances  $R_L$  and  $R_b$ . Hence, the FBT works as a current transformer, i.e., the value of the collector current  $i_{co}$  and of the return current  $i_r$  are practically independent of the feedback resistance. The value of that resistance only affects the speed of the inductance variations in the core of the FBT.

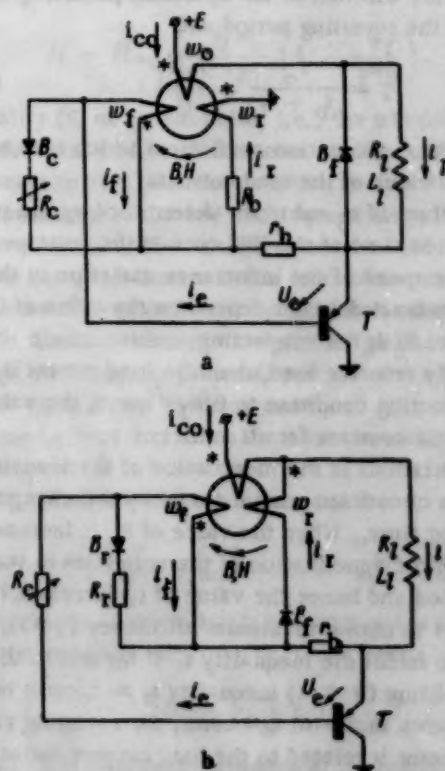


Fig. 1.

\* From a paper read at the All-Union Seminar on Magnetic Components in Automation and Computers on October 13, 1959.



Under certain conditions the circuit in Fig. 1a becomes self-oscillating. The oscillations are discontinuous, each cycle consisting of two distinct periods: a) a period when the transistor is completely conducting (both junctions being biased in the forward direction), the load voltage is near to that of the supply, the return current approaches zero, and the speed of the inductance variations in the core of the FBT is positive and is determined by the value of the load current; b) a period when the transistor is blocked (both junctions are biased in the reversed direction), the voltage across the load and the collector current approach zero, the return current is maximum and the speed of the inductance variations of the FBT core are negative and are determined by the value of the return current and of resistance  $R_C$ . The transition from one period to the other is caused by the saturation of the core and is short compared with the period of oscillations.

Moreover, owing to the existence of the feedback rectifier  $B_f$ , which shunts the load during the reversing period, the mean value of the load current  $I_L$  will equal, irrespective of the value of  $L_I$ ,

$$I_L = \frac{E}{R_L} \frac{t_o}{t_o + t_r} = \frac{E}{R_L} \gamma, \quad (1)$$

where  $t_o$  is the duration of the operation period,  $t_r$  the duration of the reversing period, and

$$\gamma = \frac{t_o}{t_o + t_r} = \frac{I_L R_L}{E} \quad (1a)$$

is the transistor conduction coefficient which is equal to the relative value of the load current.

The values of  $t_o$  and  $t_r$  are determined by the remagnetization time of the FBT core in the corresponding period. The speed of the inductance variation in the operating interval does not depend on the value of  $R_C$  (the rectifier  $B_C$  is not conducting in this period). Hence, with a purely resistive load, when the load current is equal in the conducting condition to  $E/R_L = \text{const}$ , the value of  $t_o$  will remain constant for all values of  $\gamma$ .

The variations in the mean value of the load current in Morgan's circuit are provided only by the changes in the reversing time. When the value of  $R_C$  is increased, the speed of remagnetization of the core rises in the reversing period, and hence, the value of  $t_r$  decreases.†

In order to obtain maximum efficiency ( $\gamma \approx 1$ ), it is necessary to fulfill the inequality  $t_r \ll t_o$ ; and in the unloaded condition ( $\gamma \ll 1$ ) inequality  $t_r \gg t_o$  must hold. It can be shown that with  $t_o = \text{const}$ , the reversing time variation factor is related to the load current variations factor  $k_I$  and to the maximum value of the conduction coefficient  $\gamma_{\max}$  by means of the following equation:

$$\frac{t_r \max}{t_r \min} = k_I \frac{1 - \gamma_{\max}/k_I}{1 - \gamma_{\max}}. \quad (2)$$

For instance, for  $k_I = 10$  and  $\gamma_{\max} = 0.9$ , it is necessary to provide a  $t_r \max/t_r \min \approx 90$ , i.e., the adjustable core remagnetization factor must be considerably larger than the load current variations factor.

From (1) and the condition that  $t_o = \text{const}$ , it follows that the range of the oscillating frequency  $f$  variations will be equal to

$$\frac{f_{\max}}{f_{\min}} = k_I = \frac{I_L \max}{I_L \min}. \quad (3)$$

The large variation ranges of the adjustable remagnetization time and the oscillation frequency are the important defects of the circuit in Fig. 1a, which lead to the impossibility of obtaining a large amplifier output-current variations factor. The above defect becomes worse with an inductive load. For a constant base circuit resistance, the core remagnetization time with a non-conducting transistor is in the first approximation inversely proportional to the mean value of the load current during the operation period. Providing the time constant of the load is sufficiently large, the mean value of the current  $I_L$  for time  $t_o$  is close to the mean value of the load current  $I_L$  for the whole cycle.

Thus, for an inductive impedance load, the duration of the operational period will no longer remain constant, but will change approximately in inverse proportion to the mean value of the load current:

$$t_o \approx \frac{1}{I_L}. \quad (4)$$

From (4) and (1) we obtain the following expressions for the reversing time variation factor and the self-oscillation frequency:

$$\frac{t_r \max}{t_r \min} = k_I^2 \frac{1 - \gamma_{\max}/k_I}{1 - \gamma_{\max}}, \quad (2a)$$

$$\frac{f_{\max}}{f_{\min}} = k_I^2. \quad (3a)$$

For instance, in order to obtain  $k_I = 10$  and  $\gamma_{\max} = 0.9$ , it is necessary to make  $t_r \max/t_r \min \approx 900$  and  $f_{\max}/f_{\min} = 100$ , which it is impossible to attain in practice.

The above defect can be overcome if Morgan's circuit is altered as shown in Fig. 1b. The difference between the circuits of Figs. 1a and 1b consists of the following: The control of the speed of core remagnetization is attained in the operation interval (with a conducting transistor) for this purpose the adjustable resistance  $R_C$  is connected in the base circuit in series with the feedback winding. Moreover, the demagnetization of the core in the reversing interval is accomplished by means of the load current which flows through the reversed rec-

† A photovaristor, magnetic amplifier, etc., can be used as a controlled resistance  $R_C$ .

tifier; for this purpose the return winding is connected in series with the reversed rectifier  $B_f$ .

Thus, a decrease in the adjustable resistance  $R_c$  leads to a slowing down of the core remagnetization in the operation period, and hence, to a rise in  $t_o$ . Moreover, the load current increases. The rise in the load current automatically leads to a decrease in time  $t_r$ , since current  $i_r$ , which remagnetizes the core, is equal to the load current in the reversing interval. Thus, although the control signal affects directly only the duration  $t_o$  of the transistor's conducting condition, the circuit automatically changes the duration  $t_r$  of the nonconducting condition. Moreover, for a rising  $t_o$  the value of  $t_r$  decreases, and vice versa.

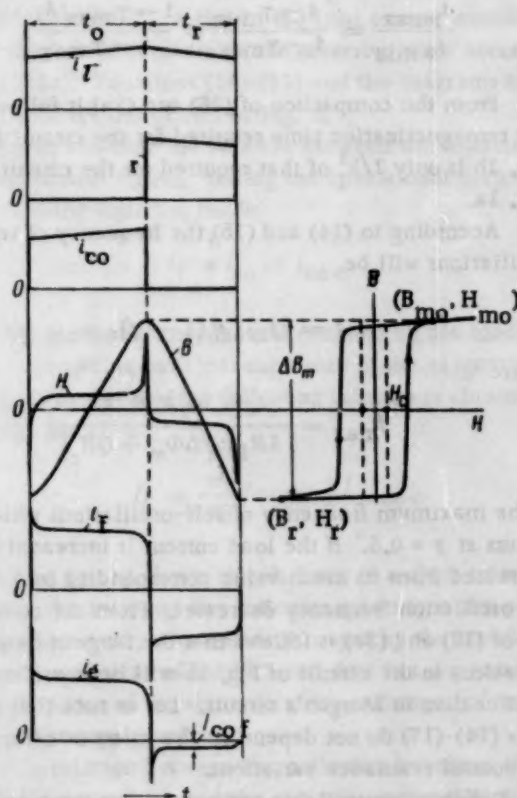


Fig. 2.

In order to obtain quantitative relations, let us examine the working of the circuit in Fig. 1b under the condition that the time constant of the load is sufficiently large compared with the period of oscillations. Moreover, let us assume that the current during this period remains practically constant (the instantaneous and mean values of the current coincide).

Diagrams of the changes in variables of Fig. 1b circuit are shown in Fig. 2. During the operation period, the transistor is conducting and the return current is zero (rectifier  $B_f$  is nonconducting), the collector current is equal to that of the load, the feedback current is positive and runs through the adjustable resistance  $R_c$  and the base of the transistor (rectifier  $B_r$  is nonconducting).

The value of the feedback current, which is the same as that of the base, is obtained from equation

$$i_f = i_e = I_f \frac{w_o}{w_f} - \frac{H l_m}{w_f} > \frac{I_l}{\beta}, \quad (5)$$

where  $H$  is the field strength in the core,  $l_m$  is the length of the mean line of force,  $\beta$  is the current gain coefficient of the transistor for  $U_{co} = 0$  and  $i_{co} = I_l$ . The fulfillment of inequality (5) provides a conducting condition for the transistor. The speed of the core inductance variations is determined by the expression

$$w_f S_c \frac{dB}{dt} = i_f (R_f + r_e + r_f + r_b), \quad (6)$$

where  $S_c$  is the cross-sectional area,  $r_e$  the emitter-base impedance of a conducting transistor,  $r_f$  the resistance of the feedback winding, and  $r_b$  the biasing resistance.

The inductance of the core increases with a speed determined by the expression (6), and its magnetic condition varies according to the rising portion of the hysteresis loop (Fig. 2). When the core becomes saturated, the field strength rises rapidly, and the feedback current decreases according to (5). When the field strength reaches a certain value

$$H = H_{mo} = \frac{I_l w_o}{l_m} \left( 1 - \frac{w_f}{\beta w_o} \right), \quad (7)$$

inequality (5) no longer holds, i.e., the transistor passes from the saturated condition to an active condition. This leads to an avalanche decrease in the base current (see Appendix); at the end of this process, the transistor becomes blocked, the voltage across the load drops almost to zero, the current in the load is completed through the reversed rectifier  $B_f$  and the return winding ( $i_r = I_l$ ), and the feedback current changes its sign and flows through circuit  $B_r, R_r$  (a small portion of the feedback current equal to the reversed current of the collector junction  $I_{cr}$  branches off to the base circuit). Thus, the reversing period is initiated.

The feedback current is then equal to

$$i_f = -i_r \frac{w_r}{w_f} - \frac{H l_m}{w_f} = -I_l \frac{w_r}{w_f} - \frac{H l_m}{w_f}, \quad (8)$$

and the speed of the inductance variations is determined from the equation

$$w_f S_c \frac{dB}{dt} = i_f (R_r + r_f + r_r) \approx i_f R_r < 0, \quad (9)$$

where  $r_r$  is the forward resistance of the rectifier  $B_r$  ( $r_f + r_r \ll R_r$ ). The emitter receives a negative voltage

$$U_e = - \left( I_l \frac{w_r}{w_f} + \frac{H l_m}{w_f} \right) R_r + I_l r_b < 0, \quad (10)$$

thus ensuring a blocking of the transistor in the reversing period.



The inductance of the core decreases with a speed determined by the expression (9), and its magnetic condition changes according to the descending portion of the hysteresis loop (Fig. 2). When the core becomes saturated in the negative direction, the field strength rises rapidly, and the value of the voltage (10) which blocks the transistor decreases ( $H < 0$ ).

When the field strength reaches the value

$$H = H_{mr} = -\frac{l_r w_r}{l_m} \left(1 - \frac{r_b w_o}{R_r w_r}\right), \quad (11)$$

inequality (10) no longer holds, and the transistor passes to an active state. This produces an avalanche breakdown of the transistor (see Appendix), and at the end of the process, an operational period is again reestablished.

Let us determine the values of  $t_r$  and  $t_o$  and the frequency of self-oscillations. By integrating Equation (9) in conjunction with (8) in the limits of  $B_{mo}$  and  $B_{mr}$ , we obtain:

$$t_r = \frac{1}{R_r} \left( \frac{w_r^2 \Delta \Phi_m + Q R_r}{I_l w_r - H_o l_m} \right), \quad (12)$$

where  $\Delta \Phi_m = S_c(B_{mo} - B_{mr}) = S_c \Delta B_m$  is the full variation of the flux in the core and  $H_o$  is the coercive force of the static hysteresis loop, and

$$Q = l_m \int_0^{t_r} (H - H_o) dt = Q(\Delta \Phi_m) \quad (13)$$

is the so-called switching coefficient of the core.

Normally,  $H_o l_m \ll I_l w_r$ ; moreover,

$$t_r \approx \frac{1}{I_l} \left( \frac{w_r^2 \Delta \Phi_m + Q R_r}{R_r w_r} \right). \quad (12a)$$

For magnetic materials with a high degree of saturation, the values of  $B_{mo}$  and  $B_{mr}$  depend to a small degree only on  $H_{mo}$  and  $H_{mr}$ ; it is therefore possible to consider approximately that  $\Delta \Phi_m$  and  $Q$  do not de-

pend on the load current and are determined only by the dimensions and the material of the core. Moreover, the reversing time will, according to (12a), change inversely proportionately to the load current.

From (1) and (12a) we can obtain the following expressions for  $t_r$  and  $t_o$ :

$$t_r = \frac{(w_r^2 \Delta \Phi_m + Q R_r) R_l}{w_r E R_r} \frac{1}{\gamma}, \quad (14)$$

$$t_o = \frac{(w_r^2 \Delta \Phi_m + Q R_r) R_l}{w_r E R_r} \frac{1}{1 - \gamma}. \quad (15)$$

It follows from (15) that variation of the core remagnetization controlled time factor in the circuit of Fig. 1b is equal to

$$\frac{t_{p \max}}{t_{p \min}} = \frac{1 - \gamma_{\min}}{1 - \gamma_{\max}} = \frac{1 - \gamma_{\max} / k_I}{1 - \gamma_{\max}}. \quad (16)$$

From the comparison of (26) and (2a), it follows that the remagnetization time required for the circuit in Fig. 1b is only  $1/k_I^2$  of that required for the circuit of Fig. 1a.

According to (14) and (15), the frequency of self-oscillations will be

$$f = 4 / \max(\gamma) (1 - \gamma), \quad (17)$$

where

$$f_{\max} = \frac{w_r R_l E}{4 R_l (w_r^2 \Delta \Phi_m + Q R_r)} \quad (18)$$

is the maximum frequency of self-oscillations which occurs at  $\gamma = 0.5$ . If the load current is increased or decreased from its mean value corresponding to  $\gamma = 0.5$ , the oscillation frequency decreases. From the comparison of (17) and (3a), it follows that the range of frequency variations in the circuit of Fig. 1b will be considerably smaller than in Morgan's circuit. Let us note that relations (14)-(17) do not depend on the value or nature of the control resistance variations.

Different controllable resistances can serve as  $R_c$ . Fig. 3 shows an amplifier circuit, of the type found in

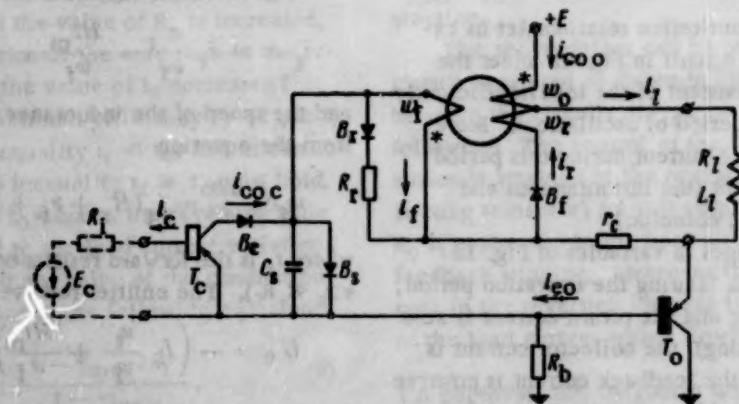


Fig. 3.



Fig. 1b, in which a transistor  $T_c$  is used as the controlled variable  $R_c$ . Rectifier  $B_c$  prevents the blocking of the operational transistor  $T_o$  by the control signal. The shunting rectifier  $B_s$  provides a path for the return current of the collector junction of the operational transistor  $T_o$  during the reversing period. The capacitance  $C_s$  improves the switching conditions and raises the stability of the oscillations. Resistor  $R_b$  provides a small initial positive bias for the operational transistor, thus helping the starting of oscillations (providing conditions of "soft" self-excitation).

The control signal (source of emf  $E_c$  with an internal resistance  $R_i$ ) is fed to the input of the controlling transistor. A rising control signal decreases the static output resistance of  $T_c$  thus leading to an increase in the duration of the operational period  $t_o$ , and hence, to a rise in the load current. A rise in the load current automatically involves a decrease in the reversing time according to (12a). Equations (14)-(17) and the diagrams in Fig. 2 hold for the circuit of Fig. 3.

Let us examine the relation between the load current and the control signal. During the operational period, the following equation holds:

$$i_f = i_{co} = i_{co c} \quad (19)$$

The feedback current is determined by the load current according to (5); if the value of the magnetizing current is neglected, the following relation is obtained from (5) and (19):

$$I_l = \frac{w_f}{w_o} I_{co} = \frac{w_f}{w_o} I_{co c} \quad (20)$$

Thus, in the above circuit there is a close relation between the load and the collector currents in the controlling transistor, which is determined by the transformation coefficient of the FBT and does not depend on the characteristics of the transistors, the resistance of the load, or the supply voltage.

The relation between the collector current of the controlling transistor and the controlling signal is determined by the  $T_c$  transistor characteristic. If the collector reaction is neglected, the following relation will hold:

$$I_{co c} = \varphi_1(E_c, R_i) \quad (21)$$

or

$$I_{co c} = \varphi_2(I_c). \quad (21a)$$

Equations (20) and (21) determine the transmission characteristic of the amplifier as a whole. This characteristic is a reproduction of the controlling transistor characteristic with its current gain amplified by a factor of  $n = w_f/w_o$ , and it does not depend on the values of  $E$  or  $R_l$ . A limitation is placed on the value of  $n$  by inequality (5), and the following condition must be observed for its fulfillment:

$$n = \frac{w_f}{w_o} < \beta_o \quad (22)$$

i.e., the resulting current gain cannot exceed the products  $\beta_c \beta_o$  ( $\beta_c$  and  $\beta_o$  are the current gains of transistors  $T_c$  and  $T_o$ ).

Below we give the experimentally obtained characteristics of an amplifier assembled according to the diagram of Fig. 3.

Its circuit parameters are: core OL 14/17-3,5-0.05-79NM,  $w_o = w_f = 20$ ,  $w_f = 300$ ,  $R_f = 60$  ohms,  $r_b = 0.4$  ohms,  $R_b = 100$  kilohms,  $c_s = 0.02$   $\mu$ f,  $T_o$  - P4B,  $T_c$  - P201,  $B_f$  - D303,  $B_b$ ,  $B_s$ , and  $B_f$  - D7B.

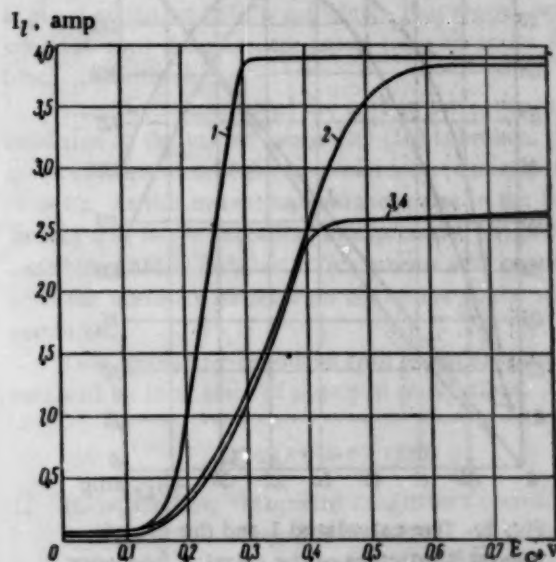


Fig. 4. Relation between the load current and the control signal emf. 1)  $R_l = 10$  ohms,  $E = 45$  v,  $R_i = 0$ ; 2)  $R_l = 10$  ohms,  $E = 45$  v,  $R_i = 50$  ohms; 3)  $R_l = 10$  ohms,  $E = 30$  v,  $R_i = 50$  ohms; 4)  $R_l = 15$  ohms,  $E = 45$  v,  $R_i = 50$  ohms. For all the curves, the value of  $L_l$  varies in the range of 0.2 to 8 h.

Figure 4 shows the relation between the load current and the control signal emf for various values of the supply voltage, the load resistance, and the internal resistance of the signal source. Over the operating portion of the characteristic, the load current is practically independent of the values of  $E$  and  $R_l$ , thus confirming the theoretical considerations. The power gain over the linear portion of the characteristics of curves 2, 3, and 4 is equal to  $4R_l R_i (\Delta I_l / \Delta E_c)^2 = 3 \cdot 10^5$ . The current ratio amounts to  $k_I \approx 40-50$ .

Figure 5 compares the calculated [from formula (17)], with the experimentally obtained, relation between the relative oscillation frequency and the load current. The experimental value of  $f_{max} = 1600$  cps, and the value calculated from Eq. (18) is 2000 cps ( $\Delta \Phi_m \approx 0.7 \cdot 10^{-5}$  v  $\cdot$  sec,  $Q \approx 0.5 \cdot 10^{-3}$  amp  $\cdot$  sec). The maximum of the ex-

perimental characteristic 2 is displaced with respect to that of the calculated characteristic 1 in the direction of the lower currents. This is probably due to the fact that, by decreasing the load current, the value of  $\Delta\Phi_m$  is slightly reduced, and hence, the value of  $f/f_{\max}$  is increased. Due to this change, the range of the oscillation frequency variations becomes smaller than the calculated value. For instance, when the load current is changed from 4 to 0.4 amp ( $k_1 = 10$ ) the value of  $f$  varies only by a factor of 2. The switching time of the power transistor amounted to 20-40  $\mu\text{sec}$ .

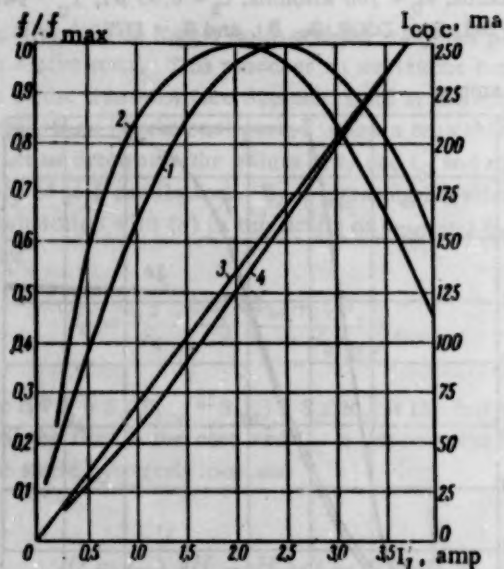


Fig. 5. The calculated 1 and the experimental 2 relations of the relative frequency of oscillations to the load current; the calculated 3 and the experimental 4 relations of the collector current of the controlling transistor to the load current.

Figure 5 shows the calculated and experimental relations of the mean collector current over time  $t_0$  of the controlling transistor to the load current, a relation which confirms expression (20). The experimental value of  $I_{CO}$  was determined as the mean value of the current over one cycle divided by  $\gamma$ .

Figure 6 provides the over-all characteristic for various ambient temperatures and several samples of transistors  $T_O$ . The curves confirm the independence of the load current from the characteristic of the operating transistor, and show the relatively small effect of temperature on the curve  $I_L = I_L(I_C)$ .

It follows from the examination of Fig. 6a that variation of the ambient temperature in the range of  $-60^\circ\text{C}$  to  $+55^\circ\text{C}$  is equivalent to a change in the emf of the input signal of  $\Delta E_c \approx 0.25$  v. If the amplifier is used in a closed-loop control system, it is easy to provide conditions which would make the effect of this variation insignificant with respect to the accuracy of the system's operation. Let us assume, for instance, that the input of the amplifier receives a control signal from a measuring element of a voltage regulator, and that it is required to make the error of regulation due to the temperature drift of the amplifier less than 1% ( $\pm 0.5\%$ ) when the temperature varies in the range of  $-60^\circ\text{C}$  to  $+55^\circ\text{C}$ . In order to fulfill this requirement, it is obviously sufficient to make the sensitivity of the measuring device equal 0.25 v per 1% of the measured voltage. Such a sensitivity is possessed, for instance, by a measuring element consisting of a nonlinear bridge circuit with two reference diodes of the D813 type.

It is important to note that normal operating conditions and the measuring range of the output variable in the amplifier of Fig. 3 are preserved over a wide range of ambient temperatures.

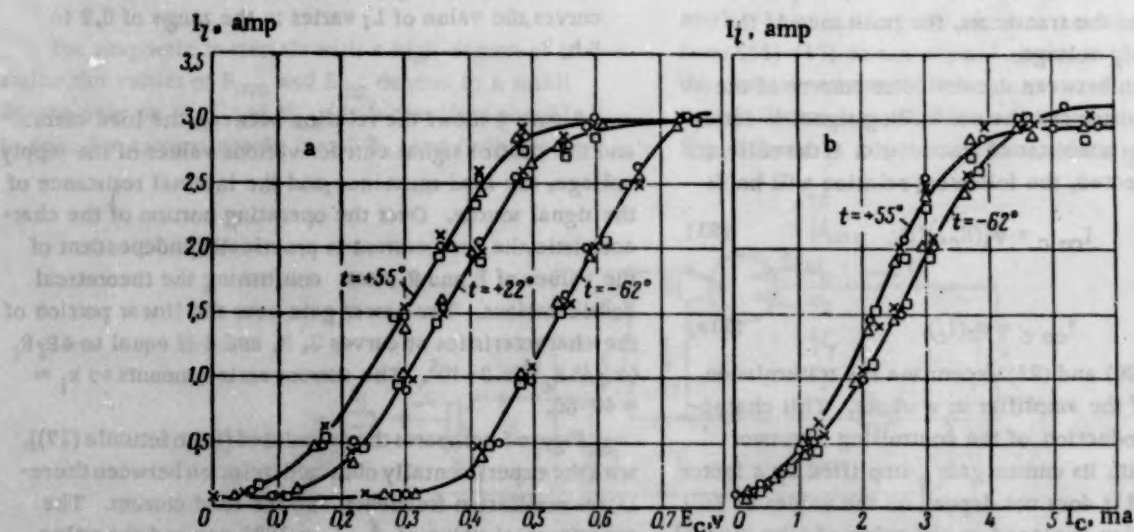


Fig. 6. Relation of the load current to the control signal emf a and to the control current b for various ambient temperatures; the experimental points correspond to various samples of transistors,  $E = 40$  v,  $R_L = 10.5$  ohms,  $R_1 = 70$  ohms.

On the basis of the results thus obtained, it is possible to make the following conclusions on the advantages of the Fig. 1b circuit (Fig. 3) as compared with Morgan's circuit:

1. Under similar conditions the Fig. 1b circuit requires a much smaller range of variations in the duration of the controlled core remagnetization time and a smaller variation of the frequency of oscillations. These factors raise considerably the stability of operation and provide a far larger ratio of load current variations.

2. The maximum oscillation frequency occurs in the circuit of Fig. 1b at  $I_f \approx 0.5 E/R_f$ , and not at  $I_f \approx E/R_f$ , which is the maximum for the Fig. 1a circuit. Thus, the mean power loss in the transistor is decreased.

3. The over-all characteristic of the Fig. 3 circuit is stable with respect to supply voltage and load resistance variations.

#### APPENDIX

After the saturation of the core and the passing of the transistor to an active condition (see Fig. 1b circuit), the following equations will hold for small increments of the variables:

$$\begin{aligned} \Delta i_{co} - \Delta i_f w_f - \Delta i_{fw} &= \Delta H l_m \\ \Delta i_{co} &= -\Delta i_f (l_{co} + l_f = I_l = \text{const}), \\ \Delta i_e &= \Delta i_f = \frac{w_f S_c d \Delta B}{R_f dt}, \\ \Delta B &= \mu_S \Delta H, \\ \tau_\beta \frac{di_{co}}{dt} + \Delta i_{co} &= \beta \Delta i_e, \end{aligned} \quad (A1)$$

where  $R_f$  is the impedance of the transistor base circuit,  $\tau_\beta$  is the time constant of transistor T,  $\mu_S$  is the permeability of the "saturated" core.

Solving the family of equations (A1) with respect to the increment of the base current, we have

$$\Delta i_e (p^2 \tau_\mu \tau_\beta - p [(b-1) \tau_\mu - \tau_\beta] + 1) = 0, \quad (A2)$$

where

$$\tau_\mu = \frac{w_0^2 S_c \mu_S}{R_f l_m}, \quad b = \frac{\beta (w_0 + w_f)}{w_f}, \quad p \equiv \frac{d}{dt}. \quad (A3)$$

The solution of (A2) with initial conditions of  $\Delta i_e(0) = 0$  and  $(d \Delta i_e / dt)(0) = \epsilon$  gives

$$\Delta i_e = \frac{\epsilon}{p_1 - p_2} (e^{p_1 t} - e^{p_2 t}). \quad (A4)$$

where  $p_1$  and  $p_2$  are the roots of the characteristic equation which corresponds to equation (A2). If condition

$$b = \beta \frac{w_p + w_f}{w_f} > 1 + \frac{\tau_\beta}{\tau_\mu}, \quad (A5)$$

is fulfilled, both roots  $p_1$  and  $p_2$  will have a positive real component, and the measuring of the current will be unstable.

After the saturation of the core in the operating period at the instant when inequality (5) no longer holds, the speed of the base current variations is negative ( $\epsilon < 0$ ). At that instant an avalanche decrease in the base current expressed by relation (A4) will therefore begin if condition (A5) is fulfilled. This process will continue until the transistor passes from an active to a blocked condition.

After the saturation of the core in the reversing condition at the instant inequality (10) is broken, the speed of variations of the base current becomes positive ( $\epsilon > 0$ ). At this instant an avalanche rise in the base current will begin according to expression (A4), providing condition (A5) is fulfilled. This process will continue until the transistor passes from the active to the saturated condition.

Thus, providing condition (A5) is fulfilled, the circuit will be in a state of sustained oscillations.

#### LITERATURE CITED

1. H. W. Collins, "Magnetic Amplifier Control of Switching Transistors," *Trans. AIME* **75** (1959).
2. V. G. Konstantinov, "A transistorized amplifier for controlling dynamo excitation," *Vestnik Élektromyshlennosti* **1** (1959).
3. Yu. A. Konev, "Functional pulse converters," Collection: *Transistor Instruments and Their Application* [in Russian] (Izd. Sovetskoe Radio, 1958).
4. O. A. Kossov, "Operation of a semiconductor switch with various load characteristics," *Élektrichestvo* **5** (1959).
5. O. A. Kossov, "Crystal-magnetic amplifier," *Avtomat. i Telemekh.* **20**, 7 (1959), ‡.
6. L. I. Setyukov and N. N. Rukovichnikov, "Transistorized power amplifiers," *Scientific papers at high schools*, *Radiotekhnika i Élektronika* **3** (1958).
7. R. E. Morgan, "A new control amplifier using a saturable current transformer and a switching transistor," *Communication and Electronics* **39** (1958).

‡ See English translation.



# A NEW METHOD OF SPECTRAL MEASUREMENTS BY MEANS OF PHOTOSENSITIVE LAYERS

W. Lueck

Berlin

Translated from *Avtomatika i Telemekhanika*, Vol. 21, No. 7, pp. 1084-1087,

July, 1960

Original article submitted July 10, 1959

Spectral measurements in the regions of visible and infrared radiation involve certain difficulties in the case where the amounts of the radiation energy to be measured are small. This problem arises when it becomes

necessary to measure the intensity of a narrow frequency band, since the radiated power

$$J_{0a} = \int_{\lambda_1}^{\lambda_2} I_{\lambda} d\lambda$$

decreases as the band narrows. For instance, if interference filters are used for selection [1], the radiated power values can be extremely small (of the order of  $10^{-10}$  w).

Along with vacuum thermoelements [2], different types of photocells, photoresistors, and phototransistors are used as sensing elements. The sensitivity of photoeffect elements is much higher than the sensitivity of vacuum thermoelements. For instance, the sensitivity of a vacuum thermoelement is approximately 30 v/w, and the sensitivity of a mass-produced PbS photoresistor is 150 v/w (for ideal blackbody radiation at 300°). In many cases, this ratio will be of the order of 1:100 in favor of photoconductors.

Figure 1 shows the spectral distribution curves for the relative sensitivity of some known photocell materials. This figure indicates that the spectral characteristics lie in the wavelength region extending from x-ray radiation to infrared radiation (approximately 10  $\mu$ ).

All these photocell materials are strongly affected by temperature as well as aging. If they are placed in thermostats, direct measurements become very complicated.

Figure 2 indicates the sharp drop in the sensitivity of lead sulfide photoresistors with temperature changes [3].

Moreover, the spectral properties change also with

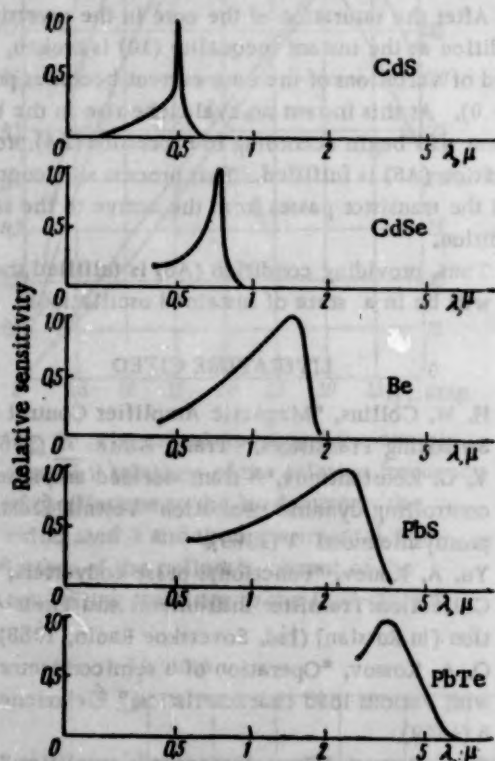


Fig. 1. Spectral distribution of the sensitivity of some sensitive layers (photoresistors).

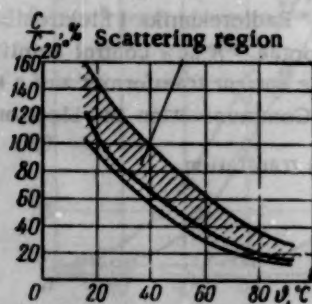


Fig. 2. Temperature dependence of the sensitivity of PbS layers.



Fig. 3. Temperature dependence of the spectral sensitivity of PbTe layers.

the cell temperature, as can be seen in Fig. 3, where the spectral sensitivity distribution of lead telluride resistors is shown [4].

Therefore, in order to eliminate the "subjective" errors of photocells, compensation methods, where the measurements are compared with measurements of known steady radiation sources, are used. The comparison is performed by alternating screening of the photocell from the measured and the standard radiation by means of rotating mirrors or disks with openings, as well as by means of oscillating diaphragms [5]. Figs. 4 and 5 show examples of such comparison methods, where mechanical diaphragming is used. Along with the presence of mechanical rotating parts, the above methods have an additional disadvantage, which consists in the fact that the "standard radiation source" device must be modified for compensation, which makes it often difficult to obtain reproducible results.

A method of eliminating the above deficiencies is proposed below [6]. According to this method, the photocell is irradiated by a variable light flux, and the indicator amplifier transconductance is regulated with respect to the alternating component of the cell current or voltage. This measurement method has the advantage that the measurements are performed directly and without compensation. Moreover, the receiver (photocell)

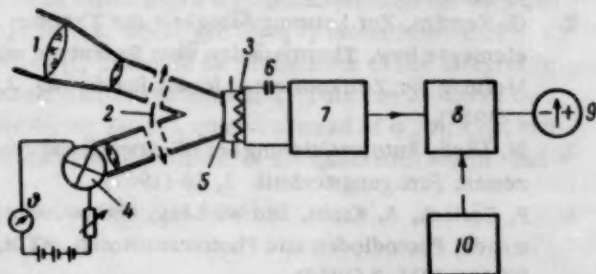


Fig. 4. Block diagram of the arrangement for temperature measurements with TMR-2000. 1) To the measurement object; 2) diaphragm which oscillates at 50 cps; 3) photoresistors; 4) comparison lamp; 5) slit diaphragm; 6) capacitor; 7) ac voltage amplifier; 8) discriminator; 9) deviation indicator; 10) line voltage.

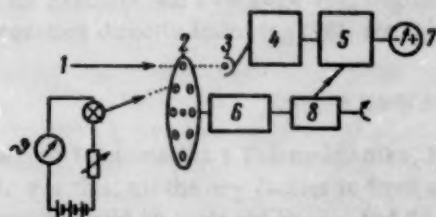


Fig. 5. Operation principle of a milliscope (Hartman and Braun). 1) To the measurement object; 2) rotating disk with openings; 3) photocell or photoconductor; 4) ac voltage amplifier; 5) discriminator; 6) motor; 7) deviation indicator; 8) generator.

receives a bias voltage due to the steady component of the variable light flux, as a result of which the noise level is exceeded and the receiver sensitivity is increased.

The operation principle is clear from Fig. 6. Along with the  $J_x(\lambda)$  radiation to be measured, light of variable intensity, which consists of the steady  $J_k(\lambda)$  and the variable  $J_k'(\lambda)$  components, is incident on the photosensitive layer. The photoconductor resistance changes in accordance with the spectral sensitivity distribution characteristic, and the sum of these variations is transformed into current and voltage variations. By  $\epsilon(\lambda)$ , we shall designate the slope of the  $dU_a/dJ(\lambda)$  transformation function, where  $U_a$  is the output voltage variation, and  $J(\lambda)$  is the variation of radiation in dependence on the wavelength for a certain given cell voltage and a given external resistance. Then the external resistance voltage  $u_a$  will be determined by the expression

$$u_a = \epsilon(\lambda) [J_x(\lambda) + J_k(\lambda) + J_k'(\lambda) + J_0],$$

where  $J_0$  is the very small photoconductor dark current.

If, for instance, by means of a spectral filter placed in front of the photosensitive layer, the wavelength range is reduced to such an extent that the frequency dependence  $\epsilon$ ,  $J_x$ , and  $J_k$  can be neglected, the resulting voltage  $u_a$  will be found from the equation

$$u_a = \epsilon (J_0 + J_k + J_x) + \epsilon J_k'.$$

where the first term on the right-hand side of the equation corresponds to the steady component, and the second term corresponds to the variable component; while  $\epsilon$  is the sensitivity, dependent on temperature and aging, whose influence on the measurement results must be eliminated.

Since the magnitude of  $J_k$  is constant, the variable component of the photocell current is the measure of this sensitivity. The variable and the steady voltage components can be readily separated. Both components can be now separately amplified, and the amplification factor of the steady-component amplifier can be varied while keeping it inversely proportional to the variable-component magnitude, so that the steady-component amplification will be

$$v_{\text{max}} = \frac{v_{\text{max}}}{v \epsilon J_k} = \frac{v_0}{\epsilon}.$$

Consequently, a voltage which is independent of the

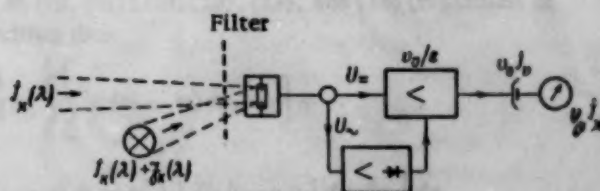


Fig. 6. Principle of radiation measurement with automatic sensitivity regulation.

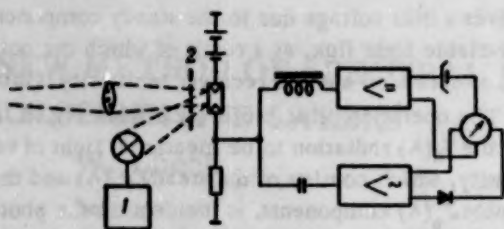


Fig. 7. Operation principle of a pyrometer for the radiation portion in automatic sensitivity regulation. 1) Constant-amplitude ac current; 2) filter.

cell sensitivity will appear at the steady-component amplifier output:

$$u_A = \frac{v_0}{s} (s J_0 + s J_k + s J_x) = v_0 J_0 + v_0 J_x,$$

where

$$s J_0 + s J_k = s J_v.$$

This voltage depends only on the intensity  $J_x$  of the radiation to be measured. The bias voltage  $v_0 J_v$  can be compensated electrically.

The radiation to be measured, which is focused by a lens or a concave mirror, is directed to a lead sulfide photoresistor through a monochromatic light filter.

With respect to the transmission frequency and the bandwidth, the light filter is selected in such a manner that the radiation component of the greatest intensity is received. Moreover, the following condition is imposed on the light filter: the change in the characteristic of the PbS spectral sensitivity distribution due to changes in the surrounding temperature and aging must not disturb the validity of the above dependences as a result of the difference between the radiator and the variable light source spectra. Thus, the variable light flux of constant amplitude falls on the PbS photoresistor after

passing through the same light filter through which the light flux to be measured passes.

For instance, an incandescent lamp with low thermal inertia, which is fed through a commutator or is supplied an ac current of constant magnitude, can be used as the constant-amplitude light source.

The shape of the variable light flux vs. time curve is not of great importance; however, it must be stable. In selecting the frequency, it should be ensured that the rise and attenuation times of the photoresistor be of the order of  $10^{-4}$ - $10^{-5}$  sec. The maximum frequency is basically determined by the variable light flux source, while the optimum value for the amplifier is 50 cps.

The resulting cell voltage is divided into the steady and variable components by means of a choke and a capacitor; both these components are then separately supplied to amplifiers with negative feedback. The output power of the amplifiers is so chosen as to make it possible to use measuring instruments with crossed coils, which are excited by the rectified variable component. The  $v_0 J_v$  steady component is compensated by the stabilized bias voltage.

#### LITERATURE CITED

1. H. Günzler, Farbläser und Metallinterferenzfilter, Feingerätetechnik 10 (1956).
2. G. Kortüm, Zur Leistungsfähigkeit der Thermoelemente bzw. Thermosäulen über Bedeutung und Messung der Zeitkonstante, Jenaer Rundschau 2, 3 (1957).
3. W. Lück, Automatisierung bei HF-Erwärmungsprozessen, Fertigungstechnik 7, 10 (1957).
4. P. Görlich, A. Krohs, and W. Lang, Photowiderstände, Photodioden und Phototransistoren, ATM, J394-1-J394-3 (1958).
5. W. Lück, Über ein neues Temperaturmessgerät, Der Industriebetrieb 2, 17-21 (1957).
6. WP, 42 I/40 406.



## LETTERS TO THE EDITOR

AN ERROR IN THE ARTICLE "EFFECT OF FLUCTUATIONS ON THE  
SIMPLEST PARAMETRIC SYSTEMS" BY V. I. TIKHONOV (AVTOMATIKA  
I TELEMEXHANIKA, VOL. 19, NO. 8, 1958)

I. A. Bol'shakov

Translated from Avtomatika i Telemekhanika, Vol. 21, No. 7, pp. 1088-1089,  
July, 1960

The article by V. I. Tikhonov is devoted to the interesting problem of the effect of fluctuations on parametric systems, which has been treated in a number of important contributions. Therefore, the conclusions reached in the article deserve the most careful study. However, this study shows that the basic results presented in the article are not correct, which is due to errors in calculation.

The errors begin with the expression for  $\Phi_2(\alpha, j)$  on page 718, where the  $2\alpha\sigma_1\sigma_2$  factor instead of  $2\alpha\sigma_2\sigma_\xi(t, u)$  should be in the front of the integral in the last part of the equation. This can be shown by considering Eq. (5), where, instead of  $\sigma_\mu\sigma_\nu R_{\mu\nu}$ , the mutual central moment of the quantities  $\alpha\eta(u)$  and  $\int_u^t \xi(x_2) dx_2$ , which is equal to

$$\alpha\sigma_1\sigma_2 \int_u^t R_{12}(u-x_2) dx_2.$$

should be substituted.

Similar errors in calculating the mutual moments are found in Eqs. (12), (13), and (14). As a result, the equations for example No. 2 on page 721, beginning with the equation directly following (16), are incorrect.

### ANSWER TO I. A. BOL'SHAKOV

My article (Avtomatika i Telemekhanika, No. 8, 1958, p. 716) contains a calculation error. It can be readily corrected. For this, all the  $\sigma_\xi$  factors in front of the integrals in Eqs. (8), (12), (13), (14), and (18) (regardless of the argument) should be replaced by  $\sigma_1$ , and Eq. (9) must be written thus:

$$m(t) = y_0 \exp \left[ -m_1(t-t_0) + \frac{1}{2} \sigma_1^2 \int_{t_0}^t \int_{t_0}^t R_1(x_2-x_1) dx_1 dx_2 \right] + \\ + \int_{t_0}^t \left[ m_2 - \sigma_1\sigma_2 \int_u^t R_{12}(u-x_2) dx_2 \right] \exp \left[ -m_1(t-u) + \frac{1}{2} \sigma_1^2 \int_u^t \int_u^t R_1(x_2-x_1) dx_1 dx_2 \right] du.$$

Actually, the output dispersion  $y(t)$  is of the following form:

$$\sigma^2 = \\ = y_0^2 \exp \left\{ -2m_1(t-t_0) + 2\sigma_1^2 \int_0^{t-t_0} (t-t_0-s) R_1(s) ds \right\} \times \\ \times \left[ \exp \left\{ 2\sigma_1^2 \int_0^{t-t_0} (t-t_0-s) R_1(s) ds \right\} - 1 \right].$$

This dispersion does not tend to infinity in every case when  $t$  increases, which follows from the results described in the article, which the author admitted to be unusual. On the contrary, the dispersion of output fluctuations tends to zero if the following condition is satisfied:

$$m_1 - 2\sigma_1^2 \int_0^\infty R_1(s) ds > 0. \quad (1)$$

As is shown by calculations for actual electronic devices which are subject to fluctuations, condition (1) is not always satisfied in these devices. Small parametric effects always occur - for instance, in electronic servosystems; however, this never leads to an infinite root-mean-square error. Therefore, the "physical explanation", whereby the author attempted to substantiate the obtained incorrect result, is obviously not valid.

The error does not affect the results in the first and the third examples. In the second example, the system will be stable with respect to dispersion if the following inequality is satisfied:

$$m_1 - 2\sigma_1^2 \int_0^\infty R(s) ds > 0.$$

If we introduce the correlation time  $\tau_k(t)$  for a random process

$$\tau_k = \int_0^\infty R(s) ds,$$

this equation can be written as

$$m_1 > 2\sigma_1^2 \tau_k. \quad (I)$$

As a rule, the correlation time  $\tau_k$  is a positive quantity, and dispersion  $\sigma_1^2$  is also basically a positive quantity. Therefore, if (I) is satisfied, also inequality (16) is automatically satisfied:

$$m_1 > \sigma_1^2 \tau_k.$$

Consequently, if (I) is satisfied, the system is statistically stable (i.e., stable with respect to the average value and dispersion). If the inverse inequality is satisfied, the system is unstable. For this case, the physical explanation given on page 722 holds. Therefore, we cannot entirely agree with L. A. Bol'shakov's remarks.

V. I. Tikhonov

## DISCUSSION

ON THE BOOK "ELEMENTS OF STRUCTURAL SYNTHESIS  
OF RELAY CONTROL CIRCUITS" BY V. N. ROGINSKII  
(AN SSSR PRESS, MOSCOW 1959; 168 pages)

V. I. Shestakov

Translated from *Avtomatika i Telemekhanika*, Vol. 21, No. 7, pp. 1090-1094,  
July, 1960

Although the development of methods for the mathematical analysis, synthesis, and simplification of relay circuits is of great importance for automation and remote control, communications, and computer techniques, no textbook or monograph which would be devoted to the latest results in the theory of relay circuits is yet available in Russian. The monograph, *Theory of Relay-Contact Circuits*, by M. A. Gavrilov, which was published in 1950 in a small edition, has become a bibliographic rarity.

It is understandable that the numerous specialists engaged in the construction of automatic devices in different branches of technology greeted with interest the book, *Elements of Structural Synthesis of Relay Control Circuits*, by V. N. Roginskii.

However, in no way does this book justify the readers' expectations. The contemporary state of the relay circuit theory and the basic trends in its development have been outlined in the book, not only in an insufficiently thorough and substantial manner, but even essentially incorrectly. In particular, the relation between the theory of relay-contact (r-c) circuits and the theory of contactless relay circuits is incorrectly defined. It is stated in the book that the "theory of relay-contact circuits is applied to an ever-increasing extent also to relay circuits with contactless elements" (p. 13). However, as is well known, r-c circuits constitute only one of the particular variants of relay circuits, and, therefore, the theory of r-c circuits cannot be generally applied to any relay circuits. At the present time, there is a fast-developing general theory of relay circuits — the theory of logic networks, which can also be applied to r-c and to contactless relay circuits. The book does not even mention the existence of this theory.

It is not mentioned, either, that the theory of r-c circuits, to the synthesis of which the book is devoted, is not so important now as it was 10-15 years ago, and that the methods of synthesis of contactless relay circuits — where electron tube, semiconductor, and magnetic switching elements are used — are becoming more important.

The book under discussion is not a textbook or a monograph, but a compilation of the author's papers on the theory of synthesis of r-c circuits, which were published in 1954-1959 in various scientific journals and

collections. The introduction defines the main tasks in electrocommunication and the main problems in its automation, and it contains a brief historical outline of the development and the contemporary state of the structural synthesis theory of relay and, mainly, r-c circuits. However, as was indicated above, this outline is not satisfactorily presented.

Chapters 1-4 present the basic postulates of the theory of r-c circuits, various methods of describing their structure and operating conditions, the basic problems in the synthesis of sequential circuits, and the algebraic transformations of contact circuits. The basic operations and principles of logic algebra (Boolean algebra) and their schematic interpretation are given in this chapter. Chapters 5 and 6 describe some methods for the transformation and simplification of contact circuits. Special attention is paid to the method based on the so-called "consideration of unused combinations." Chapter 7 considers in detail the graphic method of contact circuit synthesis. Chapters 8 and 9 present the theory of the synthesis of mixed II-type r-c circuits, which has been proposed earlier by the author; chapter 10 is devoted to the theory of the synthesis of r-c circuits with capacitors. The book ends with chapter 11, which very briefly describes a machine for the synthesis of contact (1, k)-poles, an apparatus developed by the author in 1956 in collaboration with A. A. Arkhangel'skaya and V. G. Lazarev.

The book does not contain a summary which would briefly and concisely formulate the results obtained by the author, which is especially conspicuous, since there is nowhere in the book a clear distinction between the author's own results and the well-known results contributed by other authors.

It should be also noted that those branches of r-c circuit theory to which the author has contributed are treated in least detail in the book. The papers which are the closest to the author's own contributions with respect to the subject and content are either not mentioned at all in the text or are insufficiently treated. Thus, for instance, little is said about the papers concerning the methods for the minimization of the expressions for the Boolean functions and of the corresponding circuits, which are based on the use of adjacent constituents. Neither does the book contain even a



brief survey of the work on the theory of circuits with elements with finite admittances, although chapters 8 and 9 present a synthesis theory for a particular case of such circuits — the so-called "mixed relay" circuits of the  $\Pi$ -type — which has been proposed by the author.

The author does not mention anywhere in the book that the idea of using the so-called "unused combinations," i.e., the combinations which, according to the synthesis conditions, cannot occur in the operation of the circuit to be synthesized, is not new. Neither does the author mention the fact that the terms "unused states" and "indifferent states," which he uses, are simply Russian translations of the English terms "unused output combinations" and "don't care combinations," respectively, and that the first of these terms is equivalent to the term "invalid combinations." However, these terms were used in English literature concerning the theory of relay circuits in exactly the same sense as the Russian synonyms which the author used even before the publication of his first paper in this field: "Consideration of unused combinations in the synthesis of relay-contact circuits" (*Avtomatika i Telemekhanika*, Vol. 15, No. 3, 1954).

While repeatedly applying Boolean algebra to valve elements, the author does not consider it necessary to mention the fact that the possibility of such application was first demonstrated by M. A. Gavrillov in his paper "Relay-contact circuits with valve elements" (*Izvest. Akad. Nauk SSSR, Otd. Tech. Nauk*, No. 2, 1945). This article is not even mentioned in the bibliography.

In the same manner, when introducing on page 19 a new symbol  $A \times B$  for the harmonic addition operation  $A \cdot B$ , the author does not mention that this operation has been known for a long time: it was first applied more than twenty years ago in the theory of electrical and, in particular, relay circuits.

The limited space does not permit us to adduce a number of other examples of such peculiarities in presentation, due to which a reader who is not sufficiently familiar with the literature concerning the theory of relay circuits can receive an impression that many of the already known results are new, and that they have been obtained by the author of the book.

Actually, the book contains only a small number of results contributed exclusively by its author, and this apparently explains the manner in which the state of those sections of the r-c circuit theory to which the author's own results relate is presented.

The author's work, which is presented in chapters 5 and 6, does not contain new results concerning the essence of contact circuit minimization. Actually, this was not the author's intention, as can be seen from the footnote on page 70: "The aim of the present work is the finding of suitable expressions for the subsequent transition to the circuit, and not the determination of minimum forms."

The idea of the graphic method for the synthesis of contact circuits, which is presented in chapter 7,

does not belong exclusively to the author of the book. This method was proposed in 1955 by G. N. Povarov for the synthesis of symmetric and quasi-symmetric circuits. V. N. Roginskii later showed that every circuit can be considered as quasi-symmetric if weights  $2^{i-1}$  are added to relays with the numbers  $i = 1, 2, \dots, n$  and if the numbers of combinations for which a certain given circuit must be closed are taken as the working numbers of the relay circuit. This is actually the only contribution of V. N. Roginskii to the development of this method.

Only chapters 8 and 9 contain a theory which is based on ideas belonging exclusively to the author of the book. These chapters describe the results of three papers that were published by the author in 1957, where he attempted to put forward a theory of the synthesis of  $\Pi$ -type mixed relay circuits, i.e., of such r-c circuits where the contact circuits can be connected in parallel, as well as in series, to the relay windings and to certain additional resistances of finite magnitude. However, this attempt was entirely unsuccessful, and the theory proposed by the author is far from satisfactory in the physical and mathematical sense, and is totally unsuitable for practical use.

The main principle of this theory is based on the assumption of dividing the synthesis of the relay circuits into two stages: the stage of determining the circuit structure and the stage of the electrotechnical calculation of its elements. The author assumes that the structure of a  $\Pi$ -type mixed r-c circuit can be determined if only the "orders of admittance" of its elements are known. In order to designate that a certain dipole has a finite admittance  $G$  of the same, lower, or higher order in comparison with that of relay  $A$ , the author uses the symbols  $G = A$ ,  $G < A$ , and  $G > A$ , respectively, which he defines in the following manner:  $G = A$ , if the relay  $A$  operation is not disturbed either for a series or a parallel connection of  $G$  to  $A$ , and  $G < A$  (or  $G > A$ ) if the operation of relay  $A$  is disturbed only for a series (or parallel) connection of  $G$  to  $A$ .

The author considers that the case where the operation of relay  $A$  is disturbed for a series, as well as a parallel, connection to  $G$  is possible, but of no practical importance.

The basic deficiency of the above determination is the dependence of the order of admittance on the voltage applied to the circuit and on the internal resistance of its source.

It can be readily shown through simple examples that, by changing the magnitude of the emf  $E$  and of the internal resistance  $R_E$  of its source, we can obtain any order of the admittance  $G$  for a dipole which has a constant resistance  $R$ , for instance, equal to the resistance  $R_A$  of the relay  $A$  winding. Let  $V_A$  and  $i_A$  be the minimum voltage and current sufficient for reliable operation of relay  $A$ , and  $i_A$  and  $i_p$  be the respective currents through the relay  $A$  winding when it is connected in series and in

parallel to a dipole with the resistance  $R$  equal to the resistance  $R_A$ .

By simple calculations, using only Kirchhoff's laws, we obtain

- 1)  $i_a < i_A$  and  $i_b > i_A$ , i.e.,  $G < A$  for  $V_A < E < 2V_A$  and  $R_E = 0$ ;
- 2)  $i_a > i_A$  and  $i_b > i_A$ , i.e.,  $G = A$  for  $E > 2V_A$  and  $R_E = 0$ ;
- 3)  $i_a \geq i_A$  and  $i_b < i_A$ , i.e.,  $G > A$  for  $E \geq 6V_A$  and  $R_E = 4R_A$ ;
- 4)  $i_a = i_b < i_A$ , i.e., relay  $A$  will not operate when it is connected either in series or in parallel to the resistance  $R$  for  $E = 2V_A$  and  $R_E = R_A$ .

It is perfectly obvious that similar results will be obtained in the general case, where  $R \neq R_A$ , when the voltage drop in the considered circuits connecting the relay  $A$  winding to the resistance  $R$  plays the role of the emf  $E$ .

The dependence of the order of admittance on voltage does not permit us to determine the order of admittance of all elements of the circuit to be synthesized before we begin its synthesis, since various switchings will occur during the circuit operation process, as a result of which some of the relays will be interconnected in a different way than before. Due to this, the voltage distribution among the circuit elements will change, and this, in turn, can cause a change in the beforehand-determined orders of admittance of the circuit elements. The orders of admittance of the circuit elements for different closing and dropout combinations of all relays in the circuit can be determined only after the circuit structure is known, and the electrotechnical calculation of the circuit parameters is performed.

Thus, the author's basic idea of the possibility of dividing the synthesis of a  $\Pi$ -type mixed  $r$ - $c$  circuit into two stages is illusory.

The main reason for the fallacy of the proposed synthesis theory consists in the fact that the author attempted to operate only with admittances, while ignoring the well-known physical fact that the operation of an electromagnetic relay is determined by the current passing through its windings, and that the current in circuits with finite admittances depends equally on the circuit admittance, as well as on the voltage applied to the circuit. In other words, the main reason for the fallacy of this theory is the attempt to ignore Kirchhoff's laws for electrical circuits.

This theory is unsatisfactory also from a mathematical point of view, due to the large number of fundamental mathematical and logical errors and the fact that many determinations are not satisfactory and, in some cases, nonexistent.

We shall first mention the statements which are obviously incorrect. One of such statements is, for instance, the statement contained in the following phrase (my emphasis): "We shall also assume that the admittance and parameter values of relays are chosen in such

a manner that if a finite number of admittances of the same order are connected in parallel or in series, the over-all admittance will be of the same order, i.e.,

$$A + B = A + \dots + K = A \quad (A + B + \dots + K) = A, \\ A \cdot B = A \cdot \dots \cdot K = A \quad (A \cdot B \cdot \dots \cdot K) = A. \quad (8.11'')$$

Generally speaking, this statement is not valid for any order determination, since it contradicts the basic axiom of finite quantities — the Archimedes axiom.

Expression (8.10) contains a printing error, which becomes obvious if we compare it with expression (8.7). If we eliminate this error by reversing one of the signs  $>$  and  $<$ , we obtain the following statements: If  $A > B$  and  $B > A$ , the circuit cannot be realized; if  $A < B$  and  $B < A$ , the circuit cannot be realized.

The fallacy of these statements can be readily demonstrated by adducing examples of circuits for which the  $A > B$  and  $B > A$  relations, as well as the  $A < B$  and  $B < A$  relations, are satisfied. The first of these relations holds for circuits in the above-considered example for the case (3) if relay  $B$ , which is identical to relay  $A$ , is used as dipole  $B$  with the resistance  $R = R_A$ . The second of these relations is satisfied for circuits of the case (1) in the same example, by the same substitution of relay  $B$  for dipole  $B$ .

Conditions (8.7) do not follow from determinations of the order of admittance, and, generally speaking, they are not satisfied, since the  $B = A$ ,  $B < A$ , and  $B > A$  relations and the  $A = B$ ,  $A > B$ , and  $A < B$  relations are independent of each other.

All the above reasoning on the orders of admittance apply under the assumption that the term "admittance" is used in the generally accepted sense, i.e., that it denotes the quantity reciprocal to impedance. However, in the symbols  $G = A$ ,  $G < A$ , and  $G > A$ , the sign  $G$  designates the so-called "structural admittance," which the author determined only for two values of ordinary admittance: for the 0 and  $\infty$  values. According to the determination given on page 20 in the book, the structural admittance  $G$  is equal to 0 and 1, while the corresponding ordinary admittance  $Y$  is equal to 0 and  $\infty$ , respectively. The structural admittance  $G$ , which corresponds to the  $Y$  values lying between 0 and  $\infty$ , is not determined anywhere in the book. Therefore, it is impossible to tell what is the structural admittance  $G$  of a dipole which has a certain admittance  $Y$  (for instance, admittance  $Y = 1$  mho) and, conversely, if a dipole structural admittance not equal to 0 and 1 is given, it is impossible to tell what is the ordinary admittance  $Y$  of such a dipole.

In the same manner, the operations that the author denotes by symbols  $G_1 + G_2$ ,  $G_1 \cdot G_2$ , and  $\bar{G}$  are not defined for finite admittance values. Throughout the book up to chapter 8, these operations are applied only for the values of structural admittances  $G_1$  and  $G_2$  equal to 0 and 1. For these values, the operation symbols "+,"



"+" and "-" are used in the sense of Boolean operation symbols: for addition, multiplication, and negation (complementing to 1), respectively. For structural admittances not equal to 0 and 1, these operations do not pertain to Boolean algebra operations. In this case, they represent isomorphic operations for ordinary addition, harmonic addition, and inversion — the basic algebraic operations for dipole circuits of the A-type (or of the II-type in the presently adopted terminology) — the existence of which is not mentioned in the book, although the papers where they are described are contained in the bibliography at the end of the book. By not mentioning the existence of this algebra, the author loses the possibility of offering any isomorphic presentation of the basic operations of this algebra, and, therefore, leaves the  $G_1 + G_2$ ,  $G_1 \cdot G_2$ , and  $\bar{G}$  symbols without any algebraic definition. Therefore, all the formulas where the algebraic signs "+", "·", and "-" are encountered between the structural admittance symbols which are not equal to 0 and 1 are devoid of any algebraic sense.

Neither are the  $G = A$ ,  $G < A$ , and  $G > A$  symbols defined mathematically — which is anyway essentially impossible, unless the structural admittance  $G$  is defined.

Due to the fact that the symbols of basic operations and relations are not defined and that no concrete relation exists between structural and ordinary admittances, the entire theory presented in chapters 8 and 9 is devoid of any mathematical sense and cannot be used for any calculations of admittance values.

There are no logical proofs for any statements in the book or in the papers published earlier by the author and presented in the book. A number of formulas are given without derivations and proofs. Because of this, it happens that some formulas in the book are either incorrect or contradictory. Thus, for instance, the author states that "the law of commutativity is valid for an equivalence

$$\frac{a}{b} = \frac{b}{a} \quad (5.8)$$

and, at the same time, considers that the equality  $\left(\frac{a}{b}\right) = \frac{\bar{a}}{\bar{b}}$  holds. The last equality, however, is incompatible with equality (5.8), since it can be readily shown that the inversion operation is nondistributive with respect to any commutative operation of Boolean algebra.

The equivalence symbol  $\frac{a}{b}$  is not rigorously defined. Not only in the author's different papers, but also in different places in the same paragraph — § 3 in chapter 5 — this symbol has a different meaning. By loose reasoning, the author finally arrives at the following expression for symbol  $\frac{a}{b}$  by means of Boolean algebra

operations:

$$\frac{a}{b} = ab + (a + b)\omega = a\bar{b}\omega + (a + b)\omega, \quad (5.11)$$

where  $\omega$  is any expression of this algebra. Equation (5.11) satisfies, as can be readily shown, only the following Boolean functions of the two arguments  $a$  and  $b$ :  $ab$ ,  $a$ ,  $b$ , and  $a + b$ . Only the first and the last of these functions are symmetric, so that the author's statement that formula (5.8) holds for equivalences is, generally speaking, incorrect.

It would be possible to quote other examples of internal contradictions in the equivalence calculations presented in the book.

The book contains many formulas, but they are not actually used for calculations. There are almost no calculations which would be complete and without omissions.

In conclusion, it should be noted that an absence of logic is noticeable not only in the presentation of theory, but also in the composition of the book. For instance, problems in the synthesis of sequential circuits are considered in chapter 3, and the algebraic transformations which are used for their synthesis are presented in chapter 4. The methods for describing the structure and the operating conditions of r-c circuits are treated in chapter 2, while these methods are based on the use of the algebraic apparatus presented in chapters 4 and 5. The graphic method for the synthesis of contact circuits is considered in chapter 7, and the machine for the synthesis of contact circuits according to this method is described in chapter 11. Between these naturally connected chapters, the author has for some reason inserted chapters treating r-c circuits with finite admittances, i.e., circuits, the synthesis of which cannot be secured either by the graphic method described in chapter 7 or, even less, by the machine for synthesis which is described in chapter 11. Another example showing that subjects which naturally follow each other are contained in different parts of the book are the general problems in the synthesis of sequential circuits and the synthesis of sequential circuits with capacitors. These closely related subjects are considered in chapters 3 and 10, and the intermediate chapters contain material which is only indirectly connected with these circuits.

Only an absence of proper scientific criticism can explain the publication of this book, which does not contain anything new in comparison with the papers published earlier by the author, is full of mathematical and logical errors, and also presents a false picture of the contemporary state and development trends of the theory of relay circuits, reproducing almost without changes the physically and mathematically unsubstantiated theory of the synthesis of II-type mixed relay circuits.



REPLY TO V. I. SHESTAKOV'S CRITICAL REVIEW OF THE BOOK  
"ELEMENTS OF STRUCTURAL SYNTHESIS OF RELAY CONTROL  
CIRCUITS " BY V. N. ROGINSKII

V. N. Roginskii

Translated from *Avtomatika i Telemekhanika*, Vol. 21, No. 7, pp. 1094-1098,  
July, 1960

The book under discussion is devoted to the presentation of problems connected with the structure of relay circuits. The book provides methods which the author thinks can be recommended in engineering practice, while most attention was paid to the design of the simplest circuits possible. All the methods presented in the book have been tested in practice by the author, by the team with which he works, and in a number of scientific and design organizations. For the purposes of clarifying these methods, some elements of the theory of contact and relay circuits have been presented in the book.

The book does not pretend to deal with all aspects of the theory of relay circuits, which is obvious from its title: "Elements . . . ." Moreover, only the synthesis of a narrow class of relay circuits is considered — the class of control circuits, the characteristics of which are described in the introduction. The number of branches of the modern theory of relay circuits which were not included in the book could be considerably enlarged in comparison with those V. I. Shestakov mentioned in his note.

It cannot be said that the theory of relay-contact circuits is presently of lesser importance than 10-15 years ago, since the number of relays and relay circuits which are developed and produced by the industry increases every year. Just now, when relay devices are used in enormous quantities in many fields of the national economy, the problem of the design of efficient circuits is most important. Experience shows that the application of theoretical methods (in particular, also methods presented in the book) will make it possible to simplify the existing circuits and to reduce the number of their elements sometimes by one-third. The present-day importance of this problem is emphasized by an ever-increasing number of papers in this field (including papers by V. I. Shestakov). The appearance of new elements and new theories, which also have to be developed, is another matter. I do not propose to contest their importance, but it seems to me that they cannot be set off against each other. In my opinion, the general trend of development in the nearest future is the formation of a general theory for the design of discrete action circuits, which is mentioned in the introduction. It is possible that the statement that the theory of relay-contact circuits is applied to an ever-increasing extent to relay

circuits with contactless elements, cannot be taken as completely true, but it can be hardly understood as a statement that this theory can be applied to any relay circuit (emphasis supplied by V. I. Shestakov).

Also, the book is not an historical treatise, and, therefore, it is not necessary at all to specify who was the first to use the multiplication sign for denoting consecutive connection, who was the first to analyze circuits with valve elements, who derived the formula for the calculation of admittances connected in series ("harmonic addition") and when, etc. With regard to the questions raised in the critical note, it can be said that the book contains references to papers by M. A. Gavrilov on circuits with valve elements (pages 9-10 and 28) and also to papers dealing with the problem of circuits with finite admittance elements by V. I. Shestakov, M. A. Gavrilov, and other authors (page 10).

In the same manner, there is no need to mention the translations of particular terms into foreign languages in the book.

I took the stand that the simplification of contact circuits by using so-called "unused combinations" was well known, and I did not undertake historical research in order to establish priority in this field. In my first paper concerning this problem (*Avtomatika i Telemekhanika*, Vol. 15, No. 3, 1954), to which, in particular, V. I. Shestakov refers, it was stated in the first paragraph: "A possible way of simplifying the circuit is, as is known, the consideration of those combinations which are not encountered in the operation of the circuit." The author's role is defined with sufficient clarity in the book, where it is said that ". . . a system for describing such combinations by means of connection tables and formulas, and methods for applying the conditions to circuits by taking into account the indifferent combinations, which have been developed by the author, are given" (page 11). I do not think that even readers unfamiliar with literature concerning the theory of relay circuits can draw the conclusion that all the material in the book is the author's contribution.

The book does not contain a consideration of basic problems in minimization, as V. I. Shestakov rightly notes. At the present time, minimization denotes the determination of minimum normal forms of Boolean functions, which does not always provide the possibility

of obtaining a  $\Pi$ -type contact dipole circuit with a minimum number of contacts, especially if unused combinations are present. Experience shows that in many (and, for a large number of relays, in the majority of) cases, H-type circuits are simpler for solutions which do not correspond to the minimum forms. In the same manner, the minimization of individual circuits does not provide the possibility of designing circuits with an over-all minimum number of contacts by combining these circuits into a single network (even for  $\Pi$ -type). Therefore, in practical application, the introduction of the minimization concept (in the above sense) can be even disadvantageous, since, in designing, the impression can be formed that a "minimum" circuit is secured, while a circuit with an even smaller number of contacts can be obtained if nonminimum solutions are used for individual circuits. Since, at the present time, there is no method for the design and determination of actually minimum circuits, the book provides recommendations for the design of circuits with the greatest degree of contact unification, which approaches the minimum conditions. Therefore, "minimization" has not been treated in the book, and individual minimization methods are used only for simplifying the writing of structural formulas.

At the same time, contact multipoles with a number of contacts close to the minimum, when simplifications due to indifferent combinations are automatically taken into account, can be designed by using the graphic method presented in chapter 7.

If the history of the development of this method is to be presented, one has to begin, on the one hand, with papers by M. A. Gavrilov and C. E. Shannon, which deal with the connection of multipoles, and then pass to cascade methods and methods for the design of symmetric circuits, which have been developed by G. N. Povarov (they are presented in the first part of the chapter), and, on the other hand, with papers dealing with unused combinations. In the graphic method, all operations are performed with three-valued functions, for which the concepts of "symmetry" and, even more so, "quasi-symmetry" are not defined (and, possibly, cannot be defined). This method provides possibilities (circuits with "direct lead-outs" and the consideration of unused combinations) which the above-mentioned methods do not have. In fact, the application of the graphic method principles to the G. N. Povarov method (i.e., to two-value logic) made it possible to demonstrate that all functions (two-valued, and not three-valued) are quasi-symmetrical in the sense defined by G. N. Povarov.

Another way of securing simpler circuits, is, as is known, the use of parametric dependences in the circuits, i.e., the design of such circuits where the operation of individual relays depends not only on whether the circuit is closed or open, but also on the current intensity in the closed circuit. Such circuits were designed and operated before the theory of relay circuits appeared, in the same

way as contact circuits were designed and modified for a long time before C. E. Shannon and V. L. Shestakov formulated the basic principles of the theory of such circuits. Thus, the "idea" of these circuits does not belong to the author of the book, but rather has existed a long time, and individual papers devoted to this question are available in literature. The book provides only a certain generalization of the experience gained and the definitions of rules for transforming circuits with parametric dependences for certain restrictions, which are mentioned below.

The statement that "the assumption of the possibility of dividing the synthesis process into two stages — the determination of the circuit structure and the electrical calculation of its parameters — is illusory" can be explained only by the author's total unfamiliarity with the practice of designing relay circuits and calculating their parameters.

It is awkward to talk about such truisms in an academic journal, but, since much space has been devoted to this question in the review, I shall take the liberty to dwell on it.

The division of circuit design into two interlinked stages is a necessary sequential process which is the result of long-standing experience, and only correct solutions in both stages can secure an efficient circuit. The calculation of elements can be performed only after the structure is determined, but, in composing the structure, the capabilities of relays must be taken into account.

Let us consider the simplest case, where ordinary electromagnetic relays without parametric dependences are used and where, from the structural point of view, it is only necessary that the series circuit be closed and the shunting circuit open for the relays to operate. If, for instance, it is required that relay X operate only when button A is pressed, one of the possible solutions of the circuit structure will be the series connection of the button closing contact to the relay winding, i.e., a circuit with the structural formula  $aX$ . However, even for such a circuit, the relay will operate in the required manner only if all the circuit parameters are accurately calculated (including the voltages and the current source impedances). If the calculations are erroneous, the relay may not operate, or it may "burn" and become unusable when the contact closes. A different structure can also be considered:  $\bar{a} + X$ . For such a circuit, elements with different parameters are required. However, if the structure is wrongly chosen — if, for instance, an opening, instead of a closing contact is installed in the above circuit (i.e., if the  $\bar{a}X$  circuit is chosen) — the calculation of circuit parameters will not help, and the circuit will operate in accordance with the assigned conditions.

In view of the necessity for such order, it is possible to talk about the interaction between individual elements in the circuit without first determining their parameters during the structural synthesis stage.



In a contact circuit with only two combinations — open and closed — the concept of the circuit operation coincides with the concept of its admittance: 0 or  $\infty$  (or 0 and 1 in theory). For relay circuits, such single-value correspondence between the circuit admittance and the operation of the circuit relays does not exist, and, as V. I. Shestakov rightly remarks, the operation of relays in the circuit depends on many factors, including the voltage applied. In order to take into account the influence of all circuit parameters on the operation of relays, the concept of the circuit admittance and the concept of a relay circuit operation are separated in the book, in the first place. The concept of the circuit equivalence with respect to operation is introduced. In order to express the effect of the admittances included in the circuit on the relay operation, we introduced the concept of the "order of admittance," which "does not characterize the absolute admittance (or impedance) value, but the effect of this admittance on the operation of relays in the circuit, i.e., which pertains to the actual circuit parameters and the voltage supplied to it" (page 121). Thus, the critic's statement that an attempt has been made to operate solely with "admittances" is entirely incomprehensible.

It should be remarked that the concept of the "order of admittance" characterizes the influence of different impedances on the operation of relays for certain given methods of connecting these impedances to the relay windings. Therefore, it is entirely senseless to talk either about the "magnitude" of the order, or about any well-defined correspondence between the "orders of admittance" and admittance values expressed, for instance, in mho. Since these concepts, although denoted by the same term, refer to different physical properties ("admittance" is the property of an element, and its magnitude is the reciprocal of impedance, while the "order of admittance" is the effect of this element on another in a given circuit), there is not, and cannot be, any well-defined relation between them.

In the examples given in the review, reference is made not to the order, but to the value of admittance ("the term 'admittance' is used in the generally accepted sense," as the author of the note states), and, therefore, the reasoning in the note does not essentially apply to the material presented in the book, which only confirms the absence of the above-mentioned relation.

Thus, there is a misunderstanding in this case, which is caused by the confusion in using the terms. Perhaps a term not including the term "admittance" should be found for the characteristic of the interaction of elements with finite admittance. I chose this term in order to characterize the influence which a finite admittance exerts on the relays of the circuit. Thus, for instance, an element with a "lower order of admittance" in the circuit affects the operation of the corresponding relay as a break in the circuit (very small

admittance), although, with respect to the absolute value, the admittance of this element can be equal to the relay admittance.

Let us now consider the parametric interaction of relays in the circuit. Consider a circuit with two relays, where they are connected in series or in parallel during the operation process. In both cases, in dependence on the circuit parameters (including voltage), it can happen that: 1) both relays operate; 2) only the first relay operates; 3) only the second relay operates; 4) neither of the relays operates. Thus, for the same structure and in dependence on the parameters, sixteen circuits with different modes of operation can be obtained. Therefore, in the stage of structural synthesis of a circuit with parametric dependences, it should be indicated how the relays are to operate if they are connected in parallel or in series. From all the possible combinations, I selected the three combinations which are most important in practice, and I introduced the  $A = B$ ,  $A > B$ , and  $A < B$  symbols, which indicate how these relays must operate. The existing methods for the design of relays make it possible to select parameters for which the relay will operate in correspondence with the assigned conditions (as is confirmed by examples given in the critical review). Formulas (8.7) and (8.11) are conditions which are imposed on the relays and which limit the group of the circuits under consideration, and not "statements," as V. I. Shestakov described them. As statements, they are "generally speaking, incorrect." Besides, it is difficult to find a theory for which it could not be said that its postulates and assumptions are "generally speaking, incorrect." In particular, the equivalences  $aa \dots a = a$ , and  $a + \bar{a} = 1$  in the theory of contact circuits, and some other equivalences are valid only for ideal contacts, and they are "generally speaking, incorrect." However, this in no way belittles the significance of the entire theory.

The author of the note was right in noticing the printing error in expression (8.10), which should be corrected to read: "if  $A > B$  and  $B > A$  (or  $A < B$  and  $B < A$ ), the circuit cannot be realized."

However, the statement in the review that this relation is inaccurate is not correct. Actually, if the circuit contains two relays,  $A < B$  and  $B < A$ , which are connected, for instance, in series, the relation  $A < B$  indicates that, if the circuit is closed, relay A must operate and relay B must not operate, and the  $B < A$  relation indicates that relay B must operate and relay A must not operate, i.e., both conditions are incompatible and the realization of such a circuit is an impossibility.

The "+" and "." symbols in chapters 8 and 9 correspond, as in the case of contact circuits, to parallel and series connection, and the symbol " $\sim$ " is determined by expressions (8.19) and (8.20) (page 125).

The symbols used make it possible to transform circuits containing not only contacts, but also relay windings and resistors, and to obtain circuits which are equivalent



to the relays contained in the circuit with respect to operation, and not to determine the electrical admittance of these circuits. Therefore, these operations cannot be compared with operations of the "algebra of dipole circuits of the A-type."

Thus, it is obvious that the mathematical and logical "errors" cited by V. I. Shestakov, either do not exist or are based on a conscious or unconscious confusion with regard to the concepts, "admittance value" and "order of admittance," which, as was indicated, pertain to different physical quantities.

In another place in the review, inaccuracies and contradictions in operations with equivalences are indicated.

The equivalence symbol  $a/b^*$  is used in those cases where the given conditions are satisfied by several solutions (circuits) which are characterized by the inequality (5.10), from which all particular solutions can be found by using formula (5.11). In particular,  $a/b$  indicates that, for the given conditions,  $b$  can be substituted for  $a$ , and conversely, in the formula (circuit). The commutativity of the  $a/b$  symbol is obvious from (5.10) and (5.11).

As regards the supposedly incorrect equality  $(\overline{a/b}) = \overline{a/b}$ , which is the only one indicated in the critical review, its proof is so elementary that I did not consider it necessary to provide it in the book. However, since V. I. Shestakov raised this question, I shall give the derivation. We start, for instance, with expression (5.11), and we write

$$\frac{a}{b} = ab + \omega(a + b);$$

$$\frac{\overline{a}}{\overline{b}} = \overline{ab} + \omega'(\overline{a} + \overline{b}).$$

By inverting the first of these expressions, we obtain

$$\begin{aligned} \overline{\left(\frac{a}{b}\right)} &= \overline{ab + \omega(a + b)} = (\overline{a} + \overline{b})(\overline{\omega} + \overline{ab}) = \\ &= \overline{\omega}(\overline{a} + \overline{b}) + \overline{ab}(\overline{a} + \overline{b}) = \overline{\omega}(\overline{a} + \overline{b}) + \overline{ab} = \frac{\overline{a}}{\overline{b}}. \end{aligned}$$

The other relations with equivalences can be verified in a similar manner. Therefore, it is hard to understand what is meant by other examples of "internal contradictions in equivalence calculations presented in the book" which are mentioned in the review.

In conclusion, it should be noted that V. I. Shestakov's remark on the absence of "proper scientific criticism" is completely devoid of substance. The material presented in the book was the subject of many reports

and discussions at various conferences and seminars. In particular, V. I. Shestakov twice came forward with his "criticism" (at the All-Union Conference on the Theory of Relay-Actuated Devices in 1957, and at the Session of the Scientific Council of the Moscow Electrotechnical Institute of Communications in 1959); however, he was not supported by the specialists who were present. I am also familiar with V. I. Shestakov's several negative references to the manuscripts of my papers. However, the above papers were published after they passed due criticism and discussion. Finally, V. I. Shestakov could have organized the discussion of these papers in the seminar which he heads.

In conclusion, we can say the following:

1. V. I. Shestakov's critical review presents the content of the book, as well as the individual theories, in an incorrect and tendentious manner. The only correct remark pertains to the printing error in formula (8.10).

2. In presenting the problem of transforming relay circuits, V. I. Shestakov, in spite of what is said in the book, treats the concept of the "order of admittance," which pertains to the conditions of relay operation in the circuit, as the "admittance value" and the assumptions used as "statements." Thus, all that has been said with respect to this question in the review does not pertain to my book. Moreover, the review indicates that its author is completely unfamiliar with practical methods for the calculation of relay circuit electrical parameters.

3. Neither does V. I. Shestakov's statement that the inversion operation is nondistributive with respect to any commutative Boolean algebra operation (emphasis supplied by V. I. Shestakov) pertain to the material in the book, since the "equivalence"  $a/b$  is not a Boolean operation, but a conventional way of writing the fact that the circuit  $x$  in question, which satisfies the given conditions, can have two values:  $x = a$  and  $x = b$ , which is analogous to the way of writing the general solution of the equation  $y^2 = a$  in the form  $y = \pm \sqrt{a}$ . It is true that the difference here consists in this: that, for contact circuits, the above fact results in a number of other particular values, which are determined by formula (5.11).

\*With regard to this theory, A. A. Lyapunov writes: "The methods of taking into account the so-called 'unused combinations,' which have been developed by V. N. Roginskii, who proposed a suitable algebraic tool (for the transformation of equivalences), also played an important role" (Mathematics in the USSR During the Last Forty Years [in Russian] (Fizmatgiz, 1959, Vol. 1, p. 872).

# ERRATUM

Vol. 21, No. 2, pp. 114-116, October, 1980

The article by A. A. Fel'dbaum published in *Avtomatika i Telemekhanika*, No. 2, contains errors in final derivations. In the corrected form, some of the equations in this article should be written thus:

$$L_{jk} = \delta_{jk} \alpha_k^2 \sigma^2 + (\gamma_j \gamma_k + \gamma_j B_k + \gamma_k B_j + B_k B_j) + \sum_{v=1}^m [(\gamma_j + B_j) A_{kv} + (\gamma_k + B_k) A_{jv}] \xi_v + \sum_{\mu, v=1}^m A_{kv} A_{j\mu} \xi_\mu \xi_v. \quad (37)$$

$$I_{jk, n+1} = \delta_{jk} \alpha_k^2 \sigma^2 + (\gamma_j \gamma_k + \gamma_j B_k + \gamma_k B_j + B_k B_j) + \sum_{v=1}^m [(\gamma_j + B_j) A_{kv} + (\gamma_k + B_k) A_{jv}] J_{v, n} + \sum_{\mu, v=1}^m A_{kv} A_{j\mu} I_{\mu v, n}. \quad (38)$$

$$I_{jk} = \delta_{jk} \alpha_k^2 \sigma^2 + (\gamma_j \gamma_k + \gamma_j B_k + \gamma_k B_j + B_k B_j) + \sum_{v=1}^m [(\gamma_j + B_j) A_{kv} + (\gamma_k + B_k) A_{jv}] J_v + \sum_{\mu, v=1}^m A_{kv} A_{j\mu} I_{\mu, v} \quad (j, k = 1, \dots, m). \quad (43)$$

Further, in Eqs. (49), (52), and (53), the coefficient "4" in one of the terms should be replaced by "2." With this, Eq. (55) can be reduced to the following form:

$$\varepsilon = \left(A_0 - \frac{\delta}{4}\right)^2 + \left(\frac{\delta}{k}\right)^2 \frac{1}{\left(4 - \frac{\delta}{A_0}\right)^2} + \left(\frac{k}{A_0}\right)^2 \frac{1}{1 - \left(1 - 4k + \frac{k\delta}{A_0}\right)^2}.$$